Edge Loading Effect on Total Hip Replacement

by

Ehsanollah Torabi kachousangi

A thesis submitted in partial fulfilment of the requirements for the
Degree of
Doctor of Philosophy in Engineering

University of Warwick, Department of Engineering
August 2016

Table of Contents

List of Figures

List of Tables

Acknowledgment

I would like to express my boundless thanks to Dr. Ken Mao for his unfailing support, his invaluable guidance and his inspiring comments on my work. This project never could have been completed without his support. I also appreciate the staff members of the Engineering Department for the facilities they provided me with.

Declarations

The work presented in this thesis is my own work, except where noted. None of the material of this thesis has been submitted for another degree at any other university or degree granting institution apart some common literature review previously submitted for the degree of Master of Science in Biomedical Engineering in 2011 at the University of Warwick.

Publication

Published Patent

Torabi Kachousangi, E. The University Of Warwick, (2016). ‘An acetabular cup for a hip replacement joint’. WO 2016/055783 A1.

Published Journal paper

W. Li, S. Wayte, D. Griffin, D. Chetwynd, D. Karampela, E. Torabi and K. Mao, (2014) ‘An Initial Approach on Arthritics Hip Joint using Finite Element Methods’, Applied Mechanics and Materials (668 - 669), 1557-1560.

Published Conference paper

Torabi Kachousangi, E. Asadirad, R. Mao, K. (2013), 'Prevent/Limit the Edge Loading in Total Hip Replacement′, World Tribology Congress *2013*, Torino, Italy, ISBN 978-88-908185

Poster Presentation

Torabi Kachousangi, E. Asadirad, R. Mao, K. (2013) 'Prevent/Limit the Edge Loading in Total Hip Replacement′. 40th Leeds-Lyon Symposium on Tribology, Lyon, France.

Abstract

The most important hip post-surgery problem is named Edge Loading (EL). This phenomenon significantly increases the contact pressure on the ball and the socket of the hip prosthesis hence decreasing the lifetime of the hip prosthesis drastically. Nowadays millions of patients cannot go under total hip replacement surgery due to the short lifetime of the hip prostheses. This research mainly focuses on finding solution for reducing the effect of this phenomenon.

In this research, reasons of EL are investigated and important factors in designing of the prosthesis are studied. Furthermore, a novel hip prosthesis is proposed. The model has been successfully patented with PCT number: PCT/GB2015/052933 and published with International Publication Number: "WO2016/055783Al". In this study the proposed design is analysed using three methods and the results are compared with the best available hip prosthesis in the market. The key results of the proposed design are outlined below:

- Comparison of the features of the proposed design with those of the available hip prosthesis suggests a promising outcome. This is mostly due to eliminating of the EL causes, in the new design.
- According to Hertzian Contact Theory, the proposed design reduces contact pressure during EL by 99.7% in comparison with the best available prosthesis in the market. This represents an upper limit.
- Finite element method simulation demonstrates up to 63% reduction (lower limit) of contact pressure during EL and also Neck-Rim/Ring impingement by the proposed design in comparison with the best available prosthesis in the market.

Although reduction of contact pressure by the novel design is noticeable, aforementioned methods show different results. This is due to the limitation of every method in this study. In this regard the novel design expecting to reduce contact pressure during EL / Microseparation more than 63% but less than 99.7%.

The novel design may open a new path for the total hip replacement surgery, and solve the EL problem forever.

Nomenclature

a	Contact radius
A	Cross section area
C	Dimensionless wear coefficient
c_d	Diameter clearance
C_d	Radial clearance
du	Changing displacement
dx	Changing distance
d	Head diameter
E	Elastic modulus
E'	Equivalent Elastic modulus
f	Friction factor
F	Applied force
F'	Friction force
H	Hardness
$h_{\min}$	Minimum thickness of the lubricant
i	Node i
j	Node j
k	Wear factor
$[K]^e$	Stiffness matrix
L	Linear wear rate
l	Length of the elemnt
M	Moment
$P(r)$	Distributed pressure
P_m	Mean pressure
P_0	Maximum contact pressure
R_a	Surface roughness
R_{head}	Radius of the ball
R_{Cup}	Inner Radius of the Cup/Socket
R	Equivalent radius
S_i	Shape function at node i
S_j	Shape function at node j
S'	Distance between the centre of the ball before and after separation
$\dot{s}$	Local sliding speed
S	Sommerfeld number
T	Frictional torque
u	Velocity
u^e	Displacement at different point
U	Displacement
V	Volumetric wear rate
V'	Wear volume
W	Applied load
x	Anteversion
X'	Sliding distance
X	Position vector
y	Inclination
ε	Strain
η	Lubricant viscosity

θ	Inclination angle
λ	$\frac{h_{min}}{R_a}$ Lubrication regimes
μ	Coefficient of friction
v	Poisson's ratio
ρ	Density
σ	Local mechanical stress
ω	Angular velocity
$\acute{\omega}$	Local wear rate
Δl	Changing Length

Abbreviations

1D	One dimension
2D	Two dimensions
3D	Three dimensions
ABS	Acrylonitrile-Butadiene-Styrene
AL	Alumina
ALVAL	Aseptic lymphocyte-dominated Vasculitis-associated lesion
AMC	Alumina matrix composite
BC	Boundary conditions
BDZ	Biolox Delta-Zimmer
CM	Conventional Model
COC	Ceramic on Ceramic
COP	Ceramic on Polyethylene
CPRESS	Contact pressure
CT	Computed Tomography
DOF	Degree of freedom
EL	Edge Loading
FDA	Food and Drug Administration
FDM	Finite Difference Method
FEA	Finite Element Analysis
FEM	Finite Element Method
HBW	Human Body Weight
HCLUHMWPE	Highly cross linked Ultra High Molecular Weight Polyethylene
HIP	Hot Isostatic Pressing
IM	Invented Model
MHRA	Medicines and healthcare products Regulatory Agency
MOM	Metal on Metal
MOMrs	Metal on Metal resurfacing
MOP	Metal on Plastic
MRI	Magnetic Resonance Imaging
PCT	Patent Cooperation Treaty
PMMA	Polymethylmethacrylate
PTH	Parathyroid hormone
ROM	Range of Motion
RP	Reference Point
SAA	Socket Articular Arc
SEM	Scanning electron microscopy
THR	Total Hip Replacement
UHMWPE	Ultra High Molecular Weight Polyethylene
vM	Von Mises stress

Chapter 1 : Introduction

The hip joint surgery was performed in 1821 for the first time [30]. Since then this type of surgery has progressed significantly begins with a very rudimentary surgery and materials to the modern hip replacement surgery with highly durable materials. This research studies the effect of the most important post-surgery difficulties named Edge Loading (EL), on the last possible treatment for damaged hip joint, which is total hip replacement (THR) surgery. Although THR surgery is a highly successful procedure, EL as the most important difficulty limits this surgery to patients who are fifty years old and above. Therefore, the young patients must either suffer from pain or consume medicine and use a wheelchair until they will be able to go under surgery. In this regard limiting or ideally preventing EL can promise to extend the lifetime of the prosthesis in human body; hence young patients can go under surgery and do their daily activities without pain instead of being wheelchair bound for up to thirty years. Furthermore extending the prosthesis lifetime significantly reduces the risk of revision surgery, which is critically important for the elderly.

1.1. Aims and Objectives

Our main contribution is to reduce the effect of current total hip replacement surgeries by proposing a novel hip prosthesis. To achieve this goal, we define the following aims and objectives:

- Identifying the causes of different kinds of EL.
- Finding the solution for reducing the effect of EL hence increasing the lifetime of the hip prosthesis.
- Finding the important factors in designing of the hip prosthesis that effect EL,
- Proposing a novel hip prosthesis.
- Analysing the proposed model using different methods by comparing the result of the proposed model with the most advance available hip prosthesis in the market.

In order to accomplish the above aims and objective, we combine several approaches and techniques of designing and analysis from different fields such as material science, mechanical engineering and medical science. In the following sections, we introduce the problem, its difficulties and the research gap and, sketch the structure of the approach by which the problem is tackled.

1.2. Structure of the Dissertation

This dissertation consists of 8 main chapters including the Introduction chapter, which are briefly explained below.

Literature Review

Hip joint is a ball and socket joint, which is the most weight-bearing joint in the human body. It is supported by number of cartilages, ligaments, muscles, bursa, etc. in order to have the second largest range of movement after shoulder and provide the stability of the joint. Part 2.1 mostly explains the anatomy of the hip while part 2.2 discuses hip diseases that cause pain and interrupt daily activities of patients. Some of diseases could be treated with the consideration and application of the precautions and advices made by orthopaedics such as resting or taking a medicine. However other ones such as Osteoarthritis, Rheumatoid arthritis, Traumatic arthritis, Osteoporosis, Paget's disease and fracture not only are not relieved by the lapse of time but also deteriorate and aggravate due to the degeneration of the bone or the cartilage. In this case, operation of the hip is inevitable for the patients in order to regain their activity and relieve their pain. Different treatments are explained in 2.3. Although the success rate in hip surgery is very high, always there is the risk of post-surgery problems such as infection, femoral fracture, dislocation, change in the leg length, EL and squeaking, which will be explained in 2.4.

Since 1821 many people have embarked on the investigation on the hip joint to develop new methods of surgery and highly durable artificial material to be used in the patient's body as a hip joint. The result of these investigations was the introduction of MOP, COP, MOM, COC and Composite prosthesis, which are fitted in body as a total hip, partial hip, or hip resurfacing depending on the condition of hip joint. Mechanical as well as medical conditions and properties of all materials used to make the prosthesis should be studied. Part 2.5 addresses bio tribology of prostheses and important factors such as wear, friction, lubrication, mechanical properties and biocompatibility of materials. Furthermore advantages and disadvantages of the hip prostheses made of different materials are investigated and compared with each other.

Key complication: Edge Loading

EL is the most important hip post-surgery complications, which is still under investigation in the literature and practice. Ball and socket in hip prosthesis should be contacted in conformed spherical surface. In this regard, change of the contact shape to

the edge of the socket produces high force to narrow area, which causes a high stress and respectively high wear rate. This phenomenon is named EL.

Occurrence of EL is unavoidable with current hip prostheses. This can be due to the different reasons, which can be categorised to the patient activities, surgeon experiences and engineering of the prosthesis. These are all explained in chapter 3.

Although patient can forbid some extreme activities such as specific sports like yoga or martial arts, some daily activities such as normal walking or step climbing cannot be forbidden. Unfortunately with current hip prostheses, EL happens with daily activities even if highly expert surgeons fit the prostheses.

EL as an effective factor on the lifecycle of the prosthesis, has come under investigation. Accordingly simulator machines, which measure the wear rate of the hip prosthesis, have reflected EL in simulation. Consequently different researches have been done and hip prostheses with different materials, orientations and sizes are compared with each other under several types of EL conditions. As a result, various experimental data, mathematical relationship, modelling information and anatomical evidences have been developed. Although some advice is given based on this research, the exact solution for this problem is not certain yet.

Methodology

Mathew Mak et al. [25] said: *"Potential solutions to this problem lie in alternative material and design"*. In terms of material; composite ceramic has been showing the most reliable behaviour during normal and EL conditions with the lowest wear rate and highest biocompatibility among all today available prostheses. However, a modification in the design of the prosthesis may solve the problem. In this regard the methodology in this study is based on 3 main techniques:

1. Study of the effective factors in design of the current prostheses in terms of limiting the EL, explained in 4.1.
2. Study of the Finite Element Method (FEM) in terms of analysing the current and the proposed prosthesis with Abaqus software, explained in 4.2.
3. Study of Hertzian contact theory, which mathematically compares the result of the current and the proposed model, explained in 4.3.

Design of Hip Prostheses

Based on the causes of EL and the information which have been found by studying the effective factors in designing of the most reliable hip prostheses to date, a novel model will have been proposed. This model is designed to significantly reduce or prevent the effect of EL. Furthermore, it helps to reduce the effect of Neck-Rim/Ring impingements during the extreme movement of the hip and solves another hip post-surgery complaint named dislocation. The model was successfully patented with PCT number: PCT/GB2015/052933 and published with International Publication Number: "WO2016/055783Al".

The features, specifications, advantages and disadvantages of this model are explained in chapter 5 and the rapid prototype of this model is also shown in 5.4. The model will be compared with best available hip prosthesis in the market using 3 techniques mentioned earlier

Simulation of IM and CM

In terms of comparing the proposed design and the available one in the market using finite element method, we model them in Abaqus software. For feasibility of comparison both models should be made of same materials and tested under same conditions. Chapter 6 explains the steps needed for simulating these models under following critical conditions:

- Neck-Rim/Ring impingement
- EL

Results and Discussion

Chapter 7 reports the results from comparison of two models in terms of design, FEM modelling and Hertzian contact theory and an in-depth discussion will be provided.

Conclusion and Recommendations

Future works mainly on how to make the proposed design applicable in the human body are outlined in Chapter 8.

Chapter 2 : Literature Review

2.1. Anatomy

To understand the functions of hip joint and thus their malfunctions and diseases, anatomical information seems indispensable. Without this information it is impossible to find the problems and then proceed to propose relevant medicine or surgery solution. Moreover the invention of the new artificial Total Hip Joint and improvement of the existing models require a good understanding of anatomy.

Hip joint is made of ball and socket joint, this arrangement gives the ability of large variety of motions to this particular joint and enables us to do our daily activities such as: walking, stair climbing, running and sitting.

Hip joint includes several layers of tissue. Deepest layer is the joint and the bone, the next layer is ligaments and the cartilage and the last layer comprises the muscles and the tendons, which are tightly in relation with the joint when the nerves, vessels and the skin are supporting this part of body [1]. So important structures of hip joint can be categorized as follows:

- Bone and Joint
- Articular Cartilage
- Bursa
- Synovial Membrane
- Ligaments
- Tendons
- Muscles
- Nerves and Blood vessels

2.1.1. Bone and Joint

Bones of the hip are the femur and pelvis; the femur is the longest bone in human body the head of which is shaped like a ball and named a femur head. The femur head is connected to the side of the pelvis with a joint, which is like a socket and named as an acetabulum. The femoral head is joined to the rest of the femur by a narrow bone called the femur neck. The femur neck is narrower than other parts of the femur and is located at a 125° angle with the rest of the femur [2], which enables the femur head joints to the acetabulum; and thus the stable hip joint is made.

At the top of the femur, next to the femur neck, there is a large bump named Greater Trochanter. This part of femur can be felt from the side of the hip. Different

parts of hipbone are shown in Figure 2.1. Important muscles are joined to this part of femur and posterior side of femur is called lesser trochanter.

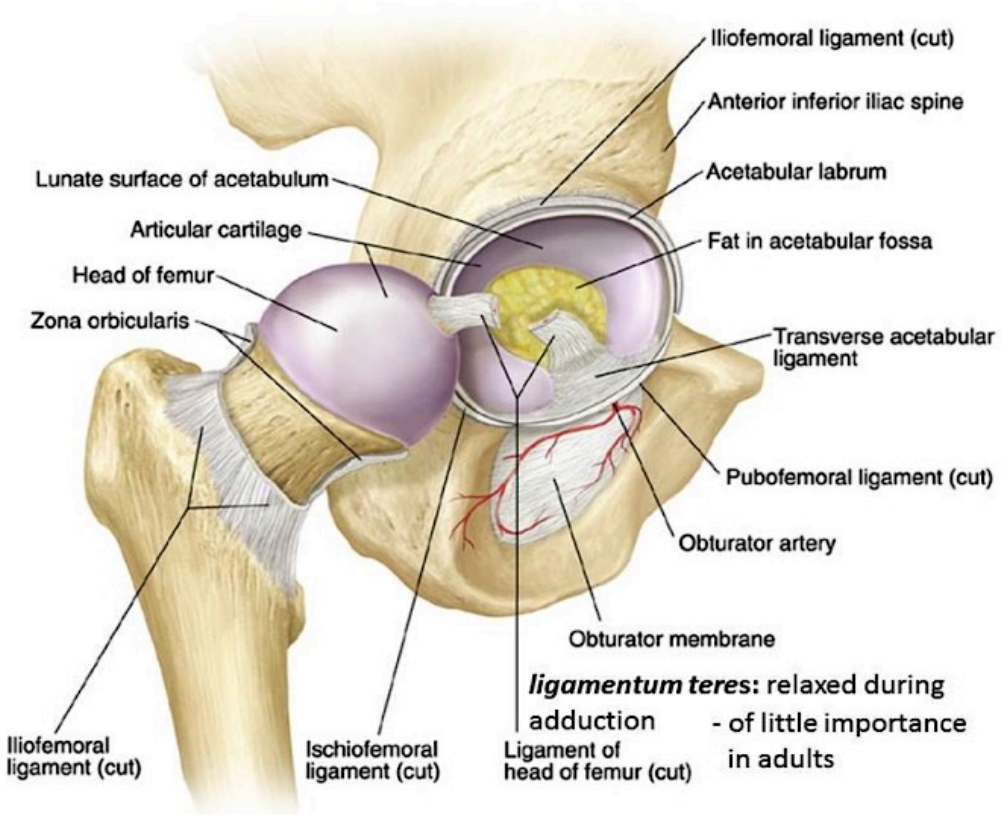

Figure 2.1. Hip anatomy, Femoral head, Neck, Greater and Lesser trochanter [1]

2.1.2. Articular cartilage

There is an articular cartilage wherever two surfaces of bones move against each other. The articular cartilage is rubbery material that covers the ends of the bones in the joint. It is white, shiny and slippery material, which supports the movement of the joint without rubbing a bone against each other. Furthermore articular cartilage acts as a shock absorber and contributes to the regular and proper motion of the joint.

Articular cartilage of the hip joint covers the head of femur and acetabulum in the pelvis. Due to the fact that the backside of the acetabulum sustains more pressure during walking, the articular cartilage is thicker in the back part of the acetabulum. Thickness of articular cartilage in hip joint is about 6 mm [3].

2.1.3. Bursa

This is a thin sac of fluid that acts as a lubricant in under friction area such as the area between the muscles, tendon and bone, tendons and ligaments and between ligaments and bone. Human body naturally produces the fluid in these sacs in response to the friction. However due to the injury or impact on the bursa, the body produces a

lot of fluid in their sacs hence it causes a problem which is called Bursitis. Since there exists plenty of muscles in the hip, there are twenty bursas available where Greater Trochanteric, Ischial Tuberosity and Iliopsoas bursas are in critical position in terms of contacting with hip joint [1].

2.1.4. Synovial Membrane

As mentioned earlier, the head of the femur and the inner layer of the acetabulum are lined with articular cartilage. Between these two cartilages there are two to three millimetres gap [4], which is covered by ligaments, hence the joint capsule is made. Inside of this capsule sealed with a thin layer, which is named as a synovial membrane. This layer, joint capsule, is filled with synovial fluid that has critical function for the hip joint. It covers the inner parts of the hip joint like ligamentum teres [4] to contain and conserve them and lubricate the joint. The cartilage is an important component in eliminating the friction and guaranteeing the smooth motion of the joint. Therefore, it needs to be healthy and supplied by oxygen and nutrition. There is no blood supply for cartilage and it entirely depends on the circulating synovial fluid, which is the oxygen and nutrition supplier for cartilage and synovial membrane. This is shown in Figure 2.2. This could be the reason for rheumatoid disease while puncturing the capsule and as a result drainage of the synovial fluid cause the necrosis of cartilage, which is the important reason for THR.

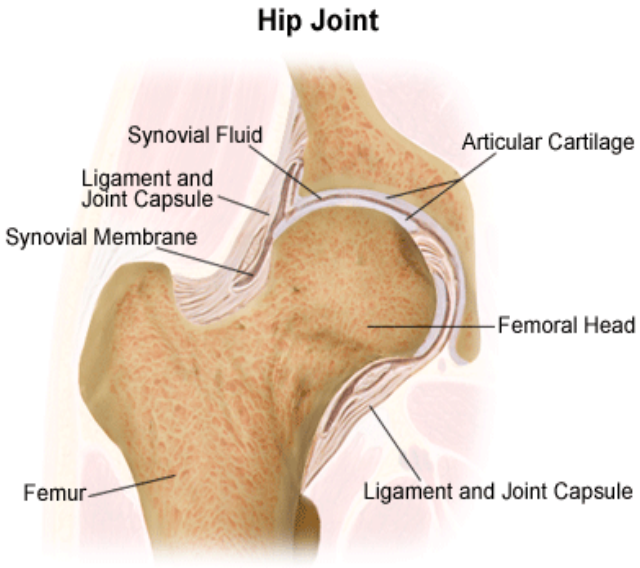

Figure 2.2. Synovial membrane and synovial fluid position [1]

2.1.5. Ligaments

Ligament is the soft tissue, which connects bone to bone. There are several ligaments located in the hip. Three important ligaments are named, Ischiofemoral, Iliofemoral and Pubofemoral ligaments, attach the femur head to the pelvis and form a joint capsule. These ligaments support the stability of the hip with holding a hip joint in place. Iliofemoral is the strongest ligament in the human body [1]. It plays an important role in maintaining the stability of human body. When the person is in the upright position, this ligament prevents the trunk from falling backward where there is no need of the muscular activity. It is relaxed while in a sitting position and allows the pelvis to tilt backward. The significant function of ligaments is to restrain the hip joint from excessive movement. Iliofemoral prevents excessive adduction and prevent the hip joint from internal rotation with cooperation of Ischiofemoral and Pubofemoral. Pubofemoral also prevents the excessive abduction of the hip joint.

There is a small ligament at the very tip of the femur head, which connects the femur head to the acetabulum and is designated as a Ligamentum Teres. It is shown in Figure 2.1. Although this ligament has no important function in controlling the joint, it plays an important role in feeding the femoral head on occasional situations. This ligament consists of a small artery, which is not the only branch of blood supply for femoral head. However, it could be the only artery if the neck of the femur is broken. Damage to this ligament and then the artery could be the cause of avascular necrosis, which is one of the reasons of the THR. This ligament similar to other ones resists the excessive movement. But due to its position, it precludes further excessive motion when the hip is dislocated.

There is a special type of ligament around the acetabulum's edge that plays a substantial role in avoiding EL and stability of the joint. It is called Labrum which is shown in Figure 2.1 (The actual picture of Labrum comes in appendix A). This ligament owing to its being located at the edge of the acetabulum, provides a deeper cup for the femoral head [6]. If this ligament is injured, it would cause the clicking and pain for the hip joint.

Inguinal ligament is another ligament in the hip that runs from Pubic Tubercle to anterior superior iliac spine. Its anatomy is important to operate the hernia patients.

2.1.6. Tendons

Tendon is a soft tissue, which connects muscle to a bone. There is a long tendon band along the femur from hip to knee, which is called Iliotibial band. Iliotibial band provides multiple points for hip muscle connectivity [1].

2.1.7. Muscles

Hip as the second most movable part of the human body and the most important part in retaining balance of the body, consists of seventeen muscles to facilitate Flexion, Extension, Abduction, Adduction, Lateral and Medial rotation of the hip joint. They are shown in Figure 2.3.

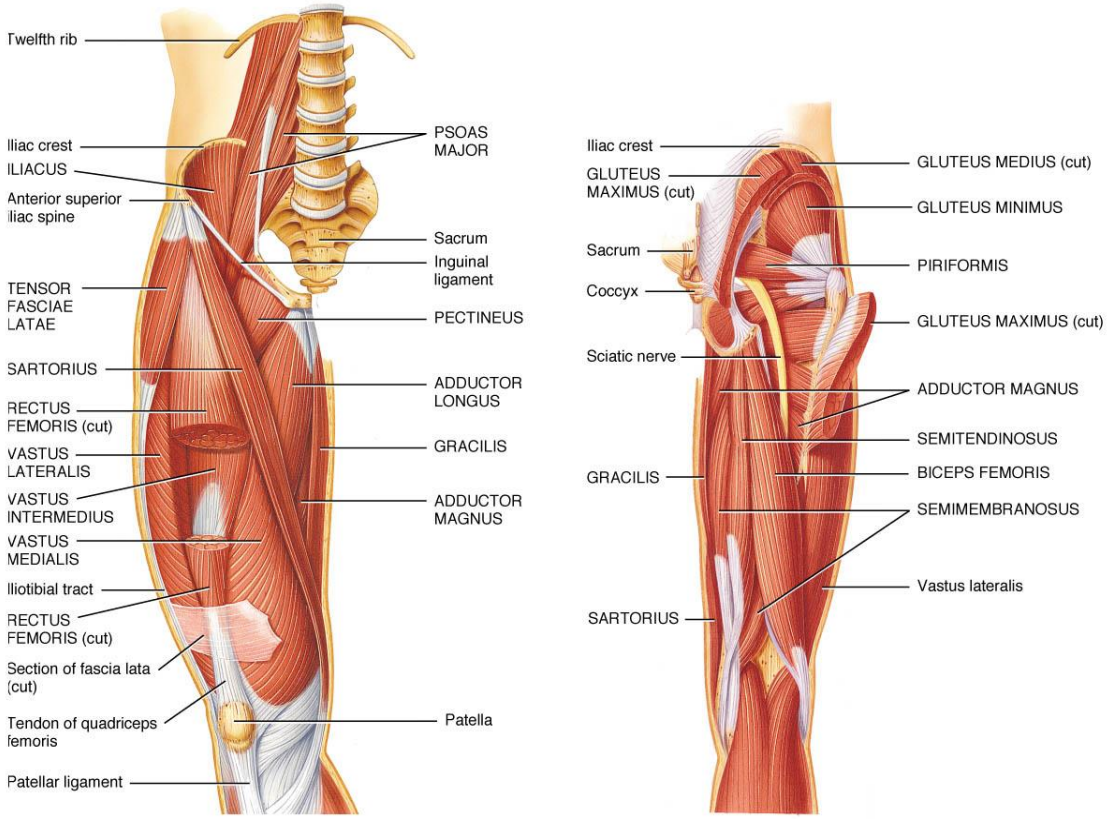

Figure 2.3. Muscles and sciatic nerve [1]

2.1.8. Nerves and Blood Vessels

Important nerves which in contact with hip joint are: Sciatic, Lateral femoral cutaneous, Femoral and Obturator nerves [5]. The joint is supported by various vessels to supply oxygen and nutrition which are Femoral artery, Internal and External Iliac artery, Obturator artery, Iliolumbar artery, Pudental artery, Profunda Femoris artery, Superior and inferior gluteal arteries.

2.2. Diseases

As explained above the hip is a complex organ while its mobility depends on the cooperation of many other organs; powerful muscles, ligaments, bursa, blood vessels, nerves etc. support it and make possible hip movement. This harmony enables hip to do

daily activity and to run or stop quickly. Malfunction in any parts of this structure causes disruption of hip mobility accompanied by severe pain (Figure 2.4).

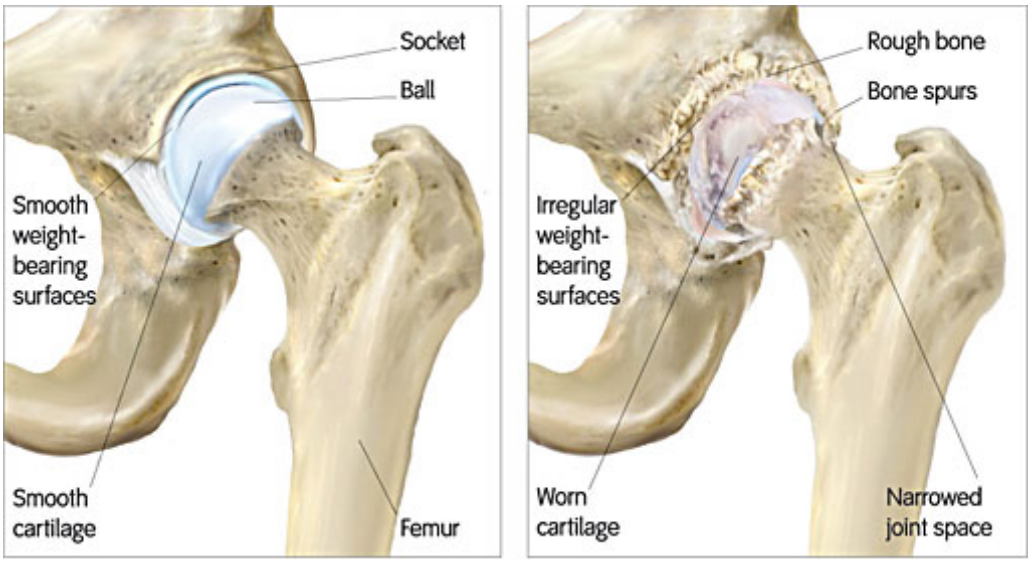

Figure 2.4. Comparing the arthritis and healthy hip joint [2]

There are many reasons for disruption of hip mobility. Many of them like Bursitis, tendonitis, muscle strain, snapping hip syndrome and numerous other diseases could be cured with non-invasive or minimal invasive medicine treatments. With respect to the subject of this dissertation, the scope of the discussion and explanation is confined to the ones lead the patient to THR surgery with considering of the age of the patients.

Arthritis [7] is the most important hip problem that disturbs the proper functioning of the hip. It is usually caused by wear and tear, disease or injury. Arthritis is the primary cause of disability and effects a huge number in Britain amounting to as many as one in five people [8].

2.2.1. Osteoarthritis

In this case articular cartilage, which covers the end of the femur head and acetabulum socket is worn out, thus the bones of femoral head and acetabulum rub against each other and eventually cause severe pain and stiffness in the hip. Osteoarthritis is a non-inflammatory degenerative joint disease. It is the most common arthritis, which is more happened in middle age and elder people with age forty-five and above [8]. There are three million people in Britain who suffer from this disease.

Although the medication and exercise can control this disease, it requires a surgery when the pain not relieved with non-invasive methods and daily activities of the patient significantly reduced.

2.2.2. Rheumatoid Arthritis

This is an autoimmune disease, which means that the immune system of the body mistakenly attacks the synovial membrane. This causes of inflammation of synovial membrane. The inflammation causes damaging the cartilage and if it is not slowed or stopped, could damage the joint.

Rheumatoid arthritis has indirect relation with the lifespan of patient and these patients have shorter life span than normal people. This is due to side effects of the medicine, which is used with the patients for controlling of synovial inflammation. Hip replacement will be done when the cartilage is worn out and thus causes the stiff joint; hence the movement of the hip is concomitant with pain.

About 1% of the people in the world have rheumatoid arthritis while 75% of this population are women. People in 40 to 55 years old are more exposed to developing this disease [9].

2.2.3. Traumatic Arthritis

This is another kind of the arthritis, which is caused by injury to the hip joint. This injury could be a result of any occurrence like sporting injury, traffic accident or falling down. If these occurrences cause the wearing out of the cartilage or fracture, lead the patient to the hip replacement surgery.

Cartilage cannot re-heal itself; therefore scar covers the torn part while scar does not have the same function as the cartilage. Scar is not only unable to act as a shock absorber; it does not work as smoothly as cartilage either. Broken bone can cause injury to other organs like ligament, muscles and tendons which makes the joint unstable.

Traumatic arthritis can arise in 2 to 5 years after the occurrence. Although pain is the first symptom of the traumatic arthritis, most of the time it disappears without the application of any medicine and re-emerges after a while. Traumatic arthritis can be accompanied with inflammation but it is not always necessarily so. In contrast with other kinds of arthritis, the traumatic one engages specific joint, which is the best way for distinguished with other ones for doctors.

2.2.4. Avascular Necrosis

Avascular Necrosis happens when blood supplying to the head of the femur is interrupted. Due to the lack of nutrition and oxygen, the joint will perish gradually. This phenomenon causes the articular cartilage to collapse and eventually the bones to rub against each other. This is mainly caused by hip fracture; however there are other

reasons for this arthritis as well: Diabetes, Kidney problem, gout, excessive use of alcohol, change the environment from high-pressure to low-pressure, cancer, use of steroid medicine etc.

The people who suffer from this arthritis, are usually age between thirty and sixty. This disease is not only healed with the lapse of time but also it gets worse and leads the patient to the surgery. This disease can be diagnosed with use of MRI. MRI can help to diagnose it in early stages of development when it is still possible to prevent cartilage collapse.

If the avascular necrosis is diagnosed in early stages, decompression surgery can save the joint from THR surgery; otherwise the use of the THR is inevitable.

Decompression surgery operates with providing a hole from damaged part of the bone to the head of the femur while it could be a spark for regeneration of the bone with linking the blood vessels to it. 80% of the patients in early stage of this disease have undergone this surgery while the success rate was as much as 75%; hence these people avoid THR in the future.

In addition to different kinds of arthritis, there are some other reasons, which lead the patients to the hip replacement surgery; and some of them are listed and discussed in the following section

2.2.5. Benign and Malignant bone tumours

Basically bone tumour is an abnormal growth of the bone cells could be noncancerous, which is called Benign; or cancerous which is called as malignant. Tumour might originate from the bone (Primary) or might be due to the spreading of the cancer from any other organs in body (Secondary).

The benign bone tumours are more pervasive in comparison with malignant bone tumours. It does not spread to other organs in the body and remains in the bone. The most common benign tumour is the one arising from the bone and cartilage together, which is called Osteochondromas. Tumour is produced by bone cells is called Osteomas and the one arising from cartilage cells is called Chondromas.

Malignant bone tumour could be primary or secondary although the primary one is very rare. It can arise from the hipbone or tangent soft tissues such as: muscles, cartilages and nerves. The most common type of primary malignant tumour is osteosarcomas [10], which arises from abnormal growth of the bone cell in end of the femur head and causes its enlargement. Therefore, it cannot fit in the acetabulum and gives rise to dislocation that is shown in Figure 2.5. Dislocated femur head can destroy

the tangent soft tissues. There are two types of primary osteosarcomas: the one which has few dividing cells and could be curable without surgery, and the one which has multiple dividing cells and can cause rapid enlargement of femoral head. The latter type not only needs surgery but also requires chemotherapy as well.

The secondary bone cancer does not arise from abnormal growth of the bone cells, while the malignant cells are from the primary tumour of other organs, which spread into the bone. This kind of cancer is hardly curable and the palliative treatment is advised [10].

Malignant bone tumour usually occurs in the age of ten to twenty; this corroborates the idea that the bone tumour is happened during the rapid growth when the males are more exposed to the risk of this tumour than females. Although the basic symptom of tumour is pain, the osteosarcoma tumour is painless and when exposed incidentally to X-ray (in other words, when X-ray is used for completely purposes or other reasons) it can be diagnosed and recognized.

Figure 2.5. 14 Years old boy with osteosarcoma of upper end of femur [4]

2.2.6. Paget's disease

There are two hormones for calcium circulation in human body: Calcitonin and Parathyroid hormone (PTH). When the calcium of blood is low, PTH is released, which triggers off the osteoclasts. These hormones break down the stored calcium in the bone and release it into blood. The calcitonin is used for the activation of the osteoblasts, which rebuilds the calcium and stores it in the bone when there is the excessive calcium in blood. This phenomenon causes the total skeletal replacement in human body; a phenomenon is called bone remodelling and occurs for children in the first year and for adults within ten years. This process is not done in the patients with Paget's disease. As

a result the bones of these patients are abnormal, large, brittle and more fracture prone, which is shown in Figure 2.6.

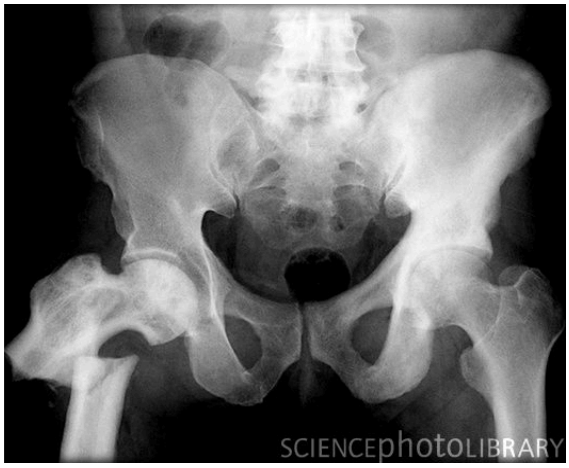

Figure 2.6. Fracture due to the paget's disease [2]

This disease is rampant in old bone of adults rather than children when it is estimated the patients with this disease are 1% in the US [11].

This disease does not have a specific symptom while it is recognized accidentally in X-ray test that is obtained for other reasons. Although there is not specific symptom, it could cause pain, fracture and stiffness and even pinch the tangent nerves by the enlarged bone. Paget is not a cancer so it is not spread to any other organs however the medicine treatment does not help it substantially and the most effective way is THR surgery [11].

2.2.7. Osteoporosis

Osteoporosis means spongy bone, which happens when the mineral density of the bone decreased. In osteoporosis, the protein of the bone is altered while a density of the bone is decreased up to two and half times less as much as the normal bone density, hence this phenomenon leads the patient to the bone fracture though it can be controlled by some precaution like preventing to fall in down, and activities like diet, exercise and losing weight. Medication such as calcium and vitamin D. could help the bone to re-heal. This disease has no symptom though it could be easily diagnosed by modern scanning. It is very common in Britain due to the low levels of sunshine, which helps the body to make up vitamin D [12]. It happens mostly in people over the age of 50, and more commonly in women than men.

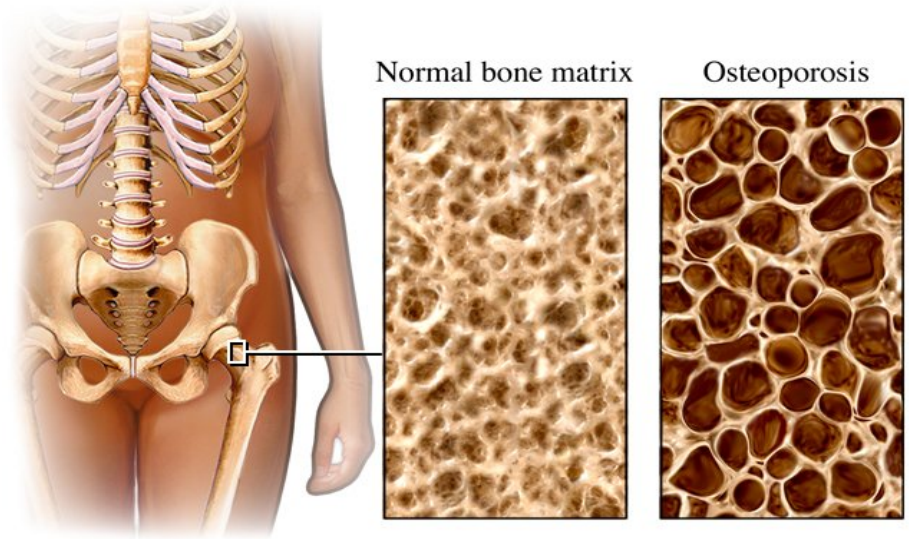

Figure 2.7. Microscopic difference between normal and osteoporosis bone [6]

2.2.8. Failed previous hip replacement surgery

Prosthesis loosening, wear, breakage, etc. lead a patient to re-surgery (Provisional surgery[1]). In this situation there is no other alternative left to the patient however the chance of success in second surgery is lower than the first one due to the deterioration apart of the bone in the first surgery. According to the University of Washington, failure is more common in women than men and it is more happened in individual more than 65 years old.

2.2.9. Femoral Fracture

Femoral Fracture could happen due to the disease mentioned earlier or severe accident in normal people. Fracture is categorized into four grades while the first three of them do not need THR surgery and can be treated with pins and nailing devices. The first grade happens when the bones are pressed to each other hence there is a stable fracture; whereas the second grade is complete fracture. However the parts are not displaced and they are still aligned. In the third grade, displacement occurs when there is some contact still existent; in the fourth grade displaced bones do not have any contact with each other hence the blood supply to the femoral head is completely disrupted and thus the THR is inevitable.

In the UK, 20% to 25% of the people following the femoral neck fracture die in a year while women constitute 80% of this population [13].

[1] Provisional surgery is conducted when the hip replacement surgery is done for the second time due to any failure in the first surgery.

2.3. Treatments

Due to the condition of the bone, disease, age and gender of the patients, the treatment could vary from simple advice of the doctor, to the THR surgery, some of these methods come in as follows.

2.3.1. Non-Surgical (Non-Invasive) methods

Non-Surgical (Non-Invasive) methods are primary methods of treatment, which would be applied before any further treatments. In these methods the patients do not undergo surgery; they rather take advice or medicine such as: Exercise, Rest, Heat Therapy, Cold Therapy, Physiotherapy (either Isometric, Isotonic or daily walking), Medicine and Drug (Corticosteroid, Anti-inflammatory agents, Glucosamine and Chondroitin, Viscos Supplementation and so on).

2.3.2. Hip Arthroscopy (Minimally-invasive)

This surgery is done through small incisions instead of a large incision, hence it has several advantages over THR surgery such as being less traumatic, faster recovery and outpatient procedure when the patient is discharged after arthroscopy [15].

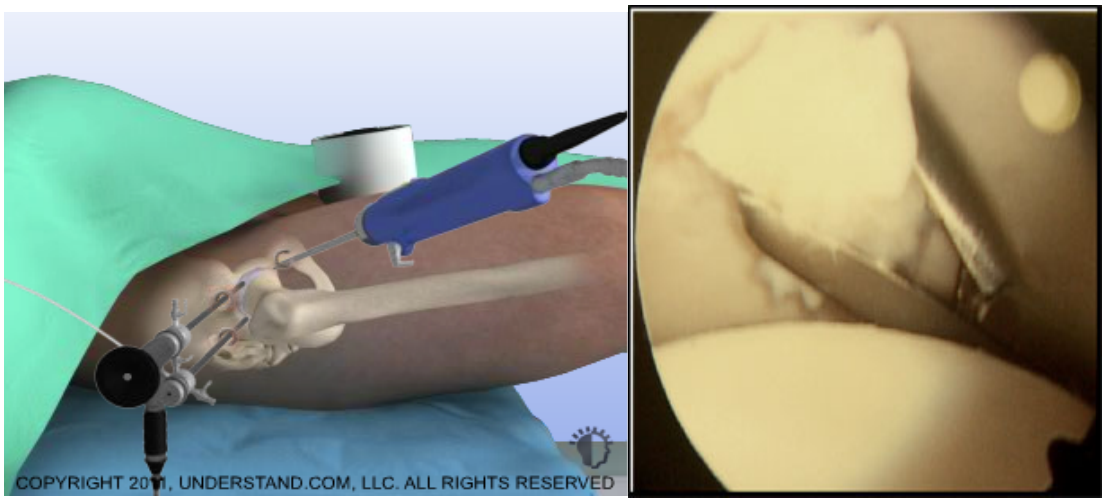

Figure 2.8. Arthroscopy instrument schema at the left side,the real picture from the arthroscopy camera at the right,the loose bpdy is removing [7]

The surgery starts with a general anaesthesia or regional anaesthesia. In the regional anaesthesia the medication is delivered to the spinal cord of the patient which numbs the lower limb. Patient's leg is slightly pulled to produce space between femoral head and acetabulum. The fluoroscope is used during the surgery to show the position of the instruments and the joint. Two to three small incisions are made while the sizes vary between 6 mm to 13 mm. The needle is inserted into the joint and placed with

guidance of the fluoroscope, saline is inserted through this needle with pressure to hold the joint open, afterward a guide wire is inserted through the needle and then the needle replaced with camera tube (cannula) to enable the surgeon to observe the condition of the joint with the monitor connected to the camera. In the second incision, another instrument is inserted to the joint to cauterize, shave or remove the tissue (Figure 2.8) depending on the joint problem such as Labrum tears, acetabulum cartilage loose body, inflammation, degeneration and bone spurs. The third or fourth incisions are rarely made and depend on the condition of the surgery. The instruments and the camera replace with each other for precise visualize and hence ease of the decision and application of the action by surgeons. The surgery lasts from thirty minutes to two hours depending on the time diagnosis and treatment taken. Eventually the incisions are sutured with two to three non-dissolvable sutures and swaddled with the bandage. The patient after surgery is advised to use walking aid for several days. Applying an ice pack could treat the swelling and pain; the sutures are removed seven to ten days after the surgery while the full recovery depends on the type of treatment prescribed by surgeon.

2.3.3. Hip replacement Surgery (Invasive/Arthroplasty)

Hip replacement Surgery is done when all other treatments, Non-invasive and minimally invasive, fail or not applicable, and the patient still feels pain for daily activities or even during the rest condition and stiffness limits a hip movement. Hip replacement surgery is one of the most successful surgeries in the world with the rate of 80% success [16] and a massive number of the convalesced amounting to more than 86,000 people in Britain in 2012 [19] and 520,000 Americans in the United State in 2006 [17]. In this surgery damaged part(s) is/are removed and replaced with artificial one(s). The surgery is mainly done through three kinds of hip replacement surgeries; depending on the condition of the joint, age, gender and type of the patient's activities, which are expatiated as follows.

2.3.3.1. Partial Hip Replacement (Hemiarthroplasty)

In this surgery the damaged part is femoral head when the acetabulum turns out to be ineffective [18]. It usually happens when the femoral head has a fourth grade fracture. In this case, it is not possible to fix it with nails and pins and thus hip replacement surgery is inevitable. An artificial femoral part consists of metallic or ceramic ball that is attached to the vertical stem, goes to the femur shaft. In this surgery

femoral head is cut off and the femur canal is prepared with a special instrument for insertion of the stem while the acetabulum is not replaced (Figure 2.9).

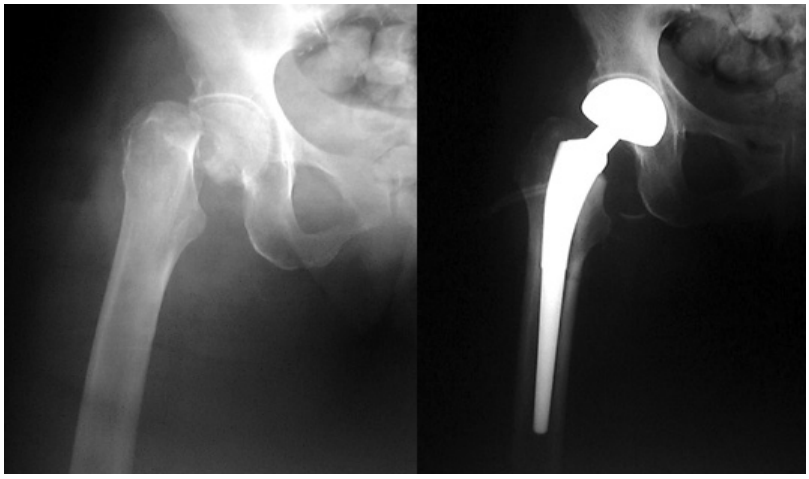

Figure 2.9. The fourth grade of fracture at left, hemiarthroplasty at right [2]

The stem is fixed inside the canal with or without cement, which will be more explained in 2.3.3.5 and 2.3.3.6. This surgery is carried out when the femoral head is broken and is no longer suitable for the arthritis patients. The reason lies in the fact that in arthritis patients the acetabulum is gradually damaged with lapse of time and eventually made unstable for preserving the prosthesis in place. Furthermore due to bearing of the metal/ceramic ball against acetabulum bone, this method is not recommended for young or active older patients and the THR is a better option for them.

2.3.3.2. Hip resurfacing

In this surgery femoral head is reshaped with a special instrument rather than being cut off, therefore most of the bone remains intact. When the patient is anesthetized, surgeon makes an incision over the patient's hip to reach to the hip joint with cutting the muscles. The leg is turned over for exposure the femoral head out of the acetabulum and acetabulum is reamed and cleaned from damaged cartilage and bone tissues. When the acetabulum part is securely installed in place with or without cement, the size of the femoral head is measured to fit the appropriate cap over it. The centre of the femur head is marked to insert the rod inside and aligns the further instruments for reshaping the femoral head to accept the cup, and eventually the cup will be placed over the remained femoral head and neck, and is fitted with cement. Size of the cup in femoral part is very important i.e., the larger size is recommended due to more stability; this will be explained later. Hip resurfacing is more suitable for the patients who

probably will have the THR in the future, such as young patient with arthritis [18]. Although this surgery has a relatively shorter recovery period than the THR and the risk of the leg length discrepancy is much lower, there is the risk of the neck fracture especially in the patient with osteoporosis such as Figure 2.10.

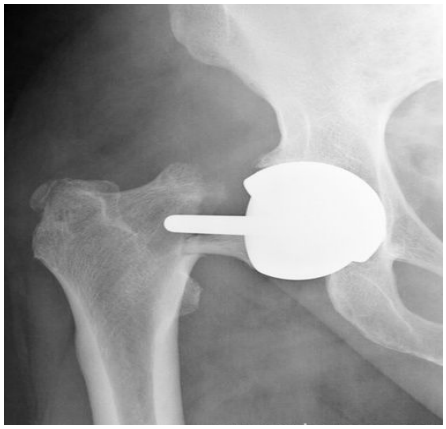

Figure 2.10. X-ray failed resurfacing due to the fracture of neck [15]

2.3.3.3. Total Hip Replacement

THR is the last option for the patients who suffer from the pain and for whom not only other types of treatments (non-Invasive and minimally invasive treatments) have been proved ineffectual but also other invasive surgeries are not effective enough. In this surgery as its name indicates, the hip joint is completely changed; so the interaction of the both acetabulum and femoral components are crucial and depend on the sizes, material and position of the prosthesis; all of which will be explained in the following chapter. The surgery takes 60-90 minutes (Appendix B) and starts with general anaesthesia or with the spinal anaesthesia when the spinal cord receives the substance through injection. Therefore the nerves going to the lower limb will be numbed and the patient will not have any sense during surgery. Because the patient in the spinal anaesthesia is awake, sedation is delivered to him/her to enable the patient not to listen to the surgery procedure such noises as produced by reaming, cutting, derailing and hammering a bone which are not gracious.

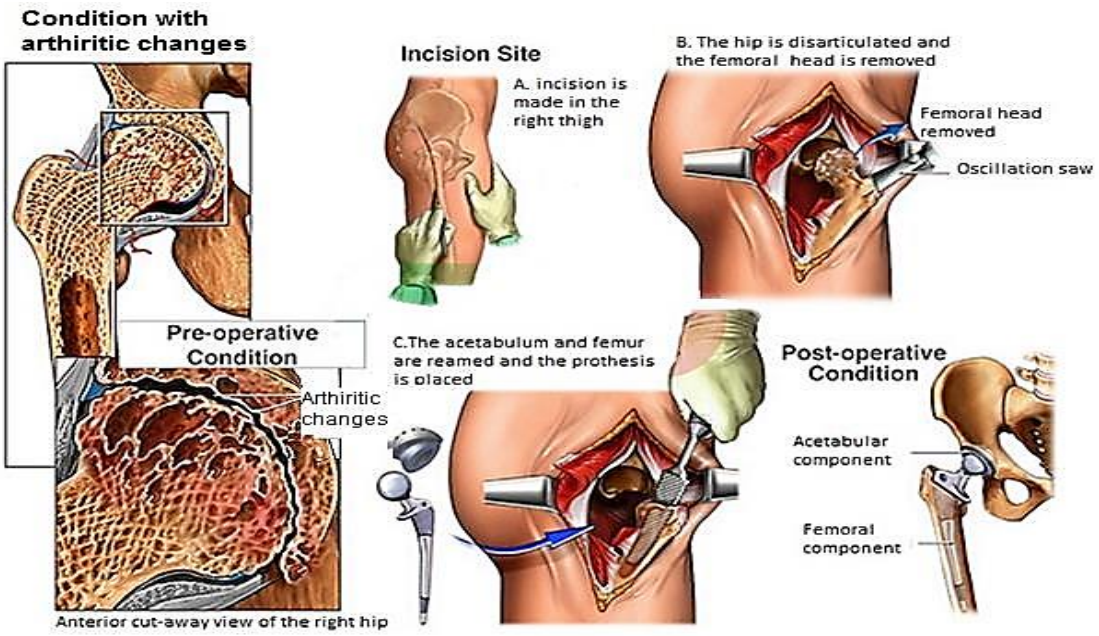

Figure 2.11. THR surgery process [7]

When anaesthesia effects, the intended region for incision is cleaned with an antiseptic substance. The incision made over the side of the hip joint, as shown in Figure 2.11, depends on the decision of the surgeon, which normally has a length of six to eight inches. The muscles and ligaments are slashed to the extent that eventually hip joint is exposed. The femur of the patient is manoeuvred for dislocation of the femoral head from acetabulum. The femoral head is cut off from the end of the femur with a saw and the acetabulum socket is reamed with special reamer to form a hemispherical shape for accepting the metal shell by screws, bone cement or by pressing which is fitted tightly and held in place by friction.

The femoral part consists of a ball and a stem. The ball fits into the socket and the stem runs through the femur. For this purpose, the head of the femur is removed by power saw and other special instruments are utilized to rasp the shaft of the femur. While the spongy bone (Cancellous) is removed from inside of the canal, it is shaped to accept the stem. Apparently the stem should be fixed into the femur as well as socket to the acetabulum either with cement or without cement which depends on the condition of the patient's bone, age and the prosthesis type. Sometimes the combination of these two is suitable while one of the prosthesis either socket or stem fixed with cement and another one is not. This method is called Hybrid total hip implant. When the stem is secured inside of the femur canal, trial balls fit into the socket to assess the proper size of the ball for each particular patient. Some patients order the customized implant,

which is made particularly according to the hip anatomy of the patient. Modularity[2] is another option for the patient which enables the surgeon to use different sizes of ball in different angles with different lengths of the stem associated with his/her anatomic feature[3].

When the appropriate ball is chosen, it is pressed on the top of the stem and locked with friction. This forms the artificial femoral head (in some prosthesis the ball is attached to the stem and are a single piece) while it gets engaged with the socket and tested again for its stability and the leg length of the patient. If the result was desirable, the ligaments are adjusted and the incision layers are sewn. Due to the excretion of the fluid by the wound a small tube comes out of the hip for draining. Sterile bandage is applied to the wound and the patient is taken to the recovery room for further services.

2.3.3.4. Bilateral THR

Sometimes it is necessary to change both hip joints due to the arthritis or stiffness. If the surgeon changes both of the hip joints with the prostheses in one surgery, that surgery is called Bilateral THR. It is presented in Figure 2.12.

The duration of this surgery is twice the time of the normal THR (about two to three hours). The patient should be under anaesthesia twice the time that the normal THR surgery takes as well. In this regard the old patients with pulmonary, cardiovascular or other diseases, for whom a longer anaesthesia and surgery might cause some problems, are recommended to undergo two separate THR surgeries.

Figure 2.12. X-ray captures bilateral THR [15]

[2] Modularity prosthesis is made of separate components while each part can be changed with different sizes

[3] There is no significant difference in the hip joint of the patient in the same gender. This is more common in knee replacement.

2.3.3.5. Cemented Method

Bone cement is made of poly-methyl-meth-acrylate (PMMA). It is used to hold the prosthesis in place. We have to keep in mind that the bone cement is not a kind of glue to stick to the prosthesis or bone, whereas it behaves as filler between the bone and prosthesis. In order to lock the prosthesis and bone together, cement must extrude into the cancellous bone either in acetabulum or femur shaft cancellous bone. Bone cement becomes very hard in fifteen minutes, which can break the weaker part of the bone if it has not penetrated into the cancellous bone properly. In order to achieve this critical purpose, fat, blood, debris and damaged cartilage are flushed out by pulse lavage[4] and then dried thoroughly to insert the permeable bone cement under pressure.

Cement method is usually used for elderly people who are less active and have weak bones (osteoporosis). The ones used this method of surgery can stand in his/her leg almost after the surgery without support and can walk within three to six weeks without walking aid.

2.3.3.6. Un-cemented method

In this method, the prosthesis has a porous surface or texture that allows the bone to grow inside the prosthesis so the bone accompanies the prosthesis and locks it within itself. Certainly this method requires enough time for growing the new bone that penetrates into the prosthesis, which is usually accompanied with pain. This interval increases the time of healing and limits the activity of the patient up to three months.

Although more long-term data are available for the cemented method due to the invention date of this method (1958 by Sir John Charnley) than the un-cemented one (1964 by Peter Ring) the results of success are comparable. However, it is recommended for the young patients who are more active and do not have osteoporosis. Figure 2.13 illustrates these two methods.

[4] Pulse lavage is a special power washer used in orthopaedic surgery.

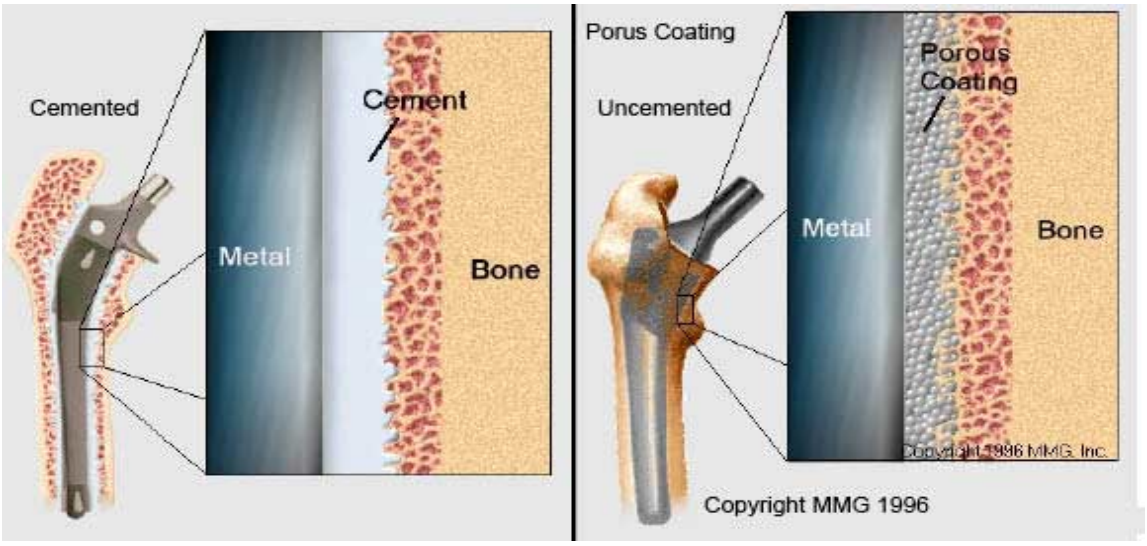

Figure 2.13. Illustration of cemented and un-cemented method [18]

2.4. Complications of Hip Replacement Surgery

Although hip replacement has been one of the most successful surgeries since its emergence, it involves some risks such as all other surgeries. There are several complications in this complex surgery while the most common, gravest and important ones in long term are respectively blood clotting, infection, loosening. EL is one of the most critical factor which is significantly increases the wear rate (26 fold in COC). These factors and possible ways to reduce the risks are discussed in following.

2.4.1. Blood clotting

Blood clotting in the veins after hip replacement surgery is a common complication. If the clot remains in the vein, it can be deemed a minor problem; whereas if it moves through blood stream and carried from the heart into the lung vessels it can cause a grave problem which is known as pulmonary embolism [20]. Pulmonary embolism can increase the death potentially. In order to prevent this phenomenon, doctors prescribe blood-diluting drug such as Coumadin. Exercise is also recommended.

2.4.2. Bleeding and vessels injury

Bleeding during surgery is normal. There is also expected to be bleeding after surgery as well. Sometimes bleeding is due to the injury to the main blood vessels[5] while the urgent surgery might be necessary by vascular surgeons to stop bleeding. In some cases excessive use of blood thinner for preventing the blood from clotting bears detrimental results, which in their own turn cause the bleeding inside the joint. Such

[5] Most of the arteries supplying the lower limb pass the hip joint closely

bleeding in the joint culminated in dislocation of the ball from socket. In case of occurrence, the wound should be opened and the blood removed from the joint promptly. It is rarely possible the blood is released into urine; however, in case of occurrence it will be temporary.

Therefore, due to the bleeding either during or after surgery the blood transfusion might be required so the patient is advised to donate his/her blood two to three weeks before surgery in order to minimize the risk of disease which is probable in transfusion of blood bank [27].

2.4.3. Nerve injury

There is a risk of injury to the Sciatic, femoral and obturator nerves when the acetabulum part changes in the THR. The risk of this complication is 1% to 2% [14] but in case of occurrence it takes the patient up to six months to recover and on rare occasions the patient may never recover. Depending on the condition of the damage to the nerve, they are classified into three main types [28], which are briefly discussed in the following sections.

- Neuropraxia: It is the least harmful nerve injury while the important parts of the nerve cell remain intact and only there is some interruption in the signals conduction. It takes six to eight weeks to recover.
- Axonotmesis: It is more severe than Neuropraxia while it not only one of the causes of signal interruption but also disrupts the neuronal axon[6] as well. In this injury the myelin sheath[7] remains intact.
- Neurotmesis: It is the most harmful injury in which the axon and myelin sheath lose their continuity.

2.4.4. Infection

Due to the massive incision for hip replacement surgery (six to eight inches) there is a higher risk of infection than other surgeries with smaller exposure area. There are several preventing measures for this purpose; sterilizing all the equipment are in contact with the blood flowing in the patient's body and all other components in the operation room such as masks, gloves and clothes used by surgeon and his/her assistances. Laminar flow operation room is another precautionary measure. Operation room is outfit with several filters, which clean the operation room from bacteria and reduce the chance of existing bacteria in the operation room environment. The antibiotic

[6] It is a long part of nerve cell, which conducts the electrical impulse from one neuron to another neuron.
[7] It is dielectric material that isolates the signal path (Axon) from other environment.

medicines, which are given to the patient before, during and after the surgery, play an important role indeed. Bacteria existing in other parts of body could travel with blood streaming and causes infection in implanted part of body so it is important to be treated that before hip replacement surgery.

Infection can be detrimental enough to cause loosening of the prosthesis while it may not appear in a year but sometimes appear as quickly as the patient haven't discharged from hospital. The People with Rheumatoid arthritis are more exposure to the risk of infection due to the disorder of their immune system [21].

2.4.5. Fracture of the femur or Acetabulum

There is a chance of the fracture either during the surgery or after surgery (Post-surgery). The fracture during the surgery is more probable in the revision surgery though there is a risk of fracture in the primary one as well. The fracture could be major or minor. The major fracture of femur needs a separate surgery to fix, which force the patient to remain on crutches from three weeks to three months depending on the extent of the fracture, while the minor fracture, crack, can be treated with the circlage wires during the same surgery. The post-surgery fracture could be due to the trauma, which is discussed in traumatic arthritis earlier, or prosthesis condition. Because femur is hollowed out and retains the femoral stem, it can be in the risk of the fracture. Acetabulum can be fractured due to the aggressive reaming on the medial [23].

2.4.6. Limb length inequality

Although all the efforts are made to maintain leg length, it is not possible in some cases. This difference of the leg length could be due to the femoral neck offset, defect of prosthesis or femoral cut but it could not cause any problems if it is less than a quarter of an inch; while a difference beyond this measure could compel the patient to use the shoe lift. Sometimes the surgeon makes this change deliberately. Increasing the leg length causes tightening of the muscles around hip which increases the stability of the joint. In the first several days after surgery, most of the patients bemoan about their leg length (they usually complain of its elongation) even if they leg length is exactly same in effect. This sense is referred to as the artificial sensation, which is resolved during the first several months after surgery [27].

2.4.7. Extra bone formation (Heterotopic ossification)

There are a few probabilities, approximating 1% of cases, for extra bone forming around the joint, which cause stiffness and pain. Although the smaller amount

of these bones appear frequently without marring the patient lifestyle, a large amount of the ectopic bones causes an acute pain and makes some difficulty for the movement of the patient. If the orthopaedic recognizes possibility of extra bone formation around the patient's hip, the radiation treatment will be advised. It should be done less than two to three days after surgery. The mature heterotopic ossification [27] is illustrated in Figure 2.14. In case of appearance of the ectopic bone it will be removed by surgery either invasive or by arthroscopy.

Figure 2.14. Class three of the heterotopic ossification [27]

2.4.8. Loosening

If any fixed parts of prosthesis, stem or socket, is loosed more than 2 mm or the position is changed, the prosthesis considered as a loosed one [22]. This is the most important difficulty in the long run after surgery while it can have several reasons, which have been outlined and explained as follows.

2.4.8.1. Patient Activity

This is an important factor in loosening prosthesis. When stress is intensified with the higher activity, there is a risk of loosening. This does not mean that the patient cannot participate in any activities such as normal walking. They are not only not forbidden but also recommended for regaining the muscle strength.

2.4.8.2. Weight of the body

It is important to keep the body weight in balance after surgery and maintain the weight as healthy as possible, because each one-pound weight makes four pounds of pressure on the hip.

2.4.8.3. Quality of the bone

If the bone is hard and relatively healthy it forms a tighter, more long-lasting bond with prosthesis. Therefore the risk of the loosening is lower, in contrast with patients with the osteoporosis bone or rheumatoid arthritis who have spongy bone and soft bone respectively [23].

2.4.8.4. Cemented or un-cemented prosthesis

Although the success of these two types of fixation is comparable, it entirely depends on the proper use of them with regard to the specific case of each patient such as age, activity and bone quality. Cemented prosthesis is usually loosed due to the cemented socket while in un-cemented prosthesis failure due to the stem as a result of osteolysis. Generally un-cemented method, due to the penetration of the bone in the porous surface of the prosthesis (The bone envelopes the prosthesis) has the lower chance of loosening in long term while cemented prosthesis has the lower chance of loosening in short term [24].

2.4.8.5. Surgeon experience

The surgeon's experience is indubitably one of the important factors for the quality of the surgery. Surgeons who work especially on the joint know the potential risks, precautions and how to tackle them in case of occurrence. Also the feedbacks of his/her patients could be the best guide in choosing the appropriate prosthesis model and surgical method [23].

2.4.8.6. Prosthesis design

From the engineering point of view prosthesis design is the most challenging problem while the material, size and positioning can be vital in loosening or fostering other problem of post-surgery life. The materials with higher abrasion rate are more prone to loosening, which are explained in 2.5.3.

2.4.9. Dislocation

Stability of the hip joint is the most important factor in the success of the surgery. The ball is held in socket with the tension of the muscles. Because the muscles are slashed in the surgery, it takes time to retrieve their strength. In this time, which is approximately about six weeks after surgery, there is more risk of dislocation, which happens when the ball slips out of the socket. Mal-alignment of socket or stem can cause of dislocation as well. This phenomenon is more likely to happen in patients with MOP and COP prosthesis due to the nature of the polyethylene and relatively small size

of the ball. To prevent this problem physiotherapists advise to avoid some certain movements such as high step climbing.

The overweight patient and the patient with poor muscle are more susceptible to dislocation; thus, they are advised to use brace in the first six weeks after surgery. In case of dislocation physiotherapists or surgeons pull intensely on the leg and pop the ball into the socket or reduces the acute setting of the prosthesis through revision surgery [24].

2.4.10. Edge Loading

If the ball contacts the edge of the lining, causes a long and narrow visible damage called wear stripe. It causes excessive erosion in the ball and the edge of the socket than the normal wear rate does while the stripe wear sign is illuminated much faster than normal abrasion signs [25]. This research addresses this problem in details at chapter 3.

2.4.11. Squeaking

It is an acoustic noise, which is seen in 6% of COC prosthesis by patients for several months (about 20 months) after surgery. Although this problem is not harmful and not associated with pain, it is annoying to the patient and may lead to change the prosthesis even if there is no any mechanical failure [26]. Walter [26] believes this phenomenon has a direct relation with the EL, which will be discussed in 3.4.

2.4.12. Other complications

Some other difficulties such as heart attack, fat embolism, anaesthetic complicity, Pain, allergy to the medicine, failure of the prosthesis or death are other risks of surgeries.

2.5. Mechanics in THR

THR is one of the most successful surgeries in terms of lowest failure rates, while its success is more than 90% [16]. More than 332,000 procedures were done in 2010 in the United States [29] and more than 75,000 ones in 2012 in the United Kingdome [19]. The rate of the surgeries is increasing every year. (i.e., more than 7% in 2013 in the United Kingdome compared to 2012 [19]). However due to the wear, the lifespan of the prosthesis is limited to 10 – 15 years only. Furthermore revision surgeries are increasing (i.e. more than 12% in 2013 in the United Kingdome compared to 2012 [19]). Increasing of revision surgery is due to the younger patients activity.

Nowadays, there are numbers of hip prosthesis brands, among which surgeons choose one of them depends on the condition of the patients (i.e. age, anatomy, gender etc.) and his/her experiences.

Although all materials are used in human body must be biocompatible, the materials are used in the head and the socket, are more essential. These are mostly plastic (P), Metal (M) and Ceramic (C). The couple surfaces in the hip prostheses are: Metal on Plastic (MOP), Ceramic on Plastic (COP), Metal on Metal (MOM) and Ceramic on Ceramic (COC). The first letter in these acronyms refers to the ball material and the last one to the socket.

This section is more focusing on the mechanical properties of the materials in hip replacement surgery since it was emerged.

2.5.1. The History of Hip Replacement

Since its emergence, THR surgery had significant progress while it begins with a very rudimentary surgery to the modern THR surgery with highly durable materials. The following material will review this development during these years.

In the first time, in 1821, Anthony White (1782-1849) of the Westminster Hospital in London had done the surgery; however he did not publicize or even make a report of it [30]. In this operation surface of the joint was changed hence it provided the mobility and relief the pain, though it failed in the case of stability.

In 1826, for the first time hipbone was cut and some part was removed by John Rhea Barton (1794-1871) in Philadelphia. He did this surgery without anaesthesia in seven minutes and the patient could walk with cane, three months after the operation. Although this surgery had primary successes, it failed in six years later. Borton was the first person who proved that the motion prevents the bone fusion. He reported the surgery in the North American Medical and Surgical Journal [31].

Vitezlav Chlumsky (1867-1943) was the Czech surgeon who experimented with many materials for the hip prosthesis like: celluloid, rubber, Magnesium, Muscle, glass, zinc, pyres, decalcified bone, wax and silver plate [32]. He tested these materials in animals before implanting in his patients.

In 1891, Professor Themistocles Glück was the first person who implanted the actual total hip prosthesis in human body. He made the femoral head and socket with ivory and screwed them to the bone with nickel plated screws. “Furthermore he experimented with mixture of plaster of Paris, and powder pumice with resin for fixation” [33]. Glück was also the first person who proposed the biocompatibility of the

material in human body. Due to this idea he used ivory for his artificial hip joint in human body, the material of which is very akin to human bone. Also he found that the cavity in the bone, bone marrow cavity, could accept the stem of the artificial hip joint if it is stably fixed in.

In early 1900, Foedre (b.ca. 1860), a French surgeon, noted that the pig bladder could withstand the stress and the intra articular pressure. In 1918, William Steven Bear (1872-1931) used pig bladder at the John Hopkins Hospital while there were not the modern surgical procedures and the surgery had been done with Hippocratic tradition which was a surgery with no anaesthesia [34].

During this period of time Sir Robert Jones (1855-1933) covers the made femoral head with a strip of gold. It was effective for twenty-one years in the body of a patient such that the patient could retain the motion of the joint for twenty-one years. He reported this success [35] as it was the longest duration of effective technique in the history of arthroplasty.

In 1924, Royal Whitman (1857- 1946) reported the first new method in surgery of osteoarthritis other than fusion. He described the surgery in annals of surgery [36] when he worked in Hospital for Rupture and Crippled in New York City. In the operation, the femoral head was removed and the trochanter and its attached muscles were cut obliquely. Hence the new area was provided together with the remained part of the neck, which could provide a secure weight.

American surgeon Marius Smith Petersen (1886-1953) made a hollow hemisphere, which was made with moulded glass, in 1923; this piece could fit on the femoral head and form the smooth interposition material between femoral head and acetabulum. He believed that the glass has not only a good biocompatibility but also it has a smooth surface with low friction. He fitted this device over the femoral head of the patient in 1932, however this method failed quickly due to insufficient withstanding of glass in the face of the stress of walking and weight pressure. Although he obtained a significant success in case of biocompatibility and smoothness, stubbornness of the patient convinced him to abandon glass. After that he used celluloid, Pyrex and Bakelite until he met his dentist in 1937 when he advised to use Vitallium by him. In that time Vitallium had recently been introduced to the dentistry market. Smith Petersen used 500 Vitallium in the hip joint [37], which had the predictable result in arthroplasty history when it had 10 years successful clinical result. Vitallium is made of cobalt, chromium

and molybdenum, which it not only does not react to the human tissues also it is very strong and resistant to the corrosion. Therefore, it is still used nowadays.

In 1948, French Judet brothers, Robert (1901-1980) and Jean (1905-1995), used acrylic to make a hip resurfacing [23] while in this process the cartilage of the femoral head is removed and replaced by the metal cap. This process could save the hip joint 20-30 years but unfortunately this material is loose and fails very quickly.

In 1950, Frederick Röeck Thompson (1907-1983), Harold R. Böhlman (1893-1979) and Austin Moore (1899-1963) refined the concept of Judet brothers and developed a use of the vitallium to make a hip joint prosthesis. They worked separately to achieve similar aims, which were to make a stable, high durable and biocompatible hip joint and could withstand the stress of walking and pressure of the human weight. By this time the mentioned aims became clear and the artificial hip joint had been made, consisting of a single piece with ball fitting to the acetabulum and a vertical stem inserted into the bone marrow cavity. Dr. Moore was honoured to be the first person, who replaced the twelve inches of the destroyed femur by a tumour, with a new vitallium prosthesis at John Hopkins in 1940 [24]. The prostheses is illustrated in Figure 2.15.

Figure 2.15. Twelve inches prothesis was replaced by Dr.Moore in 1940 [24]

Kenneth McKee (1905-1991) used dental acrylic as a cement to fix the femoral and acetabulum components. He also used Thompson prosthesis for the femoral side, which was fixed to the three-claw type cup acetabulum component. The cup was screwed into the acetabulum but it failed due to loosening. Moore and Böhlem developed the invented prosthesis to the one with pores to allow the femur bone in growth, in 1952. Although Moore and his colleagues had a significant progress in making femoral head parts, they failed to make the acetabulum component.

In 1958, a British orthopaedic surgeon, Sir John Charnley (1911-1982), introduced the new technique to reduce the wear of the socket, which was replaced under eroded parts of the socket with a Teflon material. Although Teflon component

failed, it posed the idea and paved the way for replacing the eroded part of the socket with soft material with flexibility. He used polyethylene polymer when Teflon failed. He used PMMA as a bone cement, to fix the socket to the acetabulum; and the ball and the stem to the femoral bone [40].

In 1964, another British surgeon, Peter Ring (b.1922) worked on the cement-less fixation with a metal on metal hip joint prosthesis. He achieved some good result in the first several surgeries with up to 97% success within 17 years of follow up [21]. Although his fixation method abandoned in 1970 due to the some advantages of Charnley's model (Figure 2.16), pursued by British and Swiss surgeon in 1980s. Nowadays various kinds of materials including metal on metal bearing are under investigation.

Figure 2.16. Evolution of Charnley prostheses, which is from the flat black stem to the C shape stem [21]

In the 1970's, first Ceramic on Ceramic hip prosthesis was implanted in the body of the vice president of ceramic company by French surgeon Pierre Boutin. Boutin started to work with him to develop the ceramic prosthesis. In 1974 the first generation of ceramic prosthesis, Al_2O_3, produced, which had large grain size causing low mechanical strength and failed. In 1992, the second generation of ceramic was produced with finer grain size and lower level of impurity. In 1995 using Hot Isostatic Pressing (HIP) technique, the grain size reduced further thus the mechanical properties in terms of durability, wear rate and resistance to fracture were improved in the third generation of ceramic (Biolox Forte). In 2000, the fourth generation of ceramic (Biolox Delta) was produced with composite of the 82% Alumina, 17% Zirconia, 0.3% Chromium oxide and 0.6% Strontium Oxide that reduced the wear rate by absorbing the crack energy

which will be explained further in this chapter. The properties of the ceramic prosthesis from first generation to fourth one, has been written in Figure 2.17.

Property	1st Gen	2nd Gen	3rd Gen Biolox Forte	4th Gen Biolox Delta
Density (g/cm^3)	3.94	3.96	3.98	>4.36
Grain size (µm)	<4.5	<3.2	<1.8	<1.5
4-Point bend strength (MPa)	400	500	580	1000
Fracture toughness ($MN/m^{3/2}$)	2.78	2.78	2.78	5.7
Young's modulus (GPa)			380	350

Figure 2.17. The properties of first, second, Third and Fourth generation of Ceramics [42]

2.5.2. Biotribology

Previously, scientists thought a patient walk about one million cycles a year therefore fifteen million cycles represented the 15 years activity. However nowadays, they believe younger patient and more active patients can walk up to 5 million cycles a year [43, 44]. Therefore they need better hip prosthesis to long last about 80 years, which arise 400 million cycles. This service is not only necessarily for daily activities but also should sustain sport activities, which impose excessive stresses on the joint.

The major risk factor for long-term prosthesis survival is wear and debris [45]. Mechanical Tribology studies wear, friction and lubrication between two surfaces. These are critical in designing and optimizing new prostheses. In this regard pre-clinical tests such as tribological simulation are required. Tribology of the hip joint prosthesis should consider both engineering and biological reaction of the debris computationally and experimentally.

Experimental studies mostly focus on measurement of wear volume, linear penetration, characteristic of produced debris; which is time consuming and costly. Computational studies can be an alternative. Moreover with integrating with experimental studies, the long-term effects can be predictable.

Tribology in life science known as biotribology [46] Lubrication of blood cells in capillaries; wear of artificial heart valves, screws and plates in bone and denture; friction of skin and comfort of clothes, shoes and socks; synovial fluid and different prosthesis are some example of biotribology studies.

Tribology of all bearing is related to the contact surfaces. All surfaces have specific roughness but measuring is not quite straightforward, in this regard Profilometry or Interferometry is used respectively for contacting or non-contacting method. Although average surface roughness, R_a, is the most common parameters, its

limitations e.g., two surfaces with different peaks and valley could have the same R_a, should be recognised. Therefore, other parameters are introduced to describe the roughness of hip prosthesis [47, 48]. Furthermore the roughness of the material can be changed after implantation in the body owing to wear. For example changing polyethylene roughness is reported [49] and self-polishing of metal on metal bearing reduces the asperity of the surface and helps lubrication [50]. Nevertheless R_a is the first approximation to indicate the roughness of the surfaces and the quality of finishing. Table 2.1 compares R_a of typical engineering and orthopaedic surfaces [51].

Table 2.1 R_a of typical engineering components and orthopaedic ones [51]

Components	R_a **(µm)**
Plain bearings in turbines	0.12–1.2
Rolling bearing in gear boxes	0.05-1.2
Gears in engines	0.25–1
Articular cartilage	1–6
Metal (Such as cobalt chromium)	0.005-0.025
Ceramics (such as alumina)	0.005–0.01
Plastic (such as Polyethylene)	0.1-2.5

Combined roughness of two bearing composite surface of the hip prosthesis defined by following equation [60]:

$$R_a = \sqrt{(R_a\ Head)^2 + (R_a\ Cup)^2} \tag{2.1}$$

Composite roughness values of the hip prosthesis materials are shown in Table 2.2.

Table 2.2 Composite roughness values of different hip prosthesis [60]

Bearing Couples	**Femoral**	**Acetabular**	**Composite R_a (µm)**
Metal on plastic	Cobalt Chromium	UHMWPE[8]	0.1-2.5
Metal on Metal	Cobalt Chromium	Cobalt chromium	0.0071-0.035
Ceramic on Ceramic	Alumina	Alumina	0.0071-0.014

2.5.2.1. Contact Mechanics

When two bodies contact each other, under load, a contact area is developed. Contact area and contact stress are important to solve the contact problems. This is an important factor to design the hip prosthesis, because the contact stress should not exceed the strength of contact area to prevent rapid fatigue failure. Polyethylene has

[8] Ultra High Molecular Weight Polyethylene

been tested; an increase in a thickness and conformity leads to a decrease in the stress [52]. This was an important criterion in designing the rim sleeve with polyethylene however failing of UHMWPE due to the oxidation and reduction of fatigue strength rather than contact stress. In this regard recent studies show the less contact and conformity in polyethylene can result in a reduction of the wear rate if the polyethylene has enough strength and stress is not excessive [53]. Contact stress in MOM and COC is more important in terms of preventing the EL phenomenon [54].

Finite Element (FEM) is the most common method to solve the contact mechanic problems in hip prosthesis. This is owing to complexity of available and proposal geometries and the material in used. However, the first approximation in analytical solution can be based on Hertz contact Theory [55], which will be explained in 4.3.

Theoretically, nominal contact area is considered which is smooth surface of the bearing. While real contact area includes roughness and asperity of the contact area that should be measured with sensor or pressure sensitive film [60].

2.5.2.2. Friction

Friction is defined as a resistance to motion, which can be rolling or sliding. The friction majorly is due to the reaction of the asperities, adhesion or deformation. Adhesion is only detectable in dry surfaces with no oxide or other films in between, which is not applicable to the hip prosthesis. Deformation depends on the material and the surface geometry while asperities can be deformed elastically or plastically.

Friction follows three main laws:

1. Force of friction, F', and applied load, W, are directly proportional.
2. F' is independent of apparent contact area.
3. F' kinetic is independent of sliding speed.

Coefficient of friction μ is defined in Equation (2.2). Lubricant fluid, surface roughness and materials in contact play important roles in changing the value of coefficient of friction in the hip prosthesis. For example for experimental simulation of hip prosthesis, bovine serum is used while the protein and lipids in bovine serum can significantly change the coefficient of friction.

$$\mu = \frac{F\prime}{W} \tag{2.2}$$

The coefficient of friction, μ, of steel and polyethylene combinations are shown in Table 2.3. However coefficient of friction of the ball and the socket in the hip prosthesis is modified with frictional torque, T, and the radius of the ball, R_{head}. Therefore friction factor, ƒ, computed by the following equation and the average friction factor of some combination materials are used for hip prosthesis reported in Table 2.4.

$$f = \frac{T}{WR_{head}} \tag{2.3}$$

The above equation states that, with increasing the radius of the ball, friction torque increases as well. In this regard the stress at the fixation interface can be increased which stables the fixation. For example the metal ball with diameter of 50mm and a friction factor of 0.12 under 2500 N load can provide 7.5Nm frictional torque which is a large number [60].

Table 2.3 Coefficients of friction for dry Steel and Polyethylene in the presence of air [51]

Material combination	**Coefficient of friction**
Steel on steel	0.6–0.8
Polyethylene on steel	0.3
Polyethylene on polyethylene	0.2–0.4

Table 2.4 Average friction factors for some materials are used in the hip prosthesis in the presence of bovine serum [60]

Bearing Couples	**Average friction factor**
Metal on UHMWPE	0.06
Ceramic on UHMWPE	0.06
Metal on metal	0.12
Ceramic on ceramic	0.04
Ceramic on metal	0.05

2.5.2.3. Wear

Any material loose due to the motion can be defined as a wear. There are five different types of wear explained below:

- Abrasive: Hard particles displacing the materials.
- Adhesive: Transferring of material from one surface to another surface.

- Erosive: solid particles in fluid removing the material from the solid surface. It can be impingement erosion or abrasive erosion as well. Presence of solid particles in the fluid is not compulsory such as rain erosion and cavitation.
- Fatigue: Due to the cyclic stresses, some part of the material is removed.
- Corrosive: Reaction of the chemical or electrochemical with the material such as oxidative wear.

Wear in hip prosthesis depends on the material of the components, for example in MOP prosthesis; two types of wear happen: fatigue (Pitting and delamination) and abrasive (Scratching and burnishing) wears. Wear in MOM prosthesis usually is scratching and polishing which are specific forms of abrasive wear however corrosive wear is also reported as well [56].

Wear volume, V', is proportionally related to the load, W, and sliding distance, X' which is shown in following equation; k ($^{\mathrm{mm}^3}/_{(\mathrm{Nm})}$) is wear factor [60].

$$V' = kWX' \tag{2.4}$$

Three important laws of the wear are:

1. Wear volume, V', is increasing with increasing of the load, W.
2. Wear volume, V', increasing when sliding distance, X', increases.
3. Wear volume, V', decreasing with increasing the hardness, H, of the material.

Although comparing the wear factor of material combination is very common, lubrication, multi directional motion and pressure can change this factor significantly [57]. Equation (2.4) is based on metallic bearing and derived from Archard wear law. Therefore this equation is not applicable for polyethylene in the hip prosthesis. If the elastic modulus of polyethylene is low (such as UHMPWE), the real contact area can be similar to the nominal one (A) under the load. Therefore C is a dimensionless wear coefficient and following equation will be more suitable for measuring the polyethylene wear volume [58].

$$V' = CAX' \tag{2.5}$$

Quantifying the wear and investigating the wear mechanism in hip prostheses can involve several types of laboratory equipment, methods and measuring systems. Simple screening devices and joint simulators are the two major ones. In simple

screening devices such as pin on plate, constant load and motion apply to the object while it is rotating [60].

2.5.2.4. Lubrication

Friction and wear dispute energy with heat and elastically and plastically deform asperities, however lubricant can reduce wear and friction between two surfaces and assist the motion. In biotribology, tears and synovial fluid are two lubricants that facilitate the motion of the eyelid and articular joints, respectively. Lubricant can be fluid or solid that is placed between contact surfaces to either separate asperities from each other or reduce the interaction. Lubrication depends on the thickness of the lubricant ($h_{\min}$) and the roughness of the combined surfaces (R_{a-head} and R_{a-Cup} in the hip prosthesis). λ is the ratio of these two factors which is computed by [60]

$$\lambda = \frac{h_{min}}{R_a} = \frac{h_{min}}{[(R_{a-head})^2+(R_{a-cup})^2]^{1/2}} \tag{2.6}$$

A Stribeck diagram (Figure 2.18) shows the relationship between λ and coefficient of friction as following:

- Full film lubrication ($\lambda > 3$): where contact surfaces are absolutely separated from each other then the applied load is equilibrated with lubricant pressure.
- Mixed lubrication ($1 < \lambda < 3$): where some asperities are contacted with each other hence the applied load is equilibrated partially with fluid pressure and partially with contact of the asperities.
- Boundary lubrication ($\lambda < 1$): where lubricant thickness is in the molecule scale and the applied load is equilibrated fully with the asperities that adsorbed lubricant molecules.

Friction factors are measured as a function of load (W), velocity (u) and lubricant viscosity (η) and then its variation compared with bearing characteristic number or Sommerfeld number (S) where:

$$S \propto \frac{\eta u}{W} \tag{2.7}$$

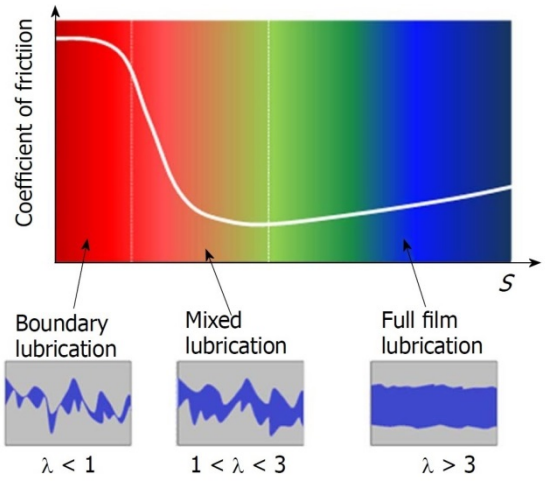

Figure 2.18. Stribeck diagram and different lubrication categories [63]

The lubrication regimes and the friction factor for the hip prosthesis are presented in Table 2.5.

Table 2.5 lubrication regimes and the friction factor for the hip prosthesis [60]

Lubrication regimes	**Friction factor**
Boundary lubrication	0.1–0.7
Mixed lubrication	0.01–0.1
Fluid-film lubrication	0.001–0.01

It is significantly important to measure the surface roughness (R_a) accurately and predict the lubricant film thickness (h_{min}), for assessment of the lubrication regimes. The first attempt for estimating the lubricant film thickness in the hip prosthesis was developed by Jin ZM et al [59] as following:

$$\frac{h_{min}}{R} = 2.8\left(\frac{\eta u}{E' R}\right)^{0.65}\left(\frac{w}{E' R^2}\right)^{-0.21} \tag{2.8}$$

Equivalent radius (R) considering the ball diameter (d) and prosthesis diameter clearance (c_d) is calculated as following

$$R = \frac{d(d+c_d)}{2c_d} = \frac{d}{2}\left(1 + \frac{d}{2c_d}\right) \tag{2.9}$$

Velocity (u) can be calculated from angular velocity (ω) as well with following formulation:

$$u = \frac{\omega d}{4} \tag{2.10}$$

Equivalent elastic modulus (E') is computed with Equation (2.11) where E and v are elastic modulus and Poisson's ratio respectively.

$$E' = \frac{1}{\left[\frac{1-v_{head}^2}{E_{head}} + \frac{1-v_{cup}^2}{E_{cup}}\right]} \tag{2.11}$$

Complex three-dimensional models need numerical method in addition to determining the lubrication thickness.

2.5.3. Biotribology in Hip Prosthesis

Although section 2.5.2 studied friction, wear and lubrication individually, participating of these in the hip prosthesis is essential [60]. Diameters (d) of the prosthesis and clearance diameters (c_d) in different kinds of the available hip prostheses are mentioned in Table 2.6.

Table 2.6 Geometries of the hip prosthesis [63]

Prosthesis	***d* (mm)**	**c_d (μm)**
MOP	22.2-44	160-400
COP	22.2-36	160-400
MOM	22.2-54	50-150
MOM_{RS}	42-62	50-300
COC	22.2-48	20-100

2.5.3.1. Materials

Contact bearing surfaces in hip prostheses are mainly made of plastics, ceramics and metals. The main mechanical properties of these materials are summarized in Table 2.7.

Table 2.7 Materials properties of the Hip Prosthesis [63]

Material	***E* (GPa)**	***v***	**R_a (μm)**
P (UHMWPE)	0.5-1	0.4	0.1-2
M (CoCrMo)	230	0.3	0.01-0.05
C (Biolox delta)	350	0.26	0.001-0.005

2.5.3.1.1. Plastic

As mentioned earlier, Sir John Charnley used plastic in 1958 for the first time in the socket due to its flexibility. Since 1958, the mechanical properties of the traditional polyethylene have been improved to the Ultra High Molecular Weight Polyethylene (UHMWPE) and then with gamma or electron beam radiation to the highly cross linked[9] UHMWPE (HCLUHMWPE) one [61, 62]. Although irradiation improves wear rate of the polyethylene, it generates some free radicals when the oxidation of them cause mechanical defect in the material [62]. In this regard the radiation dose was kept below 10 MRad[10] and further treatments had been applied. In the first generation of HCLUHMWPE (1998) one of the following techniques was chosen as a further treatment:

- Melting: this eliminates free radicals in HCLUHMWPE,
- Annealing: this maintains mechanical properties of HCLUHMWPE.

Both of the aforementioned techniques have their own advantages. In order to gain all advantages, one of the following two techniques is applied for manufacturing process of the second generation of HCLUHMWPE which was introduced in 2005 [61].

- Repetition of annealing and irradiation cycles
- Annealing in presence of vitamin E, which acts as an antioxidant

Clinical follow up of the first and the second generation of HCLUHMWPE has shown 80% reduction of the wear compared with UHMWPE [64, 65].

2.5.3.1.2. Metal

The metals are used for hip prosthesis are mainly: Cobalt Chromium Molybdenum (CoCrMo), Cobalt Chromium (CoCr) and stainless steel. However, CoCrMo is widely used. This material is obtained from either wrought or cast materials. The manufacturing process has no effect on the mechanical properties of the alloy [67, 68]; however the carbon content plays an important role in the wear resistance of the alloy. More than 0.15% carbon content reduces the wear rate 64% to 94% compared to the carbon content of less than 0.08% [66].

2.5.3.1.3. Ceramic

As it was mentioned earlier, the first generation of ceramic was implanted as a hip prosthesis in the human body in 1974. Since then the mechanical properties of this

[9] When the standard polyethylene exposure to radiation, its structure changed (The molecular bond become very tight) this changing the structured is named as a crosslinking when it is more resists to the wear.

[10] It is absorbed radiation dose while 1 RAD = 0.01Gy = 0.01 Joule/ Kilogram

material were improved with refining the grains size when in 1992, the second generation and in 1995 the third generation (Biolox Forte) were made. The fourth generation of this material was introduced to the market in 2007, which is called Biolox Delta. Biolox Delta is the gold standard ceramic that is made of the mixture of oxide ceramics and shows an excellent mechanical behaviour. It owes its behaviour to the combination of the excellent tribological behaviour of Alumina and mechanical properties of the Yttrium stabilized Zirconia [69]. Biolox Delta is made of 82% Alumina, 17% Zirconia, 0.3% Chromium oxide, 0.6% Strontium Oxide and other materials. Toughness and strength of the Alumina matrix are increased by Yttrium stabilized Zirconia when its Nano-particles are obstructing crack propagation. Furthermore Strontium Oxide deflects the crack by its platelet crystal. However the hardness of the prosthesis must be improved to enhance the wear properties. This is done by chromium oxide. The only disadvantage of this material is its cost. Figure 2.19 compares the average prices of different hip prosthesis.

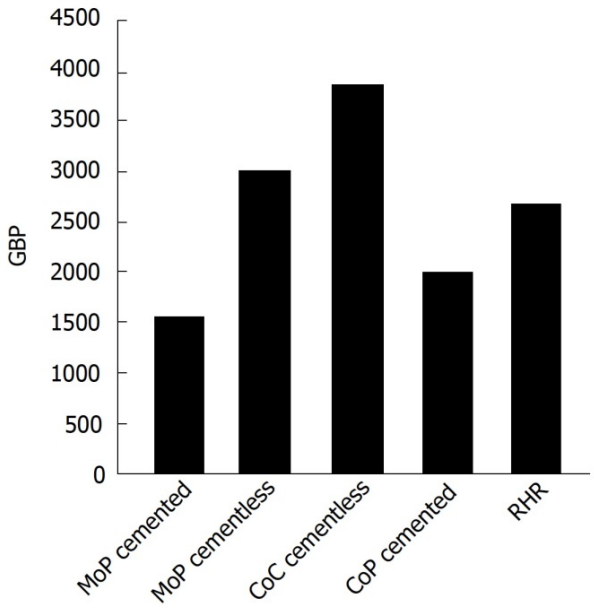

Figure 2.19. Average hip prosthesis prices [63]

2.5.3.2. Friction in Hip Prosthesis

As it was mentioned earlier, the coefficient of friction, μ, adjusts with system conditions. In hip prosthesis, geometry, lubricant fluid types, surface roughness, materials properties and loading conditions are important factors in changing the value of μ. Some experimental studies [70-71] on the hip prosthesis show that increasing the ball size decreases μ. However increasing the load increases μ. Table 2.8 compares μ of

different bearing couples in the same conditions (flexion-extension motion ±25° with 1 Hz frequency, Sinusoidal loading on the 60% of the gait cycle, with 100 N load during a constant swing phase and a peak of 2 kN, the size of the heads are 28mm except MOM_{RS} which is 55mm). They are tested with 2 lubricant types, 25% and 100% bovine serum, [70, 72]. As they are shown in this table MOM has the highest μ with average value in the range of 0.096-0.12 and COC has the lowest μ; with 0.04-0.056. Likewise, the type of the lubricant effects μ. Table 2.8 clearly shows that the values of μ in all couples are increased when they are interfaced with the lubricant with higher protein (i.e. 100% bovine serum). But this rule is not applicable when metal surfaces are contacting with each other. Metal bearing couples can get the advantage of a protein protective layer over their surfaces. In this regard for measuring μ of the hip prosthesis in vitro, the lubricant with similar rheological behaviour of the synovial fluid should be used. In the most of the hip simulators, 25% bovine serum is used more widely than 100% one [63].

Table 2.8 Coefficient of Friction (μ) of different prosthesis in 25% and 100% Bovine serum [63]

Prosthesis	**μ (in presence of 25% Bovine Serum)**	**μ (in presence of 100% Bovine Serum)**
MOP	0.062 (+ 0.008)	0.064 (± 0.01)
COP	0.056 (+ 0.01)	0.06 (± 0.012)
MOM	0.12 (± 0.02)	0.096 (± 0.012)
MOM_{RS}	0.098 (± 0.02)	0.079 (± 0.011)
COC	0.04 (+ 0.007)	0.056 (± 0.01)

2.5.3.3. Wear in Hip Prosthesis

Wear is the most critical object in biotribological aspect and it is the main reason for the hip prosthesis failure. Although experimental study of friction and lubrication is possible just in *vitro*, experimental study of the wear is possible in *vivo* as well as *vitro*. *Vivo* study is achievable by MRI[11] or testing the failed prostheses, which are discovered from hip revision surgeries.

Although the material of the prosthesis is the main effective factor in the wear rate, patient's anatomy, physiology, pathology, gender, daily activity, age, weight etc. can affect the wear rate as well. In this regard, wear rates of the prosthesis are scattered. Table 2.9 shows typical linear (L) and volumetric (V) values of the prostheses wear rate.

[11] Magnetic Resonance Imaging

Table 2.9 Linear (L) and volumetric (V) wear rate. [63]

Prosthesis	***L* (µm/Million cycles)**	***V* (mm^3/Million cycles)**
MOP	50-500 (50)	10-500 (80)
COP	30-150	15-50
MOM (New)	1-50	0.1-25
MOM (steady)	0.1-1	0.05-4
MOM_{RS} (New + Steady)	0.2-10	0.2-2.9
MOM_{RS} (Tissue reaction)	1.5-46	0.2-95
COC	0.01-1	0.005-2

Produced debris from the worn materials might have unfortunate affects in the human body which are explained in following:

2.5.3.3.1. Wear of MOP and COP

MOP and COP prosthesis have the highest wear rates due to the existing of the polyethylene as a soft bearing material. The average L and V of MOP are 50 µm/ year and 80 mm^3/year respectively. By replacing the metal ball with ceramic one, polyethylene finds the chance of interaction with smoother, harder material with lower R_a which guarantees the lower wear rate of the polyethylene in a year and reaches average L and V of COP to 30 µm/ year and 50 mm^3/ year respectively. However such a high amount of polyethylene debris in the human body motivates the enzyme that resolves the bone (osteolysis) as well as the polyethylene particles. As a result the prosthesis loosening is feasible.

2.5.3.3.2. Wear of MOM and MOM_{RS}

Eliminating the polyethylene liner increases the size of the ball to the size as big as the natural femoral head. This is increasing the range of the motion and stability with the lower risk of dislocation in long-term use of the prosthesis. Furthermore, hard bearing surfaces and protein boundary layer protectors reduce the wear rate efficiently. MOM has biphasic wear behaviour; Phase 1 starts from a day when the new prosthesis is placed in the patient's body. In this phase wear rate is relatively high with L and V of 1-50µm/year and 0.1-25mm^3/year respectively. After about 1 million cycles, phase 2 starts when the prosthesis reaches to the steady state L and V of MOM are 0.1-1µm/year and 0.05-4 mm^3/year respectively. MOM_{RS} shows slightly more wear rate due to the bigger size and fluid lubrication regime with L and V of 0.2-10 µm/year and 0.2-2.9mm^3/year respectively. Movement of the metal on metal produces metallic ions, which is harmful for the human body. Cobalt ions diffusing from prosthesis can be eliminated through urine [35] but evacuation of Chromium is very slow and passes through storage of the tissues [24] that causes of body reaction. If the concentration of

metal debris is low to moderate (i.e. phase 2), Cytokines are stimulated to release, which lead to osteolysis and respectively loosening of the prosthesis. Higher concentration of metallic debris, which can be generated by EL phenomena, is Cytotoxic. This volume of ions alters the phagocytic activity of the macrophages and will be the cause of cell death. ALVAL[12] is the name of disease which is due to the plenty of chromium and cobalt ions accumulate about the joints so it causes severe pain, inflammation near the hip, pressure on the nerves and rash. It is shown in Figure 2.20. Furthermore, if the dead cells of the inflammatory tissue are combined with the protein around the hip joint, it might cause *pseudo-tumours,* which are diagnosed by MRI, Ultrasound or CT[13] scan.

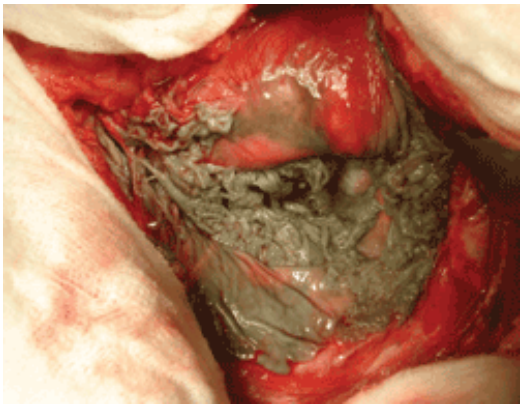

Figure 2.20. ALVAL: Due to the chromium and cobalt ions accumulation about the joint [12]

2.5.3.3.3. Wear of COC

COC is the most wear resistance prosthesis, which is getting the benefit of the hardest surface has been ever implanted in the human body. COC has L and V of 0.01-1 μm/year and 0.005-2 mm^3/year respectively. Furthermore ceramic has hydrophilic ionic surface, which attracts the polar water based fluids. This means the water based fluids are spreading over the ceramic surface and make low contact angle with ceramic rather than high angle contact which they make with polyethylene surface. This helps lubricant regime to be more effective to minimize the wear rate of the COC prosthesis. Moreover ceramic is extremely biocompatible and inert in Macro, Micro and Nano scales because of its high level of oxidation. It is classified as a bioactive material, which biologically bonds to bone (Osteoconductive property) without arising a biological reaction. The

[12] Aseptic lymphocyte-dominated Vasculitis-associated lesion
[13] Computed Tomography

only disadvantage of the ceramic is its cost while its brittleness is highly improved with the fourth generation of this material [63].

2.5.3.4. Lubrication in Hip Prosthesis

Lubrication is a complex phenomenon and depends on mechanical, chemical and tribological conditions of the hip prosthesis. In this regard, its performance cannot be generalized with specific hip replacement assessment. Nevertheless the reference test for hip is gait cycle.

Friction and wear are mainly studied experimentally while lubrication studied theoretically [73]. Hence just a few experimental tests have been done in this regard [74-75]. All studies, experimental and theoretical, aim to investigate h_{min} to compare R_a and λ.

The hip prostheses presented in Table 2.6 are made of the materials which are reported in Table 2.7 (E= 1GPa for plastic) and according to Equation (2.6), h_{min} , R_a and λ are summarized in Table 2.10. This table demonstrates that the plastic liners in MOP and COP have the boundary to mixed lubrication regime with the $\lambda \leq 1$. This is mainly due to the high value of R_a in comparison with h_{min}. Lubrication in MOM is slightly improved with $0.6 < \lambda < 2.9$. Although R_a is much lower in metal than the plastic one, h_{min} is also thinner due to the less elasticity of this material. Although lubrication regime of the MOM is mixed but the experimental test [76] shows that it can span the lubrication regime from boundary to fluid film. Theoretical and experimental studies show that λ of MOM highly sensitive to the prosthesis geometry [74, 75-77] bearing manufacturing [77] and the load condition [78,79]. More precisely; increasing the prosthesis size with decreasing the surface clearance improves the lubrication regime in MOM and $MOM_{(RS)}$ and enables the prosthesis operate in fluid film regime. COC has the best lubrication behaviour in all the prosthesis; this is mainly due to the surface finishing of the ceramic which has very low R_a that balances with the h_{min} and enables the prosthesis to operate in fluid film regime with $5.3 < \lambda < 28.3$. Radial clearance is highly important particularly in the prosthesis with hard bearing material. Large value of "C_d" leads the prosthesis to the boundary regime and the low value causes EL which disrupts the lubrication regime.

Table 2.10 Lubrication regimes measured according to Equation 2.9 [63].

Prosthesis	$\mathbf{h_{min}}$ **(μm)**	$\boldsymbol{R_a}$ **(μm)**	$\boldsymbol{\lambda}$	**Lubrication regime**
MOP	0.065-0.144 (0.105)	0.1-2	0.1-1	Boundary to Mixed
COP	0.076-0.107 (0.092)	0.1-2	0.05-0.9	Boundary to Mixed
MOM	0.020-0.061 (0.041)	0.014-0.071	0.6-2.9	Boundary to Mixed
MOM_{RS}	0.082-0.049 (0.066)	0.014-0.071	0.9-4.6	Boundary to Fluid-film
COC	0.035-0.045 (0.04)	0.0014-0.0071	5.7-28.3	Fluid-film

Figure 2.21 presents a further clarification on the effects of the sizes and the materials on the lubrication regime in the hard couple prostheses [63]. Increasing the radial clearance, C_d, decreases h_{min} and λ (Figure 2.21 A and C), however when diameter of the ball, d, is increased, h_{min} and λ are increased as well (Figure 2.21 B and D). In this regard, lower values of C_d and higher d promise more conformal couple that makes thicker lubrication film. Figure 2.21A and 2.21B respectively show if hard bearing couples have equal C_d and d, COC has the lowest h_{min} because the metal is more elastic than ceramic. However due to the smoother surface of the ceramic, COC is the only prosthesis that undergo fluid film lubrication regime almost independently from the size (Figure 2.21C and 2.21D). Figure 2.21 confirms the results of Table 2.9.

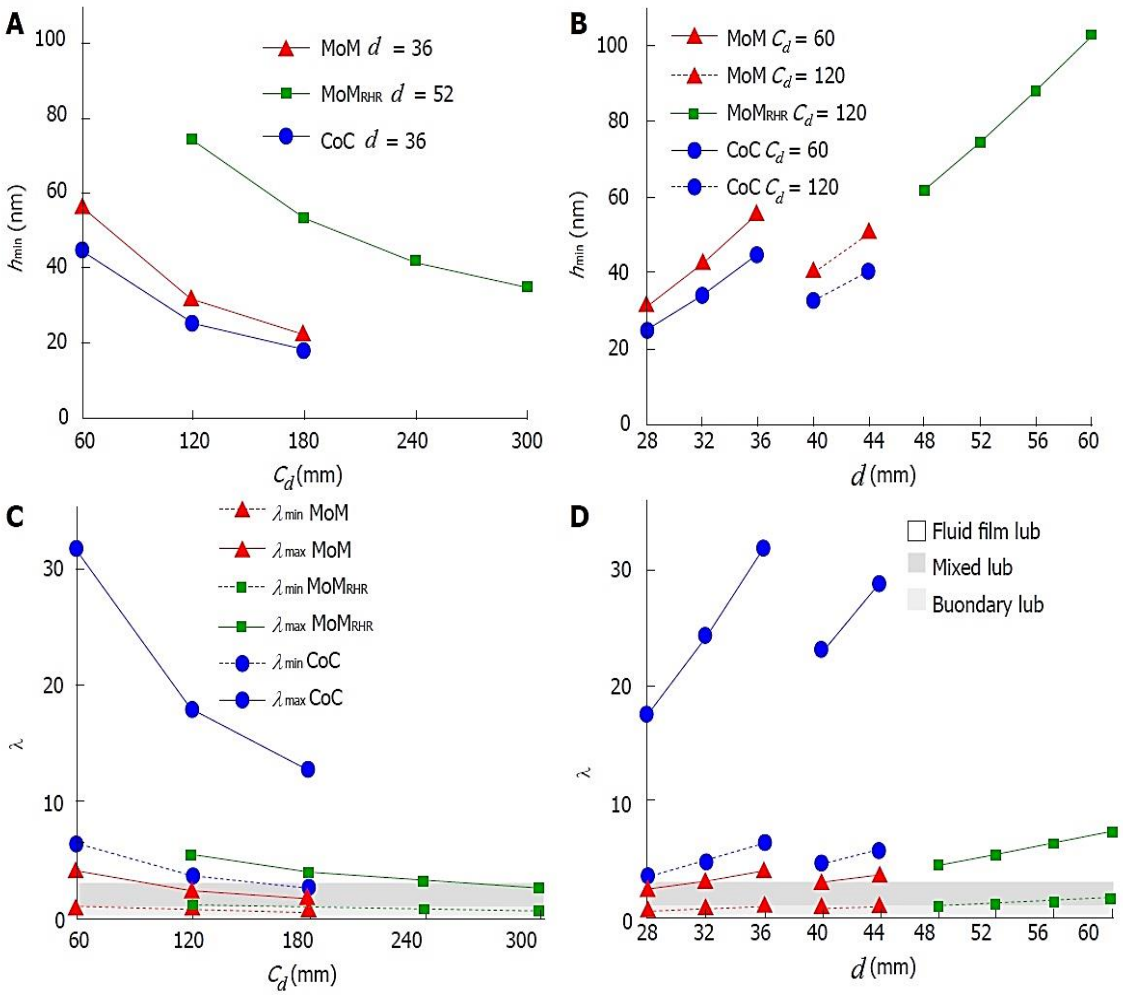

Figure 2.21. Effect of C_d and **d** of hip implants on the lubrication $\mathbf{h_{min}}$ and **λ** [63]

2.5.4. Statistical Analysis

National Joint Registry of the UK collects statistical clinical procedures data of the hip prosthesis from 2003 to 2012 [19,63]. Procedures of the prosthesis per year are illustrated in Figure 2.22 and Figure 2.23. MOP as a traditional prosthesis are still used significantly more than other prostheses, with covering of 60% to 70% of all THR surgeries. Improving the polyethylene material to HCLUHMWPE was an effective reason in this regard. Improving the ceramic material to the Biolox delta was also an effective reason to propagate the use of the COP and COC cover respectively 16% and 22% of THR surgeries in 2012. Although the usage of the metallic couples (MOM and MOM_{RS}) is increased since 2003 to 2008 (peak), from then it has been decreased significantly. The reason of this incident was the harmful effects of metallic ions in the human body, which was explained in section 2.5.3.3.2. Based on the same reason, Depuy recalled their MOM and MOM_{RS} prostheses in 2010.

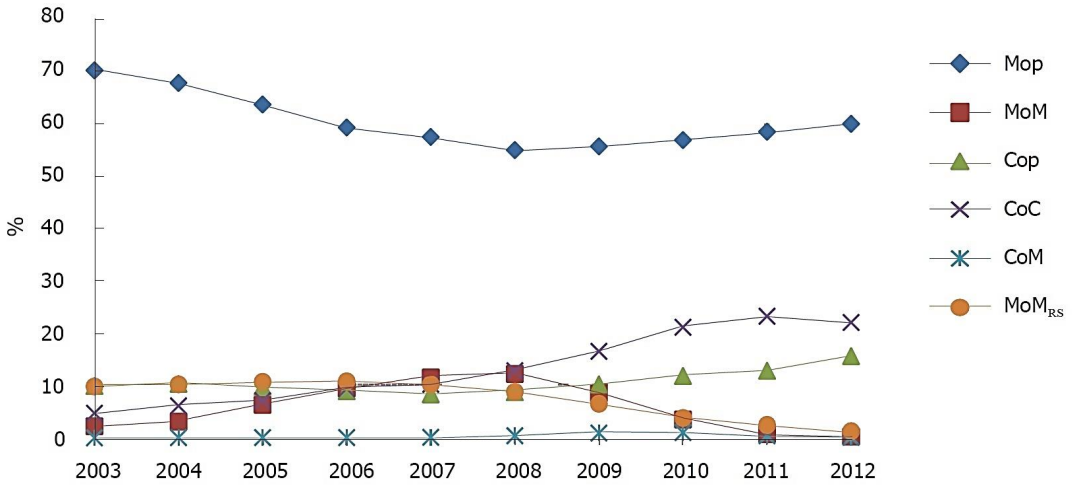

Figure 2.22. Statistical data in THR from 2003 to 2012 [63]

As it was explained earlier, larger size of the head reduces μ and increases h_{min} and λ, which makes a more conformal couple that promotes the lubrication. Furthermore, increasing the size of the head increases the range of motion and reduces the risk of dislocation and more similar to the natural femoral head size. All of which are in agreement with experimental and theoretical studies. In this regard, gradual increasing the size of the prosthesis up to the anatomical size of the femur and acetabulum is rational. Figure 2.22 also proves this claim. Since 2003, prosthesis with 22.25 mm and 26 mm are almost disappeared from the market in 2012 and usage of the 26 mm ones decreased in favour of the ones with larger balls (32 mm and 36 mm). Larger balls with diameter more than 38 mm, which are mostly metals, are decreased from 2008 (Peak) with the same reason is explained earlier.

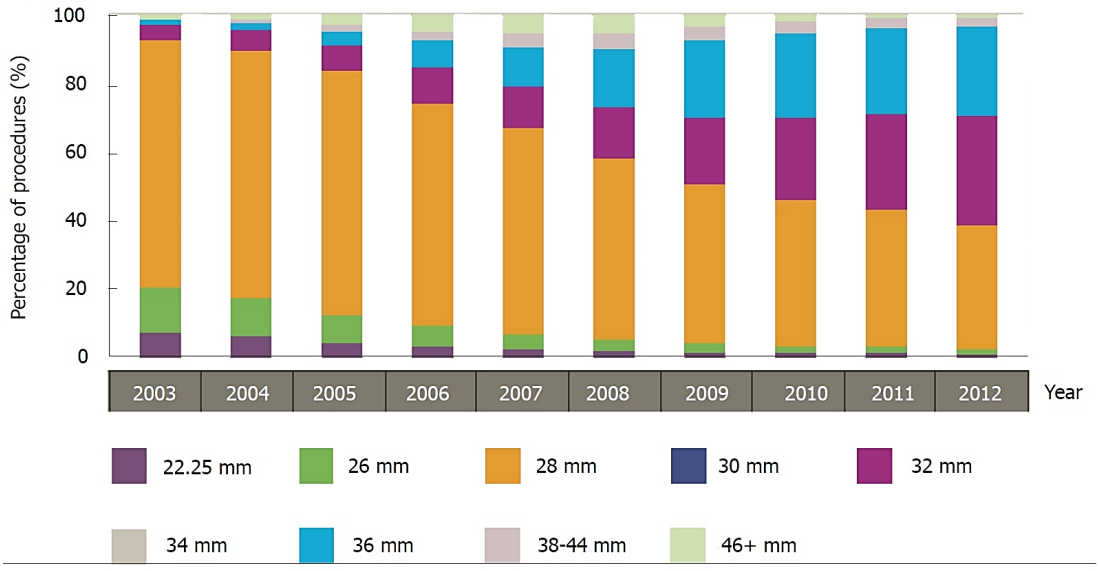

Figure 2.23. Usage of the hip prosthesis with different head sizes from 2003 to 2012 [63]

The risk of prosthesis failure according to the type of the couples and fitting methods are studied [19,63]. In this regard, the risk of revision surgeries for the hip prostheses, which are fitted with cemented and un-cemented methods during the first 9 years after primary surgery, is illustrated in Figure 2.24 and Figure 2.25 respectively. The highest risk of revision surgeries belongs to the metal couples with 17.7% and 12.3% for un-cemented MOM and MOM_{RS} respectively and 33% for cemented MOM_{RS} while the lowest rate of 2% belongs to COP, MOP and COC.

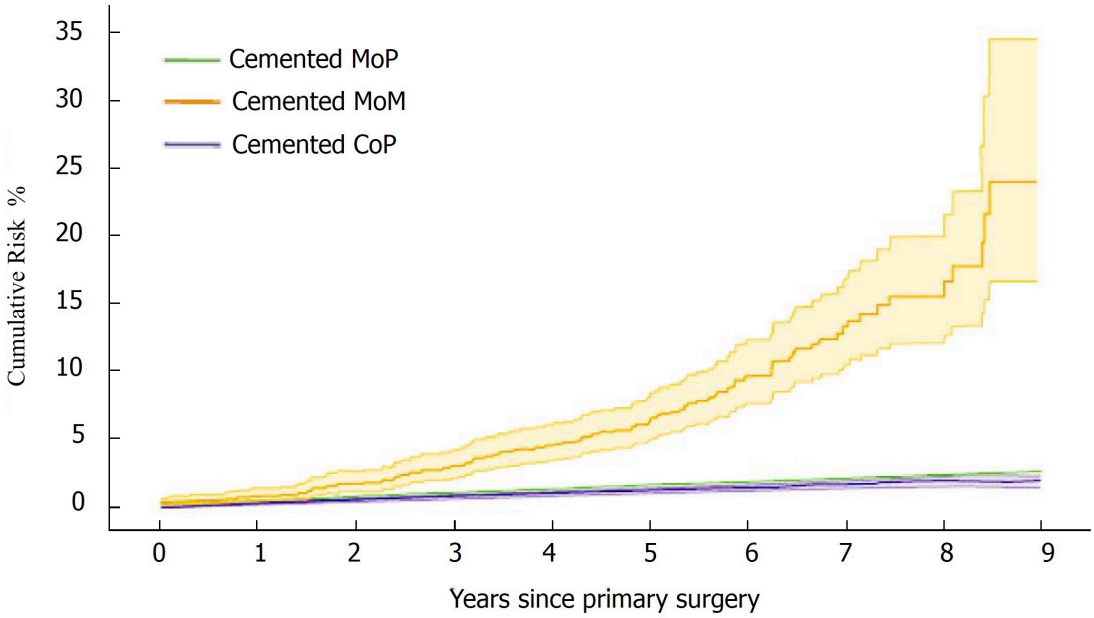

Figure 2.24. Risk of revision surgeries in the prosthesis, fixed with cemented method [63]

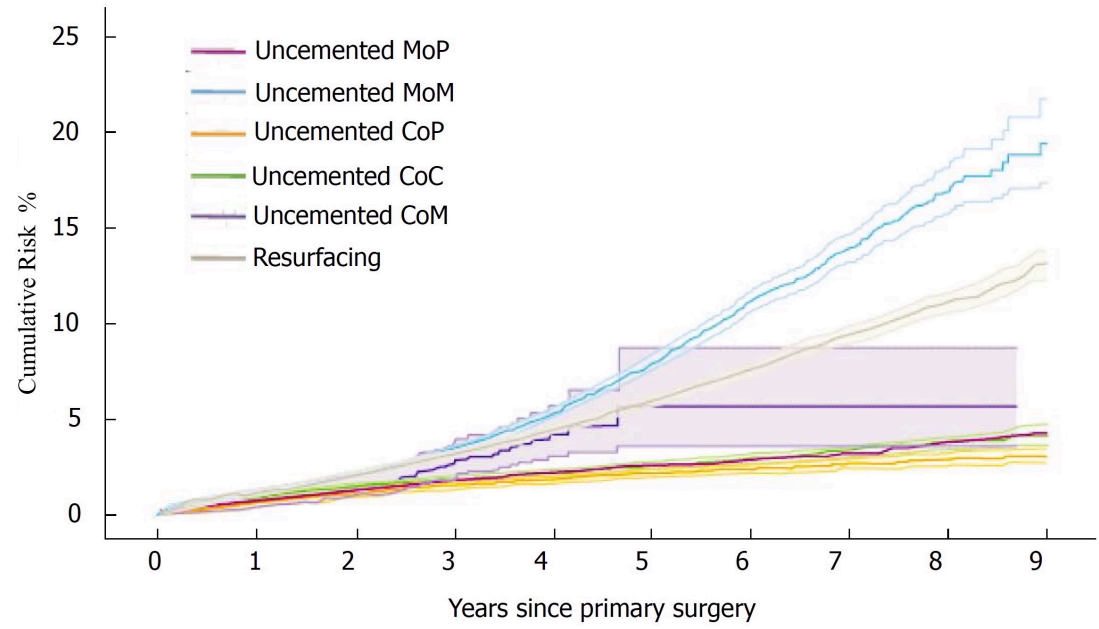

Figure 2.25. Risk of revision surgeries in the prosthesis, fixed with un-cemented method [63]

Chapter 3 : Edge Loading (EL)

The ball and the socket are in concentric contact when the ball moves on the spherical polished surface of the socket without reaching the edge of the socket [81]. Concentric wear forms a circular pattern, which is very low in the MOM [82] and negligible in the COC [83]. However EL happens when the ball does not contact with conformed spherical surface of the socket subsequently but loads the edge of the socket which is producing the excessive wear on the edge and the ball. EL is not following the circular wear pattern but it makes a long and narrow damaged area in COC prosthesis called stripe wear [84, 85]. Some authors believe that there is a close relationship between the squeaking of the COC prostheses and the stripe wear [86], which is discussed in 3.4. EL in the prosthesis with polyethylene liner makes higher wear on polyethylene, which is encountered with osteolysis and dislocation of the prosthesis [89-91] but it is unlikely that polyethylene can damage the metal or ceramic ball. EL in MOM causes some catastrophic problems such as pseudo-tumour and ALVAL [87, 88], which were explained earlier.

During the EL, ball may load the edge anterosuperiorly or posteriorly depending on the condition of the EL. They can be differentiated with studying of wear orientations on the ball [85]. They are distinguished by tilt angle which is an angle between the stripe wear and a latitude line going to the centre of the stripe wear. If superior part of the ball contacts anterosuperior part of the edge of the socket in the left hip, it produces the negative (anteverted) stripe wear on the ball. However in the case of the contact of posterior part of the edge with the ball, positive (retroverted) stripe wear is formed on the ball of the left hip prosthesis these are illustrated in Figure 3.1.

Esposito C.I et al. [92] tested 54 pairs of COC prosthesis after a mean of 3.5 years (0.2 – 10.6). He and his colleagues found 45 of the all prostheses (83%) had stripe wears while 7 of them are with anterosuperior EL, 32 of them with posterior EL and 6 of them with two kinds of stripe wears which are made by anterosuperior and posterior ELs. The median volumetric wear rate of all 54 prosthesis balls was 0.2 mm^3/year, while the balls with anterosuperior EL had 1.9 mm^3/year (0.2 – 7.2), the ones with posterior EL had 0.2 mm^3/year (0 – 3.0) and the ones with both negative and positive stripe wears had 1.5 mm^3/year. In this regard, anterosuperior EL causes higher wear rate than posterior EL while posterior EL happens more frequently than anterosuperior one.

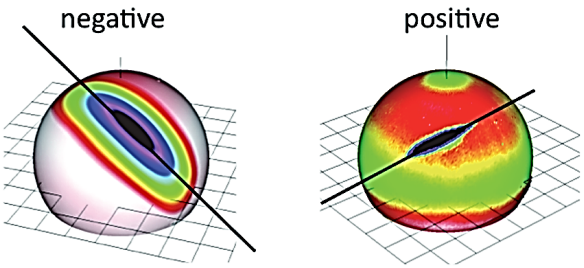

Side	Tilt angle	Edge loading
Right	Positive	Anterosuperior
Right	Negative	Posterior
Left	Negative	Anterosuperior
Left	Positive	Posterior

Figure 3.1. Tilt angle in the left and right hip prosthesis made by EL [85]

If the socket (liner) wear width of the stripe wear which is extended into the conformal surface, is more than 1 mm, then there will be a close relationship with the volume wear of the ball and the liner wear width, which is shown in Figure 3.2.

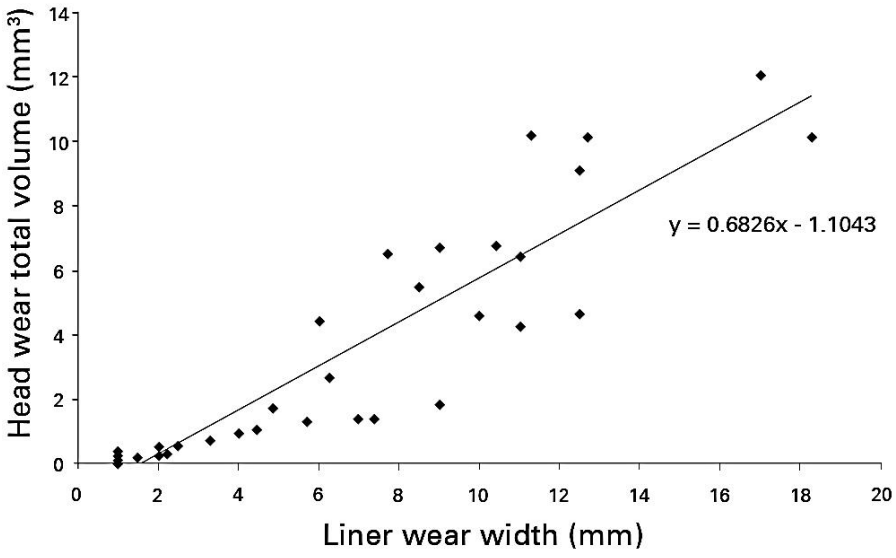

Figure 3.2. Wear relationship between the ball and the socket with EL condition [92]

Bearing surfaces of the socket comprise a concave spherical surface and the edge. However these two surfaces are machined in two separate discontinuous steps and it is difficult to merge these two surfaces to make a unit tangential smooth surface. In this regard it may present a small distinct artefact part called “crest” which has 9° to 11° deviation from edge of the sockets and is palpable by fingernail (Figure 3.3) [85]. The crest is postulated to be touched firstly during the EL.

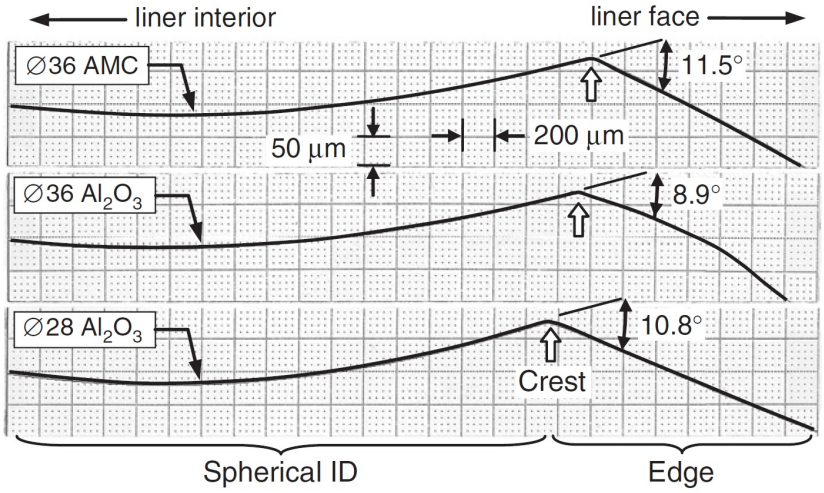

Figure 3.3. Concave spherical surface and the edge with presenting the crest [85]

Anthony P et al. [93] studied the wear volume and the size of destruction of the ball due to the contact with Crest and Edge in the prostheses which were made by Ceramtec, Germany (28mm Biolox Forte, 36mm Biolox Delta and 36mm Biolox Forte). In both cases 200N was applied to the edge and the crest of the sockets through the balls when they directly contact to the crest and smoother surface of the edge (1mm above the crest). The results showed that the wear rate due to the crest was 2 to 15 times higher than the wear rate due to the edge. Furthermore a scar made on the ball by crest was wider than the one made by an edge. Table 3.1 summarises this study and Figure 3.4A and 3.4B illustrate the worn surfaces by Crest and Edge, respectively.

Table 3.1 Wear scars on the balls due to the contact with Crest and Edge of the sockets [93]

	Volume (mm^3)		Height × Width (mm)	
Bearing	Smooth	Crest	Smooth	Crest
∅36 AMC	0.087×10^{-3}	1.362×10^{-3}	0.90 × 1.79	1.11 × 4.17
∅36 Al_2O_3	0.235×10^{-3}	0.527×10^{-3}	0.87 × 1.43	1.05 × 2.71
∅28 Al_2O_3	0.338×10^{-3}	5.080×10^{-3}	0.90 × 1.41	1.00 × 3.70

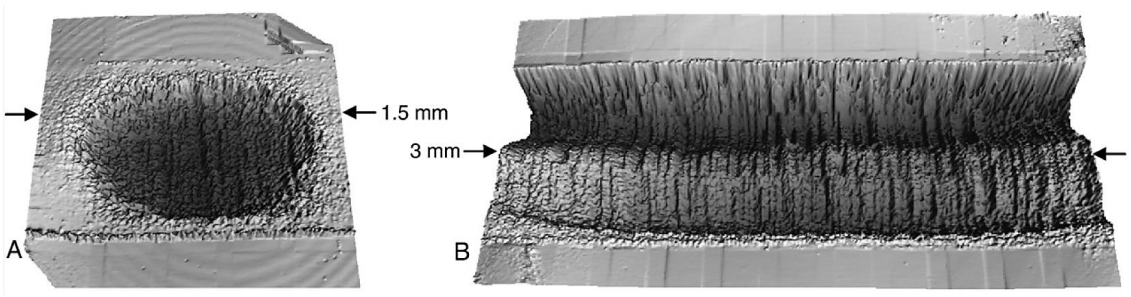

Figure 3.4. Morphology of the worn surfaces on the ball due to contact with Edge (A) and Crest (B) [93]

Another important factor in the coincidence of EL is the study of μ. Elhadi Sariali at al [94] tested 3 prostheses (32 mm Biolox forte made by Ceramtec, Germany) with Leeds Prosim simulator which can apply dynamic load similar to the *vivo* condition [95]. Sinusoidal forces with maximum amplitude of 500N, 1500N and 2500N were applied vertically and 50N during the swing phase. Prostheses are tested during EL and concentric condition. 2500N, 1500N and 500N loads in the concentric condition show $\mu \approx 0.02$, $\mu \approx 0.018$ and $\mu \approx 0.026$, respectively while during EL condition they are increased to $\mu \approx 0.12$, $\mu \approx 0.12$ and $\mu \approx 0.07$, respectively. Although EL increased μ up to 6 times, the magnitude is still low and similar to the magnitude of μ in MOM under concentric condition [70, 96].

Furthermore Elhadi Sariali at al [94] studied μ with the presence of three doses of third body particles (0.02, 0.04 and 0.08 grams of alumina powders with concentration of 0.001, 0.002 and 0.005 g/mL in the 25% bovine serum) and a large alumina particle was placed between ball and edge of the socket. Third body particles increase μ to 0.32 once alumina powders exist, and to 0.53 once alumina chips exist. Consequently, third body particles could increase the magnitude of μ, 15 to 26 times, but doses of the particles did not affect μ significantly. Likewise alumina chips smashed after first 15 cycles and μ remained in the region of 0.32.

EL could be related to an improper fixing of the socket, design and the material of the prosthesis, certain activities of the patient, surgical technique or just normal walking [97]. Understanding how this phenomenon happens, should help us to predict clinical consequences, analyse the problem more efficiently and possibly prevent EL by advising the patient or modifying prosthesis design or surgical techniques. Furthermore, we may need to improve basic hip simulators to the ones that involve EL condition which simulate more realistic behaviour of the hip in *vivo*.

3.1. Microseparation

EL was reported in the first and the second generation of COC. Researchers expected that the problem raised from the cup positioning either when it was fitted improperly or loose socket migrated to the steep position. Hence it was hoped with better positioning, proper fixing, stability of the socket and better material, EL could be prevented [98]. However, studying the third generation of COC with well positioned, well fixed and improved material showed that there is another problem that causes EL as well [99]. Lombardi et al [100] studied this phenomenon in *vivo* with video fluoroscopy and approved microseparation of the ball from the socket during normal

walking cycles. The ball is separated (up to 2 mm in MOP [100]) from the centre of the socket during the swing phase in walking cycle. Although ball was displaced in the direction of the socket axis, it did not come back to the centre of the socket in the stance phase. When the load applied at heel strike. Instead, the ball loads the socket anterosuperiorly to relocate in the socket and remains anteverted stripe wear on the ball, which was observed in most of the retrieved prostheses [101,102,103]. In this regard, modern hip simulators apply a microseparation condition as an inevitable element for testing the hip prosthesis.

3.1.1. Simulation of Microseparation

Stewart T D et al. [97] studied three bearing couples, COP, MOM, COC, with Prosim simulator (I) and Leeds II simulator (II). All of the prostheses are tested under standard and microseparation conditions. They are tested for 5 million cycles at a frequency of 1 Hz. 25% bovine serum is used as a lubricant, which was changed every 333,000 cycles. The wear rate is determined and surfaces were analysed every million cycles. Two simulators simulate the heel strike which happens in *vivo* with following methods in *vitro*:

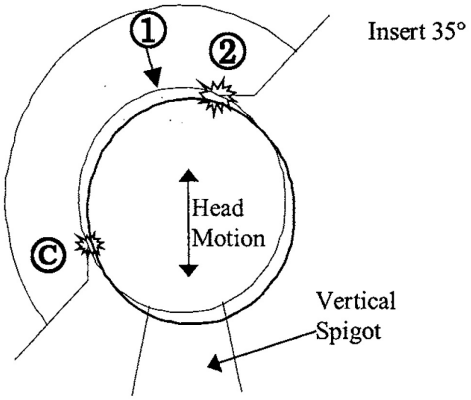

Figure 3.5. Prosim microseparation [97]

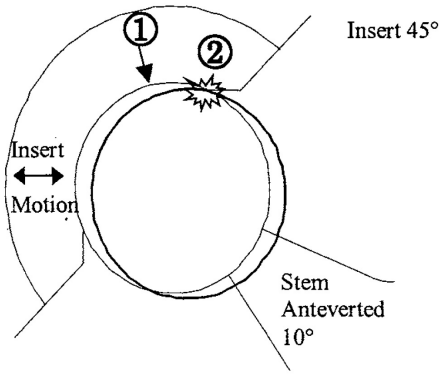

Figure 3.6. Leeds II microseparation [97]

- **Prosim hip simulator:** In this simulator, an inferior load is applied to the ball by actuator that simulates microseparation of about 0.7 mm between the ball and the socket [101]. With this separation ball contacts with inferior part of the socket; which produces lateral displacement of the ball (Figure 3.5: ball moves from position 1 to C). Then heel strike results the superior translation of the ball and contacts the ball with superior part of the socket before it was relocated in the centre of the socket (Figure 3.5: position 2).

- **Leeds II hip simulator:** In this simulator the load is applied to the socket lateromedially by a spring which makes about 0.4 mm medial and superior translation of the socket (Figure 3.6: Position 1 to 2) [102]. Thereafter superior part of the socket contacts the ball during the heel strike (Figure 3.6: Position 2) and makes a momentary stress before the ball relocated in the centre of the socket (Figure 3.6: Position 1). This simulator is able to produce mild or severe microseparations with adjusting the swing phase loads. Reducing the swing phase load from 400N to 50N makes a sever microseparation condition. Once the load is decreased, springs can overcome the friction easier and enables translation of the socket superiorly (Figure 3.7). Therefore the velocity of the socket is increased and during the impact (Figure 3.6: Position 2) momentum and impact energy are increased as well, which represent the higher laxity.

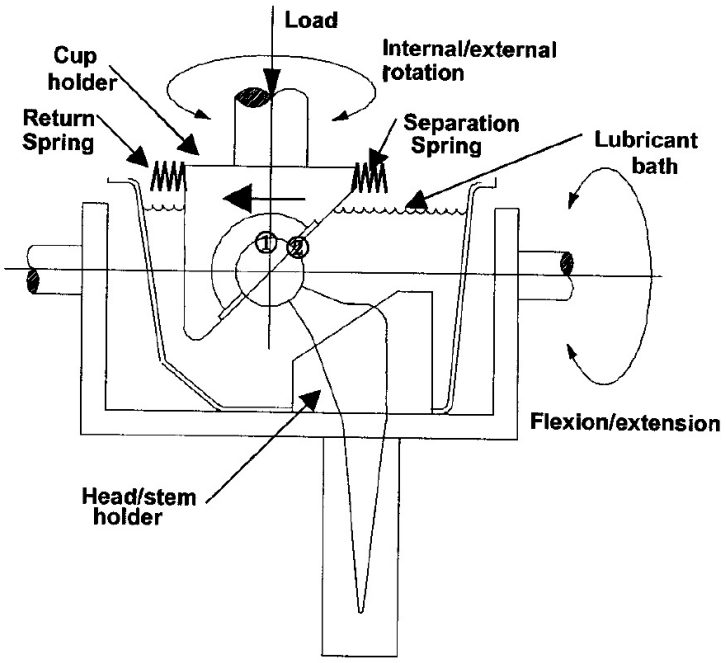

Figure 3.7. Leeds II hip simulator schematic [103]

Both simulators make a small separation between the ball and the socket to contact ball and the superior chamfer of the socket at heel-strike. Therefore, momentary stress is made before the ball is fitted in the centre of the socket. The wear is higher in the first million cycles of testing which is named bedding-in phase while it is reduced after one million cycles (steady-state phase). Average wear rate of the tested couples are listed in Table 3.2 and compared with retrieved ones in *vivo* [104]. All the tested prostheses expose higher wear rate comparing with standard condition (conventional

simulation), except COP, which showed a reduction of the wear rate by a factor of 4 [101]. This may be due to the squeezing of the film lubrication made by microseparation.

Table 3.2 Average wear rate in simulators I & II compare with vivo wear rate [97]

Component	In vivo mm^3/year	Standard mm^3/ mc	Separation mm^3/ mc
COP (I)	25-100	25.6 ± 5.3	5.6 ± 4.2
MOM (I)	0.3-5	0.09 ± 0.05	2.3 ± 1.2
COC (I)	0.1-1	0.05 ± 0.03	0.2 ± 0.03
COC (II) Mild	0.1-1	0.07 ± 0.02	0.1 ± 0.05
COC (II) Severe			1.8 ± 0.4

MOM and COC were tested with Prosim simulator. Results showed respectively 25 and 4 times higher wear rates under microseparation test condition comparing with standard one. The wear rates of the retrieved prostheses from revision surgeries are almost in contract with the wear rates of the prostheses tested with Prosim simulator [101]. Furthermore testing of the COC with Leeds II simulator showed the rising of the wear rate by a factor of 2 and 36 under mild and severe microseparation conditions respectively [101, 102]. Both simulators under microseparation made stripe wears on the ball and the socket of the COC prostheses which are the same to the colour of the alumina, they are rubbed with pencil and shown in Figure 3.8a, 3.8b and 3.8c.

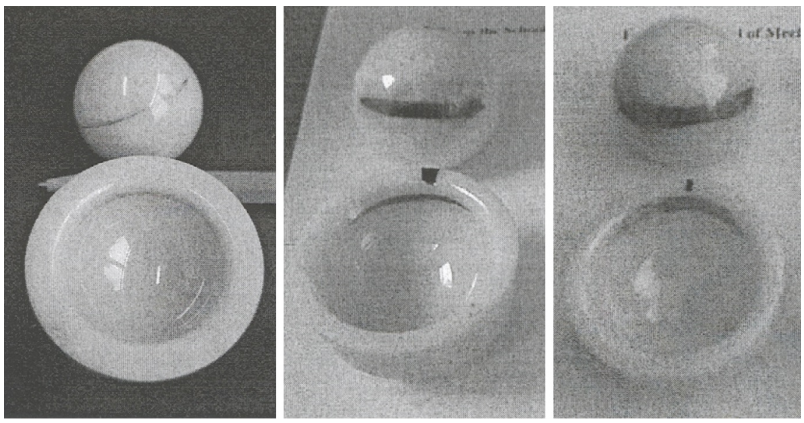

Figure 3.8. a:COC (I) [97] 3.8b: COC (II) Mild [97] 3.8c: COC (II) Severe [97]

Proceeding surgery, it takes surgically cut muscles several weeks to regain their strength. During this period of time, muscles do not have sufficient strength to keep the joint in place therefore microseparation is more probable. Bergman et al. [105] believed that contraction of the hip muscles positively loads the ball toward the socket, which reduces microseparation during the walking cycles.

3.1.2. Mild and Severe Microseparation in Bedding-in and Steady-State phases

Stewart et al [102] studied the effect of the mild and sever microseparation on the COC prostheses. They then compared results with the retrieved ones from revision surgeries and the ones tested with standard simulators. In this regard, nine pairs of Alumina Biolox Forte COC (Three with mild, three with severe and three under standard condition) are tested with Leeds II simulator using the method explained earlier. As it is shown in Figure 3.9, wear rate of the COC is significantly increased with mild and severe microseparations in comparison with COC without separation.

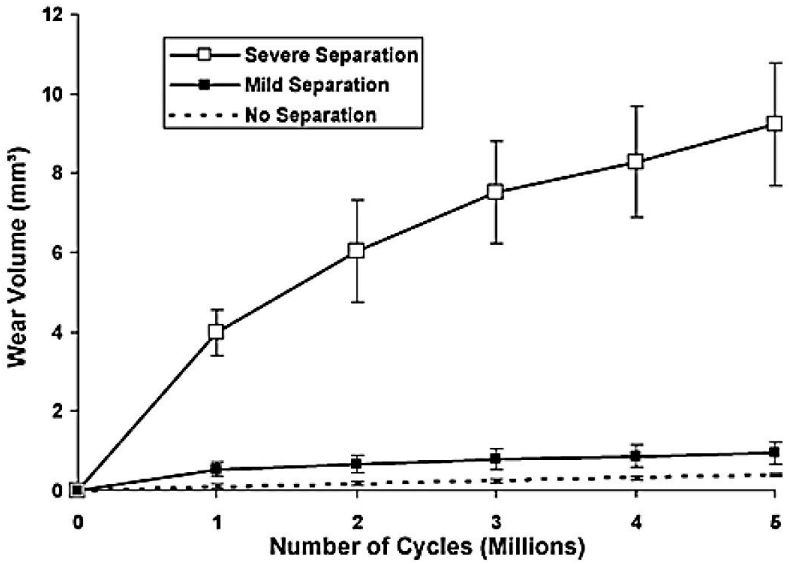

Figure 3.9. Wear volume rate of COC with mild, severe and no separations [102]

Figure 3.10 summarized the mentioned COC prostheses during Bedding-in, steady-state and overall phases. Wear rates of the COC prostheses for standard conditions were respectively 0.11±0.05 mm^3/million cycles and 0.05±0.02 mm^3 /million cycles and 0.55 mm^3/million cycles and 0.1 mm^3 /million cycles under mild separations and 4 mm^3/million cycles and 1.3 mm^3/million cycles under severe separation. As it was discussed earlier, the wear rate is relatively high in bedding-in phase and is decreased after about 1 million cycles when steady-state phase started. COC with severe microseparation shows overall wear rate of 1.8 mm^3/million cycles. The study shows mild and severe microseparation of the COC increased the wear rate by 5 and 36 fold in bedding-in phase and 2 and 26 fold in steady-state phase respectively in comparison with the standard wear rate.

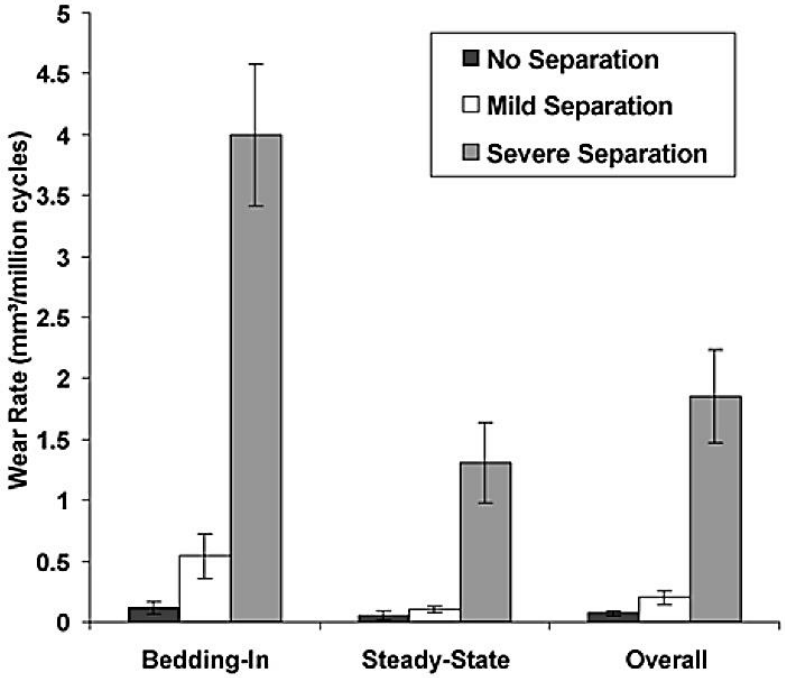

Figure 3.10. Average wears rate of COC with mild, severe and no separations in respect of Bedding-in, Steady State and Overall Phases [102].

The stripe wears (intragranular fractures) produced by mild and severe separations increase R_a from less than 0.01μm to the range of 0.14 μm to 0.3 μm. These stripe wears are similar to the ones retrieved clinically [99]. Although the stripes widths were narrower than the ones found in the first generation of COC [99], they were very similar to the retrieved HIP COC. Wear debris remained from the COC under standard condition have the size of about 10 nm while the mild and the severe microseparation leave the particles in the range of 10 nm to 1000 nm [102].

3.1.3. Advance COC behaviours under microseparation condition

Since 1970s when the first generation of the COC was made, the ceramic materials have been improved. The current one is Hot Isostatic Pressed (HIP[14]) Alumina (AL/Biolox Forte) and Alumina matrix composite (AMC/Biolox Delta). Todd D. Stewart et al. [103] tested the Biolox Delta ball against Biolox Delta socket and also against Biolox Forte socket under microseparation condition. The results developed by this study, were compared to the complete Biolox forte COC, which was studied by Stewart et al [102] and mentioned earlier in 3.1.2.

Six pairs of COC (three Biolox Delta balls against three Biolox Delta sockets and three Biolox Delta balls against three Biolox Fortes sockets) tested under severe

[14] With HIP technique, the porosity of the alumina is removed, the grain size is refined and the strength is improved significantly comparing to the 1st and 2nd generation of COC.

microseparation conditions by Leeds II hip simulator; with the same techniques are explained in 3.1.1.

Bedding-in and Steady-state wear rates of AMC heads on AL socket were respectively 0.99 mm^3/million cycles and 0.51 mm^3 /million cycles under severe microseparation. Bedding-in and steady-state wear rates of AMC couples under same condition were 0.32 mm^3/million cycles and 0.21 mm^3/million cycles respectively. Figure 3.11 summarises these results and compares them with the results are evoked from previous study (3.1.2) during bedding-in, steady-state and overall phase under severe and no microseparations.

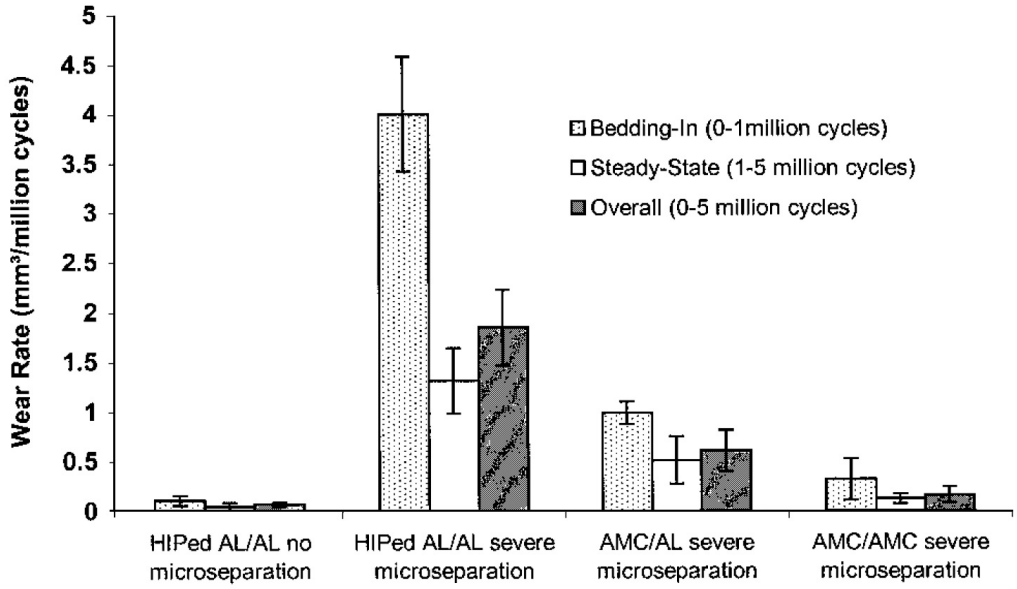

Figure 3.11. Wear rate of AMC/AMC, AMC/AL, AL/AL with severe and no separations during bedding-in, steady-state and overall phases [102]

Overall wear rate of Biolox Delta couple was 0.16 ± 0.08 mm^3/million cycles during the severe microseparation condition which is 3 times lower that overall wear rate AMC/AL couple and 12 times lower than overall wear rate of Biolox forte couple. Furthermore Todd D. Stewart found the wear of the prostheses with the ball and the socket made of same material remained equal wears while Biolox Delta ball remained 65% wear if rubbed against Biolox Forte socket [103]. Stripe wear on the Biolox Delta couples increased R_a from less than 0.005 μm to the range of 0.02 – 0.13 μm. In this regard severe microseparation increased R_a less effectively in Biolox Delta than Biolox Forte. Stripes wear on the balls of all couples (Biolox Delta, AMC/AL and Biolox Forte) are measured [103]. Stripe wear size on the ball of AMC/AL couple had 4-5 mm width and 17-53 μm deep but stripe wear on Biolox Delta was much shallower with the

size of 4-5 mm width and 1.5-16 μm depth. Stripe wear on Biolox Forte studied by Stewart et al [102] showed deep stripe wear with size of 5mm width and 90 μm depth. The prostheses were tested under severe microseparation condition and run for 5 million cycles. The images of the exposed stripe wears on the balls of AMC/AMC, AMC/AL and AL/AL prostheses were taken by scanning-electron microscopy (SEM) [102,103], which are shown on Figure 3.12, 3.13 and 3.14 respectively with scale bar of 25 μm.

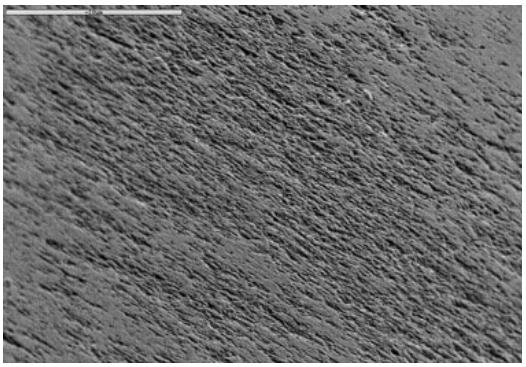

Figure 3.12. SEM of stripe wear on the head of Biolox Delta couple which is made by severe microseparation [103]

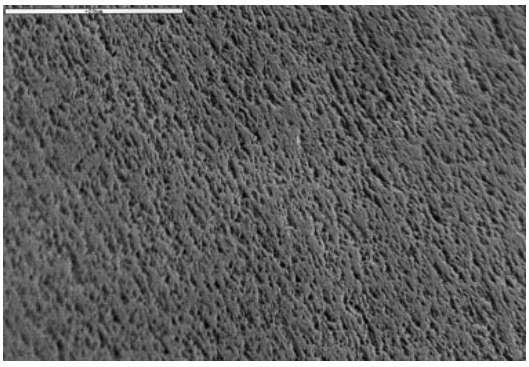

Figure 3.13. SEM of stripe wear on the head of AMC/AL couple which is made by severe microseparation [103]

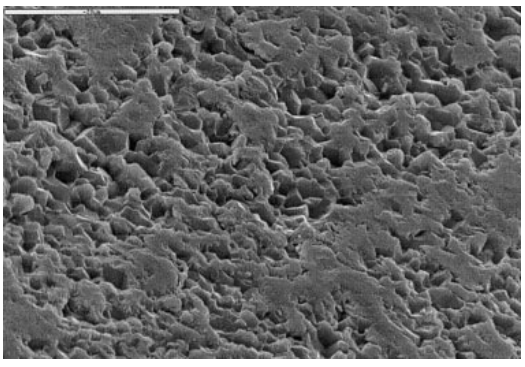

Figure 3.14. SEM of stripe wear on the head of Biolox Forte couple which is made by severe microseparation [102]

3.1.4. Numerical relationship between Microseparation and EL

M M Mak et al. [106] found a mathematical relationship between EL, microseparation, radial clearance and socket inclination. This relationship is shown as a formulation in Formula (3.1), where distance between the centre of the ball before and after separation is shown with "S'", the cup inclination angle with "θ" and the radial clearance between ball and socket with "C_d".

$$S' \geq \left(1 + \frac{1}{\tan\theta}\right) C_d \tag{3.1}$$

EL starts with the contact of the ball to the edge in point "*A*" in Figure 3.15. In this figure point "o" is the centre of the socket. A distance from the centre of the ball "C_3" to the centre of the socket "o" is the radial clearance "C_d". Having considered the triangle OC_2C_3 on the opening area of the socket we can have Equation (3.2).

$$oC_2 = \frac{C_d}{tan\theta} \tag{3.2}$$

Therefore the microseparation is needed for EL is "S'" which is described in following.

$$S' = oC_1 + oC_2 \tag{3.3}$$

From Equation (3.2) and (3.3) we can have Equation (3.4) hence Formula (3.1) can be driven from this equation.

$$S' = C_d + \frac{C_d}{tan\theta} \tag{3.4}$$

Based on Formula (3.1), a socket fixed with 45º inclination can be loaded with the ball which is displaced from the centre of the socket for more than $2C_d$. Therefore if the ball and the socket have 40 μm radial clearance [107], EL happens when ball gets more than 80 μm distance from the centre of the socket. This postulation is supported with Finite Element Analyses (FEA) as well [25].

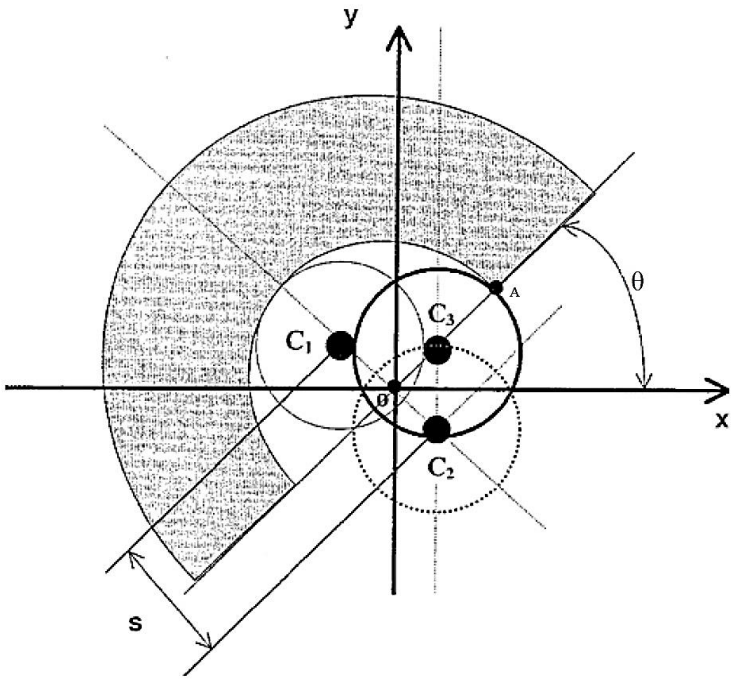

Figure 3.15. Schematic of microseparation for explaining Formula (3.1) [107]

3.2. Relationship between EL and socket positioning

Posterior EL happens even with a well-fixed socket. This is contradicting the claim that EL can be fully eliminated with proper fixing of the socket [98]. EL with current prostheses may be inevitable but can be controlled with well positioning of the socket as to reduce the wear rate effectively.

Three surgeons, WKW, WLW and BAZ [92] had done 54 revision surgeries while 32 of them were studied by radiography before revision surgery (17 Posterior, 3 anterosuperior, 6 both and 6 no wear). They had found that the prostheses with anterosuperior EL had the fixed sockets with median inclination angle of 54º (52º - 66º), which are similar to the ones with posterior EL with median inclination angle of 49º (40º - 63º). However the sockets had different anteversion angles. The ones with anterosuperior EL had fixed socket with median anteversion angle of 22º (22º - 30º) and the ones with posterior EL had fixed socket with median anteversion angle of 15º (5º - 25º). All prostheses with anterosuperior EL had high wear rate and squeaked with more than 22º anteverted sockets [92]. Figure 3.16 illustrates the median wear rate of the sockets corresponding to their positions. Well positioning of the socket is important for all prostheses including hard bearing couples [87, 108, 109]. As it is shown in Figure 3.16, positioning of the socket should be considered in a combination of inclination and anteversion. Esposito C.I et al. [92] found that a socket with 55º inclinations and 15º anteversion had low wear rate, but a socket with 55º inclination and 25º anteversion had

high wear rate. The corollary is also correct, a socket with 35º inclination and 15º anteversion had high wear rate but a socket with 35º inclination and 25º anteversion had low wear rate.

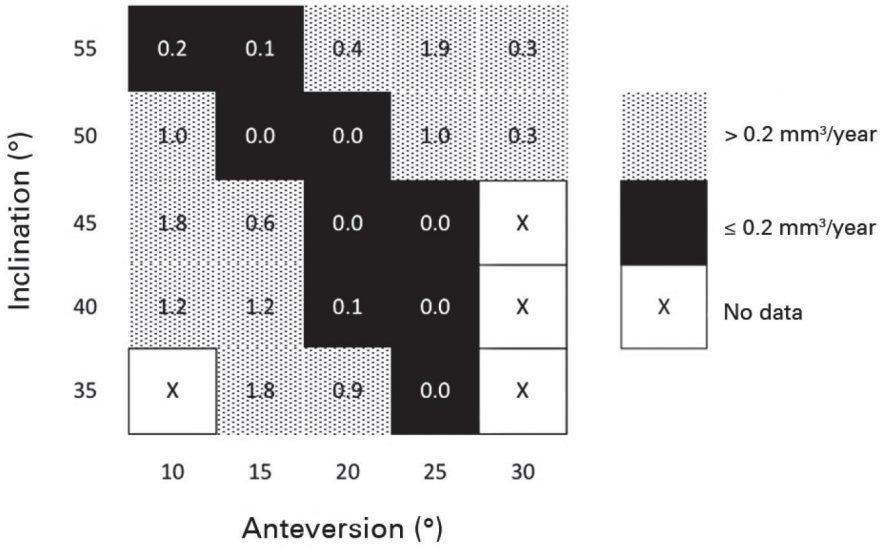

Figure 3.16. Socket median wear rate corresponding to the orientation zone [92]

Full extension may be the cause of the anterosuperior EL while deep flexion may be the cause of the posterior EL. High inclination and high anteversion tend to promote anterosuperior EL while if one of these positioning, either inclination or anteversion, is low, early anterosuperior EL may be prevented. Vice versa; low inclination with low anteversion cause the posterior EL. Socket positioning affects the contact force magnitude and direction across the hip [27] which disturbs the contact mechanics and lubrication mechanism of the prostheses [16, 28].

Although some authors [26,19, 31] believed there is a square safe zone for fixing the socket into the acetabulum to prevent dislocation and EL, and some just accepted 45º inclination and 15º anteversion as a lowest at-risk values for dislocations [29], the real safe zone is more difficult to be mathematically described. However Esposito C.I et al. [92] believed if the socket orientation satisfies (3.5), it is most likely that COC would have the lowest wear rate.

Approximated safe zone is calculated with following formulation (3.5) [92]. In this formula (y) is the inclination angle and (x) is the anteversion angle of the socket. The result further from 0° increases the risk of the wear rate. In this regard, positive value as a result leads the joint to anterosuperior EL and negative value to posterior EL. Furthermore, another study [33] showed that the inclination does not have enough

effects on EL but most of the authors [92, 84] agree the anteversion is an effective factor in this regard (i.e. posterior EL was significantly increased with less than 15º anteversion).

$$y + (7/5)\,x - 75° = 0° \qquad 35° \le y \le 55° \qquad (3.5)$$

The optimum socket position entirely depends on the anatomy of the patients and their range of the movement therefore for each patient this orientation can be different.

3.2.1. Does inclination affect EL in COC?

Some studies [114] showed that inclination does not have enough effects on EL in COC but other studies did not agree with this conclusion. Some of these studies are discussed in following.

Elhadi Sariali et al. [115] studied the combined influence of microseparation and the socket inclination to investigate the contact area and also the contact pressure, first under normal condition with no microseparation and then under EL condition. For this purpose a 32 mm COC ball and socket modelled with FEM. The material was defined to be similar to the Biolox forte and the simulation condition was similar to the Leeds II hip simulator. The radial clearance was 30 µm and socket fixed with 45º inclination.

This study showed with no microseparation and no further inclination of the socket contact area was on the centre of the head with circular shape with radius of 4.6 mm and contact pressure was 64 MPa. These values were close to the predicted values by Hertzian theory; 4.3 mm and 64.4 MPa respectively. However EL is started to be generated with displacement more than 30 µm separation and is fully generated with 60 µm displacement which confirms Formula (3.1). Increasing the microseparation shifts contacted area laterally from the centre of the ball, where 500 µm separation displaced the centre of the contact area to 10.4 mm further from the centre of the ball. EL had been starting with no microseparation but when the socket inclined more than 75º. However EL was fully developed with 90º inclination of the socket. Figure 3.17 illustrates this.

Therefore when the inclination angle of the socket was increased, the contact pressure was increased as well. During no separation, if the socket is inclined from 45º to 90º, contact pressure would be increased form 66 MPa to 137.2 MPa.

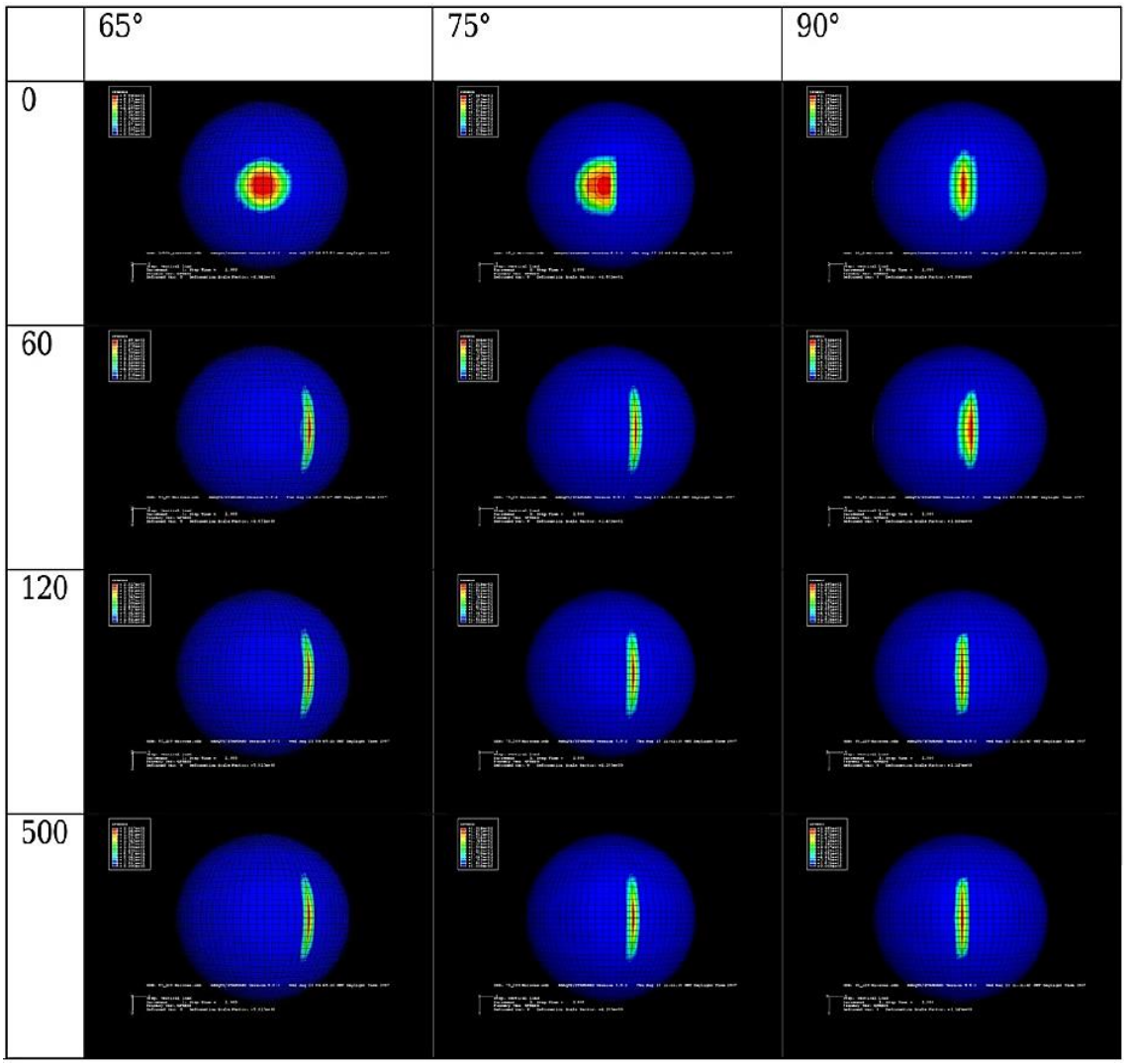

Figure 3.17. Effect of the socket inclination and microseparation on the contact pressure [115]

Despite this result, Elhadi et al. [115] believed the effect of the socket inclination would be negligible if microseparation is increased from 60 μm. However this contribution, supports the idea that microseparation is the main factor in increasing of the contact pressure rather than socket inclination or other factors.

Saverio Affatato et al. [116] tested several COC prostheses with hip simulator machine and found that the worst socket inclination angles are 23º and 63º [117,118]. In this regard, 12 pairs of 28 mm COC prostheses (made by Ceramtec) with radial clearance of 86 μm were tested with 12-station hip simulator (Shore Western, Monrovia, USA), 6 sockets mounted with 23º angle and other 6 with 63º angle. The rest of the configuration of simulation was similar to the one explained in 3.1.1. A 400N-force was applied for making 0.5 mm microseparation. The result was not the same as their first hypothesis. Although microseparation caused 12 fold higher wear rate in comparison with the standard condition, different angles did not affect the EL condition

during microseparation. Saverio Affatato et al. [116] found that after 2 million cycles 23º and 63º inclined sockets during 0.5 mm microseparation had the volumetric wear of 0.11 ± 0.03 mm^3 and 0.12 ± 0.03 mm^3 respectively which showed insignificant difference on the wear patterns as well.

Mazen Al-Hajjar et al. [119] tested 6 COC (28 mm Biolox Delta) with six-station Leeds II hip simulator, 3 mounted with 55º and other 3 with 65º inclined sockets. They are tested under standard condition and also under microseparation condition. The wear rates for both of them under standard condition were as low as 0.05 mm^3/million cycles hence inclination of the sockets had no effect on the wear rate. Moreover, inclination of the sockets under microseparation condition also had no effect on the wear rate of the Biolox delta prostheses in that study, while the mean wear rate of the COC with 55º inclined socket was 0.13 mm^3/million cycles and the mean wear rate of the COC with 65º inclined socket was 0.11 mm^3/million cycles. These are summarised in Figure 3.18.

From these studies we can conclude the COC with sockets inclined less than 75º have no effects on the wear rate and EL. Furthermore a socket with more than 75º inclination is not feasible to be fitted in human body. Therefore, inclination of the COC under microseparation has no significant effect on the wear rate any further.

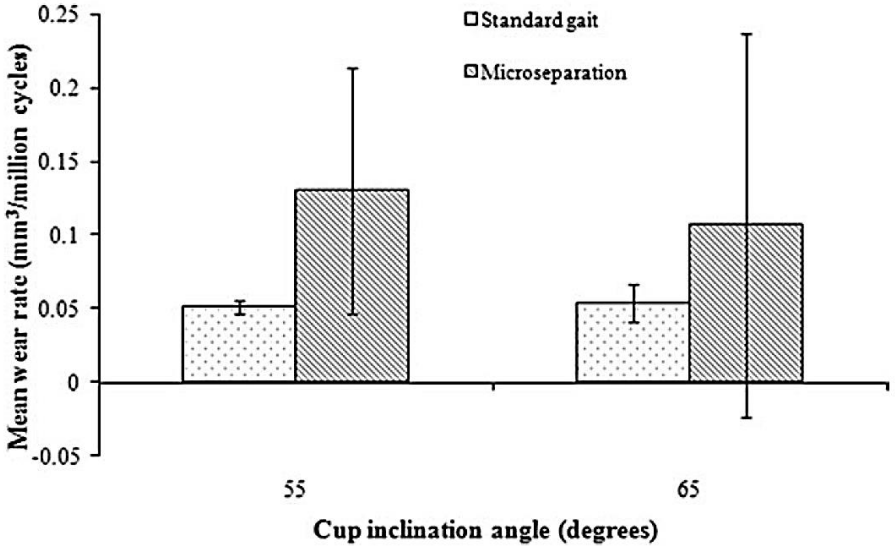

Figure 3.18. Mean wear rate of Biolox Delta prostheses with 55º and 65º socket inclinations under standard and microseparation conditions [119]

3.2.2. Does Inclination affect EL in MOM?

Some other studies in *vivo* [87, 120] investigate this issue in MOM and they believed increasing the inclination of the socket increases the wear rate of MOM,

however data from these clinical studies are not limited to the cup inclination hence the results cannot prove this assertion. Ian J. Leslie et al. [121] tested 15 MOM prostheses which had internal diameter of 39 mm, 5 fixed with 60º inclined sockets which were tested by Prosim hip simulator, 5 fixed with 45º inclined sockets which tested by the same hip simulator and the other 5 fixed with 55º inclined sockets under microseparation and tested with Leeds II hip simulator. The result showed that there were differences in the wear rate of the tested cobalt chromium prostheses under three defined conditions. The MOM prostheses with 60º inclination sockets had 9 fold and 20 fold higher wear rate than the ones with 45º inclined sockets during bedding-in and steady-state phases respectively. They believe increasing the socket inclination caused a reduction of film lubrication, hence increased the wear rate. This is in agreement with Williams S, et al. study [122]. Furthermore the amount of ions left from 60º inclined socket is similar to the one is reported by De Haan R et al. [87]. This study shows the MOM prostheses are more sensitive to the socket positioning than the COC ones [114, 115, 116, 119 and 123]. Ian J. Leslie et al. [121] found that the prostheses with 55º inclined sockets and tested with the Leeds II simulator had the highest wear rates. The reason was due to the microseparation condition applied to those set of prostheses by Leads II simulator. Where other prostheses were tested under normal condition. Figure 3.19 summarises the result.

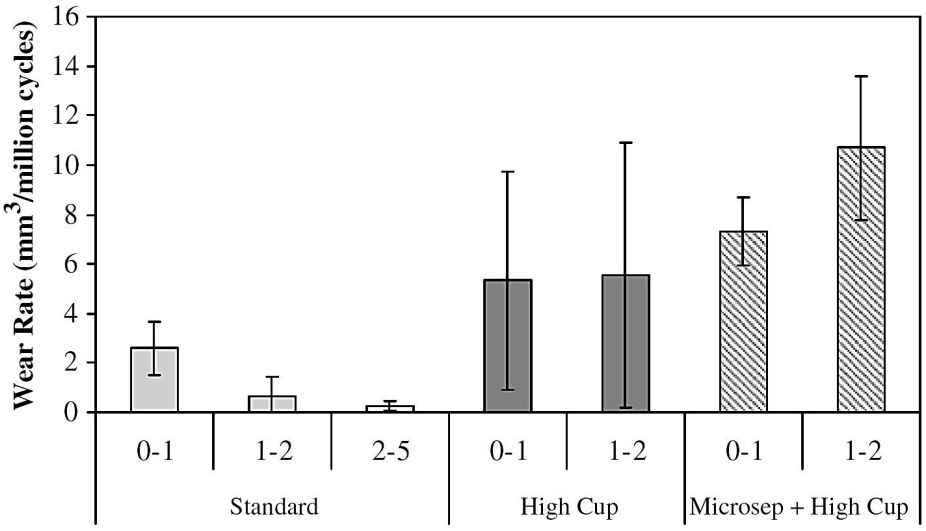

Figure 3.19. Wear rate of 39 mm MOM prostheses with 45º, 60º and 55º inclined sockets, which are tested under standard, no separation and separation conditions respectively [121]

3.2.3. Neck-Rim Impingement

A poor combination of ball and socket, dislocation, hypermobile[15] hip, misalignment of the socket or simply stoop or flexion more than 100º depending on the socket inclination [124] can cause of the Neck-Rim impingement. In case of emergence the two sides of the socket will be damaged: firstly the edge of the socket, where the neck is impinged with (It is named "impingement site" shown Figure 3.21), and secondly the opposite side of the socket where it goes under EL with superior part of the ball (It is named "egress-site" shown in Figure 3.21). Furthermore Neck-Rim impingement lifts the ball and may cause dislocation of the joint. Neck-Rim impingement is illustrated in Figure 3.20.

Figure 3.20. Neck-Rim impingement [125]

Although concern of the impingement is mainly due to its role in dislocation, attention to its role in EL is also important. Impingement was observed in 70% of the hip prostheses [126, 127]. Clinical concerns in this regard are releasing the excessive ions in MOM [128, 129], fracture in COC [130, 131] and reduce stability in general. In COC and MOM the contact area between neck and socket is physically smaller than MOP and COP and respectively the concentric stress is much higher, hence this part mainly studies the effects of this phenomenon on EL in MOM and COC. Incidentally Jacob M. Elkins et al. [132] simulated the Neck-Rim impingement with FEM to find the severity of EL and also its relation to the socket inclination. Figure 3.21 shows this model.

[15] It is referred to the joints, which stretched further than normal joints (i.e. some people can bend their thumb backward to their wrist).

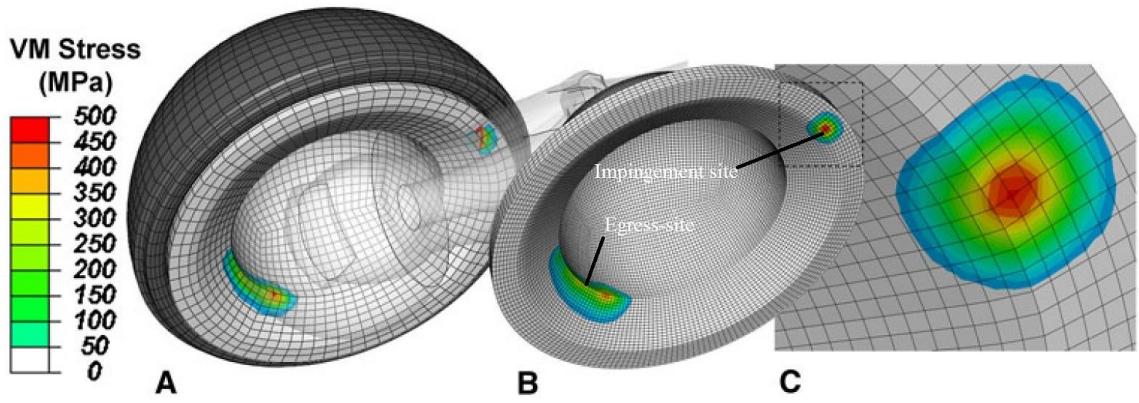

Figure 3.21. Impingement simulation model in FEM [132]

The ball size was 28 mm. MOM was defined with radial clearance of C_d= 0.029 mm, elastic modulus of E=210 GPa, friction coefficient of μ = 0.1, Poisson's ratio of v = 0.3 and density of ρ = 9.2 g/cc [70]. COC defined with C_d= 34 µm, E=380 GPa, μ = 0.04, v = 0.23 and ρ = 3.98 m/cc. The wear rate in this simulation was based on Archard–Lancaster formula, which is presented in Equation (3.6) where $\acute{\omega}$ is local wear rate, σ is local mechanical stress, k is wear factor and $\dot{s}$ is the local sliding speed of two surfaces [133].

$$\acute{\omega} = \sigma \dot{s} k \tag{3.6}$$

The aforementioned study simulated 148 times with 44 variable socket orientations (inclination and anteversion corresponding to pelvic reference [134]) and found that the orientation of the socket had linear relation with Von Mises stress of the egress-site and impingement site (Figure 3.22). Furthermore the egress-site showed a higher Von Mises stress than the impingement site. This shows the area under EL condition is damaged more severely than even the area that is impinged with neck of the stem. Additionally the study showed higher peak stress on COC than MOM at the egress-sites (Figure 3.22, A and B), but lower effect on impingement sites (Figure 3.22, C and D).

Due to the higher elastic modulus of the ceramic material in comparison with metal, higher peak stress on COC is feasible.

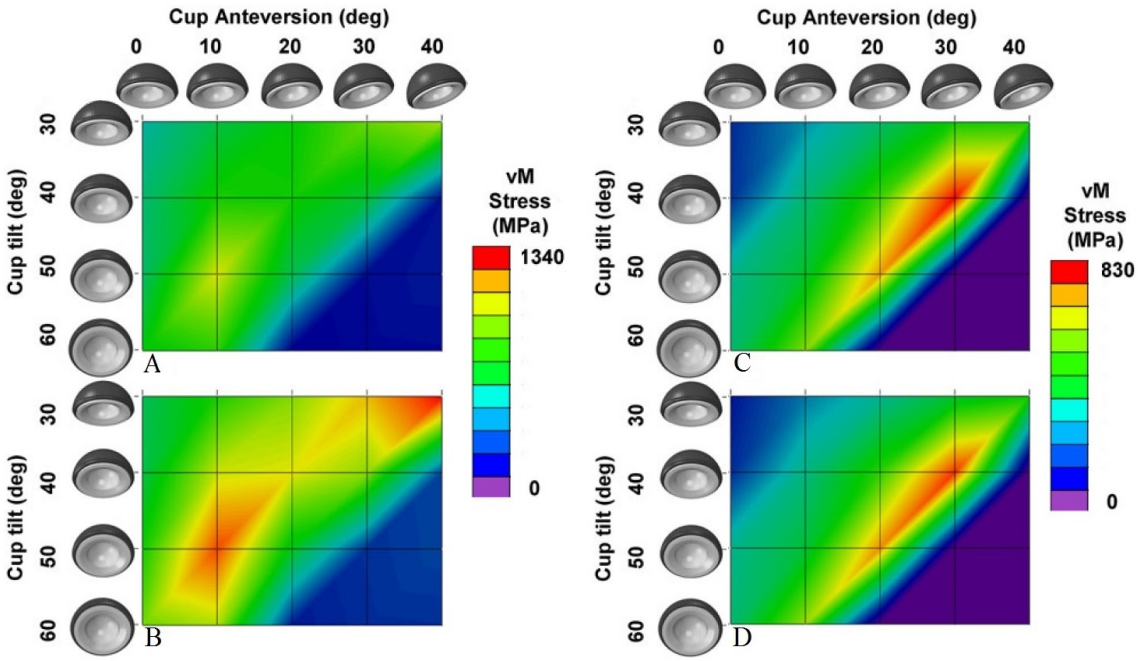

Figure 3.22. Von Mises (vM) stresses applied to the socket during impingement by stooping: A) MOM at Egress-site B) COC at Egress-site C) MOM at impingement site. D) COC at impingement site [132]

3.3. Posterior EL by Muscles contraction during Deep Flexion

Previous studies [41, 92] found that posterior EL occurs more frequently than the anterosuperior one. While the majority of the wear stripes due to the posterior EL have been observed in the absence of the impingement [85, 92, 110], this question arises: can the lines of action of the hip muscles be the reason for the posterior EL in the well positioned prostheses? If the answer is yes then: A) How does it happen? B) Is there any possible way to improve muscles line of action corresponding to the posterior EL?

In order to investigate these questions, the muscles origin and insertion points of the cadaver's right leg was developed and modelled [135, 136]. Furthermore in addition to the muscles that wrap the hip muscles, iliopsoas muscle (Originated from T12-L5 of spinal cord, wraps the pelvic and inserted to the lesser trochanter) was included in this model to ensure the femur was pulled in correct direction. Richard J. van Arkel et al. [136] discretised the full range of motion [137] to the numerous 5º of motions therefore 6,426 orientations were studied for flexion (-10° to 120°), rotation (-40° to 40°) and abduction (-25° to 40°) [138]. The model was designed with OpenSim version 2.4.0. It was modelled with MatLab version 2011b and the force vector for each muscle either its contraction pulled the ball into the socket concentrically (concentric area was 5º to edge) or contribute EL were calculated with Plugin. Diameter of the ball was 28 mm,

socket was subtended 168º and positioned with 45º inclination and 20º anteversion [139].

The result was unexpected; all muscles were inserted to the distal femur, tibia or patella can be contributed to EL even in the well-positioned socket. However large muscles like gluteus did not participate. Figure 3.23 illustrates the percentage of muscles contribution in EL during full range of motion of the hip.

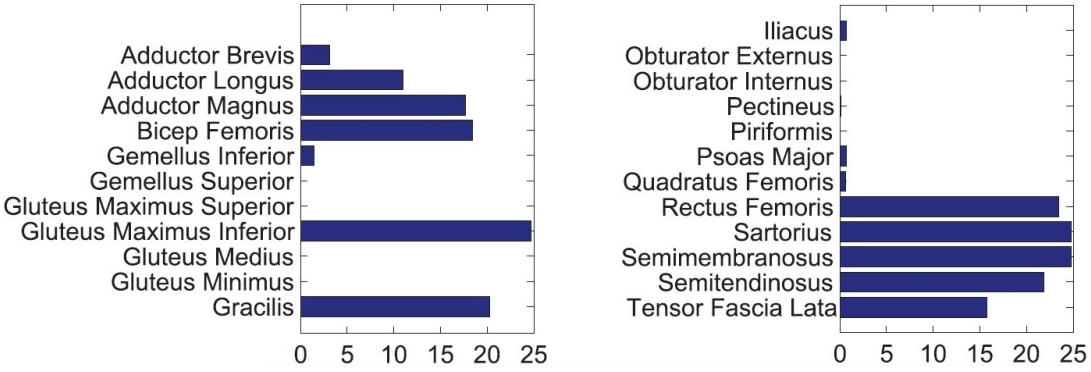

Figure 3.23. Active muscles for hip motion with percentage of their contribution in EL [136]

Posterior EL by muscles is common when the hip is deeply flexed. Rising from the chair or step climbing require about 90º flexion and -10º to 20º abduction [38, 110]. These activities require contraction of muscles, which are distally inserted to hamstrings, rectus femoris and gluteus maximus [124, 140, 141]. Therefore during sit-to-stand, the muscles which can contribute to EL, are highly active while the ones supporting a protective function are not. Morlock M. reported [142] the patient with THR rise from the chair 76 times a day and stair climbing 42 cycles a day, which are more than 27000 times and 15000 cycles per year respectively, therefore there is always a risk of posterior EL with available prostheses. During such activities, the muscles pull the femur posteriorly and levy the maximum pressure of the superior part of ball to the posterior side of socket, while joint reaction force during rising from the seat is twice as much as body weight [110] and during the stair climbing is 2.5 times as much as body weight [110]. Furthermore, the force can be increased if there is no armrest or faster rising from the seat or stair climbing. If the socket is well positioned and hip is in the neutral position of abduction and rotation, increasing the hip flexion from 80º to 100º (i.e. rising from the lower seat height or climbing the higher step), activates nine of twenty-three muscles (39%) contribute in posterior EL. This study illustrates posterior EL, which was reported clinically [88, 92, 143,144,145].

3.3.1. Abduction during flexion

Hip abduction during hip flexion can change the line of action of the muscles contributed to EL from the edge to the concentric area in the socket. This is because of tying up the line of actions of the distal femur muscles to the position of the femur [136] and adduction has the opposite effect (Figure 3.24). Internal or external rotation has little effect in this regard.

Abduction more than 20º brings the line of action of all muscles in the position of the femur with flexion up to 95º while 50º flexion of the hip can cause of EL with 20º adduction. Furthermore abduction during flexion may solve Neck-Rim impingement as well, because it moves the femoral neck away from the anterior part of the socket where it is the common area for impingement [124, 146].

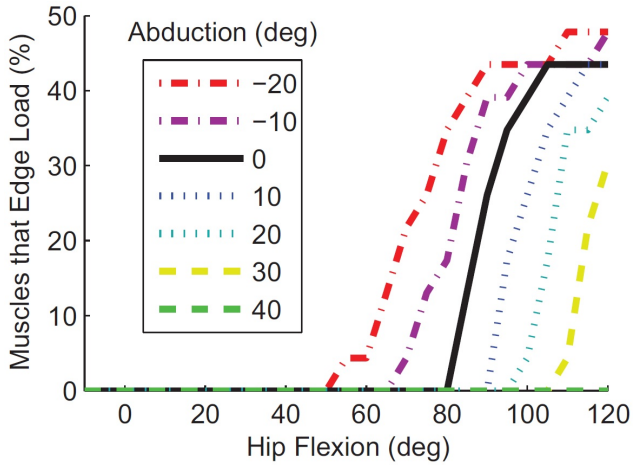

Figure 3.24. Effect of the abduction on the flexion of the hip [136]

Richard J. van Arkel et al. [136] believed abduction during deep flexion can reduce the posterior EL significantly and possibly dislocation. He believed this finding is applicable to all patients who have hip prostheses regardless to design and fixation of the prosthesis. This is simply applicable with separating of the knees before flexing the hip.

3.3.2. Relationship between socket orientation and flexion

Figure 3.25 is based on 45º inclination and 20º anteversion while orientation of the socket was the combination of anteversion of 5° (low), 20° (medium), and 35° (high) and inclination of 30° (low), 45° (medium) and 60° (high). In this regard socket with lower anteversion caused posterior EL by lower flexion of the hip and higher

anteversion had an opposite effect. It allowed the hip to flex with higher angle before the muscles contributed in EL [136].

Low inclination of the socket had two effects on the muscles action:

- Increases the number of the muscles, which can contribute to EL in all flexion angles.
- Reduces the effect of abduction during flexion of the hip.

However high inclination of the socket had four effects:

- Decreases the number of the muscles, which can contribute in EL in all flexion angles.
- Increases the effect of the abduction during flexion of the hip.
- Enables the iliopsoas muscles to contribute in EL during lower flexion or extension of the hip.
- Enables distally inserted muscles to contribute in EL with lower flexion or extension of the hip.

Therefore combination of the inclination and anteversion of the socket can be suitable as it was discussed in section 3.2. Figure 3.25 illustrates the effect of the socket orientation corresponding to the adduction or abduction of the hip.

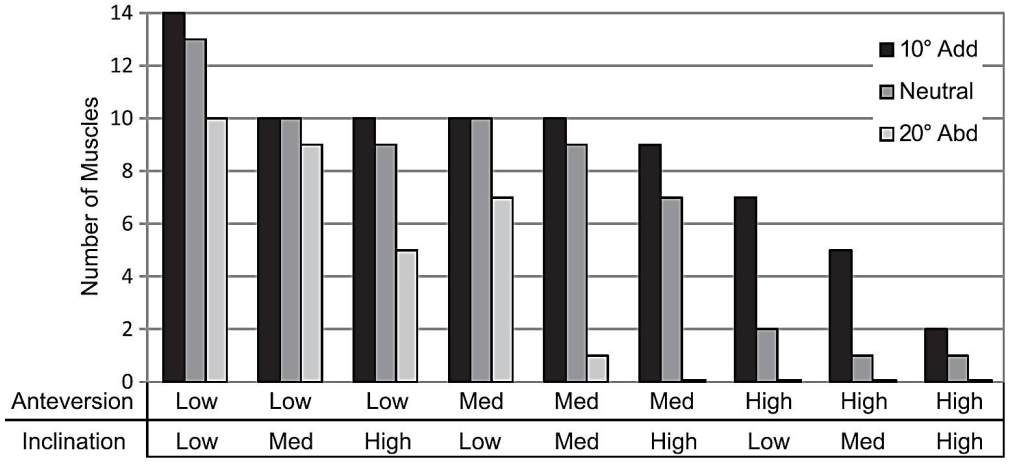

Figure 3.25. Study of hip flexion with neutral, 20º abducted and 10º adduction corresponding to the sockets orientation which is combination of inclination and anteversion [136]

3.3.3. Relationship between subtended angle of the socket and flexion

Decreasing the subtended angle of the socket arc increases the muscles contribution to posterior EL also EL with lower flexion. This is in agreement with Underwood R et al. [144], which showed the socket of MOM with decreased subtend angle suffered from sever EL and respective wear rates. Reducing the subtend angle of

the socket reduces the safe coverage area for the ball. Likewise changing the risk-zone on the edge has same effect. For example, the socket with 168º subtend angle and a risk-zone of 13º has the same performance of socket with 152º subtend angle and a risk-zone of 5º. Figure 3.26 compares the prostheses with different subtended angle corresponding to the angle of the flexion.

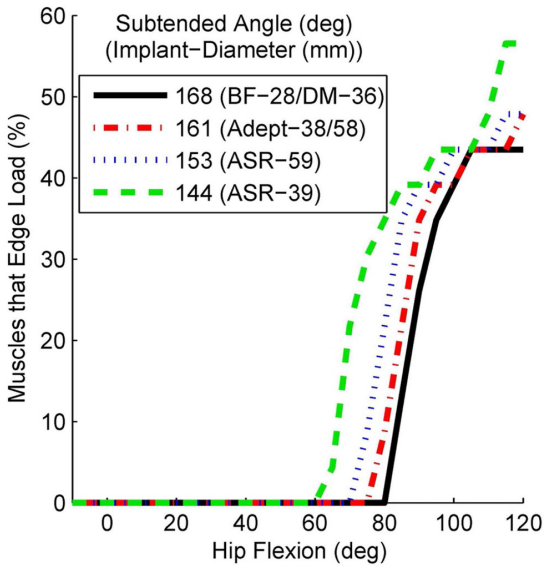

Figure 3.26. The prostheses with different subtended angle corresponding to the angle of the flexion [136].

3.4. Squeaking

Squeaking noise has been described in 1950s with the Judet acrylic Hemiarthroplasty [149]. Charnley [150] noted squeaking in vitro when he was testing Boutin COC bearing with “pendulum friction comparator” in his laboratory. However reasons of this phenomenon are still under investigation. Scientists have different beliefs about this problem. However like any other arthroplasty problems, it may be due to the prosthesis design, patient or surgical factors.

Patients who reported the squeaking with some specific activities, advised to modify their movement to eliminate the noise (i.e. to change the model of bending or to use other leg for bearing the burden). These patients are not recommended for revision surgery. Rarely patients with squeaking are advised for revision surgery due to the much higher risk of revision surgery compared with the primary THR surgery, though the people with squeaking during their walking can persuade the surgeon to do the revision surgery. Walter [26] studied squeaking in different group of patients to find the reason. He found the patients with squeaked prostheses were younger (56 years old

compared with 65, P=0.01) heavier (90 kg compared with 76, P=0.001) and taller (179 cm compared with 169, P=0.003) than the ones had non-squeaked prostheses. Some hips squeaked at the end of stance of walking when hip was extended. Other ones squeaked when the patient stooped to pick up an object from the floor when hip was flexed. He found the hips squeaked with walking had more anteverted socket (40º anteversion) than the ones squeaked with stooping (19º anteversion). He described the reasons with anterosuperior EL and posterior EL related to orientation of the socket, which were explained in Section 3.2. He said squeaking is due to passing the stripe wears of the ball over the stripe wear of the socket; the passes of stripe over each other cause the vibration in the range of the human hearing while the normal resonation of the ceramic on ceramic bearing is above enough frequency of the human hearing range. In same regard he and Restrepo C et al. [147] reported; squeaking is not occurred in first fourteen to eighteen months after surgery, while this is the time for EL to makes the stripe wear but it starts upon the stripe wear fully developed. Furthermore Lusty P.J et al. [84] reported all squeaked hip prostheses were retrieved from revision surgery had EL with stripe wear, which hypothesises EL may causes squeaking.

Squeaking more commonly reported in hard bearing couples [109]. Squeaking in COC was reported when the ball and socket made of zirconia and alumina respectively [151]. In general zirconia ball should articulate with polyethylene liner only because it has shown catastrophic wear rate in vitro when articulated either with alumina or zirconia sockets [152]. However squeaking remained unreported with ultra-low wear rate composite ceramics [109]. This can show the relationship of squeaking and wear rate. Transient squeaking also reported in MOM prostheses with incidence of 3.9% [153]. Squeaking can be transient in MOM due to the self-polishing ability of the metal while it remains in COC because ceramic has not this ability. Self-polishing of metal may hide stripe wear on MOM as well.

Elhadi Sariali at al [94] also studied squeaking in the mentioned 3 prostheses in Chapter 3. He found no squeaking in the prostheses with sockets inclined less than 75º in the absence of third body particles. He heard squeaking for the period of 1s when 0.02 gram alumina powder was added to the simulator although it was not reproducible. Likewise ceramic chip made 15s squeaking including the sound of the chip that was being crushed. Recorded sounds had major frequency of 2.6 kHz and harmonic frequencies of 5.3 kHz, 7.9 kHz and 10.4 kHz. This is shown in Figure 3.27. Major frequency of 2.6 kHz almost meets squeaking in *vivo* (2.4 kHz) which was reported

clinically [154]. Lower frequency in vivo can be due to damping effect of the soft tissues surround the prosthesis. Squeaking occurs in mentioned study with increasing of μ with 15 to 26 fold. This can show that increasing μ can produce squeaking which seems relevant with Walter study [26] also Yakoi et al. [155] who believed squeaking was made by vibration induced by friction. The vibration can be due to the instable contact of the surfaces which is made because the static μ is much higher than dynamic μ [156,157] while this differential in μ generates a "stick-slip" phenomenon. In this study although Elhadi Sariali at al. [94] could not find direct relationship between EL and squeaking, they found that adding a third body particle can cause squeaking which may be indirectly related to stripe wear and EL to the squeaking. Ecker et al. [158] found all COC with squeaking had impingement of titanium- titanium with no any damage to the ceramics which can show the effect of the metallic ions to the squeaking as it agrees with Cheviollotte et al.'s study [159] that tested COC under different conditions to study squeaking. COC was tested by hip simulator with/without lubricant fluid under metal transfer, high load, EL, stripe wear, micro fracture etc. The result showed the prostheses under all conditions squeaked with absence of lubricant. However under lubricated condition COC squeaked just under metal transferring.

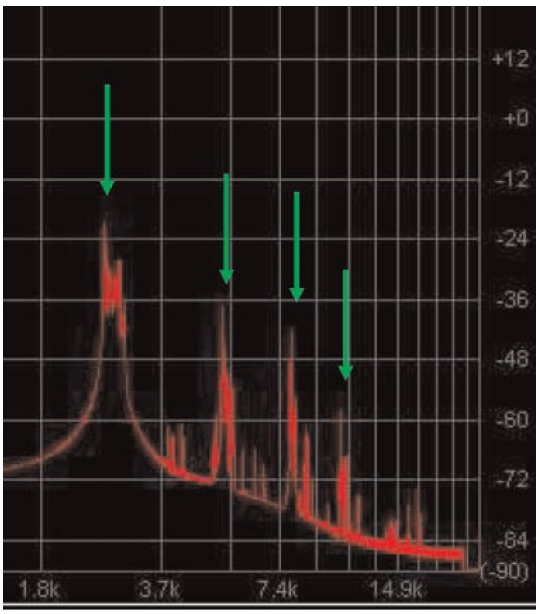

Figure 3.27. Squeaking in vitro with major frequency of 2.6 kHz [94]

Stephen B. Murphy [125] studied 2778 COC prostheses in 11 years period of time. Five patients underwent revision surgery for squeaking when all of them had neck to rim impingement and hence metal transferring. Furthermore it was found the

prostheses with beta titanium alloy stem had higher squeak rate of 7.6% and the ones with conventional titanium alloy stem had 3.1% and the ones with conventional titanium alloy and flush-mounted socket had 0.6%. Mai et al. [165] found all squeaked prostheses (10%, 32 out of 320 COC) had Trident socket. Swanson et al. [166] experienced 4 different sockets while 5 out of 6 squeaked prostheses had Stryker Trident socket and Accolade TMFZ stem. This can show the effect of the prostheses design on squeaking.

Although Walter et al. [26,109], Restrepo et al. [147], Lusty et al. [84], Glaser et al. [160] and Jarret et al. [161] believed squeaking happens with EL and microseparation. Stewart et al. [97,102,103] Elhadi et al. [94,162] didn't agree with them. They tested COC with hip simulator and found that squeaking had not been found with microseparation in COC if it is made of AL/AL or AMC/AMC. However they believed if the couple are made of zirconia head and alumina socket, squeaking occurs. This is due to the excessive wear rate of this couple which were contaminated the lubricant fluid with worn particles [151]. Therefore when the lubricating fluid was refreshed in this test, squeaking was eliminated. Elhadi et al. [162] believed passing the stripe wears of the ball over the stripe wear of the socket during EL called "chattering movement", could make a noise. But this noise is in the main frequency of 65 Hz which is although in audible range, was much lower than the squeaking frequency that was reported for COC in THR by Weiss, C et al. [163] or Parvizi et al. [164].

As a conclusion we can say squeaking is indirectly related to EL either in terms of Neck-Rim impingement or particles released in the synovial fluid made by higher wear rate due to EL or making the stripe wear.

Chapter 4 : Methodology

As it was explained in Chapter 3, many factors contribute in occurrence of EL such as patient's activities, surgical techniques, positioning of the socket, material and design of the prosthesis or simply just normal walking or contraction of the muscles. These factors are discovered with different methods. Experimental data received from patients case studies or from simulating the hip prostheses, have some limitations such as availability, cost, time and ease of use where advance development in engineering science offers other rational solutions in this regards. Virtual design and simulating of the hip prostheses with different materials, under desirable conditions in reasonably lower cost of time and fee in comparison with experimental test, encourage scientists to enjoy from analytical software that is based on Finite Element Method. Furthermore rudimentary contact theory called Hertzian contact theory can help them to have better expectation from the contact of the ball and the socket either in normal or EL condition. Therefore in this research all models are studied with FEM and Hertzian contact theory.

Certainly experimental data has helped us to have wider assessment from studying the EL phenomena and better validation of the results from virtual simulation study; all of which facilitate the understanding of the reasons of EL and may help us to solve the problem. Without these studies, hip prostheses would never have been invented or modified. We all hope with further study and analysing of the EL, this problem can be solved to increase the life cycle of the prostheses and improve the lifestyle of millions young patients.

4.1. Prostheses design

The following sections of 4.1 explain all of the effective factors in designing of hip prostheses with a focus on the significant factors in limiting EL in terms of geometry and design of the components, which have been found with other scientists to date. The information can help us to improve the available prostheses or to propose a new prosthesis, which can significantly limit the effect or ideally prevent EL.

4.1.1. Socket Design

The socket is the most important component of the hip prosthesis in terms of the occurrence of EL. The reason is that the edge of the socket is loaded with the ball and causes the EL phenomena and respective unfortunate consequences. Mathew Mak et al. [25] analysed 3 sockets under EL phenomenon to find influence of the edge geometry

on contact stress. New (With sharp edge of 90º), Worn (geometry was taken from tested socket by hip simulator under microseparation after 1 million cycles [102]) and Chamfer (Edge has 2.5 mm radius chamfer which is available in the market and reported by Mak and Jin [107] as well). The sockets were modelled with Abaqus software to have dimension of 28 mm diameter, alumina material properties (E=380 GPa and ν = 0.26) with radial clearance of C_d= 40 μm with 3 different geometry of the edges. The models analysed with FEM with 2500 N vertical force and 0 to 250 μm microseparation. Ball and socket friction assumed to be zero as they were COC prostheses, which could be well lubricated.

The results of the analysed sockets with new, worn and chamfer edge are in agreement with Formula (3.1). Where the prostheses with $C_d = 40\ \mu m$, were affected by EL with 80 μm displacement. In this regard, maximum contact pressures of 81.6 MPa were developed with all 3 sockets while increasing separation between balls and sockets significantly increased the maximum contact pressure which are shown in Table 4.1. Increasing maximum Von Mises stress are also shown in Table 4.2.

Table 4.1 Maximum contact pressure in new, worn and chamfer sockets during 80 μm to 250 μm separation [25]

	Maximum contact pressure (in MPa)		
Micro-separation distance (μm)	New	Worn	Chamfer
80	81.6	81.6	81.6
100	273	112	157
120	245	191	287
250	672	425	437

Table 4.2 Maximum Von Mises stress in new, worn and chamfer sockets during 100 μm to 250 μm separation [25]

	Maximum Von Mises stress (in MPa)		
Micro-separation distance (μm)	New	Worn	Chamfer
100	576	179	162
120	1295	333	339
250	1740	1116	646

Figure 4.1 compares the 3 sockets during 250 μm microseparation. If we use New socket as a reference, the result shows the reduction of 35% and 63% Von Mises stress in Worn and Chamfer sockets respectively. This study showed that a chamfer on the edge of the socket could reduce contact pressure and Von Mises stress effectively.

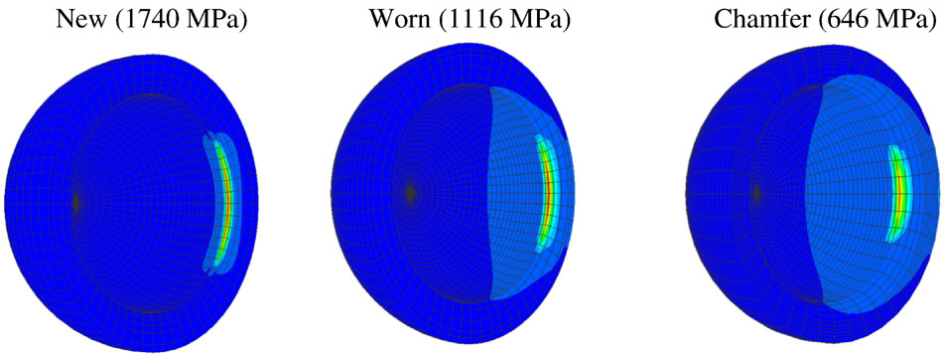

Figure 4.1. Von Mises stress in New, Worn and Chamfer sockets during 250 μm separation [25]

Socket geometry has different aspects, which are explained in following.

4.1.1.1. Edge Chamfer radius

Part 4.1.1 showed that the chamfer on the edge significantly decreases Von Mises stress during EL, however optimising geometry of the chamfer is challenging. Because decreasing the chamfer radius (i.e. from 2.5 mm to 1 mm) increases the effect of EL [25] and increasing it reduces ball coverage and socket articular arc (SAA) [87, 167] that causes EL earlier.

Jacob M. Elkins [168] considered seven pieces of 36 mm diameter MOM sockets (E=210 GPa, ν = 0.3, c= 29 μm, μ = 0.1 and ρ = 9.2 g/cm^3) with chamfer radiuses of 0, 1, 2, 3, 4, 5, 6 mm. These are modelled with FEA when the hip was in fully extension and proceeded to 103º of flexion, 7º of internal rotation and 22º of adduction. The Von Mises stress and contact pressure on the lip was registered. Jacob M. Elkins [168] studied the geometry of the edge in all 148 cases of his previous study [132], which was explained in 3.2.3. This study found that the range of motion (ROM) depends on edge geometry and socket orientation. ROM was increased with inclination of the socket regardless of the chamfer radius effect. Larger chamfer radius was more effective in increasing ROM by inclination, i.e. socket with 6 mm chamfer radius, increased 1º of ROM with every 5º inclination of the socket while ROM increased just with 0.03º with every 5º of socket inclination when the chamfer radius was 0 mm. Similar relationship was discovered with anteversion, ROM and chamfer radius although anteverted socket more than 10º, neglected the effect of chamfer radius on ROM.

Increasing the chamfer radius decreases the EL stress [25, 106] but reducing the ball coverage can make the joint unstable and promotes EL occurrence. For example if

we consider 35º inclination for socket with chamfer radius of 0 mm, EL occurs later due to the maximum coverage of the ball. However when the chamfer radius is increased to 3 mm, SAA decreases and EL occurs earlier. However the socket with chamfer of more than 3 mm radius reduces the intensity of the EL. Hence contact stress was reduced as well. Consequently chamfer radius and corresponding SAA are effective factors in occurrence of EL by different socket orientation [167, 168].

Furthermore as it was explained in 3.3.3, subtended angle, which was related to SAA affects EL as well. In general regardless of socket orientation, ROM decreases with sharper edge due to the faster Neck-Rim impingement [169].

4.1.1.2. Thickness

Mak et al. [107] studied the effect of 2.5 mm to 7.5 mm thickness of the COC sockets on contact stress and contact area of the socket. COC was modelled with Abaqus software to have dimension 28.04 mm inner diameter, alumina material properties (E=380 GPa and ν = 0.26) with radial clearance of C_d= 40 μm under 2500 N force. Furthermore these prostheses were studied with Hertzian contact theory as well to have a better analysis.

The result shows a significant effect of the socket thickness on contact pressure while this is more considerable i.e., when the thickness is decreased below 5 mm the effect is significant. For example the socket with thickness of 2.5 mm shows maximum contact pressure of 40 MPa in FEA and 94.1 MPa in Hertzian contact theory. 5 mm thickness shows 80 MPa and 94.1 MPa of contact pressure while 7.5 mm thickness shows 90 MPa and 94.1 MPa respectively in FEA and Hertzian contact theory which are summarized in Figure 4.2 and Table 4.3. [107].

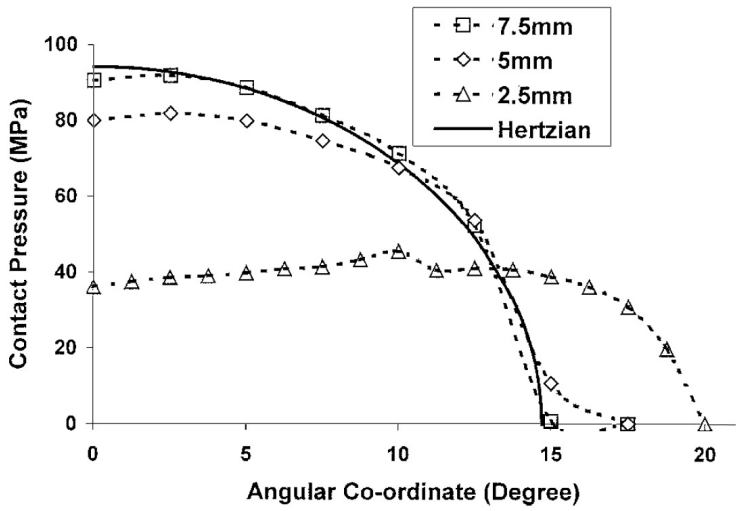

Figure 4.2. Effect of socket thickness to the contact pressure in COC [107]

Although reducing the thickness of the socket significantly reduces contact pressure, it increases tensile stress on the out of the COC socket to 96.1 MPa which can increase the likelihood of ceramic socket fracture. In this regard, choosing the thickness of the socket depends on multiple factors, which should be studied sensibly.

Similar behaviour is consistent with polyethylene liner thickness in MOP and COP. P. Triclot et al. [170] believed thickness of the polyethylene liner should not be less than 8 mm to limit the effect of the stress, fracture, fatigue and delamination of the liner by metal or ceramic balls while this thickness affects the size of the ball.

Table 4.3 Study the effect of radial clearance and thickness of the socket in FEA and Hertzian contact theory[107]

Radial clearance (μm)	Ceramic insert thickness (mm)	Contact half-angle (deg)		Maximum contact pressure (MPa)	
		Finite element	Hertz	Finite element	Hertz
40	2.5	20	14.6	40	94.1
40	5.0	17.5	14.6	80	94.1
40	7.5	15	14.6	90	94.1
20	5	22.5	18.4	50	59.3
80	5	12.5	11.6	140	149.0

4.1.2. Size of the Ball

P. Triclot et al. [170] believed a bigger head increases the head-neck ratio hence the Neck-Rim impingement was delayed therefore implant ROM was increased. Furthermore ball needs to be separated more than the radius of the socket for dislocation

where the ball with larger diameter increases the range of subluxation before dislocation occurs [171]. Burroughs et al. [172] in his experimental study found, the ball with more than 32 mm diameter increased the ROM and also reduced the risk of dislocation significantly.

Some authors [173, 174, 175] believed when the size of the balls were increased in COP and MOP, the wear rate of the polyethylene was increased. This was due to the increase of the contact distance and related speed in comparison with the smaller ball. Indeed the material of the ball is important while ceramic ball makes 50% less wear on the polyethylene than metal ball. BM. Wrobleski et al. [176] believed 22.2 mm diameter MOP caused the same wear that 32 mm COP did. As it was mentioned earlier, increasing of the liner thickness reduces the maximum size of the ball i.e. the socket with 58 mm diameter (8-10 mm polyethylene thickness, 3-5 mm metal-back insert) can receive the ball with 28 to 36 mm diameter. However HCLUHMWPE with thinner profile not only receives the balls with larger diameter up to 42 mm which improved COP and MOP in terms of dislocation but also shows a better mechanical behaviour in *vivo* [177, 178] and *vitro* [179-181].

When eliminating the polyethylene liner in MOM and COC, the size of the ball can be significantly increased (Figure 4.3). Available MOM and COC prostheses in the market have the balls with diameters up to 58 mm and 48 mm respectively which are more similar to the natural size of the femoral head of mean 48.4 mm in male [182]. AG. Rosenberg [183] believes in terms of increasing the stability of the prostheses the ball with diameter of 36 mm and above is needed. Dislocation in 28 mm COC was 4.5% while this is just 1.8% in 36 mm COC [184]. Furthermore 36 mm diameter ball in COC did not cause higher wear rate comparing with 28 mm one [185].

Although MOM comes with biggest possible size of the ball hence is the most stable prosthesis in the market, the risk of releasing ions facing this prosthesis with some difficulty, which was explained in 2.5.3.3.2 and 2.5.4.

Eric Mark et al. [186] compared 28mm diameter ball with 38 mm one in vivo and found that the ROM was not improved with increasing the diameter of the ball. This is in contrast with studies in vitro [172] where 38 mm ball has 7º and 12º ROM more than 32 mm and 28 mm, respectively. However in this study head-neck ratio was at least 2 [187] and Neck-Rim distance did not exceed 25 mm [188, 189] hence the absolute size of the ball may affect stability of the joint but does not affect ROM unless Neck-Rim or/and Neck-Ball ratio are considered.

Figure 4.3. Comparing the size of the ball in different hip prostheses [63].

4.1.3. Radial Clearance

Radial clearance between ball and socket has been addressed as a variable value. From 1977 to 1993 radial clearance was chosen between 7 µm to 10 µm [190, 191] while in last two decades relatively larger range of radial clearances, 5 µm to 86 µm [25, 107, 116, 192, 193] have been addressed. Larger radial clearances enable unmatched balls and sockets to be used. Furthermore cost of manufacturing can be reduced as well. However as it was explained earlier in 2.5.3.4, increasing the radial clearance, C_d, decreased, h_{min} and λ (Figure 2.21 A and C) at the same time it decreased the conformity of the ball and socket, which can disrupt the lubrication regime. Therefore a large value of "C_d" leads the prosthesis to the boundary regime and a low value to the EL. In this regard, radial clearance should be in the safe margin and depends on design of the socket, size of the ball and also material in use.

Mak et al. [107] also studied the effect of radial clearance on contact stress and contact area regardless to the lubrication fluid behaviour. The study showed that the reduction of C_d increased contact area and therefore contact pressure decreased significantly. This is shown in Table 4.3 and Figure 4.4.

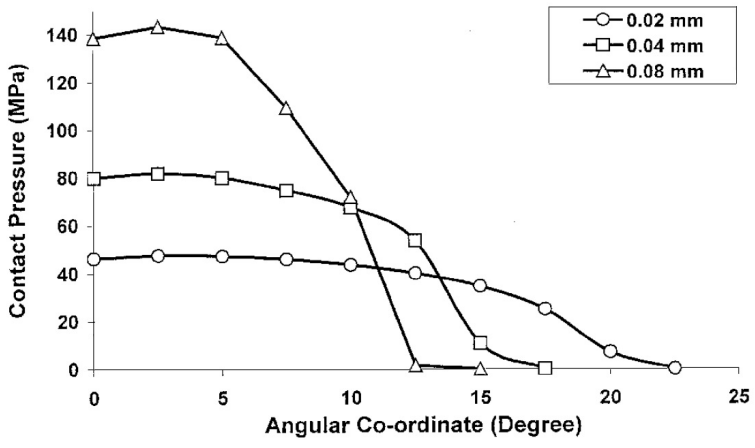

Figure 4.4. Effect of socket thickness to the contact pressure in COC [107]

4.2. Finite Element Method (FEM)

In order to analyse a mechanical problem, mathematical models called *governing equations* are defined. The resulting model is usually deferential equations with sets of initial and boundary conditions. In similar engineering problems, there are two kinds of variables that affect a system.

- The first type of variables defines the material behaviour such as Elastic modulus, Poison ratio, Viscosity etc.
- The second type of variables presents the outside situation or its impact to the object such as external forces, moment of inertia, pressure, temperature etc.

Every differential equation contains both of the aforementioned variables, which will be explained in detail. If differential equations have an exact solution, then the result will be exact. However, there are many difficult problems for which there is no exact solution. Also some other problems are very difficult to solve or computationally very expensive due to their complexity or initial and boundary conditions. In this scenario numerical methods have been used to find solutions, which are approximation to the exact solutions.

In contrast with exact solution method, which gives the absolute result in every point of indiscrete domain of equation, numerical method can provide approximations to the absolute result in discrete domain. In this regard, the domain of the differential equation is divided into the pieces (piecewise approximation). Each part is called element and each vertex of an element is named node. Numerical methods for solving the differential equations are mainly categorised into two groups:

- Finite Difference Method (FDM): In this method a differential equation of each node is written and derivatives are replaced with difference equations, hence the result will be linear in specific time. This method can solve simple mathematical problems.
- Finite Element Method (FEM): In this method a differential equation of each element considering its solved interpolation equation and other applied equations are studied. As a result of the approximation for all elements, general mathematical equation can be obtained which will be replaced with linear or nonlinear algebraic system.

FEM is a numerical method solution which is applicable to the most of the engineering problems such as analysing stress, thermal conductivity, fluid, electromagnetic etc. R. Courant [194] developed this method in 1943. He utilized the mathematical equations to find the solution for vibration systems. The next step was done with M. J. Turner [195] who applied this method in Boeing in 1950's where FEM used for analysing the wings of the airplanes. M. J. Turner et al. [195] developed a numerical analysis and published a paper with title "stiffness and deflection of complex structures". Some years later R. W. Clough [196-200] transferred this technology from aerospace engineering to a wider field of engineering. However until 1970's FEA was being only used in aeronautic and mainframe computers owned by automotive, nuclear and defence industries due to the expensive cost of the computer in that time. With dramatic decreases of computer cost, the usage of FEM has spread widely in the engineering sciences.

4.2.1. Differential equation in geometrical problem

As it was explained, governing equations of the geometrical problem is usually deferential equations with sets of initial and boundary conditions. This chapter with a simple example tries to with solving the mechanical problem with FEM method explains this method.

Figure 4.5 illustrates a trapezoid beam under horizontal force of P. Stress of Figure 4.5c is defined in Equation (4.1) where *A(x)* is the cross section area in the distance of *x* from 0 to L where *t* is a thickness of the beam, which is calculated by (4.2).

$$\sigma = \frac{P}{A(x)} \tag{4.1}$$

$$A(x) = \left[w_1 + \left(\frac{w_2 - w_1}{\mathrm{L}}\right)x\right] t. \tag{4.2}$$

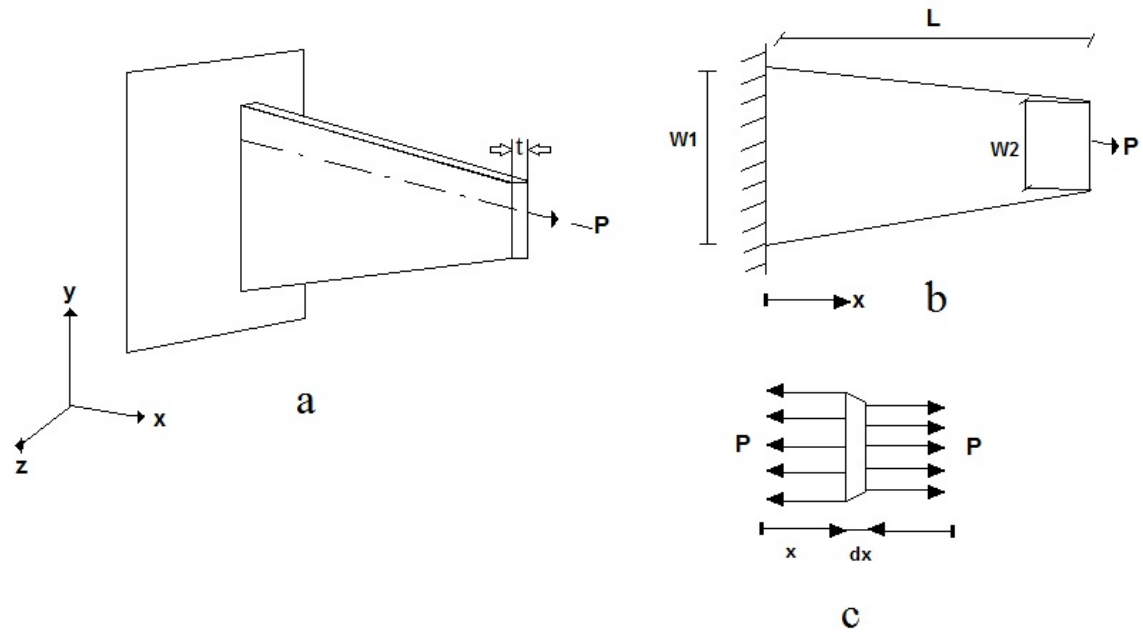

Figure 4.5. Trapezoid beam under horizontal force of P: a) 3D view b) length (L) and Width (W) are shown c) Displacement corresponding to the differential of the cross section

If changing length is defined as *du*, the strain is defined in Equation (4.3). From Hooke's law we have Equation (4.4).

$$\varepsilon = \frac{du}{dx} \tag{4.3}$$

$$\sigma = E\varepsilon \tag{4.4}$$

Replacing Equation (4.1) and Equation (4.3) in Equation (4.4) will result in differential equation of this problem defined by Equation (4.5), which is a first degree differential equation and can be solved easily. This equation can be solved with numerical methods of differential equation solution as well.

$$\frac{P}{A(x)} = E\,\frac{du}{dx} \quad \rightarrow \quad A(x)E\,\frac{du}{dx} - P = 0 \tag{4.5}$$

In this study, the differential equation is solved to obtain the result of whole model while in FEM, differential equations of every element will be solved instead of entire model. Weighted residual methods are among the most common methods in solving the numerical solution of differential equations. The solution is based on postulated results which should meet initial and boundary conditions; thus the result is

not an exact amount i.e. the residue always exists. This method solves through collection method, subdomain method, Galerkin method and least square method.

In general steps of the FEM are as follows:

1. Discretize a domain of the governing equation to the piecewise domain.
2. Define shape functions for every element.
3. Define the equations for every element.
4. Assemble the elements and find the general equations for the model.
5. Apply initial and boundary conditions.
6. Solve the general equations of the model.
7. Carry out post processing and find other important information.

4.2.2. Discretize a domain of the governing equation to the piecewise domain

Regarding to the condition of the problem, the domain of the differential equation can vary. For example in Equation (4.5) in Figure 4.5, a domain of differential equation (x) is a distance between 0 to L. Hence, the domain of this equation contains the whole physical range of the model. In this equation, we denote the applied force by P and a displacement, which is the answer of the question, by u. In other words the result of this equation shows a displacement in every point of trapezoid beam during the applied load of P. studying of this example in FEM only provides an approximate solution to some discrete points in the domain (approximated domain), which is illustrated in Figure 4.6. The points are known as nodes and the area confined between the nodes are called elements. In this regard, instead of solving the equations in all points of the domain, the equation will be approximately solved in the nodes and the final result for the whole domain will be suggested with solving the interpolation equations. The number of effective variables in every node of the system is called degree of freedom (DOF). For example in Figure 4.5 the model has 1 DOF, which is the displacement (*U*) in x-axis and the result of the differential equation.

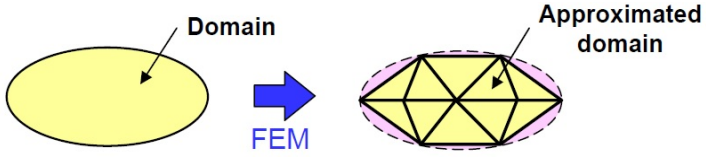

Figure 4.6. Domain and Approximated domain

In Figure 4.5, x domain is between 0 to L. Figure 4.7 discretizes the continuum domain to 4 elements and 5 nodes in one-dimension scale. Figure 4.8a and 4.8b show this element which contains 2 nodes, i and j. Both nodes have one DOF which is a displacement in x-axis. The relationship is defined in (4.6) and (4.7). The symbol of e on $\{U\}^e$ and $\{F\}^e$ means that these relationships belong to the nodes of each element. U_i and U_j are displacements in node i and j, and F_i and F_j are applied forces to these nodes, respectively. F_i and F_j are external forces applied to one element when all elements are integrated into an entire model, these node forces cancel internally and are therefore not considered.

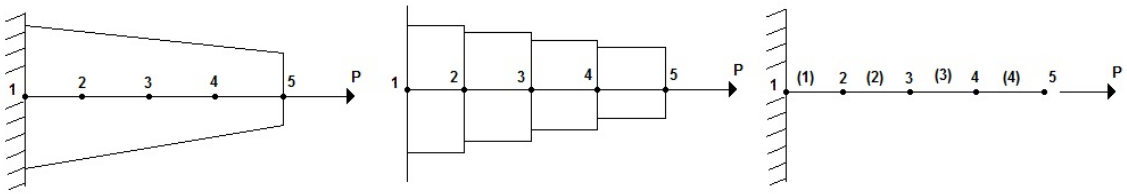

Figure 4.7. Discretised Trapezoid domain of Figure 4.5 to 4 elements and 5 nodes in one-dimension scale

$$\{U\}^e = \{U_i\,, U_j\} \tag{4.6}$$

$$\{F\}^e = \{F_i\,, F_j\} \tag{4.7}$$

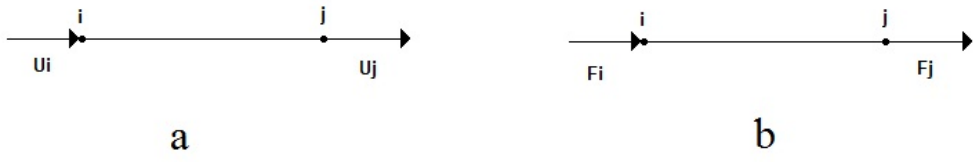

Figure 4.8. 2 nodes of 1D element: a) $\boldsymbol{U_i}$ and $\boldsymbol{U_j}$ are displacements in node i and j b) $\boldsymbol{F_i}$ and $\boldsymbol{F_j}$ are applied forces to node i and j

2D and 3D elements have more nodes and depend on the existing variables (i.e. forces on x-axis, y-axis, z-axis, moments and respective displacements) have different DOF. For example $\{U\}^e$ and $\{F\}^e$ in Figure 4.9a and 4.9b and Figure 4.10a and 4.10b mentioned in (4.8), (4.9), (4.10), and (4.11) respectively.

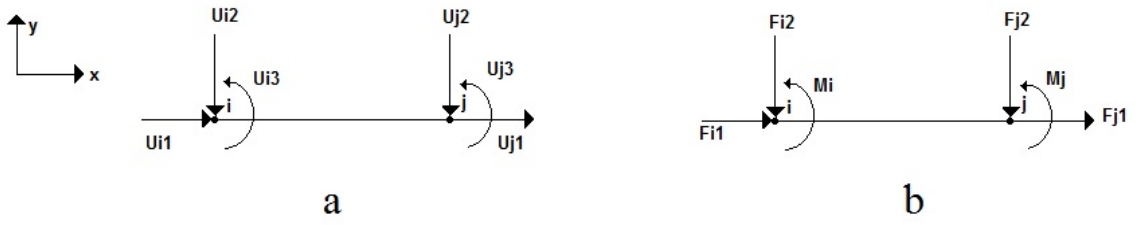

Figure 4.9. 2 nodes of 1D element with 2 forces and moments a) U_{i1} , U_{i2} , U_{i3}, U_{j1}, U_{j2}, U_{j3} are displacements in node i and j b) F_{i1} , F_{i2} , M_i, F_{j1}, F_{j2}, M_j are applied forces and moments to node i and j

$$\{U\}^e = \{U_{i1}\ , U_{i2}\ , U_{i3}, U_{j1}, U_{j2}, U_{j3}\} \tag{4.8}$$

$$\{F\}^e = \{F_{i1}\ , F_{i2}\ , M_i, F_{j1}, F_{j2}, M_j\} \tag{4.9}$$

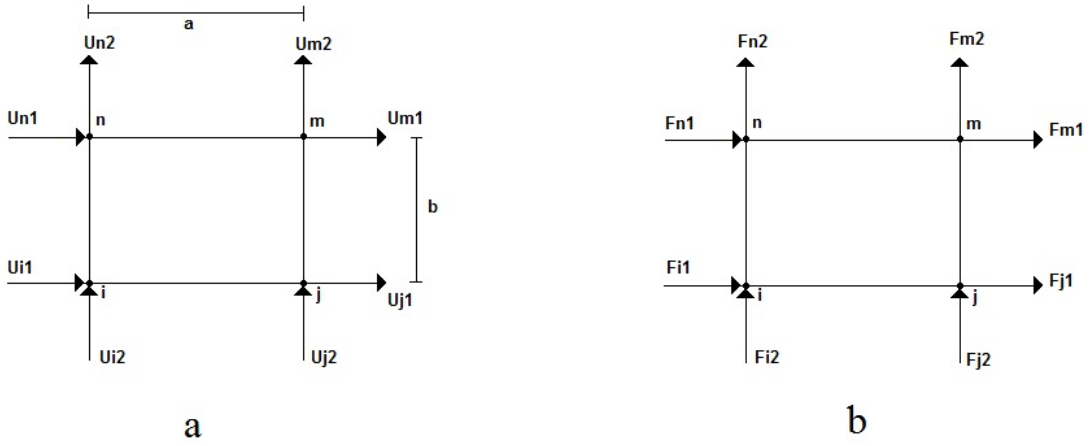

Figure 4.10. 4 nodes of 2D element with 2 forces to every node a) U_{i1} , U_{i2} , U_{j1}, U_{j2}, U_{n1} , U_{n2} , U_{m1}, U_{m2} are displacements in node i, j, n and m b) F_{i1} , F_{i2} , F_{j1}, F_{j2}, F_{n1} , F_{n2} , F_{m1}, F_{m2} are applied forces to node i, j, n and m

$$\{U\}^e = \{U_{i1}\ , U_{i2}\ , U_{j1}, U_{j2}, U_{n1}\ , U_{n2}\ , U_{m1}, U_{m2}\} \tag{4.10}$$

$$\{F\}^e = \{F_{i1}\ , F_{i2}\ , F_{j1}, F_{j2}, F_{n1}\ , F_{n2}\ , F_{m1}, F_{m2}\} \tag{4.11}$$

4.2.3. Definition of shape functions for every element

Shape function is the function that finds a solution of every point in one element corresponding to the value of nodes. Therefore, if the values of the nodes in the element are known, this function explores all other points in the element. In other words this function is a simple first, second or third degree of interpolation function.

Shape function can be linear (one degree), quadratic (second degree) or cubic (third degree) in 1D[16], 2D[17] and 3D[18] elements. The cubic elements are more matching

[16] One dimension
[17] Two dimensions

to the real geometric domain which can be seen in Figure 4.11. For the sake of explanation, we here describe the basic one, which is linear in 1D element as follows.

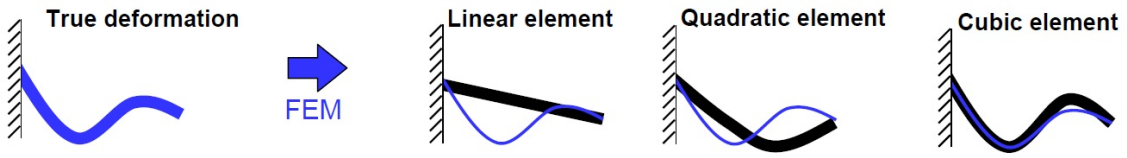

Figure 4.11. Linear (one degree), quadratic (second degree) and cubic (third degree) Shape functions in FEM

4.2.3.1. Linear shape equation in one dimension element

As explained before, the displacement of node i and j were shown by U_i and U_j. Displacement in every point of the element is shown by u^e written as a linear function (4.12) where c_1 and c_2 are unknown constants and X is a position vector in relation to the coordinate system.

$$u^e = c_1 + c_2 X \tag{4.12}$$

With replacing the nodes values in (4.12) the following equations are defined with Equation (4.13) and Equation (4.14):

$$U_i = c_1 + c_2 X_i \tag{4.13}$$

$$U_j = c_1 + c_2 X_j \tag{4.14}$$

With solving of linear system of Equation (4.13) and Equation (4.14), c_1 and c_2 are explained with Equation (4.15) and Equation (4.16) respectively.

$$c_1 = \frac{U_i X_j - U_j X_i}{X_j - X_i} \tag{4.15}$$

$$c_2 = \frac{U_j - U_i}{X_j - X_i} \tag{4.16}$$

Therefore, displacement distribution along the element can be written in (4.17).

[18] Three dimensions

$$u^e = \frac{U_i X_j - U_j X_i}{X_j - X_i} + \frac{U_j - U_i}{X_j - X_i} X \quad \rightarrow \quad u^e = \left(\frac{X_j - X}{X_j - X_i}\right) U_i + \left(\frac{X - X_i}{X_j - X_i}\right) U_j \tag{4.17}$$

From (4.17), shape function of S_i and S_j are shown in Equation (4.18) and Equation (4.19), respectively where l , is a length of the element.

$$S_i = \frac{X_j - X}{X_j - X_i} = \frac{X_j - X}{l} \tag{4.18}$$

$$S_j = \frac{X - X_i}{X_j - X_i} = \frac{X - X_i}{l} \tag{4.19}$$

Hence displacement distribution along the element can be formulated in (4.20) or the matrix shape of (4.21).

$$u^e = S_i U_i + S_j U_j \tag{4.20}$$

$$u^e = (S_i \quad S_j) \begin{pmatrix} U_i \\ U_j \end{pmatrix} \tag{4.21}$$

Shape functions have three interesting features, which are presented as follows:

- In every node of the element, one shape function is equal to 1 and the other one is equal to 0. ((4.22) and (4.23))

$$S_i|_{X=X_i} = \frac{X_j - X_i}{l} = \frac{l}{l} = 1 \qquad S_i|_{X=X_j} = \frac{X_j - X_j}{l} = \frac{0}{l} = 0 \tag{4.22}$$

$$S_j\big|_{X=X_i} = \frac{X_i - X_i}{l} = \frac{0}{l} = 0 \qquad S_j\big|_{X=X_j} = \frac{X_j - X_i}{l} = \frac{l}{l} = 1 \tag{4.23}$$

- Summation of the shape functions is equal to 1 (4.25).

$$\frac{X_j - X}{X_j - X_i} + \frac{X - X_i}{X_j - X_i} = \frac{X_j - X_i}{X_j - X_i} = \frac{l}{l} = 1 \tag{4.25}$$

- Summation of their derivatives respect to X equals to 0 (4.26).

$$\frac{dS_i}{dX} + \frac{dS_j}{dX} = \frac{-1}{X_j - X_i} + \frac{1}{X_j - X_i} = 0 \tag{4.26}$$

Normally increasing the shape function degree to 2 or 3 increases the accuracy of the interpolation functions as well as more conforming of the elements with the whole model feature (Figure 4.11). In this regard one or two nodes need to be added to the each 1D element respectively, because for solving the second degree equations at least 3 known points and for third degree equations, 4 known points are required.

4.2.4. Definition of equations for every element

Always applying a force to the element changes the value of the nodes in that element. The relation between force and nodes value is shown in (4.27). In this mathematical relation, $[K]^e$ is named a stiffness matrix which is the most important part in FEA. In other word, finding the stiffness matrix is equivalent to the solution of the problem in domain of one element. Let $\{F\}^e$ be the force vector and $\{U\}^e$ be displacement vector.

$$\{F\}^e = [K]^e\{U\}^e \tag{4.27}$$

There are three methods to find $[K]^e$ which are: 1) direct stiffness method, 2) minimum potential energy method, and 3) weighted residual method. In this chapter, direct stiffness method will be explained due to its application to the underlying problem.

4.2.4.1. Direct stiffness method

If one of the elements in Figure 4.5 is given, the stress and strain of this part are defined in Equation (4.28) and Equation (4.29) respectively where l is the length of the element.

$$\sigma = \frac{F}{A} \tag{4.28}$$

$$\varepsilon = \frac{\Delta l}{l} \tag{4.29}$$

With replacing of Equation (4.28) and (4.29) in Equation (4.4) (Hooke's law), Equation (4.30) is formulated where *E* is elastic modulus.

$$\sigma = E\varepsilon \;\Rightarrow\; \frac{F}{A} = E\frac{\Delta l}{l} \;\Rightarrow\; F = \left(\frac{AE}{l}\right)\Delta l \tag{4.30}$$

Corresponding to Figure 4.8a Δl can be defined with Equation (4.31) and due to the equilibrium of the element in Figure 4.8b, Equation (4.32) is explainable.

$$\Delta l = U_j - U_i \tag{4.31}$$

$$F_j = -F_i \tag{4.32}$$

Substituting Equation (4.31) and Equation (4.32) in Equation (4.30) results in Equation (4.33) and the matrix form of this equation can be written as (4.34).

$$F_j = -F_i = \left(\frac{AE}{l}\right)(U_j - U_i) \tag{4.33}$$

$$\begin{Bmatrix} F_i \\ F_j \end{Bmatrix} = \frac{AE}{l}\begin{bmatrix} 1 & -1 \\ -1 & 1 \end{bmatrix}\begin{Bmatrix} U_i \\ U_j \end{Bmatrix} \tag{4.34}$$

Respecting to (4.27), the stiffness matrix for this element is formulated with (4.35).

$$[K]^e = \frac{AE}{l}\begin{bmatrix} 1 & -1 \\ -1 & 1 \end{bmatrix} \tag{4.35}$$

4.2.5. Assembling the elements and find the general equations for the model

When the stiffness matrix of the element is computed, all elements of the model should be assembled together to find the stiffness matrix of the entire model. Figure 4.7 discretizes Figure 4.5a to 4 elements and 5 nodes and (4.35) is the stiffness matrix of every element in this model. Therefore, the stiffness matrix of the first element in this model is presented in (4.36), and (4.38) shows the position of this matrix in the whole model stiffness matrix, respecting to the all nodes DOF. (4.37) is a DOF vector in this model.

$$[K]^1 = \frac{A_1 E}{l}\begin{bmatrix} 1 & -1 \\ -1 & 1 \end{bmatrix} \tag{4.36}$$

$$\{u\} = [U_1 \quad U_2 \quad U_3 \quad U_4 \quad U_5]^T \tag{4.37}$$

$$[K]^{(1G)} = \frac{A_1 E}{l}\begin{bmatrix} 1 & -1 & 0 & 0 & 0 \\ -1 & 1 & 0 & 0 & 0 \\ 0 & 0 & 0 & 0 & 0 \\ 0 & 0 & 0 & 0 & 0 \\ 0 & 0 & 0 & 0 & 0 \end{bmatrix}\begin{matrix} U_1 \\ U_2 \\ U_3 \\ U_4 \\ U_5 \end{matrix} \tag{4.38}$$

Furthermore, the positions of the second, third and fourth elements stiffness matrix are presented in (4.39), (4.40) and (4.41) respectively.

$$[K]^{(2G)} = \frac{A_2 E}{l}\begin{bmatrix} 0 & 0 & 0 & 0 & 0 \\ 0 & 1 & -1 & 0 & 0 \\ 0 & -1 & 1 & 0 & 0 \\ 0 & 0 & 0 & 0 & 0 \\ 0 & 0 & 0 & 0 & 0 \end{bmatrix}\begin{matrix} U_1 \\ U_2 \\ U_3 \\ U_4 \\ U_5 \end{matrix} \tag{4.39}$$

$$[K]^{(3G)} = \frac{A_3 E}{l}\begin{bmatrix} 0 & 0 & 0 & 0 & 0 \\ 0 & 0 & 0 & 0 & 0 \\ 0 & 0 & 1 & -1 & 0 \\ 0 & 0 & -1 & 1 & 0 \\ 0 & 0 & 0 & 0 & 0 \end{bmatrix}\begin{matrix} U_1 \\ U_2 \\ U_3 \\ U_4 \\ U_5 \end{matrix} \tag{4.40}$$

$$[K]^{(4G)} = \frac{A_4 E}{l}\begin{bmatrix} 0 & 0 & 0 & 0 & 0 \\ 0 & 0 & 0 & 0 & 0 \\ 0 & 0 & 0 & 0 & 0 \\ 0 & 0 & 0 & 1 & -1 \\ 0 & 0 & 0 & -1 & 1 \end{bmatrix}\begin{matrix} U_1 \\ U_2 \\ U_3 \\ U_4 \\ U_5 \end{matrix} \tag{4.41}$$

Stiffness matrix of the entire model is the summation of all elements stiffness matrices. (4.42) is the stiffness matrix, $[K]^{(G)}$, for entire model in Figure 4.5 which was separated by four 1D elements. This can be written with (4.43) where $K_i = \frac{A_i E}{l}$

$$[K]^G = [K]^{1G} + [K]^{2G} + [K]^{3G} + [K]^{4G} \tag{4.42}$$

$$[K]^{(G)} = \begin{bmatrix} K_1 & -K_1 & 0 & 0 & 0 \\ -K_1 & K_1 + K_2 & -K_2 & 0 & 0 \\ 0 & -K_2 & K_2 + K_3 & -K_3 & 0 \\ 0 & 0 & -K_3 & K_3 + K_4 & -K_4 \\ 0 & 0 & 0 & -K_4 & K_4 \end{bmatrix} \quad (4.43)$$

4.2.6. Apply initial and boundary conditions

When $[K]^{(G)}$ is computed, the application of the initial and the boundary conditions to the models leads to DOF of the model (i.e. the value of nodes displacements). The relation between total stiffness matrix, displacement and applied forces is shown in (4.44) where G denotes this relation is for the entire model.

$$\{F\}^G = [K]^G\{U\}^G \quad (4.44)$$

Equation (4.44) is a basis of the most static problems where $\{F\}$ can be force, heat, charge etc. $[K]$ may denote stiffness, conductivity, viscosity etc. and $\{U\}$ is usually the answer of the equation which can be displacement, temperature, velocity etc. Figure 4.12 summarizes all. In a static system, time is not considered while in reality all systems performing dynamically where time is addressed. However, if the application of the load or displacement was slow enough, system is assumed to behave statistically where the inertial forces were neglected. Dynamic system needs more complex equations, which is not the concern of this study. For dynamic analysis of the hip joint, we refer to El'Sheikh [201] and Senalp [202].

Unknown

	Property $[\mathbf{K}]$	Behavior $\{\mathbf{u}\}$	Action $\{\mathbf{F}\}$
Elastic	stiffness	displacement	force
Thermal	conductivity	temperature	heat source
Fluid	viscosity	velocity	body force
Electrostatic	dialectri permittivity	electric potential	charge

Figure 4.12. Different parts of Governing equation in static system

In Figure 4.5, the external force, P, is applied to the end of the Trapezoid beam. Therefore a force (actually P) is applied only to the fifth node of the elements in Figure 4.7. Therefore, the force matrix can be written in (4.45). Furthermore, the first node in Figure 4.7 is unable to have displacement due to the attachment of the beam to the wall leading to $U_1 = 0$ hence (4.46) is a general equation for this model.

$$\{F\} = \begin{Bmatrix} 0 \\ 0 \\ 0 \\ 0 \\ P \end{Bmatrix} \tag{4.45}$$

$$\begin{bmatrix} 1 & 0 & 0 & 0 & 0 \\ -K_1 & K_1 + K_2 & -K_2 & 0 & 0 \\ 0 & -K_2 & K_2 + K_3 & -K_3 & 0 \\ 0 & 0 & -K_3 & K_3 + K_4 & -K_4 \\ 0 & 0 & 0 & -K_4 & K_4 \end{bmatrix} \begin{Bmatrix} U_1 \\ U_2 \\ U_3 \\ U_4 \\ U_5 \end{Bmatrix} = \begin{Bmatrix} 0 \\ 0 \\ 0 \\ 0 \\ P \end{Bmatrix} \tag{4.46}$$

4.2.7. Solution of the general equations of the model

The final step in FEM is to solve the general equation of the model. In the example of Figure 4.5, if $E = 10.4\times10^6 \ \frac{\mathrm{N}}{\mathrm{m}^2}$, $P = 1000$ N, $w_1 = 2$ m, $w_2 = 1$ m, $t = 0.125$ m and $L = 10$ m from Equation (4.2), the cross section area of the Trapezoid beam along x is provided by Equation (4.47). Therefore, cross-section areas of the model in five mentioned nodes in Figure 4.7 are as follows. $\mathrm{A}_1 = 0.25\ \mathrm{m}^2$, $\mathrm{A}_2 = 0.21875\ \mathrm{m}^2$, $\mathrm{A}_3 = 0.1875\ \mathrm{m}^2$, $\mathrm{A}_4 = 0.15625\ \mathrm{m}^2$ and $\mathrm{A}_5 = 0.125\ \mathrm{m}^2$.

$$\mathrm{A(x)} = \left[\mathrm{w}_1 + \left(\frac{\mathrm{w}_2 - \mathrm{w}_1}{\mathrm{L}}\right)\mathrm{x}\right]\mathrm{t} = \left[2 + \left(\frac{1-2}{10}\right)\mathrm{x}\right](0.125) = 0.25 - 0.0125\mathrm{x} \tag{4.47}$$

Cross section area of one element is equal to the summation of the cross section areas of its nodes divided by the quantity of them where in this example $A = \frac{\mathrm{A_i} + \mathrm{A_{i+1}}}{2}$. If $L = 10$ m, every node in Figure 4.5 has the length of 2.5 m and the stiffness matrixes ($\mathrm{K_i} = \frac{\mathrm{A_i E}}{\mathrm{l}}$) of the four elements in this figure are as following: $\mathrm{K}_1 = 975\times10^3 \ \frac{\mathrm{N}}{\mathrm{m}}$, $\mathrm{K}_2 = 845\times10^3 \ \frac{\mathrm{N}}{\mathrm{m}}$, $\mathrm{K}_3 = 715\times10^3 \ \frac{\mathrm{N}}{\mathrm{m}}$ and $\mathrm{K}_4 = 585\times10^3 \ \frac{\mathrm{N}}{\mathrm{m}}$ and the matrices are as following. Assembling these matrixes results in the general equation matrix of this example in (4.48).

$$[K]^1 = 10^3 \begin{bmatrix} 975 & -975 \\ -975 & 975 \end{bmatrix}$$

$$[K]^2 = 10^3 \begin{bmatrix} 845 & -845 \\ -845 & 845 \end{bmatrix}$$

$$[K]^3 = 10^3 \begin{bmatrix} 715 & -715 \\ -715 & 715 \end{bmatrix}$$

$$[K]^4 = 10^3 \begin{bmatrix} 585 & -585 \\ -585 & 585 \end{bmatrix}$$

$$[K]^{(G)} = \begin{bmatrix} 975 & -975 & 0 & 0 & 0 \\ -975 & 975+845 & -845 & 0 & 0 \\ 0 & -845 & 845+715 & -715 & 0 \\ 0 & 0 & -715 & 715+585 & -585 \\ 0 & 0 & 0 & -585 & 585 \end{bmatrix} \quad (4.48)$$

Having taken the initial and boundary conditions of this example into account, the general equation of this example is developed in (4.49).

$$10^3 \begin{bmatrix} 1 & 0 & 0 & 0 & 0 \\ -975 & 1820 & -845 & 0 & 0 \\ 0 & -845 & 1560 & -715 & 0 \\ 0 & 0 & -715 & 1300 & -585 \\ 0 & 0 & 0 & -585 & 585 \end{bmatrix} \begin{Bmatrix} U_1 \\ U_2 \\ U_3 \\ U_4 \\ U_5 \end{Bmatrix} = \begin{Bmatrix} 0 \\ 0 \\ 0 \\ 0 \\ 10^3 \end{Bmatrix} \quad (4.49)$$

Solving the general equation (4.49) leads to the results which are displacement of every nodes in Figure 4.7 as follows:

$U_1 = 0\ m$

$U_2 = 0.001026\ m$

$U_3 = 0.002210\ m$

$U_4 = 0.003608\ m$

$U_5 = 0.005317\ m$

4.2.8. Post processing and other important information

In terms of post processing, other important information can be obtained by model stiffness matrix. For example, the average stress of every element in Figure 4.7 can be defined by Equation (4.50). Hence the stress of the four elements are obtained as following:

$$\sigma = E\varepsilon = E\left(\frac{U_{i+1} - U_i}{l}\right) \quad (4.50)$$

$$\sigma^{(1)} = E\left(\frac{U_2 - U_1}{l}\right) = 4268\,\frac{N}{m^2}$$
$$\sigma^{(2)} = E\left(\frac{U_3 - U_2}{l}\right) = 4925\,\frac{N}{m^2}$$
$$\sigma^{(3)} = E\left(\frac{U_4 - U_3}{l}\right) = 5816\,\frac{N}{m^2}$$
$$\sigma^{(4)} = E\left(\frac{U_5 - U_4}{l}\right) = 7109\,\frac{N}{m^2}$$

4.2.9. FEM with Abaqus software

Abaqus software analyses models with FEM. From sketching the geometry of the model to analysing, there are 9 modules, which are briefly explained here:

1. Sketch module: This module enables us to sketch the geometry of desired models.
2. Part module: With this module different parts of the model are made in 2D or 3D.
3. Property module: This module defines the properties of the material(s) is/are used in the parts.
4. Assembly module: With this module the parts can be sit together, in other words this montages the model.
5. Step module: Different types of analyses are explained in this module.
6. Interaction module: This module defines a type of contact between different surfaces.
7. Load module: Initial and boundary conditions are set in this module.
8. Mesh module: When the above 7 steps have been done; this module discretizes a domain of the model.
9. Job module: In this module, a completed finite element model is transferred to one of the analysers i.e. Abaqus/Standard or Abaqus/Explicit.

4.2.10. Different types of elements in Abaqus software

In Abaqus, elements can be categorised with their dimensions or the method of analysing.

Elements in terms of dimension divided to 1D, 2D, 3D and in terms of analysing are divided to the following:

- Stress-Strain elements
- Coupled Temperature-Displacement
- Acoustic
- Cohesive
- Continuum shell
- Heat transfer
- Piezoelectric
- Pore Fluid/Stress
- Thermal electric
- User defined

To analyse our model in this research, 3D elements are chosen with Stress-Strain analysing. DOF in this type is displacement and chosen elements are quadric continuum elements with the name of C3D20R in Abaqus. This name in Abaqus shows the information of the element. For example in the aforementioned element, C means Continuum, 3D means three dimensions element, 20 is the number of the nodes in every element and R means reduced integration. If this element is changed to the linear one number of the nodes reduced to 8, hence the name of the element will be C3D8R. Reduced integration means, the number of the chosen points for calculating of integration is reduced. This increases the speed of calculation but slightly reduces the accuracy of computation. There can be some other elements in naming of the element for example C3D20RHT, where H means hybrid which is used when the model is not dense, and T means this element is used for coupled temperature-displacement. However because it is not our concern in this study will not be explained further.

4.3. Hertzian Contact Theory

As explained in part 2.5.2.1, the best method to study the contact mechanic behaviour of the hip prostheses is FEM, however the first approximation in analytical solution can be based on Hertzian contact Theory [203] which is both explained in this chapter and used to analyse EL phenomena in Chapter 7.

When any two curved surfaces contact each other, the contact initiates with point or along a line. With a small load, elastic deformation spreads these into contact areas and the load is distributed as a pressure. This is first explained by Hertz in 1881 [203] based on four assumptions, which are:

1. Material should be homogeneous, isotropic and linear elastic

2. Contact surfaces should be smooth and frictionless
3. Contact surfaces should be continues and non-conformed
4. Contact radius should be much smaller than radius of the surfaces are in contact.

In our study there is a contact of the ball and socket which is named conformal contact and also EL contact which is not conformal contact and basically ball is contacted with smaller ball which is the chamfer part of the edge of the socket. In this regard just the spherical contact of Hertzian contact theory explained in this dissertation and parallel or inclined axis cylinders are not explained further.

If elastic sphere 1 with radius of R_1 pushed to the sphere 2 with radius R_2 with force of W (Figure 4.13), the contacted area will be circular with radius of (a) this can be defined by Equation (4.51). The effective contact modulus E' is defined in Equation (4.52) and R which is the effective radius of curvature, is defined by Equation (4.53) where convex curvature (ball in our study) has a positive radius and the concave one (socket in our study) has negative radius. Equation (4.52) and Equation (4.53) can be rewritten as following when they apply to the ball and socket of our study. v and E are Poisson's ratio and Young's modulus, respectively and $C_d = R_{cup} - R_{head}$ is the radial clearance between ball and socket [60].

$$a = \{\frac{3WR}{4E'}\}^{⅓} \tag{4.51}$$

$$\frac{1}{E'} = \frac{1-v_1^2}{E_1} + \frac{1-v_2^2}{E_2} \quad \rightarrow \quad \frac{1}{E'} = \frac{1-v_{head}^2}{E_{head}} + \frac{1-v_{cup}^2}{E_{cup}} \tag{4.52}$$

$$\frac{1}{R} = \frac{1}{R_1} + \frac{1}{R_2} \quad \rightarrow \quad R = \frac{R_{cup}R_{head}}{R_{cup}-R_{head}} = \frac{R_{head}(R_{head}+C_d)}{C_d} \tag{4.53}$$

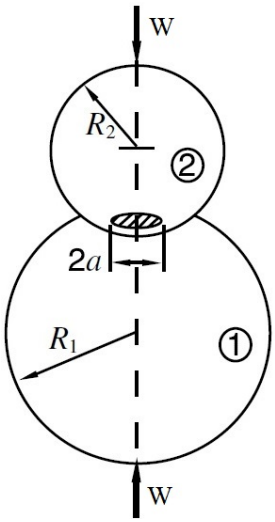

Figure 4.13. Elastic sphere 1 with radius of $\boldsymbol{R_1}$ contacts with force of *W* to the sphere 2 with radius $\boldsymbol{R_2}$ and made circular area with radius of ($\boldsymbol{a}$)

The result of the distributed pressure *P(r)* is presented as a semi elliptical, it is shown in Figure 4.14 and calculated with Equation (4.54). The mean pressure, P_m, is defined with Equation (4.55), which can be rewritten in the favour of finding P_0.

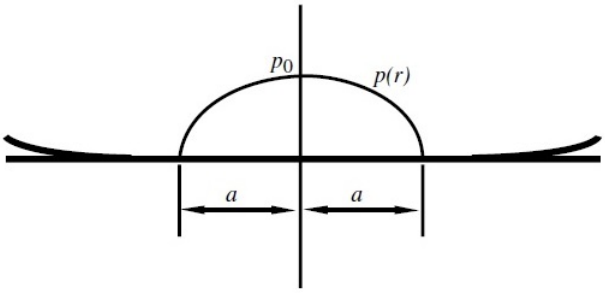

Figure 4.14. Contact of 2 surfaces result of the distributed pressure *P(r)* as a semi elliptical

$$P(r) = P_0\sqrt{1 - \frac{r^2}{a^2}} \tag{4.54}$$

$$P_m = \frac{2P_0}{3} = \frac{W}{\pi a^2} \qquad \rightarrow \qquad P_0 = \frac{3P_m}{2} = \frac{3W}{2\pi a^2} \tag{4.55}$$

From Equation (4.51) and Equation (4.55) we can have Equation (4.56), which helps us to find P_0 without having to consider the contacted area of a.

$$P_0 = \{\frac{6WE'^2}{\pi^3 R^2}\}^{1/3} \tag{4.56}$$

Proof:

$$P_0 = \frac{3W}{2\pi a^2} = \frac{3W}{2\pi(\{\frac{3WR}{4E'}\}^{1/3})^2} = \frac{3W}{2\pi\{\frac{9W^2R^2}{16E'^2}\}^{1/3}}$$

$$P_0{}^3 = \frac{27W^3}{\frac{8\pi^3*9W^2*R^2}{16E'^2}} = \frac{27W^3*16E'^2}{8\pi^3*9W^2*R^2} = \frac{3W*2E'^2}{\pi^3*R^2} \Rightarrow P_0 = \{\frac{6WE'^2}{\pi^3R^2}\}^{1/3}$$

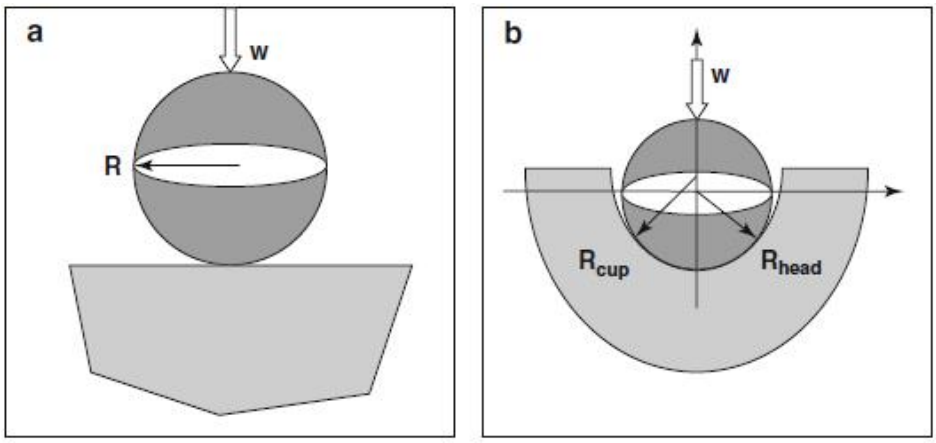

Figure 4.15. Application of Hertzian contact theory to a) Ball-on-plane b) Hip prosthesis [60]

4.3.1. Analysis of EL with Hertzian Contact Theory

Hertzian theory validated FEA [107] while this method is more applicable to the EL condition than the normal condition. This is due to its closer condition to the main four assumptions of the Hertzian contact theory. The first two assumptions are mainly related to the material of the prostheses, where ceramic in both studies can closely meet the assumptions, however assumptions three and four mostly meet the EL condition more than the normal one. Firstly, this is due to the fact that in EL condition, the ball is not conformed with edge of the socket (which is the reason of the EL). Although in both cases surfaces are not continues, in EL condition the ball surface can be assumed continuous with respect to the surface of the contacted area but this is not the case for edge surface or for conformal contact in first case where the surfaces were conformed and non-continues. Secondly, a ball with much bigger radius (i.e. 24 mm) contacts the chamfer of the edge has a radius of almost one-tenth of the ball radius (i.e. 2.5 mm). This meets the Hertzian fourth assumption for ball surface in EL condition but not in the normal condition.

Nevertheless part 5.2 explains a novel hip prosthesis that accommodates ball with conformal contact area of the socket, which ideally can prevent EL. In this regard

Hertzian contact theory less applicable to study of this prosthesis during EL condition, because the new design provides similar condition that the conformal contact of the ball and the socket does before EL; hence the same limitation would be existed. This is more explained in Chapter 7.

Chapter 5：Design of Hip Prostheses

As mentioned in Chapter 3, many factors contribute in the occurrence of EL while some of them can be limited with improving the surgical technique, well positioning of the prostheses or patient's activities. However other ones have not been improved yet. The problem such as microseparation happens with every walking cycle and causes EL. In this regard, scientists have been investigating EL with different techniques such as those explained in Chapter 3 and Chapter 4. Nevertheless; in all circumstances, solution of EL may only be, change of the material and/or design of the prostheses [25, 39, 107]. Mathew Mak et al. [25] states:

"Potential solutions to this problem lie in alternative material and design"

In terms of material; ceramic has shown the most reliable behaviour during normal and EL conditions with the lowest wear rate and highest biocompatibility among all today available prostheses. Furthermore as discussed in 3.1.3, AMC as a gold standard ceramic material has the best mechanical behaviour comparing with other available COC. Although we hope future science develops a new material that shows even better mechanical properties than AMC, it seems it will be unlikely to solve EL without modifying the design of prostheses. Moreover, we believe a modified/new design can solve the problem even with the available materials.

5.1. Important factors in conventional hip prostheses

The most effective factors in design of the hip prostheses which were explained in methodology of designing in Chapter 4, are summarised below:

- Increasing the chamfer radius decreases the EL stress [25, 106] but coincidently reduces the ball coverage which can make the joint unstable and promotes EL occurrence. 2.5 mm chamfer is usually chosen by manufacturer and scientists [25, 107, 206, 207]
- According to Part 4.1.1.2 when the thickness of the socket was decreased below 5 mm, the effect of the contact pressure and Von Mises stress are reduced but tensile stress would be increased significantly which was a reason of a crack in COC [107]. This is in line with Ceramtec decision in using of the socket with 5 mm thickness for their Biolox delta prostheses [102,103, 204, 205, 206].

- Higher ratio between neck and ball increases ROM and the bigger ball can stabilise the joint. Nowadays there are hip prostheses with the maximum size of 60mm in MOM and 48mm in COC [170].
- Increase in C_d, decreases h_{min} and λ (Figure 2.21 A and C) and at the same time decreases the conformity of the ball and socket which can disrupt the lubrication regime. Therefore large value of the "C_d" leads the prosthesis to the boundary regime and the low value to the EL. CeramTec [204] addressed the radial clearance of 40 μm as the most reliable C_d, for their COC with 28mm to 48mm diameter balls [25, 107, 204, 205, 206].

  All the above features can improve performance of the hip prosthesis in terms of effecting on EL. However, they cannot solve it yet. Biolox Delta which considers all above features show the best performance in terms of mechanical behaviour between all available hip prostheses in the market while EL in this prosthesis still shows significant wear rate in comparison with prostheses with no EL (Figure 3.12, 3.13 and 3.14). Therefore, the presence of EL is still affecting the prostheses significantly unless the ball is restricted to the radial clearance which may disable EL.

5.2. Novel design

Part 5.1 explained important factors in designing of the hip prosthesis in terms of reducing the effect of EL and improving the mechanical behaviour of the prostheses during patient's activity. Considering these factors and understanding EL phenomena, which were explained in depth in Chapter 3, paved the way to invent a new hip prosthesis that is patented with PCT number: PCT/GB2015/052933 and published with International Publication Number "WO2016/055783Al" with Title of "AN ACETABULAR CUP FOR A HIP REPLACEMENT JOINT" (Appendix D). The Invented Model (IM) feature is explained in this chapter and will be tested, analysed and compared with the best available prostheses in the market in Chapter 6 and 7.

As explained earlier, EL occurs if the ball loads the edge of the socket. For this purpose; firstly the ball should be able to get enough distance from the centre of the socket for loading the small area of the socket's edge (Formula (3.1)) and secondly the ball must reach to the edge of the socket. In this regard, limiting these two factors were the main objectives in devising the IM.

The IM is designed with minimum changes applied to the features of the conventional prosthesis, which are known to be reliable and simultaneously obtains the

maximum improvement in mechanical behaviour of the prostheses in terms of EL. Furthermore the ease of use, practicality and simplicity of the IM encourage manufacturers, surgeons and patients to appreciate the design and facilitates the way of being accepted as a new hip prosthesis in the market. The IM is designed to be very user friendly, in this regard the IM preserves the main structure of conventional model (CM) prostheses and just a tiny ring is attached to the main socket in specific way which is explained in following.

5.2.1. Features of the IM

In IM, only an acetabulum component is modified and the ball remains as it was in all other hip prostheses. The ring of the IM effectively continues the inner surface of the main socket with no interruption, to narrow the opening area of the IM socket. This feature stops the ball from coming out of the socket. The end face of the main socket (Figure 5.1b) and the corresponding face of the ring (Figure 5.1c and 5.1e) are provided with complimentary alignment features to align the ring with respect to the main socket. This alignment feature is in the form of a circumferential rib and groove extending around the circumference of the ring and the cup respectively to joint these two together. The attachment of the groove and the rib (Figure 5.6d) could be done by biocompatible adhesive (Loctite made by Henkel-Germany) for all IM prostheses or simply press fitting if they are made of metal (i.e for MOM). In terms of using the adhesive, the rib and groove have enough spaces between the bonding surfaces for placing the adhesive. Having a number of these surfaces increases the bonding strength significantly. These are shown in Figure 5.1d and Figure 5.2b. In terms of press fitting, the rib may be slightly larger than the groove or provided with some barbs (Figure 5.1e and Figure 5.1f) to undergo plastic deformation and lock the main socket to the ring and makes the complete IM socket. Press fitting is possible with or without using of biocompatible adhesive. In press fitting, adhesive can be placed between the spaces which are between barbs and/or the end surfaces of the ring and groove.

The face of the ring is flat with the same slope of the neck in the time of meeting the ring in extensive motion of the hip. Therefore neck and ring are conformed in this occasion. Furthermore the inner (Figure 5.2c) and outer (Figure 5.2d) edges of the ring at the end of the ring have convexly curved chamfers. This feature prevents the contact of the sharp edge to the neck or ball interiorly and eliminates the risk of contacting of the soft tissues around a joint to the sharp outer edge of the socket in the human body which may causes injury.

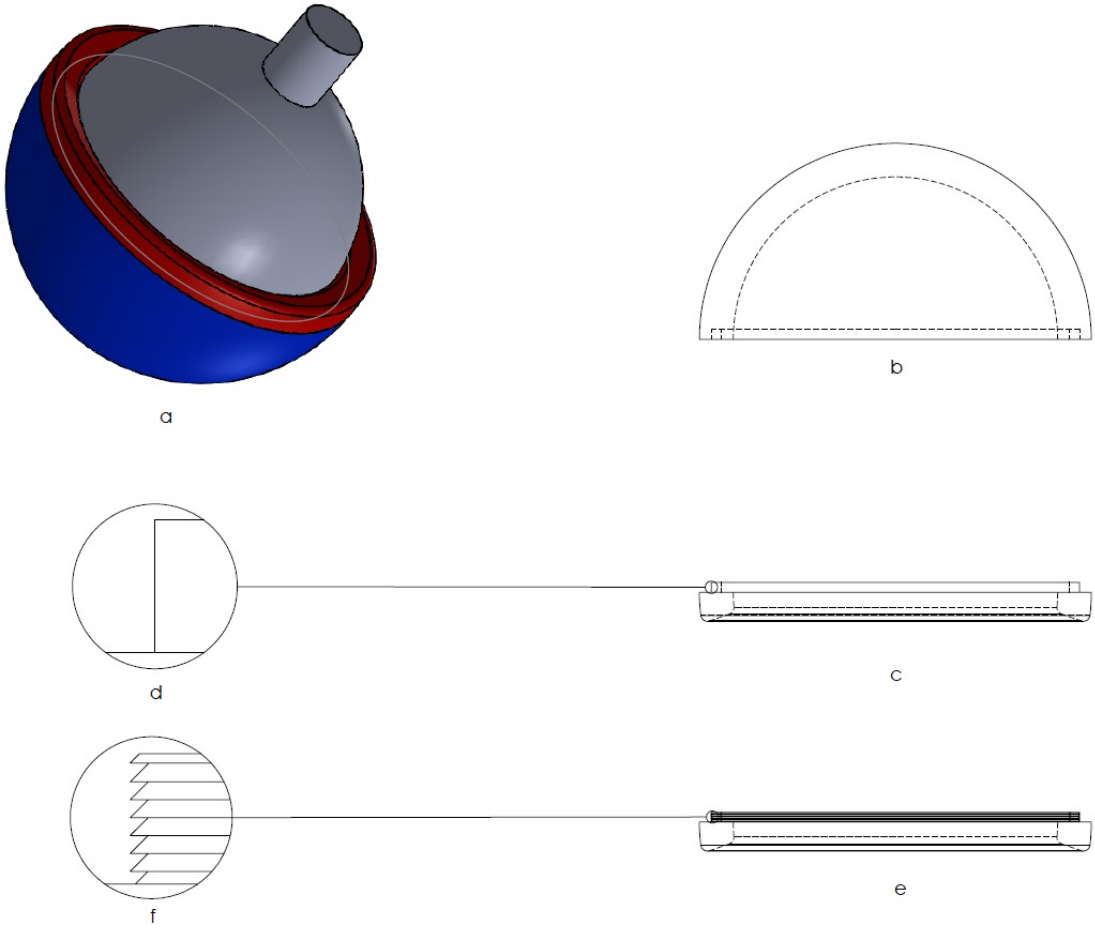

Figure 5.1. IM a) Complete set. b) Main socket. c) Ring for adhesive. d) Rib. e) Ring for press fitting f) Rib with barbs

5.2.2. Main advantages of the IM

As is conceived from the features of IM, the opening area of the IM socket is smaller than the diameter of the ball hence ball cannot move out of the IM socket or separated more than radial clearance in all directions. This limitation not only solves the dislocation problem but also increasing the coverage area, and prevents the ball from meeting the edge of the socket. Furthermore, dispersing the load to the wider area (ring circumference) significantly reduces the stresses which possibly prevents EL or significantly limits it. In comparison with conventional prostheses the reduction of stress in the IM is postulated either during normal activity where microseparation is inevitable or during Rim-Neck impingement. The next chapter explores this hypothesis further.

The flat surface of the ring enables the neck to contact a more conformed surface of the ring and the load will be distributed respectively across the surfaces more

than on the point on the edge. The inner chamfer of the ring (Figure 5.2c) effectively eliminates the impingement of the ball and the neck to the sharp edge. The outer chamfer (Figure 5.2d) makes smoother contact of the IM socket with human tissues as well as the neck. The radius of the chamfer is small to leave maximum contact area during Neck-Ring impingement (Figure 5.3).

The low profile nature of the IM ring has following advantages:

1. The size of the ball can be maximised for any given anatomy.
2. The cost of manufacturing is minimized.
3. Simple design is more acceptable for manufacturer, surgeon and patient.
4. Makes it applicable to all kind of hip prostheses with any size, though it is more preferable for MOM and COC with reasonably larger size of the ball.
5. ROM is maximised and just decreased about 10% (Figure 5.3) in comparison with CM (Figure 5.4).

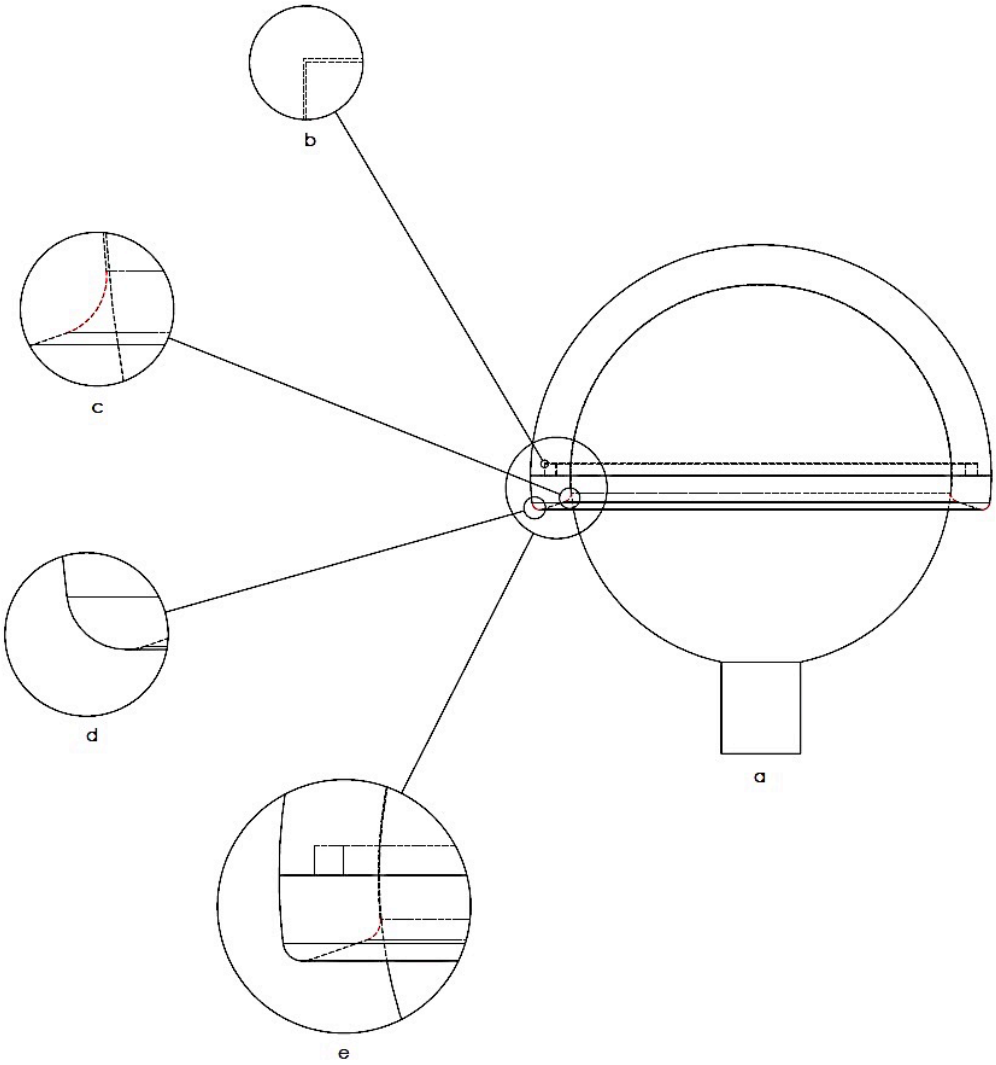

Figure 5.2. Schematic of IM in detail which are sketched with Solid Work. a) Complete IM prosthesis b) bonding surface tolerance in COC c) Inner chamfer of the ring d) Outer chamfer of the ring e) ring in detail

5.3. Range of Motion in IM and CM

The schematic and range of motions of the IM and conventional hip prostheses (Biolox Delta COC) are shown in Figure 5.3 and Figure 5.4 respectively. The size of the IM ball is 48mm which is the maximum size of the ball which has been used in COC (Biolox Delta made by Ceramtec) with radial clearance of 40µm. IM and Biolox Delta 48 mm Alumina-Zirconia which is the best available hip prostheses in the market, are compared and analysed under same condition in Chapter 6 and 7

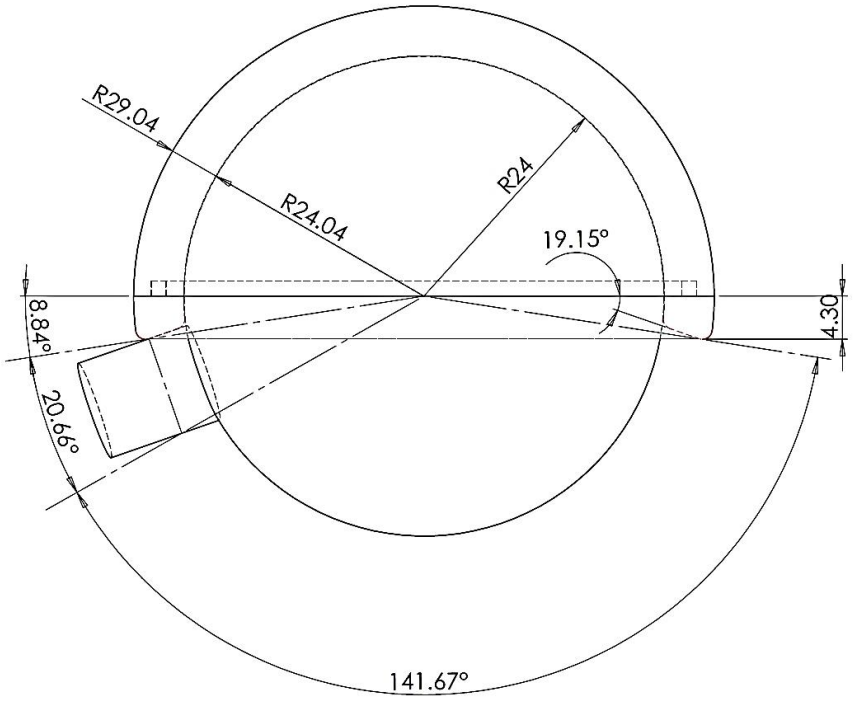

Figure 5.3. Dimensions and range of motion in 48mm IM hip prostheses

Although the range of motion in IM was slightly reduced by the ring, still the remained range of motion is more than enough for patient's daily activities in normal conditions. Boone DC et al. [137] believed the full range of motion of the hip joint is as following:

- Flexion: -10° to 120°
- Rotation: -40° to 40°
- Abduction: -25° to 40°

Hence the maximum range of motion which belongs to flexion with 130° of range of motion, is still less than ROM of the IM with 141°. Indeed this is applicable to the normal daily activities and does not include some sports which include hypermobility of the hip such as yoga, gymnastic and martial arts. Furthermore, the

optimum fixation of the prosthesis in the acetabulum should be considered which was explained earlier.

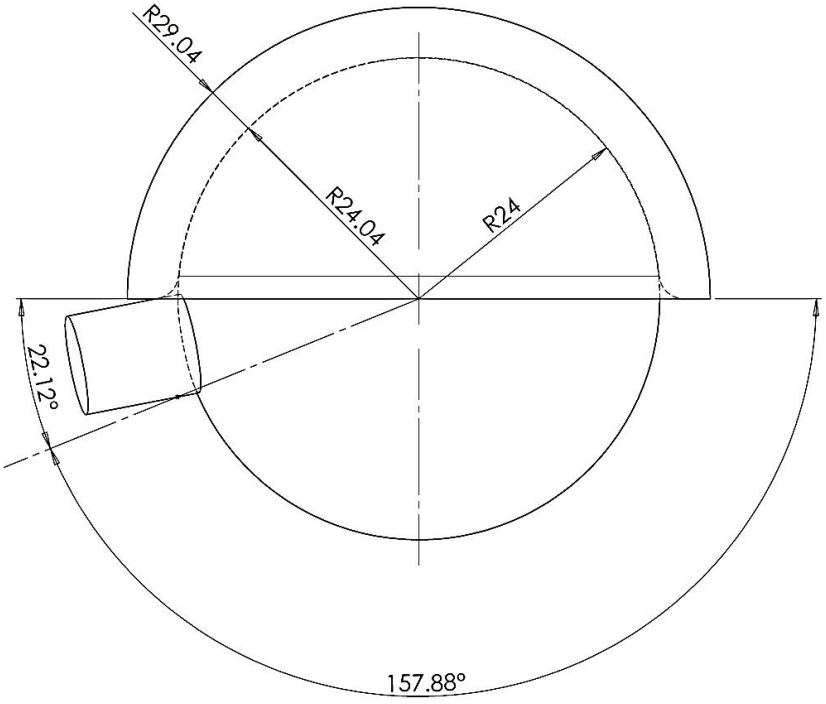

Figure 5.4. Dimensions and range of motion in 48mm Biolox Delta hip prostheses

5.4. IM Rapid Prototype

Physical examination of the prototypes showed that the design is workable and could easily be handled by surgeons in theatre, furthermore IM and CM can be compared in all aspects.

There are two 3D-Printing machines available in our School which are UP Plus (Figure 5.5a) and Stratasys Objet24 (Figure 5.5b). UP Plus prints/makes the object by Acrylonitrile-Butadiene-Styrene (ABS) plastic with minimum layer resolution of 150μm which is relatively rough. Low cost of printing is the main advantage of this machine in comparison with Stratasys Objet24 which prints the object by rigid white opaque photopolymers (VeroWhitePlus) with layer resolution of 28μm.

The rapid prototype of IM is made with UP Plus 3D printer in the Engineering laboratory of The University of Warwick. Three components of full IM prosthesis are shown in Figure 5.6a when they are disassembled. Figure 5.6b shows it when they are assembled. Figure 5.6c shows the face of the ring and the groove of the main socket and Figure 5.6d shows rib of the ring which is fitted in the groove of the main socket.

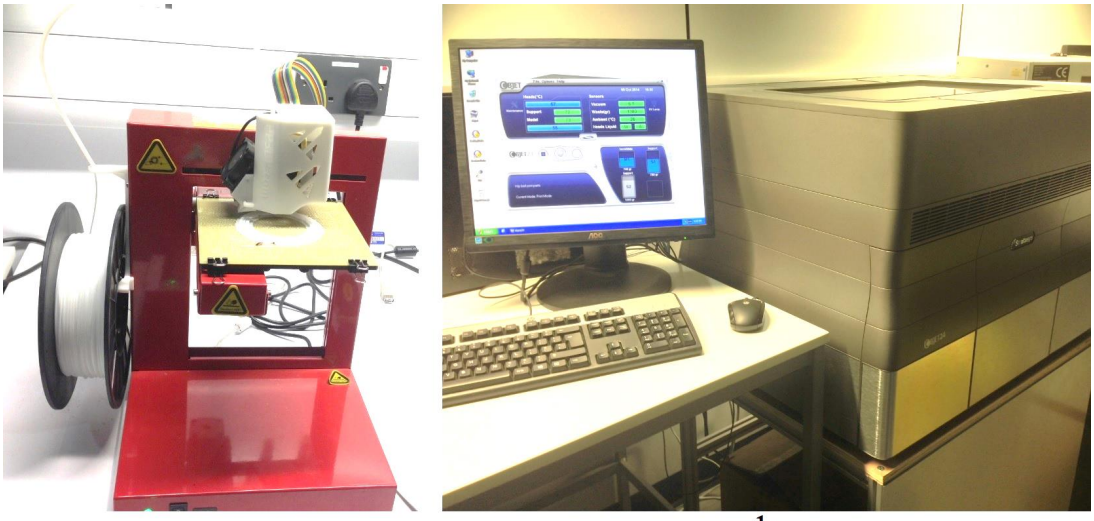

a b

Figure 5.5. 3D Printers in The University of Warwick. a) UP Plus. b) Stratasys Objet24

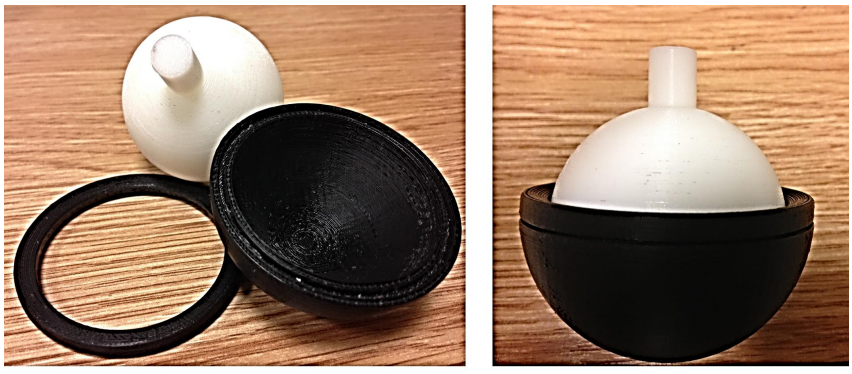

a b

c d

Figure 5.6. IM prototype which is made with UP Plus 3D printer in The University of Warwick. a) Dissembled IM. b) Assembled IM. c) Face of the ring. d) Rib and groove

Chapter 6： Simulation of the Invented Model (IM) and the Conventional Model (CM)

The most common method for studying contact mechanic is FEA [175] which was explained in Section 4.2. Contact mechanics study of the hip joint is studied with this technique due to the complexity of the geometry and material involved [176, 177] in the prostheses. Furthermore simulating with FEA is not only cost effective comparing with hip simulator machines, but also can comprehensively analyse behaviour of the prostheses in different mechanical points of view and save enormous amount of time. Indeed experimental data from the latest hip simulators that tested the hip joint under EL conditions and Hertzian contact theory enables us to validate the results.

In this chapter the best hip prosthesis in the market [205, 207] (Biolox Delta-Zimmer (BDZ)) is compared with the IM to find whether the design of the IM is effective in reducing of the EL phenomenon and respective wear rate. Abaqus is one of the most advance software packages in analysing the problems with FEM. Therefore this software is used for this study with the same sequences explained in 4.2.8.

FEM compares IM and CM in 2 main aspects, which are:

- Analysing EL in IM and CM
- Analysing the Neck-Rim/Ring impingement in IM and CM

6.1. Defining Features of IM and CM

Important factors in designing CM are explained in Section 4.1 which are all considered in the BDZ [207] and will be considered for simulation in this chapter. The same aspect is considered in making IM, which is based on the given details in Chapter 5. These two prostheses will be analysed by Abaqus software. For most accurate result with the lowest cost of time which is possible in simulation, the components are divided to critical parts (Region 1) and non-critical parts (Region 2) where the Region 1 is in the domain of our study and the Region 2 is not. In terms of studying EL, Region 1 will be a close region to the latitude of the ball and the area near to the edge of the socket. However Region 1 in Neck-Rim/Ring impingent study is the neck and the ring/rim of the socket. During both studies usually only the half of the region 1 is under maximum contact pressures while more than half are not, due to the symmetry feature of the prostheses.

6.1.1. CM Design feature

Based on Section 4.1, ball of the BDZ is sketched with diameter of 48 mm which involves the cavity for receiving a taper 12/14.

Due to the reason explained in Section 6.1, femoral parts are divided to 5 parts and made with sketching of 3 main features. Figure 6.1 and Figure 6.2 show the features of the Region 1 and Region 2 of the ball, respectively. They make 2 halves of every region. The cavity is illustrated in both regions in Figure 6.1 and Figure 6.2 is for receiving a 12/14 taper/neck, which is the other component of the femoral part and sketched in Figure 6.3 with slope angle of 5.66º (based on BDZ dimension which is shown in appendix C). Femoral stem is attached to the ball through the taper. However the stem is not studied in this paper due to its irrelevancy to the mentioned studies.

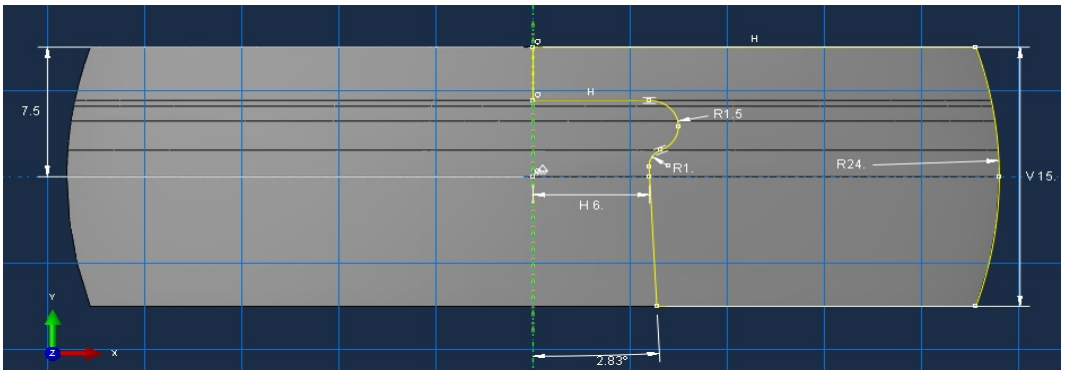

Figure 6.1. Feature of Region 1 of the ball in CM and IM

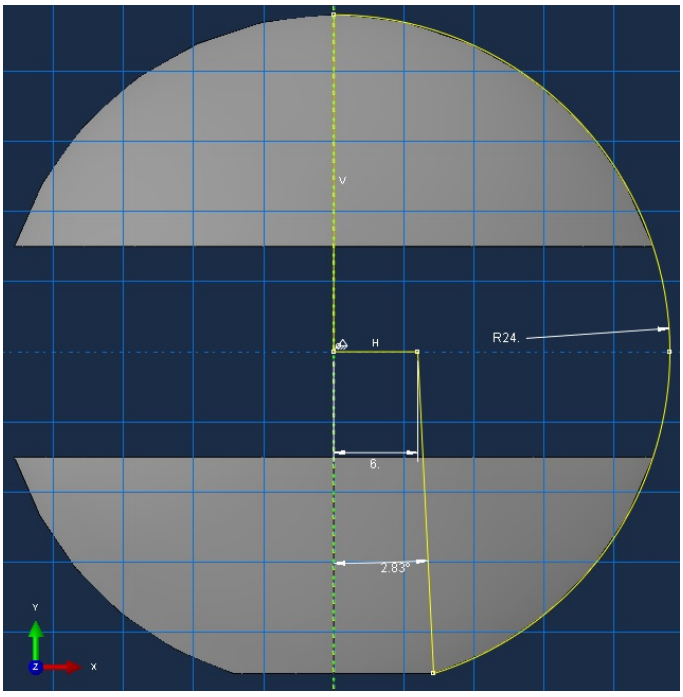

Figure 6.2. Region 2 of IM and CM ball

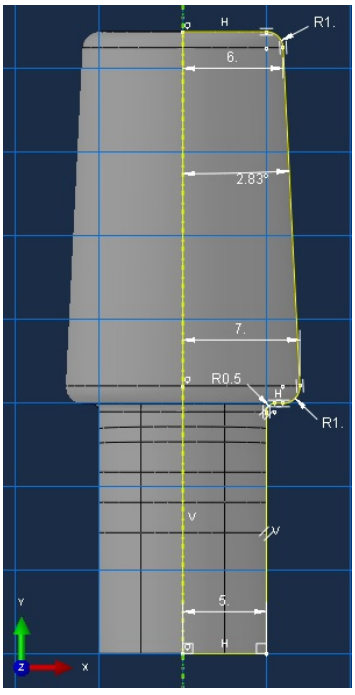

Figure 6.3. Taper 12/14 in CM and IM

A CM socket is sketched in Figure 6.4. It is made of two halves where one half contains Region 1 and the other one Region 2. The socket inner surface diameter is 48.08µm to leave 40µm radial clearance for assembling of the ball. The CM socket has 2.5mm chamfer of the edge and thickness of 5mm.

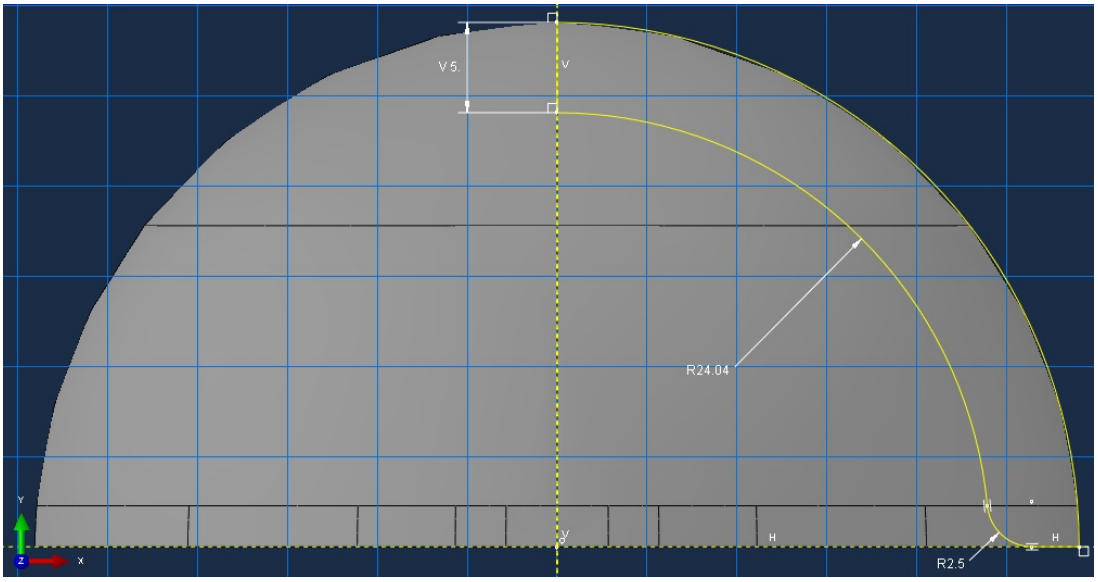

Figure 6.4. Feature of the CM socket

6.1.2. IM Design feature

All femoral parts of IM are made exactly the same as the ones explained in Section 6.1.1. The IM socket also has the same dimension of CM with 48.08 mm inner diameter and 58.08 mm outer diameter. The IM socket includes the ring that explained in Chapter 5. The angle between surface of the ring and the horizontal axis is 19.15º in this study that makes conformal contact between neck and ring during impingement. The IM socket also contains Region 1 and Region 2, which is made of 2 halves. The feature is shown in Figure 6.5.

In both CM and IM, all parts are sketched accurately with help of variable tools in Abaqus such as for adding different constraints to make the most desirable sockets and ball. CM socket must have an open area with diameter of 48.08 mm. The IM socket should have 48.08 mm diameter where the ring attaches to the main socket. However opening area becomes 0.25% narrower with the ring therefore 99.75% of the inner diameter, which is 47.95 mm in this study, prevents ball from coming out of the socket. This is also sufficient to provide a reasonable contact surface between the ring and the ball to spread the load as mentioned earlier. However, it also allows the greatest ROM for the ball as it can move more than 141º before the neck meets the ring, which was explained in Chapter 5.

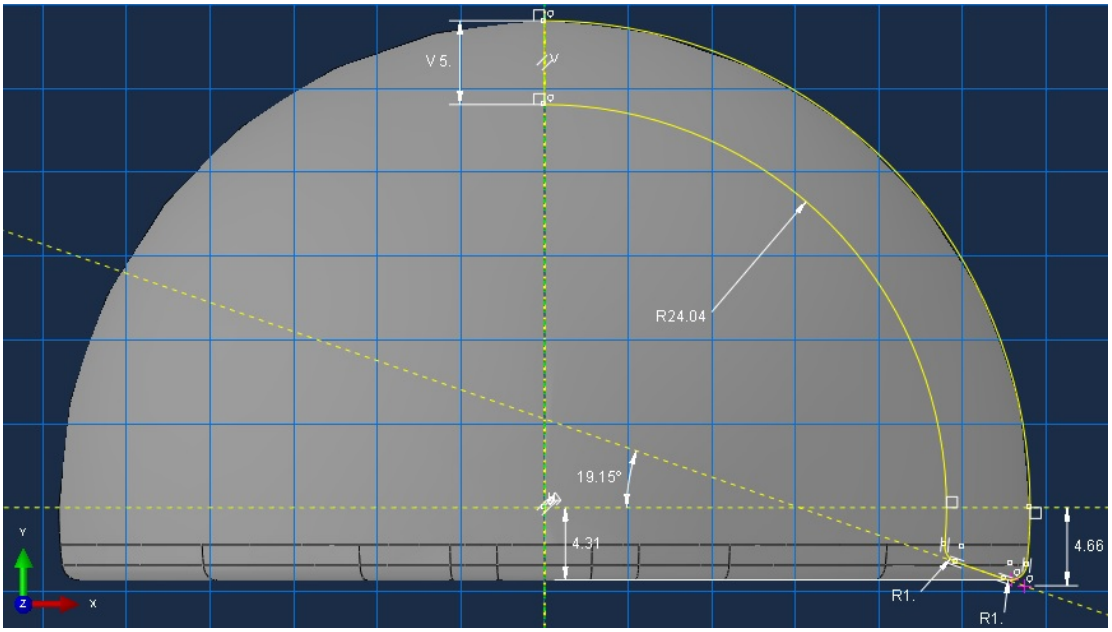

Figure 6.5 Feature of the IM socket

6.2. Part module for IM and CM in Abaqus

Due to the symmetric nature of CM and IM, all components are made by the revolving technique. In this regard, sketched parts in Figure 6.1, Figure 6.2, Figure 6.4 and Figure 6.5 are revolved vertically by 180º around the vertical line passed from the centre point. Therefore 8 halves are made. Figure 6.6 shows Region 1 (for EL analysis) of the ball and Figure 6.7 shows half of the region 2 of the ball. Figure 6.9 and Figure 6.10 show half of the CM and IM sockets, respectively. The other halves of these parts are made by mirroring about x-y plane to complete the features with pair attachments. The sketched taper in Figure 6.3 is revolved by 360º vertically around the vertical axis passed through centre point to make the whole taper which is shown in Figure 6.8.

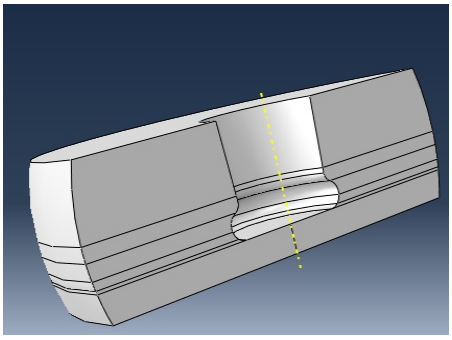
Figure 6.6. half of the region 1 of the ball

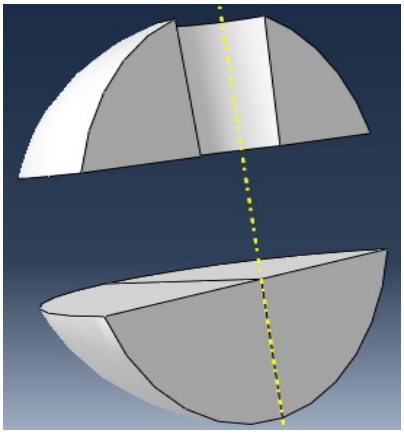
Figure 6.7. half of the region 2 of the ball

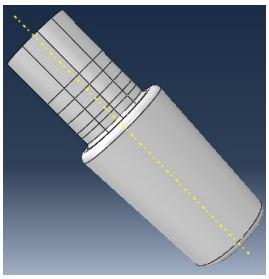
Figure 6.8. The Neck

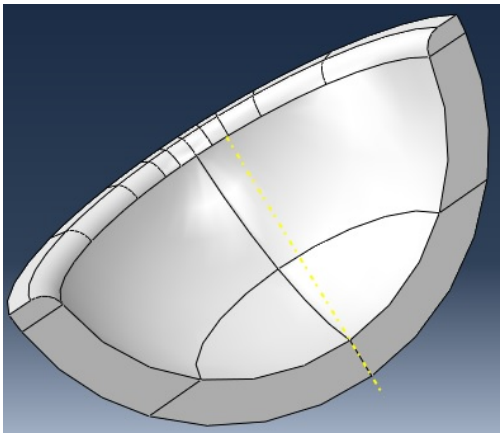

Figure 6.9. Region 1 of CM socket

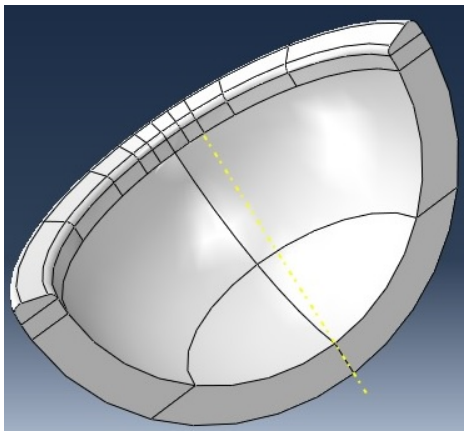

Figure 6.10 Region 1 of IM socket

6.3. Properties of the material

Both models, CM and IM, are made of Biolox Delta, which is an Aluminium oxide matrix composite ceramic that consists of approximately 82% Alumina (Al_2O_3), 17% Zirconia (ZrO_2) and other trace elements, such as chromium oxide (Cr_2O_3) which was explained in 2.5.3.1.3. This material has shown the best mechanical and biological performance during EL condition which was discussed in 3.1.3 in depth. Table 6.1 shows the mechanical properties of this material which has been assigned to the all components of CM and IM in this study. However the Taper/Neck should be fitted into taper cavity in the ball with press fitting technique, hence needs more elastic material than ceramic. The taper of BDZ made of titanium alloy (Ti_6Al_4V), which is appointed to the taper for this study. The property of this material is described in Table.6.2

Table 6.1. Alumina Zirconia Properties

Hardness (HV)	1925
Density (g/cm^3)	4.37
Young's modulus (GPa)	350
Fracture toughness	8.5
Poisson's ratio	0.22

Table 6.2. Titanium Alloy Properties

Hardness (HV)	349
Density (g/cm^3)	4.43
Young's modulus (GPa)	113.8
Fracture toughness	75
Poisson's ratio	0.342

6.4 Assembly and Positioning

Before getting started, the simulation parts should be assembled and positioned in the study situation. In this regard, Region1 and Region 2 of the ball are matched and the taper is fixed in the cavity. Afterward femoral components are tied together to make the union shape of the femoral component which is shown in Figure 6.11 and Figure 6.12.

Region 1 and Region 2 of the CM and IM are also assembled and shaped the final shape of CM and IM sockets. They are also obliged to be union shapes with tie constrain. They can be seen in Figure 6.11 and Figure 6.12 respectively. Subsequently the balls are accurately fitted into the centre of the sockets.

In this module, desirable surfaces of the balls, sockets and tapers, which are 18 surfaces, described for every model. Furthermore, 2 reference points (RP) are defined for every model for an easier control of the ball and the socket during loading or displacing. In this regard, RP-1, either in CM or IM, is coupled with the taper or taper cavity (in terms of eliminating the taper for study of the EL) and RP-2 is coupled with outer surface of the sockets.

In order to analyse the contact pressure which is caused due to the impingement of the neck to the rim of CM and to compare the result with the same coincident in IM, the neck should be positioned just about to contact with the CM rim or IM ring. These are shown in Figure 6.11 and Figure 6.12 respectively.

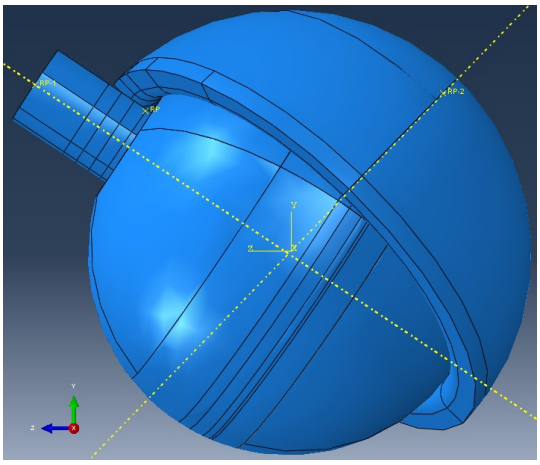

Figure 6.11. CM assembly for Neck-Rim impingement

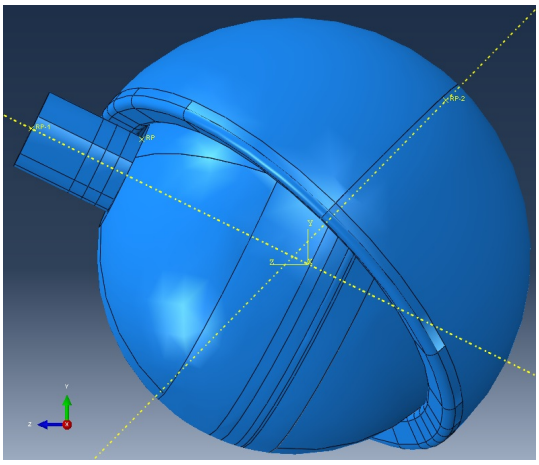

Figure 6.12. IM assembly for Neck-Ring impingement

As it was mentioned earlier in Chapter 3, EL happens when ball is separated from the centre of the socket and gets enough distance to load the edge. For simulating of EL in Abaqus ball and socket should get enough distance from each other (based on

Formula 3.1). In this regard, the latitude of the ball should contact the edge of the CM socket or in case of IM it may contact the ring. These are shown respectively in Figure 6.13 and Figure 6.14. Furthermore, the completed IM and CM prostheses should be well located for simulation. As it was explained in Sections 3.2 and 3.2.1, positioning of the socket in the acetabulum may affect EL. Therefore, the ideal positioning of 45º inclination and 20º anteversion of the sockets are considered from Formula (3.5) and applied to the final location of CM and IM in all cases in different studies.

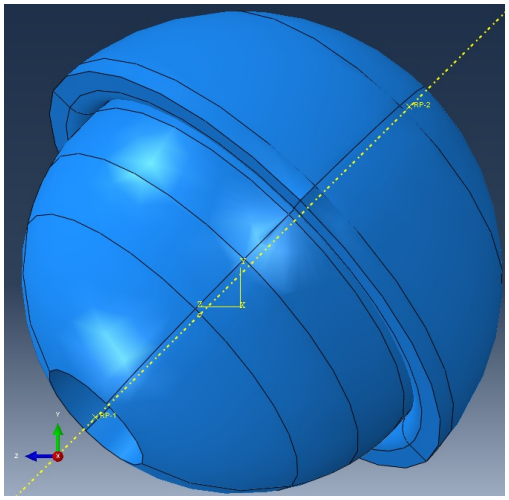

Figure 6.13. CM assembly for EL study

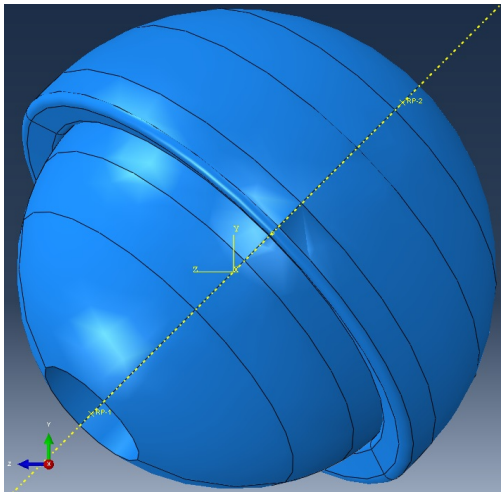

Figure 6.14. IM assembly for EL study

6.5. Step module

The type of analysing must be described in advance to the loading, displacing and meshing of the models, as the analysing type can affect them. Steps module in Abaqus not only allows us to describe type of the analysis in every model but also enables a user to define several steps if needed.

Here, the models are analysed statically and the equations are solved with direct method, which was studied in 4.2.4.1. Time period is set to be $1\,s$, however this does not mean a real time in static study. Time period is divided to the maximum number of 1,000,000 increments in this study, to satisfy the static behaviour of the model as it was discussed earlier in 4.2.6. The initial increment size is $1\,ms$ but it is set to be controllable with Abaqus in the range of Min: $10^{-11}\,s$ to Max: $1\,s$. Increasing or decreasing the size of the increment is due to the accuracy of the assumption in numerical solution by Abaqus. This software based on initial boundary condition and shape functions, tries to find the solution for every element as it was explained in 4.2 and 4.2.3, however if the model is complex, the initial value should be small enough for

solving the differential equations. The result from the first increment defines the next increment condition. In this regard in every increment, equations are solved several times and the result is compared with the result of the previous increment to be used for the next increment. If the error of the obtained results in every increment is less than the certain amount, iterations will be stopped and the equation will be ready for solving the next increment. Hence if the result is being converged, the increments are solved one by one up to the final increment to give final result, which is the final position of the model. In this regard, if the initial increment size is much higher than the one it should be, Abaqus automatically reduces the size of the increment gradually up to the minimum possible increment size to find more accurate result and convergence result. Vice versa, if the chosen initial increment size is too small, the software increases the increment size gradually to the maximum possible increment size to speed up the processing and find the final solution faster. In this case some increments are eliminated from calculation and will not be shown in results increments.

Depending on the condition and requested data of the study, step module can be defined differently. When analysing is completed, software gives some output as a result of its analysis. By default, some outputs are requested and selected in step module while the user can change them. In our study, during all circumstances, default output is not changed and accepted to be shown either in contour shape (Field output) or graphically (History output).

IM and CM will be analysed during impingement by different loads ranged from 1kN to 6kN. The load will be applied to the neck when it only contacts the rim of CM or ring of IM. In this study our concern is the contact pressure (CPRESS), which directly affects wear rate of the prosthesis. However Von Mises stress (S) and translation and rotation (U) are also selected for further investigation. The time increment starts with 0.001 s which will be gradually increased to 0.292 s by Abaqus due to the excellent meshing technique of the regions under study. Respectively, because the load is applied by ramp linearly over step, first increment analysed with just 0.1% of the applied load which was 6N (in terms of study with 6kN load) while it is gradually increased to 29.2% of the load after 16 increments. The increase leads to the result within 17 increments. It is shown in Appendix E.

For analysing EL due to microseparation, the same steps are defined while different displacements are applied to the ball and the socket of IM and the CM. In this regard ball is separated from the centre of the socket for 50 μm - 0.5 mm which loads

the edge of the sockets. CPRESS will be studied in this test, and CM and IM are compared with each other. For example during 250µm, the first increment starts with 1 ms which will be gradually increased to 0.292 s due to the excellent meshing which was easing the calculation for Abaqus. Respectively displacement is also started with 250 nm and increased to 72.98 µm, which also will give the result within the same 17 increments of Neck-Rim/Ring Impingement study (Appendix E).

6.6. Interaction module

In all circumstances of this study surface to surface contact is studied. During Neck-Rim/Ring impingement, surface of the neck and surface of the CM rim or IM ring contact each other. However during EL study, surface of the ball contacts with the surface of the CM rim or may IM ring. Region 1 of the IM and CM sockets are our concern hence they should be meshed finer and selected as a slave while ball components are always defined as a master. Master and slave parts are shown with red and purple colour respectively in both conditions in Figure 6.15 and Figure 6.16. Furthermore slaves are adjusted only to remove over closure and all surfaces are automatically smoothed for 3D geometry surfaces when applicable.

All contacts in this study are defined to be frictionless during tangential contact and Hard when they are in a normal contact. Therefore the contacted parts cannot penetrate in each other.

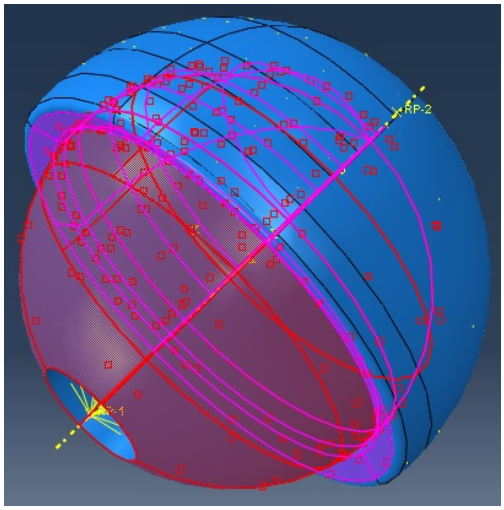

Figure 6.15. Interaction for studying EL

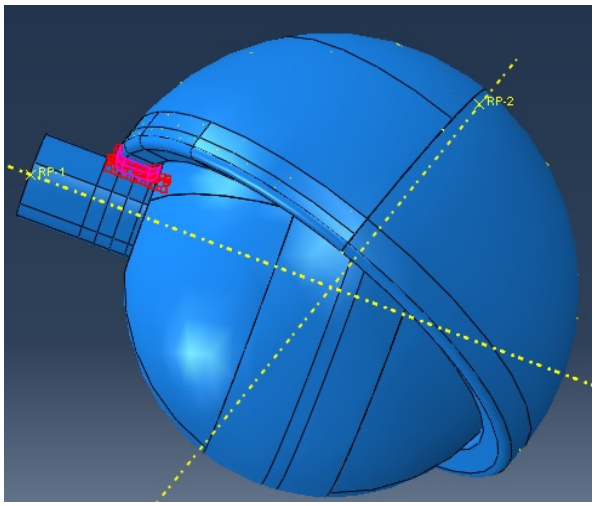

Figure 6.16. Interaction for studying Neck-Rim/Ring Impingement

6.7. Load and Boundary Conditions

In every study of this paper all boundary conditions (BC) and loading conditions are applied to both IM and CM exactly in the same manner. As explained earlier, these

two prostheses are studied under 2 different circumstances hence they have different loading and boundary conditions for every study.

During Neck-Rim/Ring impingement, socket should be fixed while neck is contacting ring/rim with different forces. In this scenario, socket is fixed by defining the displacement/rotation BC to the RP-2 where it is restricted to zero displacement and rotation in every direction (Appendix F-b). However ball and neck, which are tied together and controlled by RP-1, should be able to move in y-axis only. Therefore they are restricted to zero displacement and rotation in every other direction (Appendix F-a). Consequently several concentric loads are applied to the y-axis of the RP-1 (Appendix F-c).

In terms of studying EL, no load is defined and simulation of EL based on the natural incidence that is microseparation. Therefore in this study RP-1 disables the ball to move or rotate in every direction (Appendix G-a) and RP-2 restricts the socket to move only in x-axis with the selected displacement with no any rotation or displacement in all other directions (Appendix G-b). Although microseparation is not applicable to IM due to the nature of this design, it will be applied to study IM in the same condition that is applied to CM.

6.8. Mesh

As it was explained in 4.2.2, the geometric domain of balls and sockets components should be discretised to the element base domain. In this regard, every part explained in 6.1.2 is discretised to the several elements which is known as Meshing. This module directly effects on the result of the processing. In this regard different parts may mesh with different type of the elements, seeding, and meshing techniques, which are explained in following.

Size of the element is crucial. If the size of the element is small, the mesh density will be improved which causes increasing the number of the elements. Discretising of geometric domain with extensive number of elements increases the accuracy of the processing while it results in extremely high processing time. In this regard, not only critical parts are made separately but also they are well meshed with local seeds (elements with 1 mm in EL study and 0.1 mm in Neck-Rim/Ring impingement study and maximum deviation factor of 0.05). However the parts which are not under investigation, are meshed with rough elements with global size of 3 mm.

IM and CM have complex features thus they should be divided to the simpler parts to be well meshed[19]. In this regard, every part has been partitioned into the several particles which can be meshed, with structured and/or sweep techniques which are suitable for these models. Because every partition can be meshed with local seed, desirable parts of the IM and CM are partitioned well. For Neck-Rim/Ring impingement study; the expecting contact parts of the neck, the rim of CM and the ring of IM are partitioned well that results in the excellent meshing of these areas which are shown in Figure 6.17. Contacting parts of the ball and the sockets in IM and CM during EL position, which are at the middle of the ball and edge of the sockets, are also well partitioned and meshed in the same way which are shown in Figure 6.18.

All models are made of hex-dominated elements with advancing front algorithm. When the parts are made with revolution type, Hex-dominated elements tries to use mostly hexahedral elements while use tetrahedral elements in the areas were contacted with centreline in part module. This enables the nodes of the elements matched with seeds. Advancing front algorithm fills the front borders of the partitions with hexahedral elements and tries to follow the same manner into the parts where it is possible. This helps the seeds and nodes to be matched together as well.

The element type (shape function) in meshing has an important effect on simulation processing which was discussed in 4.2.3. Regions 2 are made of the elements with linear geometric order (C3D8R), while the expected contact parts in regions 1 are made of the elements with quadratic geometric order with 20 nodes (C3D20R). These elements were explained in 4.2.10.

Figure 6.17a and Figure 6.17b respectively show meshed CM and IM during Neck-Rim/Ring impingement. The expected contact areas of IM and CM in this study are meshed with fine local seeds, while the rest of the areas are roughly meshed. The number of elements which make the ball components, is 21,227 (4,067 elements for ball which is region 2 in this study and 17,160 elements for the neck which is Region 1 in this study). This is shown in Figure 6.17c. CM and IM sockets respectively are 15,672 (15,084 elements for Region 1 and 588 elements for Region 2) and 16,434 elements (17,650 elements for Region 1 and 760 elements for Region 2), which are shown in Figure 6.17d and Figure 6.17e respectively.

[19] If these models are not well partitioned, the only technique possible to be applied for meshing, will be free technique with Tet shape elements which is the easiest but the most inaccurate meshing technique.

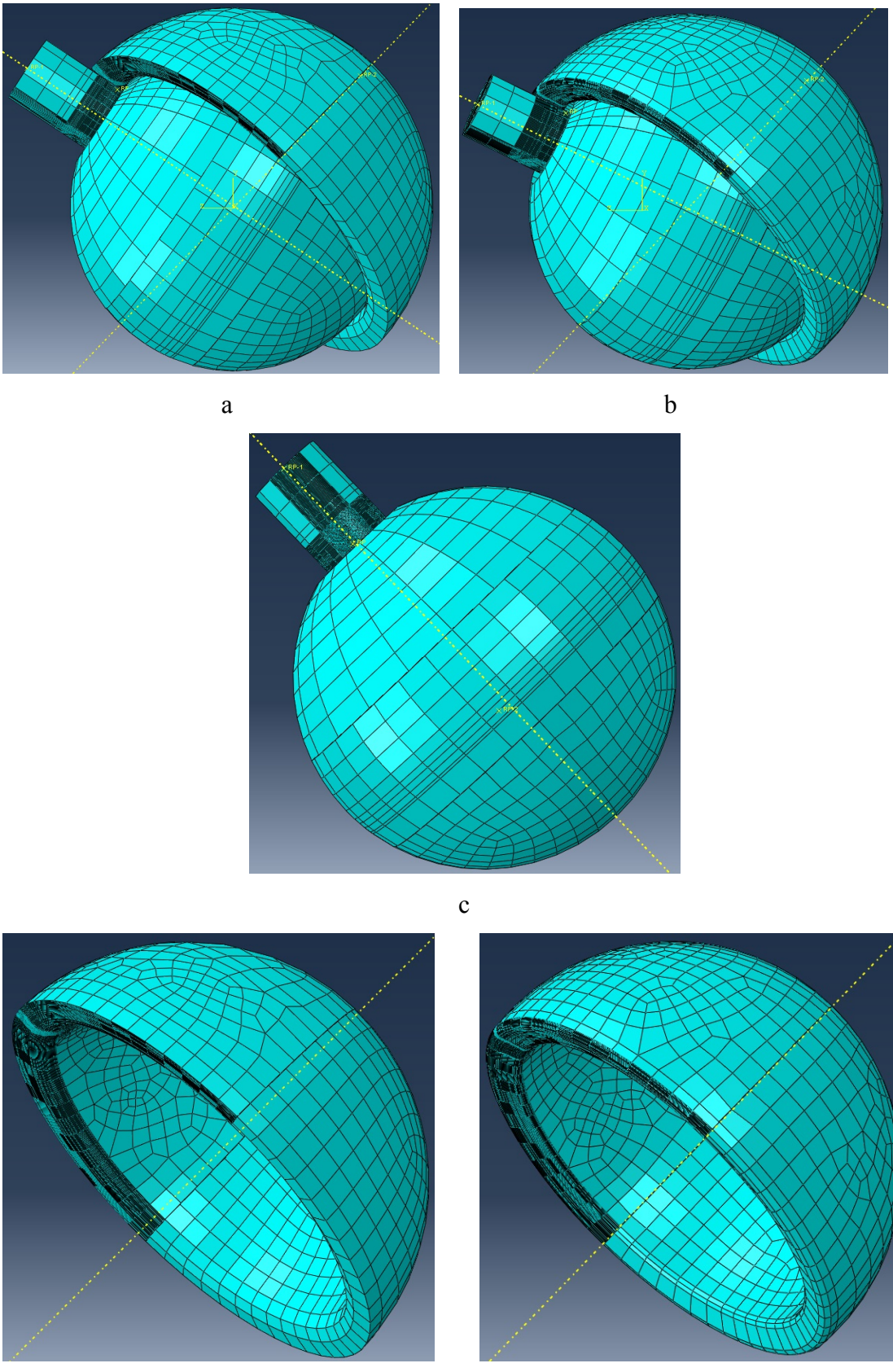

Figure 6.17. CM and IM meshed components for Neck-Rim/Ring impingement study a) Assembled meshed CM b) assembled meshed IM c) Meshed ball and neck d) Meshed CM socket e) Meshed IM socket

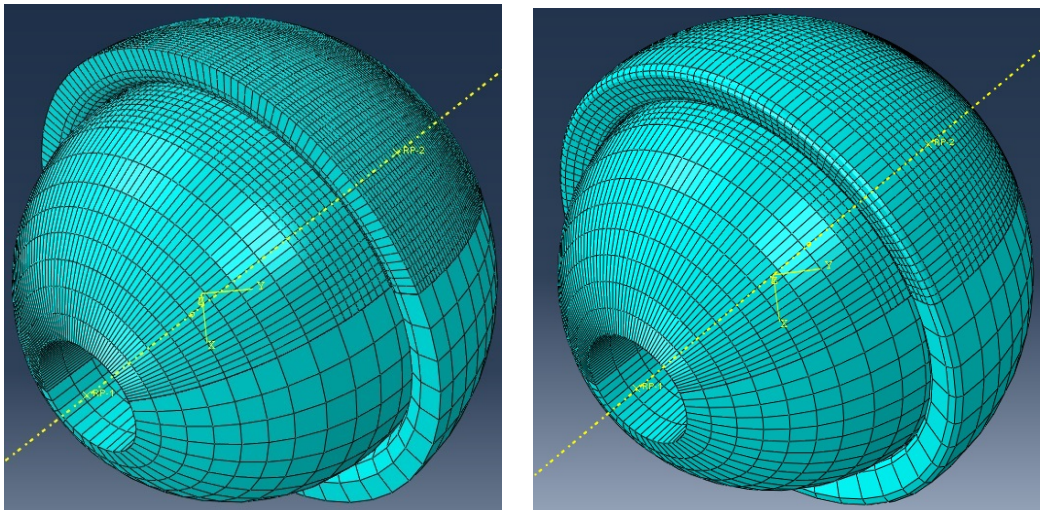

a b

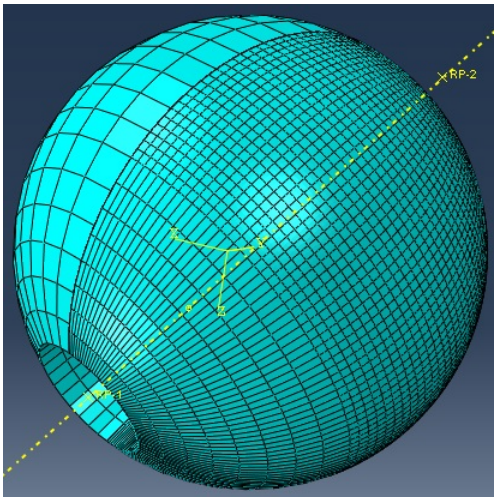

c

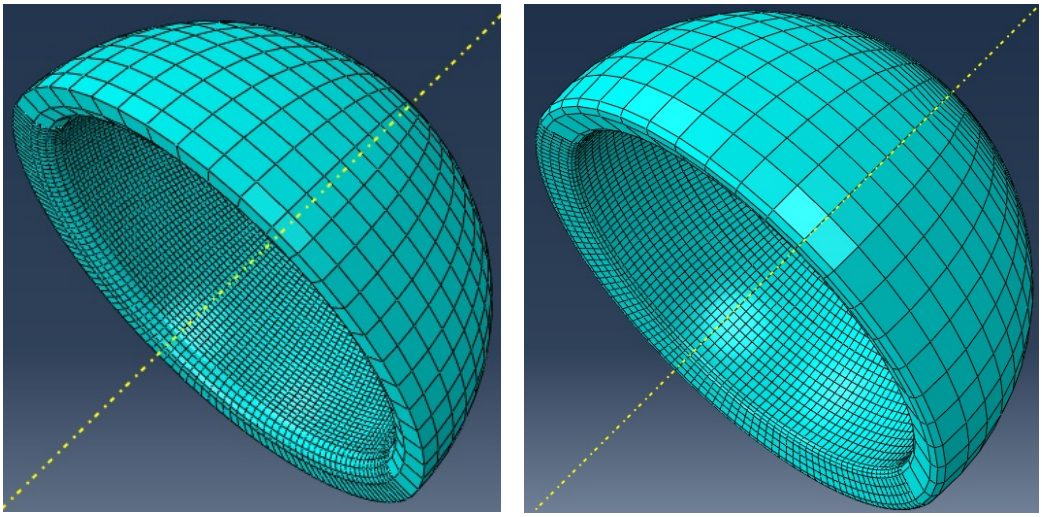

d e

Figure 6.18. CM and IM meshed components for EL study a) assembled meshed CM b) Assembled meshed IM c) Meshed ball d) Meshed CM socket e) Meshed IM socket

Figure 6.18a and Figure 6.18b show meshed IM and CM for EL study. They are finely meshed on the Region 1 of this study, which is almost half of the ball and the socket in IM and CM. However Region 2 for this study is roughly meshed. Total elements made the ball domain in this study are 11,073 (3132 elements for ball which is region 2 in this study and 7,941 elements for region 1 in this study) which are shown in Figure 6.18c. CM and IM sockets respectively are 8,432 (7,392 elements for the half in region 1 and 1040 elements for the other half in region 2) and 10,125 elements (8,500 elements for the half in region 1 and 1625 elements for other half in region 2) which are shown in Figure 6.18d and Figure 6.18e respectively.

6.9. Job

Here, two situations are studied, while IM and CM are studied in exactly same condition in every situation. Therefore, the results could be comparable.

In Neck-Rim/Ring impingement 5 different loads are applied to the neck when it contacts the rim in CM and the ring in IM hence 10 jobs should be run in this situation. In EL condition, IM and CM prostheses are studied under 6 different microseparation to contain the following situations:

- Before incidence of EL on CM.
- When EL is developing on CM.
- Fully developed EL on CM.
- Extreme EL condition.

All created 22 jobs run with parallelization of all 8 available processors cores of our computer to minimize the processing time. Processing of the simulation can be seen in a monitor page (Appendix E).

Chapter 7 : Result and Discussion

IM and CM are analysed based on 3 different methods mentioned in Chapter 4. Although improving the design of IM, which eliminates the EL requirements, postulates promising results, Chapter 6 studied IM and CM with Abaqus. Furthermore Hertzian contact theory investigates EL in CM and IM for further verification in 7.3. The main concern in this study is limiting EL, which is likely to happen with IM. However Neck-Rim/Ring impingement is also considered with IM as an additional advantage of this design. In every condition of this study, CM and IM are tested under same condition, orientation and sizes but design feature, hence comparing the results of CM and IM are meaningful.

7.1. Analysis of Neck-Rim/Ring impingement with FEM

Boone et al. [137] believed that the hip maximum range of motion during normal daily activities is 130° (-10° to 120°) which is during a hip flexion, Therefore in both CM and IM respectively with 157° and 141° range of motion there should be low risk of impingement in normal daily activities. However if surgeon does not ideally fix the prosthesis, patient performs some excessive hip flexing activities either voluntary or involuntary etc., the risk of impingement will be increased significantly. Surprisingly impingement have been observed in 70% of all kinds of the hip prostheses [126,127,131] as it was shown in Figure 3.20 and explained in 3.2.3. In this regard, with small change on design of the socket, IM tries to reduce the impact of impingement as well as EL problem, which is our main concern in this study.

IM socket consists of a flat surface, which is conformed with neck during impingement. There are 2 small inside and outside 1mm chamfers as well to eliminate a point contact with sharp edges during impingement (Figure 5.2). However CM only get the benefit of 2.5 mm chamfer which reduces the stress and contact pressure during impingement and EL in comparison with the older prostheses with sharper edges which was explained in 4.1.1 in depth. Although 2.5 mm radius chamfer has been selected with most of the manufacturer nowadays ([204, 205, 206, 207]), the nature of the CM design not only disables providing the flat surface on the edge but also encounters with the optimum chamfer radiuses which explained in 4.1.1.1. In this study Abaqus analyses the IM ring with the 2.5 mm radius chamfer of BDZ [207]. The neck of the ball contacts the CM rim with 5 different loads which are 1kN, 2kN, 2.8kN, 3.4kN and 6kN and the same loads are applied to IM when the neck is impinged with the ring of the IM.

7.1.1. CM and IM under 1kN force during Neck-Rim/Ring impingement

When 1 kN force is applied to the neck in y-axis, the neck is displaced vertically and presses the chamfer of the CM rim, or the flat surface of the IM ring. Distribution of the load on the flat surface of the IM ring shows the reduction of contact pressure by 63% in comparison with CM one. Figure 7.1a and Figure 7.1b are showing the contour results of contact pressures in CM and IM respectively due to the neck impingement.

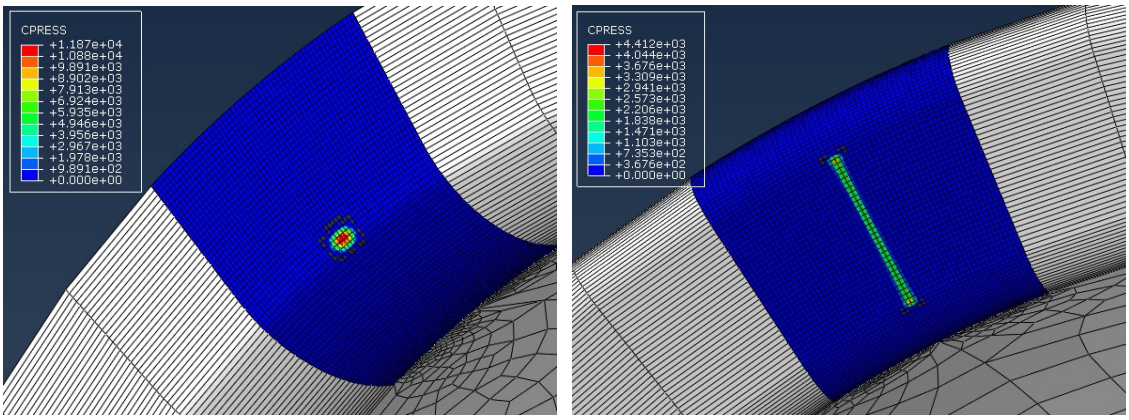

a b

Figure 7.1. Contour results of Neck-Rim/Ring impingements on CM and IM under 1kN load a) Maximum 11.87 GPa Contact pressure on CM b) Maximum 4.4 GPa Contact pressure on IM

7.1.2. CM and IM under 2kN force during Neck-Rim/Ring impingement

Walking speed of 1 km⁄h could apply 280% of Human Body Weight (HBW) to the hip [95]. If the average patient HBW is 70 kgs, hip will be loaded under about 2kN force. With this assumption, the neck loads the rim of CM and the ring of IM with 2kN. The result shows excellent behaviour of the IM ring under 2 kN force with reduction of contact pressure by 59%. The contour result is illustrated in Figure 7.2a for CM rim and Figure 7.2b for IM ring.

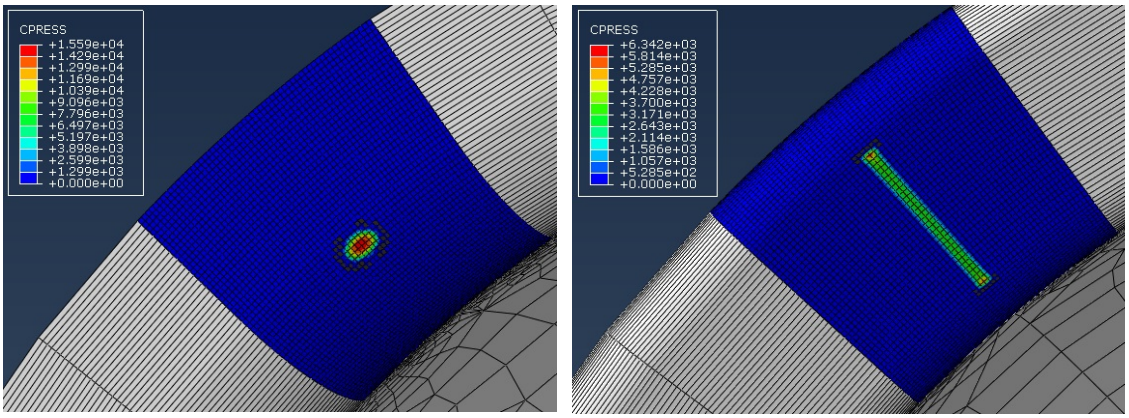

a b

Figure 7.2. Contour results of Neck-Rim/Ring impingements on CM and IM under 2 kN load a) Maximum 15.6 GPa Contact pressure on CM b) Maximum 6.3 GPa Contact pressure on IM

7.1.3. CM and IM under 2.8 kN force during Neck-Rim/Ring impingement

Stair climbing may increase the force on the hip by 400% of HBW [208, 209], which can be a source of Neck-Rim/Ring impingement during high step climbing. In terms of occurrence almost 2800N force is applied to the neck which is pushed to the rim of CM or the ring of IM. Fortunately the result showed that the IM ring reduces the impact of neck impingement in comparison with the conventional rim of CM. Therefore contact pressure is reduced by 57%. This is illustrated in Figure 7.3a and Figure 7.3b.

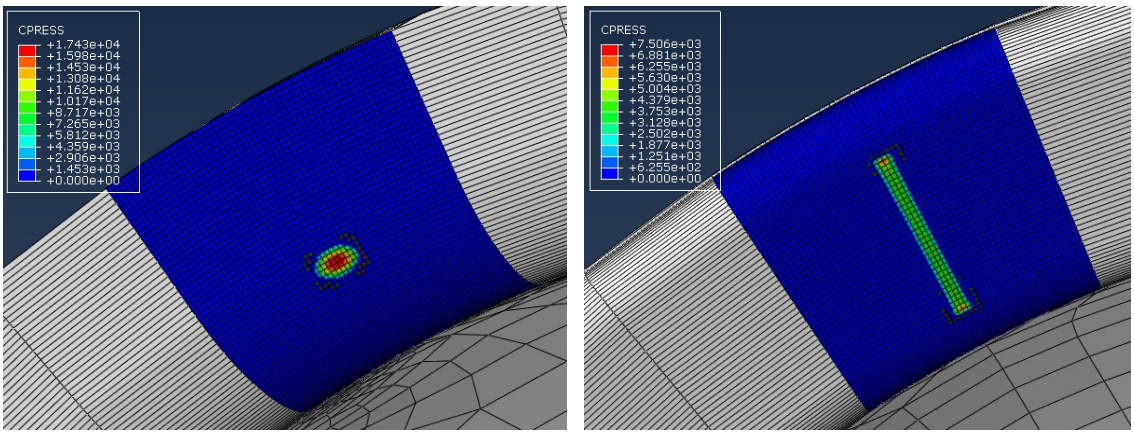

a b

Figure 7.3. Contour results of Neck-Rim/Ring impingements on CM and IM under 2.8 kN load a) Maximum 17.4 GPa Contact pressure on CM b) Maximum 7.5 GPa Contact pressure on IM

7.1.4. CM and IM under 3.4 kN force during Neck-Rim/Ring impingement

If walking speed is increased from 1 km⁄h to 5 km⁄h, the median peak force would be increased from 280% HBW to 480% HBW [95, 209, 210]. In this regard a 3.4 kN force will be applied to the neck when it impinges the rim of CM or the ring of IM. The result in this test also shows the reduction of 56% of contact pressure by IM ring. Figure 7.4a and Figure 7.4b compare the contact pressures made by neck to the CM rim and the IM ring, respectively.

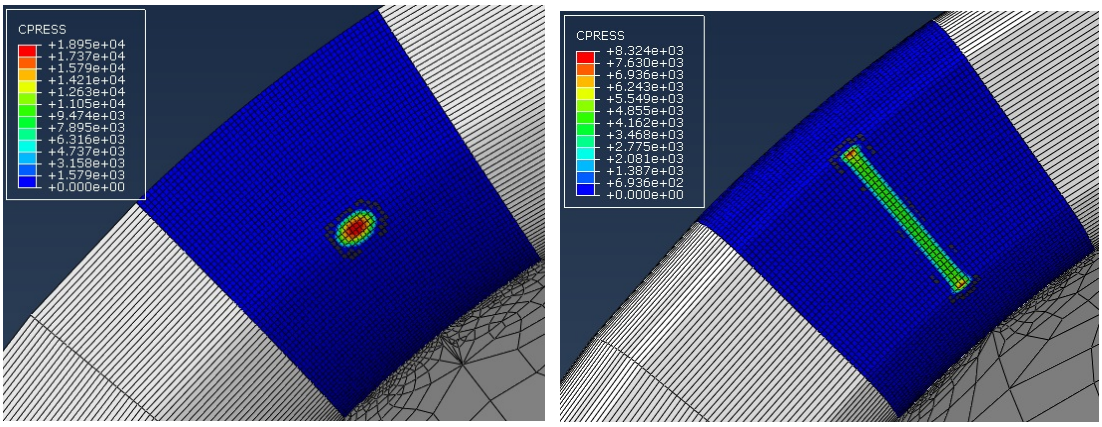

a b

Figure 7.4. Contour results of Neck-Rim/Ring impingements on CM and IM under 3.4 kN load a) Maximum 18.9 GPa Contact pressure on CM b) Maximum 8.3 GPa Contact pressure on IM

7.1.5. CM and IM under 6kN force during Neck-Rim/Ring impingement

Bergmann G et al. [95] reported the maximum applied force to the hip was due to the stumbling when the force was raised to 870% HBW. Figure 7.5a and Figure 7.5b compare CM and IM contact pressures during stumbling when IM ring shows 52% reduction in association with CM rim. Fortunately the hip joint can withstand up to 1500% HBW before fracture [209].

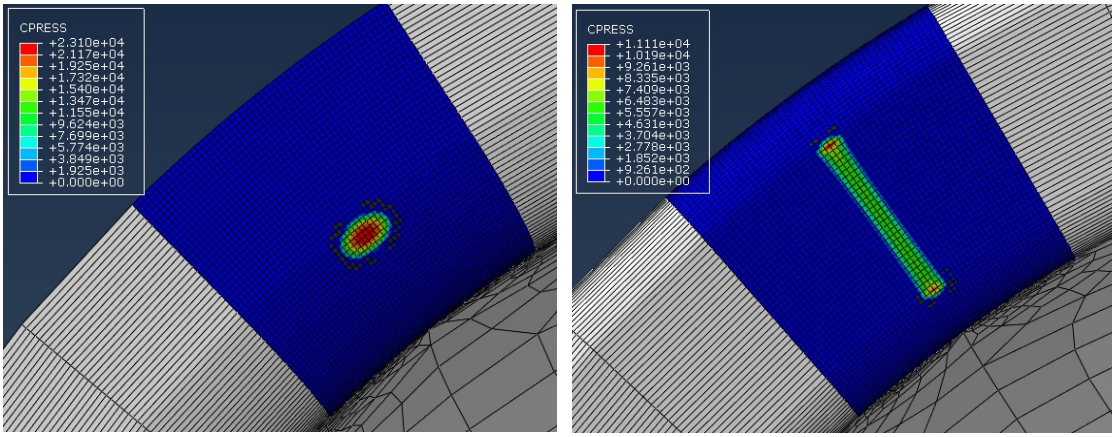

a b

Figure 7.5. Contour results of Neck-Rim/Ring impingements on CM and IM under 6 kN load a) Maximum 23.1 GPa Contact pressure on CM b) Maximum 11.1 GPa Contact pressure on IM

7.1.6. Discussion

All results showed significant reduction of contact pressure by the IM ring in comparison with the CM rim. The result was predictable in general term from the IM design, because once the given forces press the neck to the CM rim, relatively small part of the neck loads small area of the rim chamfer, which is more similar to point-to-point contact. Conversely when the same forces push the neck to the IM ring, relatively wider part of the neck loads the conformed flat surface of the IM ring (Figure 7.1b, 7.2b, 7.3b 7.4b and 7.5b demonstrates this graphically as well). This is more like surface-to-surface contact than point contact. Hence the distribution of the loads on the surfaces can reduce the contact pressure effectively. In terms of practicality of this idea, crowning technique may be needed for manufacturing. Table 7.1 and Figure 7.6 summarise the results of this study. The level of improvement shown give added confidence in the benefits of the new design.

Table 7.1. Comparison of the maximum contact pressure due to the impingement of the neck to CM rim and IM ring under 1kN, 2kN, 2.8kN, 3.4kN and 6kN

Load (kN)	Contact pressure (GPa)	
	CM	IM
1	11.87	4.4
2	15.9	6.34
2.8	17.43	7.5
3.4	18.95	8.32
6	23.1	11.11

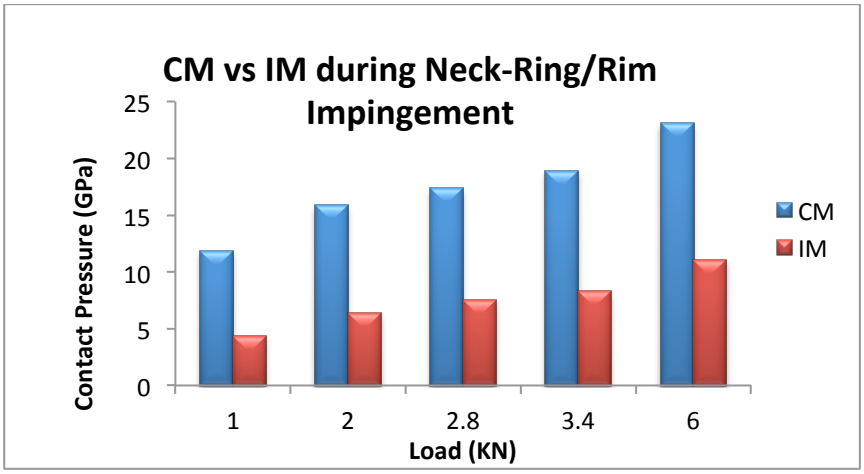

Figure 7.6. Maximum contact pressure of CM (blue bars) and IM (Red bars) during Neck-Rim/Ring Impingement under 1kN, 2kN, 2.8kN, 3.4kN and 6kN

7.2. Analysing EL with FEM

Surgeon or patient's cautions can eliminate some EL sources, but microseparation as the most effective factor in EL, cannot be prevented. Due to microseparation inevitability, EL happens with every walking cycle and affects the wear rate significantly. Therefore to simulate EL in this study, ball and socket are separated from each other with specific distances. We again stress that to investigate EL, IM and CM are studied under the same conditions such as boundary conditions, displacements, material properties, dimensions etc. Therefore, any differences observed in the results of comparing CM and IM are due to the difference in their designs.

Analysing EL has the 4 following milestones:

- Microseparation, which does not cause of EL
- Microseparation that may develop EL
- Developed EL
- Extreme microseparation condition and EL

The above conditions are reviewed with 6 studies for every model (12 in total) to evaluate contact pressures which are made by EL on the CM and IM sockets.

The numerical method in Section 3.1.4 (Formula (3.1)) proves that prosthesis with radial clearance of 40 µm could experience EL with 80µm separation if the ball can reach to the edge of the socket. However, the nature of the IM design disables the ball from coming out of the socket or being separated more than radial clearance (40 µm in this study), Therefore, sources of EL by microseparation can be eliminated in the IM design. Therefore, we will have reduction of contact pressure and respective wear rate. To validate this claim, CM and IM are analysed with FEM and Hertzian contact theory in this chapter.

7.2.1. Microseparation, which does not cause of EL (50µm)

Based on Formula (3.1), ball should be separated from the centre of the socket by at least twice of the radial clearance, to load the edge of the CM. Therefore; microseparation below 80µm in this study cannot make EL. In this regard, if 50µm displacement is applied to CM and IM in this study, none of them will experience EL. This statement is verified with simulation and corresponding contour results shown in Figure 7.7a and Figure 7.7b where maximum contact pressures in both CM and IM are relatively low and almost equal with 99.6 MPa and 99.5 MPa, respectively. This means ball and socket in both CM and IM should be in conformal contact surface, which can be graphically seen in Figure 7.7a and 7.7b as well. Hence CM and IM under microseparation of 50µm show the similar behaviour and none of them experience EL, which is in agreement with Formula (3.1).

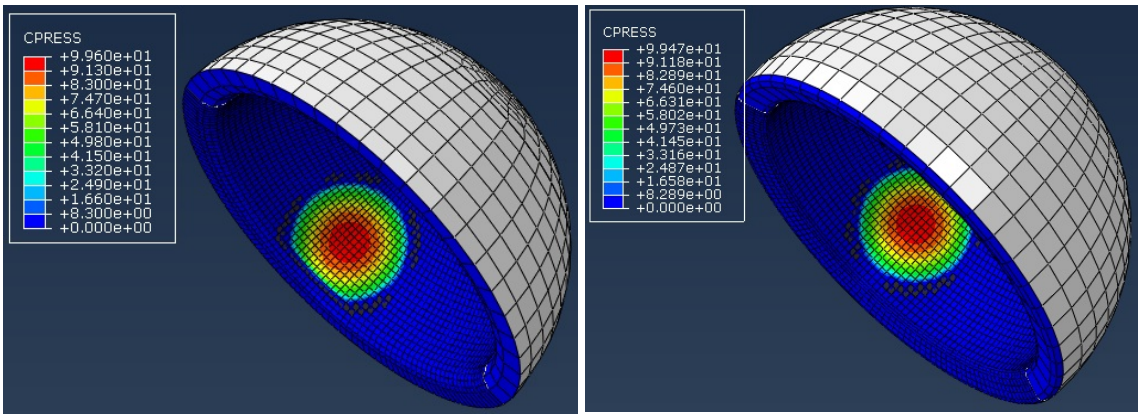

a b

Figure 7.7. Contour results of EL made by 50 µm displacement a) Maximum 99.6 MPa Contact pressure on CM socket. b) Maximum 99.5 MPa Contact pressure on IM socket

7.2.2. Microseparation that may develop EL (80µm)

As mentioned earlier, based on Formula (3.1), 80µm separation can be a critical value that may cause EL. Therefore 80µm distance is applied to CM and IM to analyse their performance. This study also agrees with Formula (3.1) and shows conformal contact of the ball and the socket in CM just are interrupted by moving toward the edge, while the majority part of the ball and socket are in conformal contact. However the ball and the socket of IM are perfectly in conformal contact. Therefore as it was suggested with Formula (3.1), CM socket with maximum contact pressure of 212.2 MPa slightly is affected by EL and shows marginally higher value of contact pressure in comparison with IM socket in Figure 7.8b with maximum contact pressure of 207.2 MPa which is not affected by EL at all.

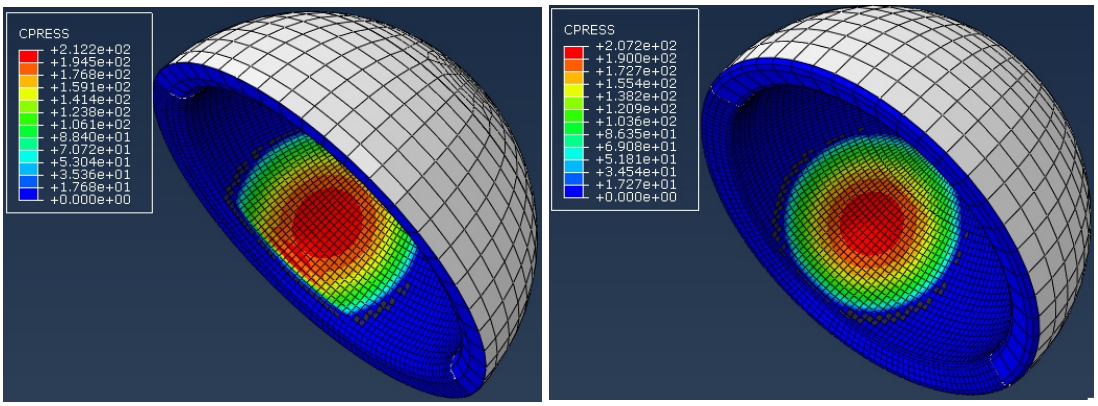

a b

Figure 7.8. Contour results of EL made by 80 µm displacement a) Maximum 212.2 MPa Contact pressure on CM socket. b) Maximum 207.2 MPa Contact pressure on IM socket

7.2.3. Developed EL (150 µm - 250 µm)

Section 7.2.2 shows that microseparation more than 80µm develops EL in CM but not postulated in IM. In this regard, different microseparation (150µm, 200µm and 250 µm) are applied to our study to investigate EL in CM and IM when they are well beyond the critical microseparation distance of 80µm.

7.2.3.1. Study EL in CM and IM under 150 µm displacement

Microseparation of 150 µm is well beyond the critical value of the microseparation; hence we expect that EL should be developed in CM. Microseparation of 150 µm is simulated with Abaqus to investigate EL in CM and IM. Figure 7.9a and 7.9b respectively show contact pressure due to this microseparation on CM and IM. Contour result shows EL is fully developed in CM while it was not developed in IM. Consequently, IM shows 26% reduction of contact pressure comparing with CM socket.

Figure 7.9a shows maximum contact pressure of 513 MPa on the edge of CM and Figure 7.9b shows maximum contact pressure of 378 MPa on the conformal area of the IM socket.

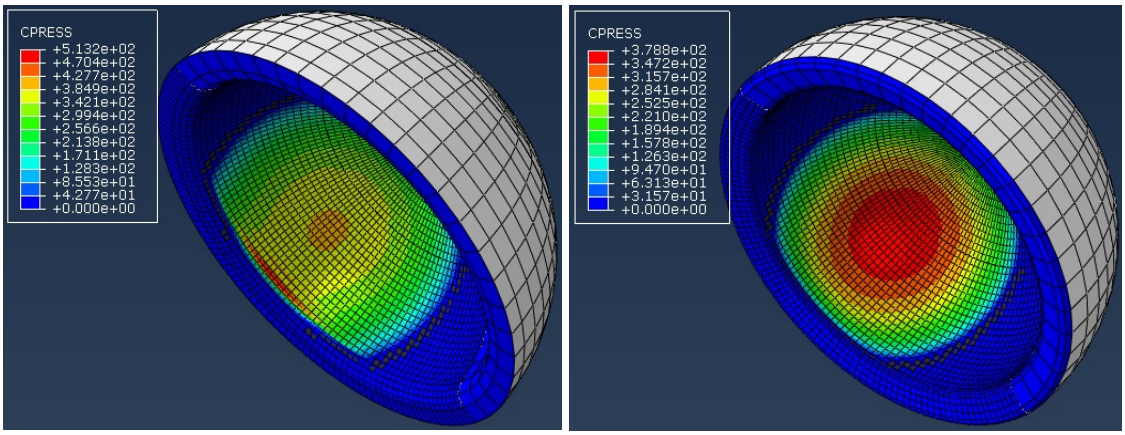

a b

Figure 7.9. Contour results of EL made by 150 µm displacement a) Maximum 513.2 MPa Contact pressure on CM socket. b) Maximum 378.8 MPa Contact pressure on IM socket

7.2.3.2. Study EL in CM and IM under 200 µm displacement

Microseparation of 200 µm shows maximum contact pressure of 914.6 MPa on the edge of the CM socket and 489 MPa on the conformal contact surface of the IM socket. In this regard under the same condition, IM reduces contact pressure by 46% comparing with the CM socket, which are shown in Figure 7.10a and Figure 7.10b, respectively.

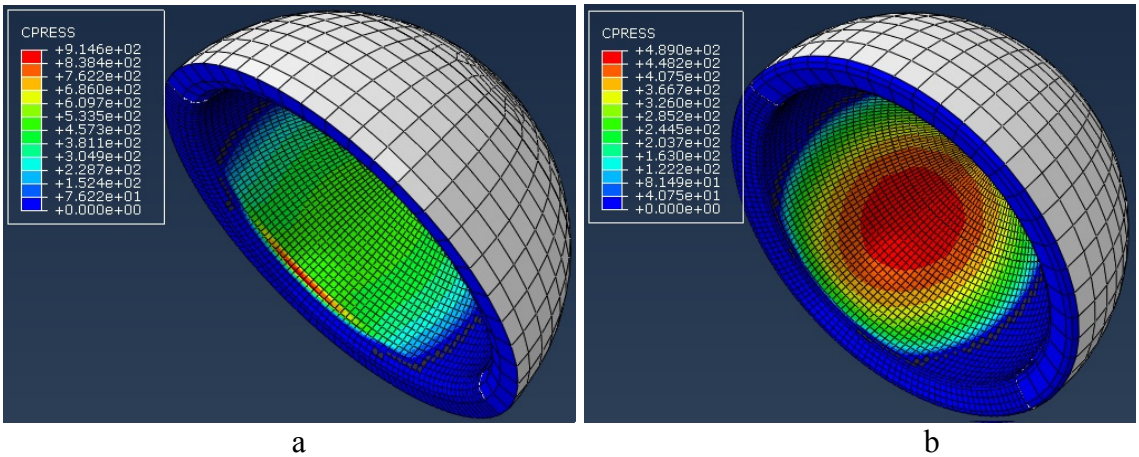

a b

Figure 7.10. Contour results of EL made by 200 µm displacement a) Maximum 914.6 MPa Contact pressure on CM socket. b) Maximum 489 MPa Contact pressure on IM socket

7.2.3.3. Study EL in CM and IM with 250 µm displacement

250 µm is the maximum displacement applied to the ball and socket for investigating the EL phenomenon [25, 97, 106]. A 250 µm displacement is also applied to CM and IM in our study. The result shows maximum contact pressure of 1.44 GPa on the narrow area of the CM edge (Figure 7.11a) while IM with 59% less contact pressure shows the maximum contact pressure of 590 MPa. Contour result remarkably shows conformal contact in IM under 250 µm displacement which is illustrated in Figure 7.11b.

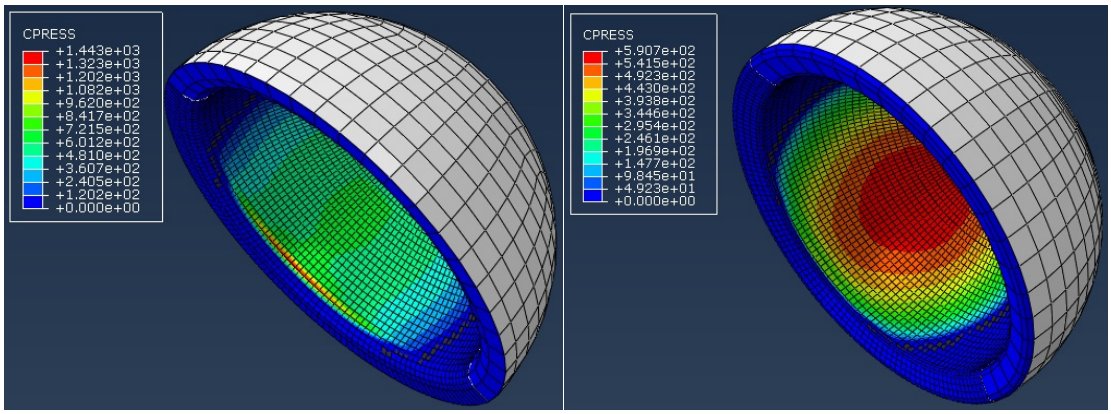

a b

Figure 7.11. Contour results of EL made by 250 µm displacement a) Maximum 1.44 GPa Contact pressure on CM socket. b) Maximum 590.7 MPa Contact pressure on IM socket

7.2.4. Extreme EL condition on CM

Although 250 µm was a maximum displacement applied to CM in some other studies [25, 97, 106], in our study 500 µm displacement is also considered for further investigation and test CM and IM in exaggerated conditions as well.

The result of this test is interesting where the edge of CM is significantly loaded with maximum contact pressure of 4.39 GPa in comparison with own conformal surface of the socket with maximum contact pressure of 1.09 GPa. This can be recognisable with colour spectrum Figure 7.12a as well. In other words the edge of CM is pressed 300% more than the maximum contact pressure of the conformal part of the CM socket. However, the IM ring is loaded with maximum contact pressure of 1.62 GPa where the conformal surface of the socket is loaded with maximum contact pressure of 1.27 GPa which means the IM ring is loaded only 27% more.

In this scenario IM not only shows better performance with 63% reduction of the contact pressure in comparison with CM design but also corresponding to the

distribution of the load on the IM socket which is shown in Figure 7.12b EL cannot be defined for IM.

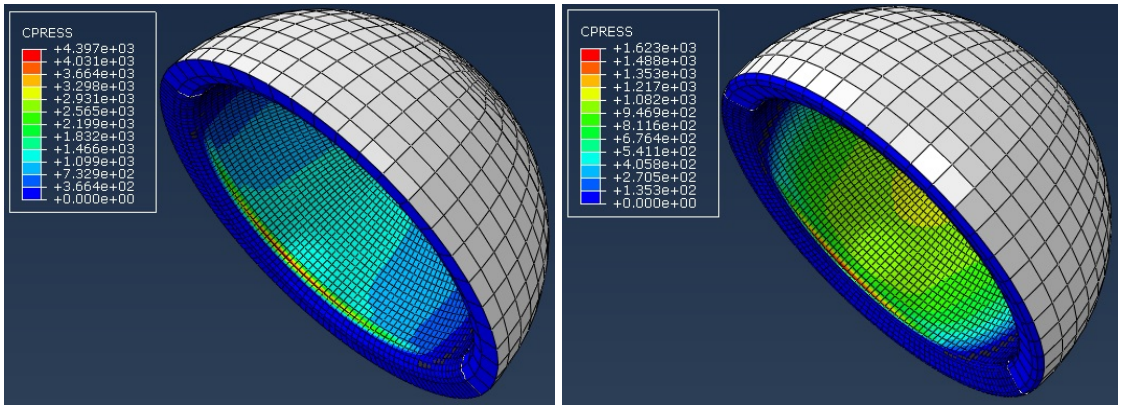

a b

Figure 7.12. Contour results of EL made by 500 µm displacement a) Maximum 4.4 GPa Contact pressure on CM socket. b) Maximum 1.62 GPa Contact pressure on IM socket

7.2.5. Discussion

EL happens if the ball can load the edge of the socket. If the ball is limited to the conformed surface of the socket, it does not reach to the edge of the socket. Therefore, the main requirement for EL to occur is eliminated and EL may be prevented. The IM Ring with unique design restricts the ball to the radial clearance. Also it makes the conformed surface in the socket for encountering with the ball even when it tries to come out of the socket during swing phase of walking cycle when the limb is lifted from the ground. The result from FEM shows the effectiveness of the IM design which is summarised in table 7.2.

Table 7.2. Summarising results of CM and IM in term of maximum contact pressure

Microseparation (µm)	**Contact pressure (GPa)**	
	CM	**IM**
50	99.6	99.4
80	212.2	207.2
150	513.2	378.8
200	914.6	489
250	1443	590.7
500	4397	1623

The results show that displacement under 80 µm has the same effect on IM and CM performances due to the conformal contact of the ball and the socket when EL is

not happened. However when the patient with CM prosthesis lift his/her leg from the ground to start walking cycle, ball gets more than 80 µm distance from the centre of the socket. In this case CM ball reaches to the edge of the CM socket and loads it with strike hill. However even in a normal condition like walking cycle, this may reach to 250 µm depending on the strength of the soft tissues surround the joint and in an unusual condition such as accident it can be fully dislocated from the socket. In terms of increasing the microseparation distance ball can more significantly loads the edge of the CM socket which is studied with FEM as well and illustrated in Figure 7.13. However the IM ring withstands the weight of the leg and prevents ball to get more than 40 µm separation from the centre of the IM socket and consequently the IM ball cannot load the IM socket with strike hill. In order to compare the results of CM and IM under microseparation, the same displacements are applied to CM and IM. The conformability of the IM ring shows a significant reduction of the contact pressure, which is reported in Figure 7.13.

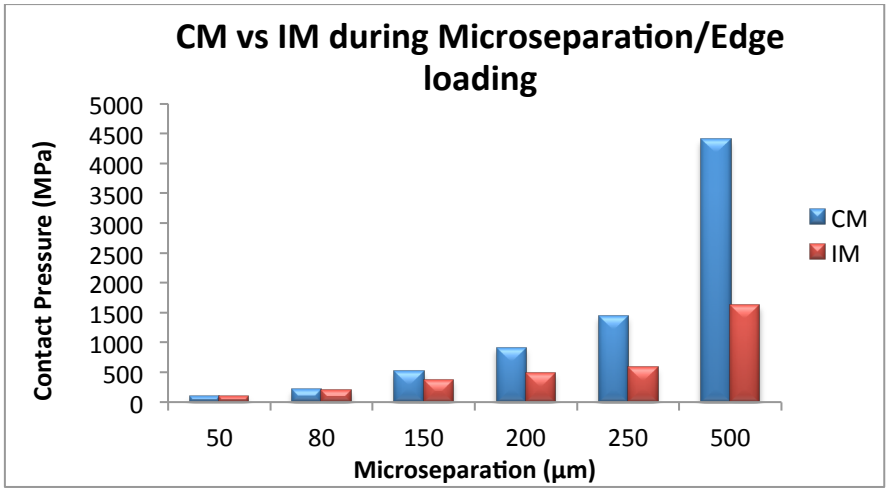

Figure 7.13. Contact pressure of CM vs IM during Microseparation of 50 µm to 500 µm

Increasing the microseparation between the ball and socket of CM and IM better indicates the advantage of the IM socket. When EL is fully developed by 150 µm microseparation, the CM socket is affected by contact pressure of 513.2 MPa, while the same microseparation is 26% less effective on IM socket. However when microseparation is increased to 500 µm, IM is affected with 63% less contact pressure than CM socket. Figure 7.14 compares the CM and IM socket when the microseparation increases.

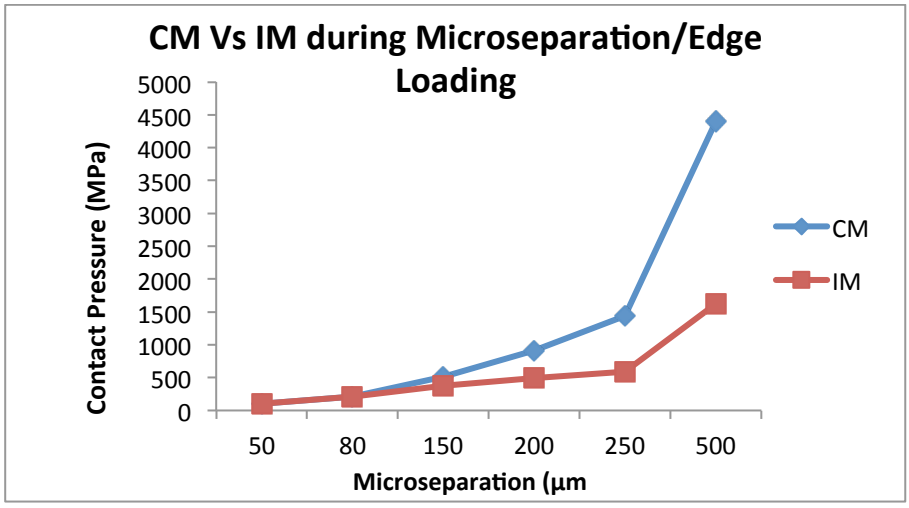

Figure 7.14. Reduction of maximum contact pressure by IM during Microseparation of 50 µm to 500 µm

7.3. Analysing EL with Hertzian Contact Theory

As explained in 4.3, we can study EL in CM and IM using Hertzian contact theory as well. When CM is undergone the EL condition, ball comes out of the socket and loads the CM chamfer. In terms of applying the Hertzian contact theory in this situation, we can assume that 2 balls with different radiuses ($R_{1\,CM} = 24\,mm$ and $R_{2\,CM} = 2.5\,mm$ in this study) contact each other. However IM ball only can loads the conformal surface of the IM socket either only to the concave area of the main socket or to the concave area of the IM Ring. Therefore, we can apply Hertzian contact theory to the ball with radius of 24 mm and the socket with 24.04 mm radius ($R_{1\,IM} = 24\,mm$ and $R_{2\,IM} = -24.04\,mm$).

CM and IM analysed with Hertzian contact theory and then compared based on this theory as well. From Table 6.1, Young's modulus and Poisson's ratio of the material which are used in CM and IM, are 350 GPa and 0.22 respectively. Therefore, the effective contact modulus E′ can be calculated by Equation 4.52 as following:

$$\frac{1}{E'} = \frac{1-(0.22)^2_{head}}{350\times10^9} + \frac{1-(0.22)^2_{cup}}{350\times10^9} = \frac{1.903}{350\times10^9} = 5.437\times10^{-12}$$

$$=> \quad E' = 1.839\times10^{11}\ \text{Pa}$$

7.3.1. Analysis of the CM with Hertzian Contact Theory:

In this study microseparation makes a contact between ball with 24 mm radius and chamfer with 2.5 mm radius. Thus using Equation (4.53), the effective radius of curvature of CM chamfer and ball is equal to:

$$\frac{1}{R}=\frac{1}{R_1}+\frac{1}{R_2} \quad => \quad \frac{1}{R_{CM}}=\frac{(24+2.5)\times10^{-3}}{24\times10^{-3}\times2.5\times10^{-3}}$$

$$=> \quad R_{CM}=2.264\times10^{-3}\ \text{m}$$

From Equation (4.51), contact radius of a is calculated as following:

$$a=\{\frac{3WR}{4E'}\}^{⅓} \quad => \quad a_{CM}=\{\frac{3\times W\times2.264\times10^{-3}}{4\times1.839\times10^{11}}\}^{⅓}$$

$$=> \left(\frac{W\times6.792\times10^{-3}}{7.356\times10^{11}}\right)^{⅓} = (W)^{⅓}\times(9.233\times10^{-15})^{⅓}$$

$$=> \quad a_{CM}=2.098\times10^{-5}\times(W)^{⅓}\ \text{m}$$

and maximum contact pressure of P_0 is computed by Equation (4.55) as follows:

$$P_0=\frac{3W}{2\pi a^2} \quad => \quad P_{0\,CM}=\frac{3W}{2\times3.14\times(2.098\times10^{-5}\times(W)^{⅓})^2}$$

$$=> \quad P_{0\,CM}=\frac{3W}{2.765\times10^{-9}\times W^{2/3}}$$

$$=> \quad P_{0\,CM}=1.085\times10^{9}\times W^{1/3}\ \text{Pa}$$

$P_{0\,cm}$ can be calculated with Equation (4.56) as well which does not need the value of the CM contact radius (This method for this study is explained in Appendix H).

7.3.2. Hertzian Contact Theory in IM

In this study, microseparation makes a contact between ball with 24mm radius and the concave ring of the IM socket with 24.04 mm radius. As it was explained earlier, ball has a positive radii and the concave ring has negative radii. Therefore using Equation (4.53), the effective radius of curvature of IM ring and ball is equal to:

$$R = \frac{R_{cup}R_{head}}{R_{cup} - R_{head}} => \quad R_{IM} = \frac{24\times24.04\times10^{-6}}{4\times10^{-5}}$$

$$=> R_{IM} = 14.424 \text{ m}$$

From Equation (4.51) contact radius of "a" is calculated as following:

$$a = \{\frac{3WR}{4E'}\}^{⅓} => \quad a_{IM} = \{\frac{3\times W\times14.424}{4\times1.839\times10^{11}}\}^{⅓}$$

$$=> \left(\frac{W\times43.272}{7.356\times10^{11}}\right)^{⅓} = (W)^{⅓}\times(5.882\times10^{-11})^{⅓}$$

$$=> a_{IM} = 3.889\times10^{-4}\times(W)^{⅓} \text{ m}$$

Therefore maximum contact pressure of $P_{0\,IM}$ is computed based on Equation (4.55) as following

$$P_0 = \frac{3W}{2\pi a^2} => P_{0\,IM} = \frac{3W}{2\times3.14\times(3.889\times10^{-4}\times(W)^{⅓})^2}$$

$$=> P_{0\,IM} = \frac{3W}{9.503\times10^{-7}\times W^{2/3}}$$

$$=> P_{0\,IM} = 3.156\times10^{6}\times W^{1/3} \text{ Pa}$$

$P_{0\,IM}$ also can be directly computed with Equation (4.56) which is s explained in Appendix I.

7.3.3. Discussion

Once the load (W) in Equations (7.1) and (7.2) is set, the maximum contact pressure on of CM and IM can be determined, respectively. Comparing Equation (7.1) and Equation (7.2) clearly demonstrates that the IM design reduces the maximum contact pressure by 99.7%.

$$P_{0_{CM}} = 1.085\times10^{9}\times W^{1/3} \quad \text{Pa} \tag{7.1}$$

$$P_{0_{IM}} = 3.157\times10^{6}\times W^{1/3} \quad \text{Pa} \tag{7.2}$$

Furthermore once the load (W) in Equations (7.3) and (7.4) is set, the maximum contact radius of CM and IM can be calculated respectively. CM and IM are made of the same material, therefore, if the same load is applied to Equations (7.3) and (7.4), then higher contact radius shows higher conformity. Equation (7.4) shows an increase in the IM contact radius by 94.6% in comparison with CM contact radius which is calculated by Equation (7.3).

$$a_{CM} = 2.098\times10^{-5}\times(W)^{1/3} \quad \text{m} \tag{7.3}$$

$$a_{IM} = 3.889\times10^{-4}\times(W)^{1/3} \quad \text{m} \tag{7.4}$$

As it was explained in part 4.3.1, studying of EL with Hertzian contact theory is extremely rational. However the assumptions of this theory, which are explained in part 4.3, are more compatible with CM than IM. Third assumption of Hertzian contact theory said; “Contact surfaces should be continues and non-conformed”, while the ring of IM makes conformed contacted surfaces to the ball, even though during microseparation.

Although both of the studies either with FEM or Hertzian contact theory clearly show better performance of the IM comparing to CM during EL, the result from Hertzian contact theory is better than the expected one. Contrary the result from FEM is worse than the expected one. Therefore we can expect the reduction of contact pressure during microseparation / EL by the IM will be at least 63% with an upper bound of more than 99%.

Chapter 8 : Conclusion, Recommendations and Future works

8.1. Conclusion

Edge loading (EL) is a key effective reason for increasing the wear rate of the total hip replacement prosthesis. This reduces the lifetime of the hip prostheses, which stops millions of young patients to go under THR surgery. Therefore these patients must remain wheelchair bound until they reach the right age for surgery.

Although there are many different reasons in occurrence of EL, some of them can be related to surgeons or patient cautions. However, some others could not be prevented or limited yet. Microseparation as the most important factor in occurrence of EL appears in every walking cycle. When the ball is separated from the centre of the socket, loads the edge of the socket before it is relocated in the centre of the socket. All kind of EL satisfy following conditions:

- Ball is separated from the centre of the socket.
- Ball loads the edge of the socket.

Consequently if these two reasons can be eliminated, EL can be limited respectively. The anatomy of the healthy hip joint prevents joint from EL while THR destructs this harmony as following:

- Hip capsule, which is sealed the joint with Ischiofemoral, Iliofemoral, Pubofemoral ligaments are slashed and punctured for exposing the hip joint for THR surgery.
- Labrum, which is an anatomical ring surrounding the acetabulum is completely removed for THR.
- Ligamentum teres attaches the tip of femoral head to the inside of the socket does not exist after THR.

We have proposed a novel hip joint prosthesis which reduce the effect EL in current total hip replacement surgeries. This research has studied the new hip joint prosthesis both medically and mechanically to be suitable for Biomedical research. Investigating the effective factors in EL and designing of the new hip prosthesis to preventing EL developed a novel design (IM) which has been patented with International Publication Number: WO2016/055783Al.

The IM not only eliminates the mentioned factors in EL but also solves dislocation problem. Moreover it significantly reduces the impact of the Neck-Rim/Ring impingement during excessive movement.

The IM has been analysed with three methods and the results are compared with the best available hip prosthesis in the market which is Biolox Delta Hip prosthesis. All results considerably support the effectiveness of the IM design.

Comparing the IM design with the available hip prosthesis suggests a promising result. This is mostly due to the eliminating of the EL causes by IM. Further analysing with FEM and Hertzian contact theory supports this theory as well. Hertzian contact theory shows reduction of contact pressure during EL by 99.7% and FEM simulation shows up to 63% reduction of contact pressure during EL and also Neck-Rim/Ring impingement.

99.7% reduction of contact pressure by Hertzian contact theory might be better than the expected results that postulated from IM. Third assumption of Hertzian theory said: Contact surfaces should be continuous and non-conformed, while this assumption was not exactly met by the IM. In contrast a considerably better result than 63% reduction of contact pressure by FEM is predictable. This is mostly due to the nature of the IM. IM disables the ball to get more than 40 μm dislocation; hence applied displacements more than 40 μm cannot be applicable to the IM. However due to the condition of the tests it was examined at all the same displacements as the CM.

If IM successfully passes the experimental tests and satisfies MHRA[20] in the UK and FDA[21] in the US, it can be implemented in human body. This not only significantly improves the lifestyle quality of younger patient but also with increased lifetime of the prosthesis, elderly rarely go under revision surgery which eliminates the respective risk of this surgery as well.

[20] Medicines and Healthcare products Regulatory Agency
[21] Food and Drug Administration

8.2. Recommendation and Future works

There are some challenging points in the IM design, which can be improved, by further research in the future as follows:

- Fixing the IM ring on the IM main socket: Although there are some recommendations in this thesis about fixing of the ring with press fitting for MOM or using biocompatible adhesive (Loctite made by Henkel-Germany) for COC and MOM, further study needs for ideal fixing method or making better adhesive for this purpose.
- Material of the IM Ring: Although ring can be made with the same material of the main socket, it might be more flexible material can be used to prevent the joint dislocation during outrageous condition.
- Manufacturing of IM and getting an experimental data.
- Approving by MHRA and/or FDA.
- Implementing in the human body.

References

1. Ranawat,A.S. Kelly,B.T . (July 2005). Anatomy of the Hip: Open and Arthroscopic Structure and Function . *Operative Techniques in Orthopaedics*. 15 (3), 160-174

2. Karlsson,K.M. Sernbo,I. Obrant,K.J. Redlund-Johnell,I. JohnellO. (April 1996). Femoral neck geometry and radiographic signs of osteoporosis as predictors of hip fracture. *ScienceDirect* . 18 (4), 327-330

3. Cheng,Y. Wang,S. Yamazaki,T. Zhao,J. Nakajima,Y. Tamura,S . (December 2007). Hip cartilage thickness measurement accuracy improvement. *Computerized Medical Imaging and Graphics*. 31 (8), 643-655

4. Gray,A. Villar,R. (October 1997). The ligamentum teres of the hip: as arthroscopic classification of its pathology. *The Journal of Arthroscopic & Related Surgery*. 13 (5), 575-578

5.Cook,P. Stevens,J. Gaudron,C. (August 2003). Comparing the effects of femoral nerve block versus femoral and sciatic block on pain and opiate consumption after total knee arthroplasty. *The Journal of Arthroplasty*. 18 (5), 583-586

6. Kesson,M. Atkins,E . (2005). Chapter 10- The hip. In: Patsy Cyriax,*Orthopaedic Medicine* . 2nd ed. London: Elsevier. 353-402

7. Habermann,E.T. Feinstein, P.A. (February 1978). Total hip replacement artheoplasty in arthritis conditions of the hip joint.*ARTHRITIS & RHEUMATISM*. 7 (3), 189-231

8. Lanyon,P. Muir,K. Doherty,S. Doherty,M. (2003). Age and sex differences in hip joint space among asymptomatic subjects without structural change: implications for epidemiologic studies. *Arthritis Rheum* . 48 (4), 1041–1046

9. Boutry,N. Khalil,C. Jaspart,M. Marie-Hélène,V. Demondion,X. Cotton,A. (July 2007). Imaging of the hip in patients with rheumatic disorders. *European Journal of Radiology*. 63 (1), 49-58

10. Jain,R. Grimer,R.J. Carter,S.R. Tillman,R.M. Abudu,A.A. (November 2005). Outcome after disarticulation of the hip for sarcomas. *European Journal of Surgical Oncology (EJSO)*. 31 (9), 1025-1028

11. Rousière,M. Michou,L. Cornélis,F. Orcel,P. (December 2003). Paget's disease of bone. *Best Practice & Research Clinical Rheumatology*. 17 (6), 1019-1041

12. Morgan,S.L . (February 2001). Calcium and Vitamin D in Osteoporosis.*Rheumatic Disease Clinics of North America*. 27 (1), 101-130

13. Goldacre MJ, Roberts SE, Yeates D. (October 2002). Mortality after admission to hospital with fractured neck of femur: database study.*BMJ*. 325 (7369), 771–775

14. Baltzan,M.A. Suissa,S. Bauer,D.C. Cummings,S.R. (April 1999). Hip fractures attributable to corticosteroid use. *The Lancet*. 353 (9161), 1327

15. Simpson,J. Sadri,H. Villar,R . (December 2010). Hip arthroscopy technique and complications. *Orthopaedics & Traumatology*. 96 (8), S68-S76

16. Panagis,J. Khaled,J. Saleh,M. Clement, B. (July 2013). *Hip Replacement.* Available: http://www.niams.nih.gov/Health_Info/Hip_Replacement/default.asp. Last accessed NOV 2013

17. Buie,V.C. Owings,M.F. DeFrances,J.C. Golosinskiy,A. (December 2010). *National Hospital Discharge Survey*. Available: http://www.cdc.gov/nchs/nhds/nhds_publications.htm. Last accessed Feb 2014

18. Turner,S. (2001). Research in Orthopedic Surgery. In: Souba,W.W. Wilmore,D.W *Surgical Research*. London: Academic Press. 1137-1200

19. Porter,M. Borroff,M. Gregg,P. MacGregor,A.Tucker,K. (2013). *10th Annual Report 2013*. Available: http: //www.njrcentre.org.uk. Last accessed DEC 2014

20. Dickens,P. Knight,B.H. Ip,P. Fung,W.S.Y. (December 1997). Fatal pulmonary embolism:: A comparative study of autopsy incidence in Hong Kong and Cardiff, Wales. *Elsevier*. 90 (3), 171-174.

21. Berthelot,J. Bataille,R. Maugars,Y. Prost,A. (October 1996). Rheumatoid arthritis as a bone marrow disorder.*ARTHRITIS & RHEUMATISM*. 26 (2), 505-514

22. Miller DM. (2004). Adult Reconstruction. In: Deputy *Review of orthopedics* . 4th ed. Saunders: Elsevier. 266-308

23. Judet,J. Judet R. (MAY 1950). The use of an artificial femoral head for arthroplasty of the hip joint. *The Bone and Joint Journal*. 32 (2), 166–173

24. Moore,A.T. Böhlman, H.R. (JUL 1983). The classic. Metal hip joint. A case report. *Clin Orthop*. (176), 3–6

25. Mak,M. Jin,Z. Fisher,J. Stewart,T.D . (January 2011). Influence of acetabular cup rim design on the contact stress during edge loadin in ceramic on ceramic hip prostheses. *The Journal of Arthroplasty*. 26 (1), 131-136

26. Walter,W.L. Lusty,P.J. Watson,A. O'Toole,G. Tuke,M.A. Zicat,B. Walte,W.K. (December 2006). Stripe wear and squeaking in ceramic total hip bearings. *Seminars in Arthroplasty*. 17 (3), 190-195

27. Kantor,S.R. Cummins,J. Tanzer,M . (June 2005). Complications after Total Hip Arthroplasty:Heterotopic Ossification.*Seminars in Arthroplasty*. 16 (2), 105-113

28. Chelly,J.E. Uskova,A.A. Plakseychuk,A . (June 2010). The role of surgery in postoperative nerve injuries following total hip replacement.*Clinical Anesthesia*. 22 (4), 285-293

29. Dennison,C. Pokras.R. (2010). *Number of all-listed procedures for discharges from short-stay hospitals, by procedure category and age.* Available: http://www.cdc.gov/nchs/data/nhds/4procedures/2010pro4_numberprocedureage.pdf. Last accessed Jan 2015

30. Anthony White (Obituary) Lancet. 1849;1:324.

31. Barton,JR. (Jan-Feb 1984). On the treatment of anchylosis, by the formation of artificial joints. *North American Medical and Surgical Journal* . 3 (1827), 279-292

32. Chlumsky V. Zentralblatt für or thopaedische Chirurgie. 1896. Continued Centralblatt für orthopaedische Chirurgie un mechanik from 1887-1890

33. Rang,M. (1966). *Anthology of Orthopaedics*. Edinburgh, London, New York: E. & S. LIVINGSTONE . 117-180

34. Baer,WS. (1918). Arthroplasty with the aid of animal membrane.*Amer Jour Orth Surg*. 16 (1), 171

35. Jones R, Lovett RW. (1929). *Orthopaedic*. Wm Wood: Baltimore. 110-130

36. Whitman,R. (1924). The Reconstruction Operation for Arthritis Deformans of the Hip-Joint . *Annals of Surgery*. 80 (5), 779–785.

37. Smith-Petersen,M. (1948). Evolution of mould arthroplasty of the hip joint. *The Bone and Joint Journal*. 30 (1), 59-75

38. Nadzadi,ME. Pedersen,DR. Yack,HJ. et al. (2003). Kinematics, kinetics and finite element analysis of commonplace maneuvers at risk for total hip dislocation. *J Biomech* .36,577–591.

39. Affatato,S. Goldoni,M. Testoni,M. Toni,A.(2001) Mixed oxides prosthetic ceramic ball heads. Part 3: effect of the ZrO2 fraction on the wear of ceramic on ceramic hip joint prostheses. A long-term in vitro wear study. *Biomaterials*,22(7),717–723.

40. Wroblewski,B.M. Siney,P.D. (1992). Charnley low-friction arthroplasty in the young patient. *The Bone and Joint Journal*. 80 (285), 7-45

41. Kwon,Y-M. Mellon,SJ. Monk,P. (2012). In vivo evaluation of edge-loading in metal-on-metal hip resurfacing patients with pseudotumours. *Bone Joint Res,* (1),42–49

42. Amanatullah,D.F. Landa,J. Strauss,E.J. Garino, JP. Kim,SH. Di Cesare,P.E. (September 2011). Comparison of Surgical Outcomes and Implant Wear Between ceramic- ceramic and ceramic-Articulations in Total Hip Arthroplasty. *the Journal of Arthroplasty*. 26 (6), 72-77

43. Goldsmith,A.A. Dowson,D. Wroblewski,B.M. Siney,P.D. Fleming,P.A. Lane,J.M. Stone,M.H. Walker,R. (2001). Comparative study of the activity of total hip arthroplasty patients and normal subjects. *the Journal of Arthroplasty*. 16 (5), 613–619

44.Schmalzried,T.P. Szuszczewicz,E.S. Northfield,M.R. Akizuki,K.H. Frankel,R.E. Belcher,G. Amstutz,H.C.(1998). Quantitative assessment of walking activity after total hip or knee replacement. *The Bone and Joint Journal*. 80 (1), 54-59

45.Ingham,E. Fisher,J. (2005). The role of macrophages in osteolysis of total joint replacement. *Biomaterials*. 26 (11), 1271–1286

46. Dowson,D. (1970). Whither tribology. *Wear*. 16 (4), 303–304

47. Hall,R.M. Siney,P. Unsworth,A. Wroblewski,B.M. (1997). The effect of surface topography of retrieved femoral heads on the wear of UHMWPE sockets. *Medical Engineering & Physics*. 19 (8), 711-719

48. Sychterz,C.J. Engh,Jr.CA. Swope,SW. McNulty,DE. Engh,CA. (January 1999). Analysis of prosthetic femoral heads retrieved at autopsy.*Clinical Orthopaedics & Related Research*. 358, 223–234

49. Hood,RW. Wright,TM. Burstein,AH. (1978). Retrieval analysis of total knee prostheses: a method and its application to 48 total condylar prostheses. *JOURNAL OF BIOMEDICAL MATERIALS RESEARCH*. 17 (5), 829 - 842

50. Vassiliou,K. Elfick,AP. Scholes,SC. Unsworth,A. (2006). The effect of 'running-in' on the tribology and surface morphology of metal-on-metal Birmingham hip resurfacing device in simulator studies. *engineering in medicine*. 220 (2), 269 - 277

51. Dowson,D. Wright,V. (1981). *Introduction to the Biomechanics of Joints and Joint Replacements*. London: Wiley. 254

52. Bartel,DL. Burstein,AH. Toda,MD. Edwards,DL. (1985). The effect of conformity and plastic thickness on contact stresses in metal-backed plastic implants. *BIOMECHANICAL ENGINEERING* . 107 (3), 193–199

53. Galvin,AL. Kang,L. Udofia,I. Jennings,LM. McEwen,HM. Jin,Z. Fisher,J. (2009). Effect of conformity and contact stress on wear in fixed-bearing total knee prostheses. *Journal of Biomechanics*. 42 (12), 1898–1902

54. Udofia,IT. Williams,S. Brockett,C. Jin,ZM. Fisher,J . (2009). Effect of acetabular cup orientation on the contact mechanics of metal-on-metal hip resurfacing prostheses. *the Orthopaedic Research Society*. 34 (2278), 1

55. Johnson,KL. (1987). *Contact mechanics*. Cambridge: Cambridge University Press. 242-312

56. Figueiredo-Pina,CG. Yan,Y. Neville,A. Fisher,J. (2008). Understanding the differences between the wear of metal-on-metal and ceramic-on-metal total hip replacements. *Engineering in medicine*. 222 (3), 285-296

57. Kang,L. Galvin,AL. Fisher,J. Jin,ZM. (2009). Enhanced computational prediction of polyethylene wear in hip joints by incorporating cross-shear and contact pressure in additional to load and sliding distance: Effect of head diameter. *Journal of Biomechanics*. 42 (7), 912–918

58. Liu,F. Galvin,A. Jin,ZM. Fisher,J. (2011). A new formulation for the prediction of polyethylene wear in artificial hip joints. *Mechanical Engineering*. 225 (1), 16-24

59. Jin,ZM. Dowson,D. Fisher,J. (1997). Analysis of fluid film lubrication in artificial hip joint replacements with surfaces of high elastic modulus.*Mechanical Engineering*. 211 (3), 247-256

60. Jin,Z. Fisher,J. (2014). Tribology of Hip Joint Replacement. In: George Bentley *European Surgical Orthopaedics and Traumatology*. London,UK: European Federation of National Associations of Orthopaedics and Traumatology. 2365-2377

61. Dumbleton,JH. D'Antonio,JA. Manley,MT. Capello,WN. Wang,A. (December 2006). The basis for a second-generation highly crosslinked UHMWPE. *Clinical Orthopaedics & Related Research*. 453, 265-271

62. McKellop,H. Shen,FW. Lu,B. Campbell,P. Salovey,R. (1999). Development of an extremely wear-resistant ultra high molecular weight polyethylene for total hip replacements. *Orthopaedics Research*. 17 (2), 157-167

63. Di Puccio,F. Mattei,L. (January 2015). Biotribology of artificial hip joints. *World Journal of Orthopedics*. 6 (1), 77-94

64. D'Antonio,JA. Capello,WN. Ramakrishnan,R. (2012). Second-generation annealed highly cross-linked polyethylene exhibits low wear. *Clin Orthop Relat Res* . 470 (6), 1696-1704

65. Reynolds,SE. Malkani,AL. Ramakrishnan,R. Yakkanti,MR. (2012). Wear analysis of first-generation highly cross-linked polyethylene in primary total hip arthroplasty: an average 9-year follow-up. *Arthroplasty*. 27 (6), 1064-1068

66. Firkins,PJ. Tipper,JL. Saadatzadeh,MR. Ingham,E. Stone,MH. Farrar,R. Fisher,J. (2001). Quantitative analysis of wear and wear debris from metal-on-metal hip prostheses tested in a physiological hip joint simulator. *Biomed Mater Eng* . 11 (2), 143-157

67. Chan,FW. Bobyn,JD. Medley,JB. Krygier,JJ. Tanzer,M. (1999). The Otto Aufranc Award. Wear and lubrication of metal-onmetal hip implants.*Clin Orthop Relat Res* . 369 (369), 10-24.

68. Dowson,D. Hardaker,C. Flett,M. Isaac,GH. (2004). A hip joint simulator study of the performance of metal-on-metal joints: Part I: The role of materials. *the Journal of Arthroplasty*. 19 (8), 118-123

69. Jenabzadeh,A-R. Pearce,SJ. Walter,WL. (2012). Total hip replacement: ceramic-on-ceramic. *Arthroplasty*. 23,232-240

70. Brockett,C. Williams,S. Jin,Z. Isaac,G. Fisher,J. (2007). Friction of total hip replacements with different bearings and loading conditions. *J Biomed Mater Res B Appl Biomater*. 81 (2), 508-515

71. Scholes,SC. Unsworth,A. (2000). Comparison of friction and lubrication of different hip prostheses. *Proc Inst Mech Eng H* . 214 (1), 49-57

72. Brockett,C.L. Williams,S. Jin,Z.M. Isaac,G. Fisher,J. (2007). A comparison of friction in 28 mm conventional and 55 mm resurfacing metal-on-metal hip replacements. *Journal of Engineering Tribology*. 221 (3), 391-398

73. Mattei,L. Di Puccio,F. Piccigallo,B. Ciulli,E. (2011). Lubrication and wear modelling of artificial hip joints: a review. *Tribology International*. 44 (5), 532–549.

74. Smith,SL. Dowson,D. Goldsmith,AAJ. Valizadeh,R. Colligon,JS. (2001). Direct evidence of lubrication in ceramic-on-ceramic total hip replacements. *Journal of Mechanical Engineering Science*. 215 (3), 265-268

75. Smith,SL. Dowson,D. Goldsmith,AAJ. (2001). The lubrication of metal-on-metal total hip joints: A slide down the Stribeck curve. *ournal of Engineering Tribology*. 215 (5), 483-493

76. Dowson,D. McNie,CM. Goldsmith,AAJ. (2000). Direct experimental evidence of lubrication in metal-on-metal total hip replacement.*Journal of Mechanical Engineering Science*. 214 (1), 75-86.

77. Liu,F. Jin,Z. Roberts,P. Grigoris,P. (2007). Effect of bearing geometry and structure support on transient elastohydrodynamic lubrication of metal-on-metal hip implants. *Journal of Biomechanics*. 40 (6), 1340–1349

78. Gao,L. Wang,F. Yang,P. Jin,Z. (2009). Effect of 3D physiological loading and motion on elastohydrodynamic lubrication of metalon- metal total hip replacement. *Medical Engineering & Physics*. 31 (6), 720-729

79. Smith,SL. Unsworth,A . (2000). Simplified motion and loading compared to physiological motion and loading in a hip joint simulator.*Proc Inst Mech Eng H* . 214 (3), 233-238

80. Mattei,L. Di Puccio,F. Piccigallo,B. Ciulli,E. (2010). *Elastohydrodynamic lubrication in total and resurfacing hip implants: effect of materials and geometries* . Singapore: Springer.

81. Fisher,J. (2011). Bioengineering reasons for the failure of metal-on-metal hip prostheses: an engineer's perspective. *Bone joint surgery*. 93 (8), 1001–1004

82. Tuke,MA. Scott,G. Roques,A. Hu,XQ. Taylor,A. (2008). Design considerations and life prediction of metal-on-metal bearings: the effect of clearance. *Bone joint surgery*. 90 (3), 134–141

83. Lusty,PJ. Tai,CC. Sew-Hoy,RP. Walter,WL. Walter,WK. Zicat,BA. (2007). Third-generation alumina-on-alumina ceramic bearings in cementless total hip arthroplasty. *Bone joint surgery*. 89 (12), 2676–2683

84. Lusty,P.J. Watson,A. Tuke,M.A. Walter,W.L. Walter,W.K. Zicat,B. (2007). Orientation and wear of the acetabular component in third generation alumina-onalumina ceramic bearings: AN ANALYSIS OF 33 RETRIEVALS. *The Bone and Joint Surgery*. 89 (B), 1158–1164

85. WalterWL. Insley,GM. Walter,WK. Tuke,MA. (2004). EL in third generation alumina ceramic-on-ceramic bearings: stripe wear.*Arthroplasty*. 19 (4), 402-413

86. Walter,WL. Kurtz,SM. Esposito,C. Hozack,W. Holley,KG. Garino,JP. Tuke,MA. (2011). Retrieval analysis of squeaking alumina ceramic-on-ceramic bearings. *Bone joint surgery*. 93 (12), 1597–1601

87. De Haan,R. Pattyn,C. Gill,H.S. Murray,D.W. Campbell,P.A. De Smet,K. (2008). Correlation between inclination of the acetabular component and metal ion levels in metal-on-metal hip resurfacing replacement.*The Bone and Joint Journal*. 90 (B), 1291-1297

88. Kwon,Y.M. Glyn-Jones,S. Simpson,D.J. Kamali,A. McLardy-Smith,P. Gill,H.S. Murray,D.W. (2010). Analysis of wear of retrieved metal-on-metal hip resurfacing implants revised due to pseudotumours. *Bone joint surgery*. 92 (B), 356–361

89. Isaac,GH. Dowson,D. Wroblewski,BM. (1996). An Investigation into the Origins of Time-Dependent Variation in Penetration Rates with Charnley Acetabular Cups—Wear, Creep or Degradation?. *Journal of Engineering in Medicine*. 210 (3), 209–216

90. Parvizi,J. Wade,FA. Rapuri,V. Springer,BD. Berry,DJ. Hozack,WJ. (2006). Revision hip arthroplasty for late instability secondary to polyethylene wear. *Clinical Orthopaedics & Related Research*. 447 (A), 66-69

91.Wroblewski,BM. Siney,PD. Dowson,D. Collins,SN. (1996). Prospective clinical and joint simulator studies of a new total hip arthroplasty using alumina ceramic heads and cross-linked polyethylene cups. *The Bone and Joint Surgery*. 78 (B), 280-285

92. Esposito,CI. Walter,WL. Roques,A. Tuke,MA. Zicat,BA. Walsh,WR. Walter,WK. (2012). Wear in alumina-on-alumina ceramic total hip replacements: a retrieval analysis of EL. *Bone joint surgery*. 94 (7), 901-907

93. Anthony,P. Sanders,MS. Parth,J. Dudhiya,B. Brannon,R.M. (2012). Thin Hard Crest on the Edge of Ceramic Acetabular Liners Accelerates Wear in EL. *The Journal of Arthroplasty*. 27 (1), 150-152

94. Elhadi Sariali, Todd Stewart, Zhongming Jin, John Fisher (2010). In Vitro Investigation of Friction under EL Conditions for Ceramic-on-Ceramic Total Hip Prosthesis. *Wiley Inter Science*. 28 (8), 979-985

95. Bergmann,G. Graichen,F. Rohlmann,A. (1993). Hip joint loading during walking and running, measured in two patients. *J Biomechanics* . 26 (8), 969–990

96. Scholes,SC. Green,SM. Unsworth,A. (2001). The wear of metal-on-metal total hip prostheses measured in a hip simulator. *Proc Inst Mech Eng* . 215 (6), 523–530

97. Stewart, T.D. Williamsa,S. Tipperb,JL. Inghamb,E. Stonec,MH. Fishera,J. (2003). Advances in simulator testing of orthopaedic joint prostheses. *Tribology Series*. 41,291–296

98. Nevelos,J.E. Prudhommeaux,F. Hamadouche,M. Doyle,C. Ingham,E. Meunier,A. Nevelos,A.B. Sedel,L. FisherJ. (2001). Comparative analysis of two different types of alumina-alumina hip prosthesis retrieved for aseptic loosening. *The Bone and Joint Journal*. 83 (4), 598-603

99. Nevelos,J. Ingham,E. Doyle,C. Streicher,R. Nevelos,A. Walter,W. Fisher,J. (2000). Microseparation of the centers of alumina-alumina artificial hip joints during simulator testing produces clinically relevant wear rates and patterns. *Arthroplasty*. 15 (6), 793-795

100. Lombardi,AV. Mallory,TH. Dennis,DA. Komistek,RD. Fada,RA. Northcut,EJ. (2000). An in vivo determination of total hip arthroplasty pistoning during activity. *Arthroplasty*. 15 (6), 702-709

101. Williams,S. Stewart,T.D. Ingham,E. Stone,M.H. Fisher,J. (2003). Influence of microseparation and joint laxity on wear of ceramic on polyethylene, ceramic on ceramic and metal on metal total hip prostheses. *The Bone and Joint Journal*. 85 (B)

102. Stewart,T. Tipper,J.L. Streicher,R. Ingham,E. Fisher,J. (2001). Long Term Wear of HIPed Alumina on Alumina Bearings for THR Under Microseparation conditions. *Journal of Material Science*. 12 (10), 1053-1056

103. Stewart,TD. Tipper,JL. Insley,G. Streicher,RM. Ingham,E. Fisher,J.(2003). Long-Term Wear of Ceramic Matrix Composite Materials for Hip Prostheses Under Severe Swing Phase Microseparation. *J Biomed Mater Res B Appl Biomater*. 66 (2), 567–573

104. Tipper,J.L. Firkins,P.J. Besong,A.A. MBarbour,P.S. Nevelos,J. Stone,M.H. Ingham,E. Fisher,J. (2001). Characterisation of wear debrisfrom UHMWPE on zirconia ceramic, metalon-metal and alumina ceramic-on-ceramic hip prostheses generated in a physiological anatomical hip joint simulator. *Wear*. 25, 120-128

105. Bergmann,G. Graichen,R. Rohnmann,A . (2002). *Investigation of potential separation between head and cup of total hip implants.*Available: http://www.ors.org/Transactions/48/0982.pdf. Last accessed 2015

106. Mak,M.M. Besong,A.A. Jin,Z.M. Fisher,J . (2002). Effect of microseparation on contact mechanics in ceramic-on-ceramic hip joint replacements. *Proceedings of the Institution of Mechanical Engineers*. 216 (6), 403-408

107. Mak,M.M. Jin,Z.M . (2002). Analysis of contact mechanics in ceramic-on-ceramic hip joint replacements. *Proc Inst Mech Eng* . 216 (4), 231-236.

108. Nevelös,AB. Evans,PA. Harrison,P. Rainforth,M. (1993). Examination of alumina ceramic components from total hip arthroplasties. *Proc Inst Mech Eng H* . 207 (3), 155-162

109. Walter WL. O'Toole,GC. Walter,WK. Ellis,A. Zicat,BA. (2007). Squeaking in ceramic-on-ceramic hips: the importance of acetabular component orientation.. *Arthroplasty*. 22 (4), 496-503

110. Bergmann,G. Deuretzbacherb,G. Hellerc,M. Graichena,F. Rohlmanna,A. Straussb,J. Dudac,G.N. (2001). Hip contact forces and gait patterns from routine activities. *Journal of Biomechanics*. 34 (7), 859-871

111. Lewinnek,GE. Lewis,JL. Tarr,R. Compere,CL. Zimmerman,JR. (1987). Dislocations after total hip-replacement arthroplasties. *The Bone and Joint Surgery*. 60 (2), 217-220.

112. McCollum,DE. Gray,WJ. (1990). Dislocation after total hip arthroplasty: causes and prevention. *Clinical Orthopaedics & Related Research*. 261, 159-170

113. Biedermann,R. Tonin,A. Krismer,M. Rachbauer,F. Eibl,G. Stöckl,B . (2005). Reducing the risk of dislocation after total hip arthroplasty: the effect of orientation of the acetabular component. *The Bone and Joint Surgery*. 87, 762-769

114. Johansson,HR. Johnson,AJ. Zywiel,MG. Naughton,M. Mont,MA. Bonutti,PM. (2011). Does acetabular inclination angle affect survivorship of alumina-ceramic articulations?. *Clinical Orthopaedics & Related Research*. 469 (6), 1560-1566

115. Sariali,E. Stewart,T. Jin,Z. Fisher,J. (2011). Effect of cup abduction angle and head lateral microseparation on contact stresses in ceramic-on ceramic total hip arthroplasty. *Journal of Biomechanics*. 45 (2), 390-393

116. Affatato,S. Traina,F. Toni,A. (2011). Microseparation and stripe wear in alumina-on alumina hip implants. *Int J Artif Organs*. 34 (6), 506-512

117. Affatato,S. Bersaglia,G. Foltran,I. Emiliani,D. Traina,F. Toni,A . (2004). The influence of implant position on the wear of alumina-onalumina studied in a hip simulator. *Wear*. 256 (3-4), 400–405

118. Taddei,P. Affatato,S. Fagnano,C. Toni,A. (2006). Photoluminescence investigations on alumina ceramic bearing couples tested under different angles of inclination in a Hip joint simulator. *Journal of Materials Science*. 41 (2), 399-407

119. Al-Hajjar,M. Leslie,IJ. Tipper,J. Williams,S. Fisher,J. Jennings,LM. (2010). Effect of cup inclination angle during microseparation and rim loading on the wear of BIOLOX delta ceramic-on-ceramic total hip replacement. *J Biomed Mater Res B Appl Biomater*. 95 (2), 263-268

120. Morlock,MM. Bishop,N. Zustin,J. Hahn,M. Ruther,W. Amling,M. (2008). Modes of implant failure after hip resurfacing: morphological and wear analysis of 267 retrieval specimens. *The Bone and Joint Surgery*. 90 (3), 89-95

121. Leslie,I.J. Williams,S. Isaac,G. Ingham,E. Fisher,J. (2009). High Cup Angle and Microseparation Increase the Wear of Hip Surface Replacements. *Clinical Orthopaedics & Related Research*. 467 (9), 2259–2265

122. Williams,S. Leslie,I. Isaac,G. Jin,Z. Ingham,E. Fisher,J. (2008). Tribology and wear of metal-on-metal hip prostheses: influence of cup angle and head position. *Bone joint surgery*. 90 (3), 111-117

123. Nevelos,JE. Ingham,E. Doyle,C. Nevelos,AB. Fisher,J. (2001). The influence of acetabular cup angle on the wear of ‘‘BIOLOX Forte’’ alumina ceramic bearing couples in a hip joint simulator. *J Mater Sci Mater Med*. 12 (2), 141–144

124. Bartz,RL. Nobel,PC. Kadakia,NR. Tullos,HS. (2000). The effect of femoral component head size on posterior dislocation of the artificial hip joint. *Bone joint surgery*. 82 (9), 1300-1307

125. Daniel,T.Le. Stephen,B.M. (2014). Ceramic-on-ceramic total hip arthroplasty: A new standard—Affirms. *Seminars in Arthroplasty*. 25 (2), 107–115

126. Lundberg,HJ. Liu,SS. Callaghan,JJ. Pedersen,DR. O'Rourke,MR. Goetz,DD. Vittetoe,DA. Clohisy,JC. Brown,TD. (2007). Association of third body embedment with rim damage in retrieved acetabular liners.*Clinical Orthopaedics & Related Research*. 465, 133-139

127. Shon,WY. Baldini,T. Peterson,MG. Wright,TM. Salvati,EA. (2005). Impingement in total hip arthroplasty: a study of retrieved acetabular components. *The Journal of Arthroplasty*. 20 (4), 427–435

128. Barrack,RL. Schmalzried,TP. (2002). Impingement and rim wear associated with early osteolysis after a total hip replacement : a case report. *Bone joint surgery*. 84 (7), 1218-1220

129. Urban,RM. Tomlinson,MJ. Hall,DJ. Jacobs,JJ. (2004). Accumulation in liver and spleen of metal particles generated at nonbearing surfaces in hip arthroplasty. *Arthroplasty*. 19 (8), 94-101

130. Barrack,RL. Burak,C. Skinner,HB. (2004). Concerns about ceramics in THA. *Clinical Orthopaedics & Related Research*. 429 (A), 73-79.

131. Holley,KG. Furman,BD. Babalola,OM. Lipman,JD. Padgett,De. Wright,TM. (2005). Impingement of acetabular cups in a hip simulator— comparison of highly cross-linked and conventional polyethylene.*the Journal of Arthroplasty*. 20 (3), 77–86

132. Elkins,J.M. O'Brien,MK. Stroud,NJ. Pedersen,DR. Callaghan,JJ. Brown,TD. (2011). Hard-on-Hard Total Hip Impingement Causes Extreme Contact Stress Concentrations. *Clinical Orthopaedics & Related Research*. 469 (2), 454-463

133.Archard,JF. (1953). Contact and rubbing of flat surfaces. *J Appl Phys*. 24 (8), 981 - 988

134. Pedersen,DR. Callaghan,JJ. Brown,TD. (2005). Activity-dependence of the 'safe zone' for impingement versus dislocation avoidance. *Medical Engineering & Physics*. 27 (4), 323-328

135. Klein Horsman MD, Koopman HF, van der Helm FC, et al. (2007). Morphological muscle and joint parameters for musculoskeletal modelling of the lower extremity. Clin Biomech,22,239–247.

136. Richard J. van Arkel, Luca Modenese, Andrew T.M. Phillips, Jonathan R.T. Jeffers (2013), Hip Abduction Can Prevent Posterior EL of Hip Replacements, *JOURNAL OF ORTHOPAEDIC RESEARCH*, 1 pp. 1172–1179

137. Boone DC, Azen SP. (1979). Normal range of motion of joints in male subjects. J Bone Joint Surg,61,756–759.

138. Delp S, Anderson F, Arnold A, et al. (2007). OpenSim: opensource software to create and analyze dynamic simulations of movement. IEEE Trans Biomed Eng 54:1940–1950.

139. Murray DW. (1993). The definition and measurement of acetabular orientation. J Bone Joint Surg,75,228–232.

140. Yoshioka S, Nagano A, Hay DC, et al. (2012). The minimum required muscle force for a sit-to-stand task. J Biomech,45,699–705.

141. Doorenbosch CAM, Harlaar J, Roebroeck ME, et al. (1994). Two strategies of transferring from sit-to stand; The activation of monoarticular and biarticular muscles. J Biomech, 27,1299–1307.

142. Morlock M, Schneider E, Bluhm A,(2001) et al: Duration and frequency of everyday activities in total hip patients. J Biomech,34,873

143. Walter WL, Waters TS, Gillies M, et al. (2008). Squeaking hips. J Bone Joint Surg,90A,102–111.

144. Underwood R, Matthies A, Cann P, et al. (2011). A comparison of explanted Articular Surface Replacement and Birmingham Hip Resurfacing components. J Bone Joint Surg,93B,1169–1177.

145. De Haan R, Campbell PA, Su EP, et al. (2008). Revision of metal-on-metal resurfacing arthroplasty of the hip: the influence of malpositioning of the components. J Bone Joint Surg,90,1158–1163

146. Kessler O, Pati S, Stefan W, et al.(2008). Bony impingement affects range of motion after total hip arthroplasty: a subject-specific approach. J Orthop Res,26,443–452.

147. Restrepo C, Parvizi J, Kurtz SM, Sharkey PF, Hozack WJ, Rothman RH,(2008) The noisy ceramic hip: is component malpositioning the cause? J Arthroplasty,23, 643-9.

149. Amstutz HC, Clarke IC(1991): Evolution of hip arthroplasty, in Amstutz HC: Hip Arthroplasty. New York, NY, Churchill Livingstone,1-14

150. Charnley J(1979): Low Friction Arthroplasty of the Hip. Berlin, Germany, Springer-Verlag.

151. Morlock M, Nassutt R, Janssen R, et al.(2001) Mismatched wear couple zirconium oxide and aluminum oxide in total hip arthroplasty. J Arthroplasty,16,8.

152.Willmann G ,Fruh HJ, Pfaff HG,(1996), Wear characteristics of sliding pairs of zirconia (Y-TZP) for hip endo-prostheses. Biomaterials 17:2157-2162.

153. Back DL, Dalziel R, Young D, et al.(2005) Early results of primary Birmingham hip resurfacings. An independent prospective study of the first 230 hips. J Bone Joint Surg Br,87,3.

154. Sariali E, Stewart T, Jin Z, et al. (2009). In vitro and in vivo analysis of squeaking frequencies in ceramic-on-ceramic total hip protheses. 55th Orthopaedic Research Society, Las Vegas

155. Yokoi M, Nakai M.(1979). A fundamental study on Frictional noise. 1st Report, the generating mechanism of rubbing noise and squeal noise. Bull JSME 22:1665–1671.

156. Van de Velde F, De Baets P. (1998). A new approach of tick-slip based on quasi harmoic tangential oscillations. Wear 216:15–26.

157. Van de Velde F, De Baets P. (1998). The relation between frcition force and relative speed during the slip-phase of stick-slip cycle. Wear 219:220–226.

158. Ecker T, Robbins C, Van Flandem G, et al. (2008). Squeaking in total hip replacement: No cause for concern. Orthopedics 31:875.

159. Chevillotte C, Trousdale R, Chen Q, et al. (2009). The 2009Frank Stinchfield Award: ‘‘Hip squeaking’’: a biomechanical study of ceramic-on-ceramic bearing surfaces. Clin Orthop Relat Res [Epub ahead of print.

160. Glaser, D., Komistek, R., Cates, H., Mahfouz, M., (2008). Clicking and squeaking: in vivo correlation of sound and separation for different bearing surfaces. J.Bone Jt. Surg.Am.90 (Suppl.4), 112-120.

161. Jarret, C., Bruzzone, M., Rodriguez, J., Ranawat, C., (2007). The squeaking hip: an under-reported phenomenon of ceramic-on-ceramic total hip arthroplasty. In: Proceedings of the AAOS, Poster No.198, San Diego, USA.

162. Elhadi Sariali, Todd Stewart, Zongmin Jin, John Fisher (2010), Three-dimensional modelling of invitro hip kinematics under micro-separation regime for ceramic on ceramic total hip prosthesis: An analysis of vibration and noise, *Journal of Biomechanics*, 43, 326–333

163. Weiss, C., Hothann, A., Hoffman, N., Morlock, M., (2008). Squeaking ceramic-on- ceramic total hip replacements. A numerical vibration approach. In: Proceedings of the 16th Congress of the European Society of Biomechanics, Luzern, Switzerland.

164. Parvizi J, Adeli B, Wong JC, et al (2011).A squeaky reputation: the problem may be design dependent. Clinical Orthopaedics and Related Research, 469,1598–605.

165. Mai K, Verioti C, Ezzet KA, et al.(2010) Incidence of 'squeaking' after ceramic-on-ceramic total hip arthroplasty. Clinical Orthopaedics and Related Research, 468, 413–7.

166. Swanson TV, Peterson DJ, Seethala R, et al.(2010) Influence of prosthetic design on squeaking after ceramic-on-ceramic total hip arthroplasty. Journal of Arthroplasty,25,36–42.

167. Griffin WL, Nanson CJ, Springer BD, et al. (2010). Reduced articular surface of one-piece cups: A cause of runaway wear and early failure. Clin Orthop Relat Res ,468,2328– 2332.

168. Jacob M. Elkins, Karen M. Kruger, Douglas R. Pedersen, John J. Callaghan, Thomas D. Brown (2012), Edge-Loading Severity as a Function of Cup Lip Radius in Metal-on-Metal Total Hips—A Finite Element Analysis, *J Orthop Res,* 30,169–177.

169. Richard J Underwood, Angelos Zografos, Ritchie S Sayles, Alister Hart and Philippa Cann (2012), Edge loading in metal-on-metal hips: low clearance is a new risk factor Proceedings of the Institution of Mechanical Engineers, Part H: Journal of Engineering in Medicine, 217 – 226

170. P. Triclot, F. Gouin, (2011) Update - "Big-head": The solution to the problem of hip implant dislocation? *Orthopaedics & Traumatology: Surgery & Research,* 97 (4), S42-S48

171. Sariali E, Lazennec JY, Khiami F, Catonné Y.(2009) Mathematical evaluation of jumping distance in total hip arthroplasty. Acta Orthop,80,277—82.

172. Burroughs BR, Hallstrom B, Golladay GJ, Hoeffel D, Harris WH. (2005), Range of motion and stability in total hip arthroplasty with 28-32-38 and 44mm femoral head size. J Arthroplasty,20,11—20.

173. Shaju KA, Hassan ST, D'Souza LG, McMahon B, Masterson EL. (2005),The 22mm vs 32mm femoral head in cemented primary hip arthroplasty long-term clinical and radiological follow-up study. J Arthroplasty,20(7),903—8.

174. Livermore J, Ilstrup D, Morrey B. (1990)Effect of femoral head size on wear of the polyethylene acetabular component. J Bone Joint Surg Am, 1990,72(4),518—28.

175. Clarke IC, Gustavson A, Jung H, Fujisawa A.(1996) Hip-simulator ranking of polyethylene wear: comparison between ceramic heads of different sizes. Acta Orthop Scand,67(2),128—32.

176. Wrobleski BM, Siney PD, Fleming PA. (2000), Wear of ultra-high molecular weight polyethylene cup in the Charnley LFA, using metal and ceramic 22.2 diameter head. Total Hip Arthroplasty: what will the 21st century prosthesis be like? Acora Group ed,4(4),111—3.

177. Shen FW, Lu Z, McKellop HA. (2011),Wear versus thickness and other features of 5-Mrad cross-linked UHMWPE acetabular liners. Clin Orthop Relat Res,469,395-404.

178. Muratoglu OK, Orhun K, Wannomae K, Christensen S, Rubash H, Harris WH. (2005), Ex vivo wear of conventional and crosslinked polyethylene acetabular liners. Clin Orthop Relat Res, 438,158—64.

179. Triclot P, Grosjean G, El Masri F, Courpied J, Hamadouche M.(2007), A comparison of the penetration of two polyethylene acetabular liners of different levels of cross-linking. J Bone Joint Surg Br,89(11),1439—45.

180. Leung SB, Egawa H, Stepniewski A, Beykirch S, Engh Jr CA, Engh Sr CA. (2007), Incidence and volume of pelvic osteolysis at early followup with highly cross-linked and non cross-linked polyethylene. J Arthroplasty,22(2),134—9.

181. Geerding CH, Grimm B, Vencken W, Heyligers IC, Tomino AJ. (2009),Cross-linked compared with histological polyethylene in THA: an 8-year clinical study. Clin Orthop Relat Res,467,979—84

182. Milner GR, Boldsen JL. (2012). Humeral and femoral head diameters in recent white American skeletons. *Journal of Forensic Science* .; 57(1) pp. 35-40.

183. Rosenberg AG. AAOS (2010), SympoVI; podium presentation

184. Zagra L, Ceroni GR, Corbella M. (2004),THA ceramic-ceramic coupling with bigger heads. 9th Biolox Symposium, www.biolox.com.

185. Clark C, Green D, Williams P, Donaldson T, Pezzotti G.(2006) US perspective on hip simulator wear testing of BIOLOX Delta in severe test modes. 11th Biolox Symposium,www.biolox.com.

186. Hammerberg EM, Wan Z, Dastane M, Dorr LD (2010) Wear and range of motion of different femoral head*, The Journal of Arthroplasty* 25(6), 839-843

187. Usrey MM, Noble PC, Rudner LJ, et al. (2006),Does neck/liner impingement increase wear of ultrahigh molecular-weight polyethylene liners. J Arthroplasty,21:65.

188. Dorr LD.(2008),Acetabular cup position: the imperative of getting it right. Orthopedics,31:898.

189. Kelley SS, Lachiewicz PF, Hickman JM, et al.(1998) Relationship of femoral head and acetabular size to the prevalence of dislocation. Clin Orthop Relat Res,355:163.

190. Nizard, R. S., Sedel, L., Christel, P., Meunier, A. Soudry, M. and Witvoet, J. (1992), Ten-year survivorship of cemented ceramic–ceramic total hip prosthesis. Clin. Orthop. Related Res., 282, 53–63.

191. Sedel, L. Evolution of alumina-on-alumina implants: a review. Clin. Orthop. Related Res.,(2000), 379, 48–54.

192. 7 Saikko, V. and 5 CONCLUSIONS PfaV, H. G. (1998)Low wear friction in alumina/alumina total hip joints: a hip simulator study. ActaOrthopaedica Scand.,69(5), 443–448.

193. Ueno, A., Amino, H., Okimatu, H. and Oonishi, H.(1999) Wear, friction, and mechanical investigation and development of alumina-to-alumina combination total hip joint. In Joint Arthroplasty (Eds S. Imura,M.Wada andH. Omori),119–131 (Springer-Verlag, Tokyo).

194. R. L. Courant, (1943)"Variational Methods for the Solution of Problems of Equilibrium and Vibration," Bulletin of the American Mathematical Society, 49, 1-23.

195. M. J. Turner, R. W. Clough, H. C. Martin and L. J. Topp,(1956) "Stiffness and Deflection Analysis of Complex Structures," J. of Aero. Sci., 23 (9)

196. CLOUGH, R.W.(1958) "Structural analysis by means of a matrix algebra program", Proc. A.S.C.E. Conf. on Electronic Computation, Kansas City,109-132.

197. CLOUGH, R.W.(1960) "The finite element method in plane stress analysis", Proc. 2nd A.S.C.E. Conf. on Electronic Computation, Pittsburg, Pa.

198. CLOUGH, R. (1965) "The finite element method in structural mechanics", in: Stress Analysis, Chapter 7, edited by O.C. ZIENKIEWmZ and G.S. HOLISTER, Johil Wiley and Sons, Ltd, 85-87.

199. CLOUGH, R.(1979) "The finite element method after twenty-five years: A personal view", Int. Conf. on Engineering Application of the Finite Element Method, Computas, Veritas Center, Hovik, Norway, 1.1.

200. CLOUGH, R.W. and E.L. WILSON,(1962) "Stress analysis of a gravity dam by the finite element method", Proc. Symposium on the Use of Computers in Civil Engineering, Laboratorio Nacional de Engenliaria Civil, Lisbon, Portugal, .

201. H. F. El'Sheikh, B. J. MacDonald, and M. S. J. Hashmi, (2003)"Finite element simulation of the hip joint during stumbling: a comparison between static and dynamic loading," Journal of Materials Processing Technology,143,(144),249-255.

202. A. Z. Senalp, O. Kayabasi, and H. Kurtaran, (2007), "Static, dynamic and fatigue behavior of newly designed stem shapes for hip prosthesis using finite element analysis,", (28),1577-1583.

203. Hertz, H.(1882), On the contact of rigid elastic solids and on hardness. In: Schott, J.A. (Ed.), Miscellaneous papers by H.Hertz. Mac Millan, London,164–183.

204. Cai P, Hu Y, Xie J. (2012), Large-diameter Delta Ceramic-on-ceramic Versus Common-sized Ceramic-on-polyethylene Bearings in THA. Orthopedics, (35),1307-1313

205. Kuntz M, (2006),Validation of a New High Performance Alumina Matrix Composite for use in Total Joint Replacement, Seminarsin Arthroplasty (17), 141–5.

206. CeramTec GmbH, Medical Products Division. (2000).'BIOLOX delta Scientific Information and Performance Data'. Retrieved from https://www.ceramtec.com/files/mt_biolox_delta_en.pdf

207. Zimmer Personal Fit. Renewed Life. (2010). 'Continuum Acetabular System'. Retrieved from http://www.zimmersouthafrica.co.za/medical-professionals/products/hip/continuum-acetabular-system-ous.html

208. Nordin M, Frankel VH, eds(1989).Basic Biomechanics of the Musculoskeletal System. Philadelphia: Malvern, PA: Lea & Febiger,135-151

209. Saudek C E. The hip. In J. Gould, G. J. Davies (Eds.)(1985) Orthopaedic and Sports Physical Therapy. St. Louis: Mosby, 365-407

210. Soderberg, G. L. (1986). Kinesiology: Application to Pathological Motion. Baltimore: Williams & Wilkins, 243-266.

Appendixes

Appendix A: Labrum; the Natural Ring

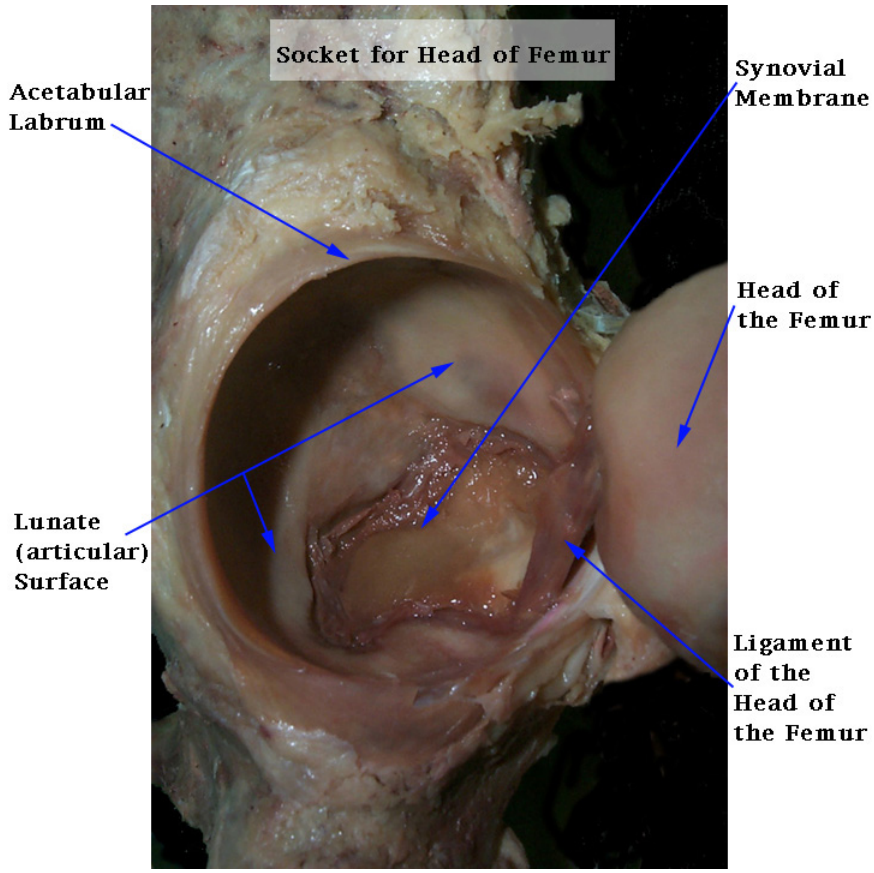

Labrum, a natural ring of the socket

Appendix B: Total Hip Replacement Surgery video

COC Total Hip Replacement Surgery video can be found in following link:

https://www.youtube.com/watch?v=fN10ycgxw_c

Appendix C: Taper properties

Neck and Taper cavity (Biolox Delta, CearmTec [206])

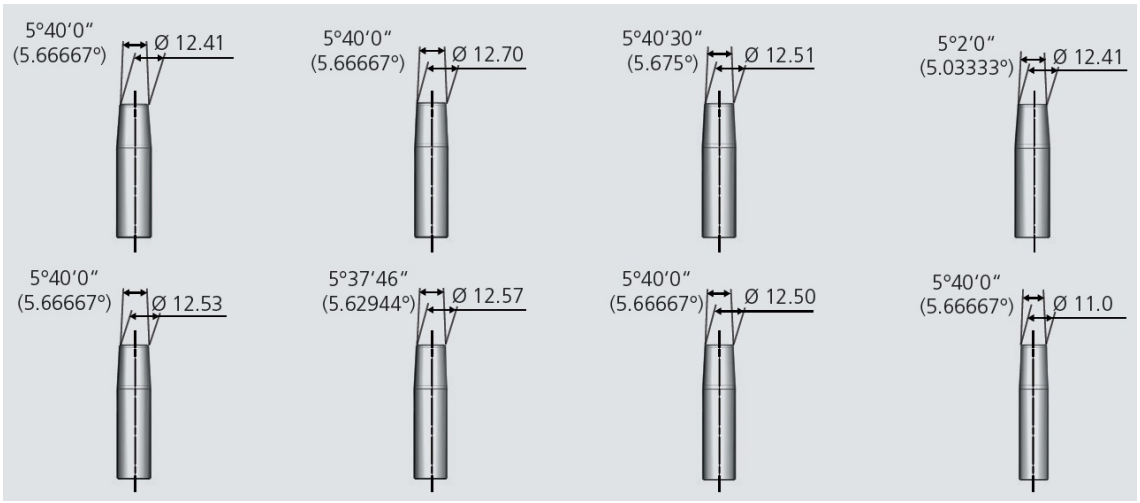

Different tapers where all of them are designated "12/14" [206]

Taper size: 12/14 [206]

Appendix D: IM Patent file

All 28 pages of this patent with international publication number: WO2016055783A1 available in the following link: http://www.sumobrain.com/patents/wipo/Acetabular-cup-hip-replacement-joint/WO2016055783A1.pdf

(12) INTERNATIONAL APPLICATION PUBLISHED UNDER THE PATENT COOPERATION TREATY (PCT)

(19) World Intellectual Property Organization
International Bureau

(43) International Publication Date
14 April 2016 (14.04.2016)

WIPO | PCT

(10) International Publication Number
WO 2016/055783 A1

(51) International Patent Classification:
A61F 2/34 (2006.01)

(21) International Application Number:
PCT/GB2015/052933

(22) International Filing Date:
7 October 2015 (07.10.2015)

(25) Filing Language: English

(26) Publication Language: English

(30) Priority Data:
1417694.5 7 October 2014 (07.10.2014) GB

(71) Applicant: **THE UNIVERSITY OF WARWICK** [GB/GB]; Coventry Warwickshire CV4 7AL (GB).

(72) Inventor: **TORABI KACHOUSANGI, Ehsanollah**; Apartment 15, The Town House, 2 Kenilworth Road, Leamington Spa Warwickshire CV32 5TE (GB).

(74) Agent: **BOULT WADE TENNANT**; Verulam Gardens, 70 Gray's Inn Road, London WC1X 8BT (GB).

(81) Designated States *(unless otherwise indicated, for every kind of national protection available)*: AE, AG, AL, AM, AO, AT, AU, AZ, BA, BB, BG, BH, BN, BR, BW, BY, BZ, CA, CH, CL, CN, CO, CR, CU, CZ, DE, DK, DM, DO, DZ, EC, EE, EG, ES, FI, GB, GD, GE, GH, GM, GT, HN, HR, HU, ID, IL, IN, IR, IS, JP, KE, KG, KN, KP, KR, KZ, LA, LC, LK, LR, LS, LU, LY, MA, MD, ME, MG, MK, MN, MW, MX, MY, MZ, NA, NG, NI, NO, NZ, OM, PA, PE, PG, PH, PL, PT, QA, RO, RS, RU, RW, SA, SC, SD, SE, SG, SK, SL, SM, ST, SV, SY, TH, TJ, TM, TN, TR, TT, TZ, UA, UG, US, UZ, VC, VN, ZA, ZM, ZW.

(84) Designated States *(unless otherwise indicated, for every kind of regional protection available)*: ARIPO (BW, GH, GM, KE, LR, LS, MW, MZ, NA, RW, SD, SL, ST, SZ, TZ, UG, ZM, ZW), Eurasian (AM, AZ, BY, KG, KZ, RU, TJ, TM), European (AL, AT, BE, BG, CH, CY, CZ, DE, DK, EE, ES, FI, FR, GB, GR, HR, HU, IE, IS, IT, LT, LU, LV, MC, MK, MT, NL, NO, PL, PT, RO, RS, SE, SI, SK, SM, TR), OAPI (BF, BJ, CF, CG, CI, CM, GA, GN, GQ, GW, KM, ML, MR, NE, SN, TD, TG).

Published:
— *with international search report (Art. 21(3))*

(54) Title: AN ACETABULAR CUP FOR A HIP REPLACEMENT JOINT

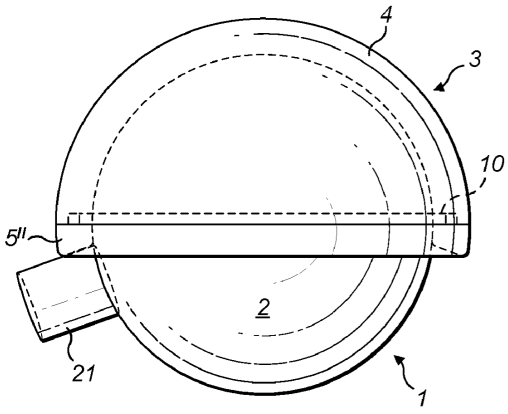

FIG. 4

(57) Abstract: An acetabular cup for a hip replacement joint. The cup comprises a main body (4) which has a substantially hollow hemispherical shape with an inner surface for receiving, in use, a ball (2) of a femoral component (1). The main body has an end face (6) at the open end of the hollow hemisphere for which a ring (5) is connected. The ring continues the inner surface of the main body without interruption to narrow the opening of the cup. The inner edge of the ring (5) at the end of the ring furthest from the main body having a convexly curved chamfer (12). The face (20) of the ring furthest from the main body is substantially frustoconical.

WO 2016/055783 A1

Appendix E: Monitoring of the increments in the Abaqus job page

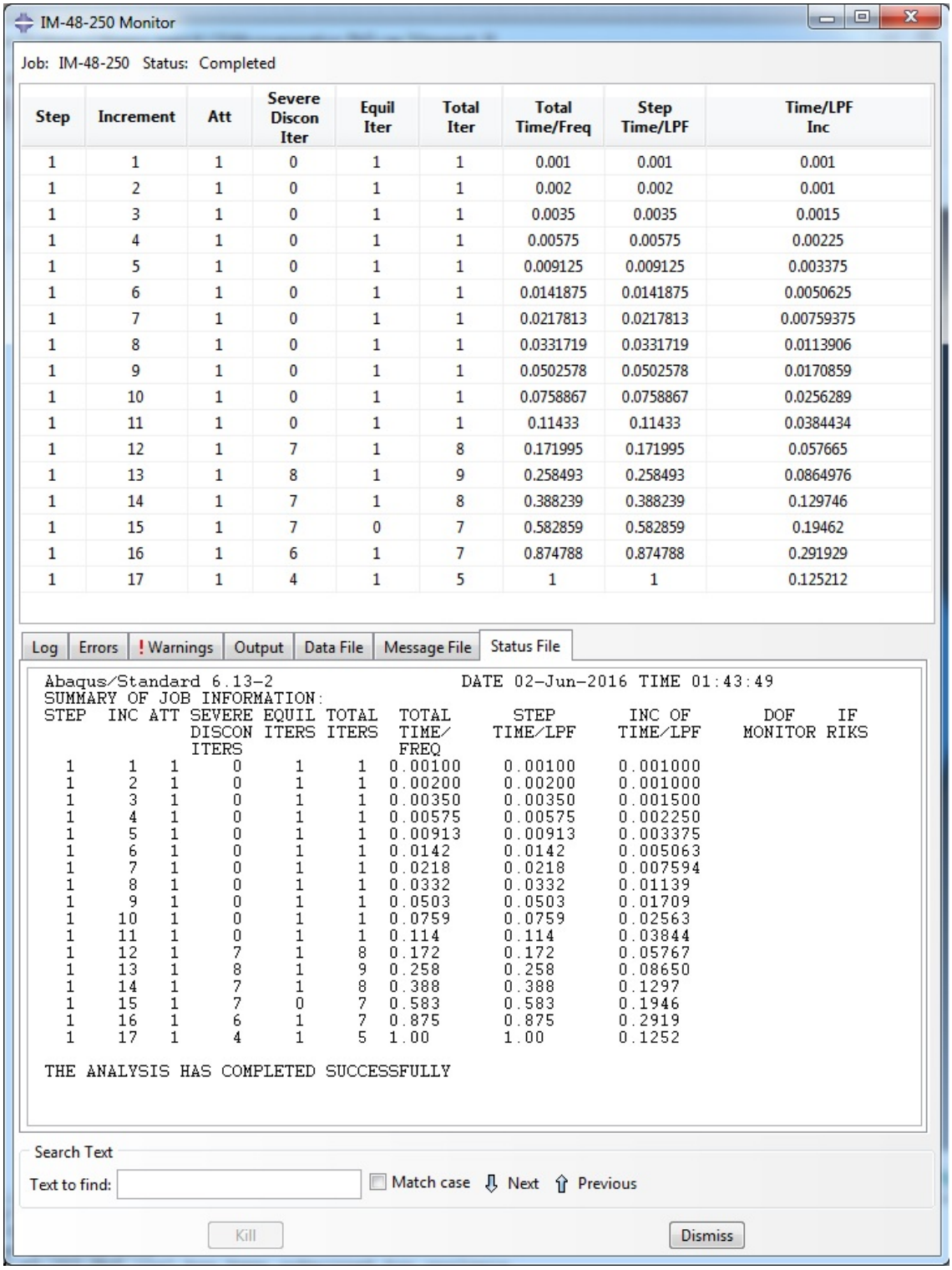

Step	Increment	Att	Severe Discon Iter	Equil Iter	Total Iter	Total Time/Freq	Step Time/LPF	Time/LPF Inc
1	1	1	0	1	1	0.001	0.001	0.001
1	2	1	0	1	1	0.002	0.002	0.001
1	3	1	0	1	1	0.0035	0.0035	0.0015
1	4	1	0	1	1	0.00575	0.00575	0.00225
1	5	1	0	1	1	0.009125	0.009125	0.003375
1	6	1	0	1	1	0.0141875	0.0141875	0.0050625
1	7	1	0	1	1	0.0217813	0.0217813	0.00759375
1	8	1	0	1	1	0.0331719	0.0331719	0.0113906
1	9	1	0	1	1	0.0502578	0.0502578	0.0170859
1	10	1	0	1	1	0.0758867	0.0758867	0.0256289
1	11	1	0	1	1	0.11433	0.11433	0.0384434
1	12	1	7	1	8	0.171995	0.171995	0.057665
1	13	1	8	1	9	0.258493	0.258493	0.0864976
1	14	1	7	1	8	0.388239	0.388239	0.129746
1	15	1	7	0	7	0.582859	0.582859	0.19462
1	16	1	6	1	7	0.874788	0.874788	0.291929
1	17	1	4	1	5	1	1	0.125212

```
Abaqus/Standard 6.13-2                    DATE 02-Jun-2016 TIME 01:43:49
SUMMARY OF JOB INFORMATION:
STEP   INC ATT SEVERE EQUIL TOTAL  TOTAL      STEP       INC OF       DOF    IF
                DISCON ITERS ITERS TIME/     TIME/LPF   TIME/LPF     MONITOR RIKS
                ITERS              FREQ
  1     1   1      0     1     1  0.00100    0.00100    0.001000
  1     2   1      0     1     1  0.00200    0.00200    0.001000
  1     3   1      0     1     1  0.00350    0.00350    0.001500
  1     4   1      0     1     1  0.00575    0.00575    0.002250
  1     5   1      0     1     1  0.00913    0.00913    0.003375
  1     6   1      0     1     1  0.0142     0.0142     0.005063
  1     7   1      0     1     1  0.0218     0.0218     0.007594
  1     8   1      0     1     1  0.0332     0.0332     0.01139
  1     9   1      0     1     1  0.0503     0.0503     0.01709
  1    10   1      0     1     1  0.0759     0.0759     0.02563
  1    11   1      0     1     1  0.114      0.114      0.03844
  1    12   1      7     1     8  0.172      0.172      0.05767
  1    13   1      8     1     9  0.258      0.258      0.08650
  1    14   1      7     1     8  0.388      0.388      0.1297
  1    15   1      7     0     7  0.583      0.583      0.1946
  1    16   1      6     1     7  0.875      0.875      0.2919
  1    17   1      4     1     5  1.00       1.00       0.1252

THE ANALYSIS HAS COMPLETED SUCCESSFULLY
```

17 Processed increments monitoring in the job page

Appendix F: BC and Load in Neck-Rim/Ring impingement

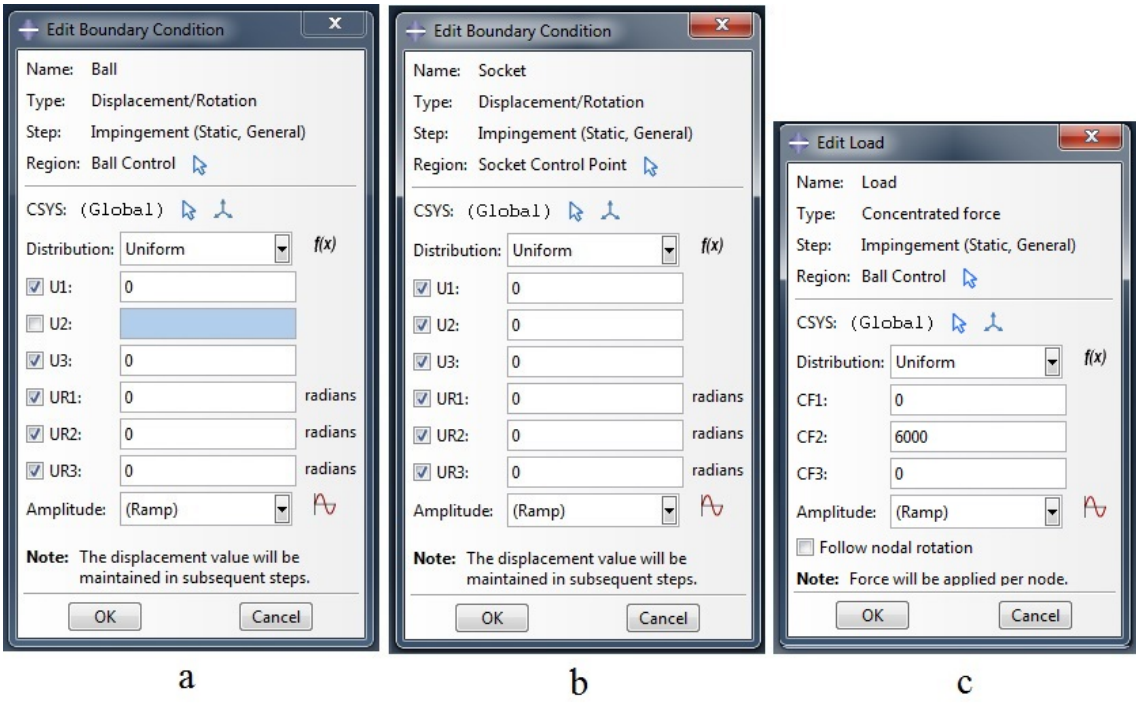

a) BC of the ball b) BC of the socket c) Applied load to the neck

Appendix G: BC in EL study

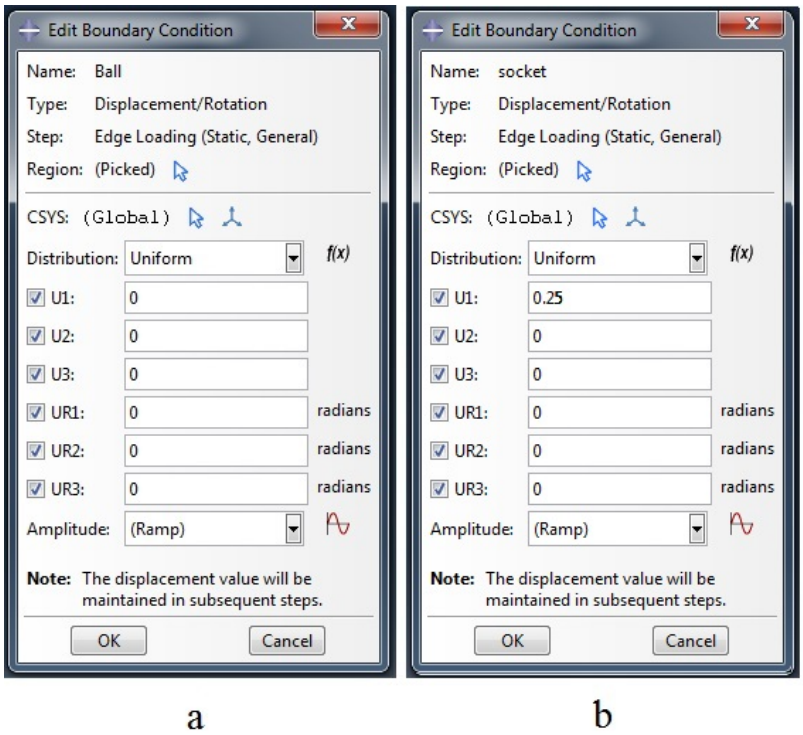

a) BC of the ball, b) BC of the socket

Appendix H: Direct solution to find maximum contact pressure in CM

$$P_0 = \{\frac{6WE'^2}{\pi^3 R^2}\}^{1/3} \Rightarrow P_{0\,cm} = \left(\frac{6\times W\times(1.839\times10^{11})^2}{31\times(2.264\times10^{-3})^2}\right)^{1/3}$$

$$\Rightarrow P_{0\,cm} = \left(\frac{2.03\times10^{23}\times W}{1.589\times10^{-4}}\right)^{1/3}$$

$$\Rightarrow P_{0\,cm} = 1.085\times10^{9}\times W^{1/3}$$

Appendix I: Direct solution to find maximum contact pressure in IM

$$P_0 = \{\frac{6WE'^2}{\pi^3 R^2}\}^{1/3} \Rightarrow P_{0\,IM} = \left(\frac{6\times W\times(1.839\times10^{11})^2}{31\times(14.424)^2}\right)^{1/3}$$

$$\Rightarrow P_{0\,IM} = \left(\frac{2.03\times10^{23}\times W}{6.45\times10^{3}}\right)^{1/3}$$

$$\Rightarrow P_{0\,IM} = 3.157\times10^{6}\times W^{1/3}$$